

AD A101657

AFWAL-TR-81-3041
VOLUME 1

LEVEL

2
135



EFFECT OF VARIANCES AND MANUFACTURING TOLERANCES ON THE DESIGN STRENGTH AND LIFE OF MECHANICALLY FASTENED COMPOSITE JOINTS

VOLUME 1 - METHODOLOGY DEVELOPMENT AND DATA EVALUATION

S.P. Garbo and J.M. Ogonowski

McDonnell Aircraft Company
McDonnell Douglas Corporation
P.O. Box 516
St. Louis, Missouri 63166

DTIC
JUL 21 1981

April 1981

Final Report for Period 15 February 1978 - 15 April 1981

Approved for public release; distribution unlimited

FILE COPY

WRIGHT DYNAMICS LABORATORY
AIR FORCE WRIGHT AERONAUTICAL LABORATORIES
AIR FORCE SYSTEMS COMMAND
WRIGHT-PATTERSON AIR FORCE BASE, OHIO 45433

81 7 21 009

NOTICE

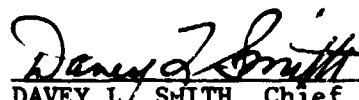
When Government drawings, specifications, or other data are used for any purpose other than in connection with a definitely related Government procurement operation, the United States Government thereby incurs no responsibility nor any obligation whatsoever; and the fact that the government may have formulated, furnished, or in any way supplied the said drawing, specifications, or other data, is not to be regarded by implication or otherwise as in any manner licensing the holder or any other person or corporation, or conveying any rights or permission to manufacture, use, or sell any patented invention that may in any way be related thereto.

This report has been reviewed by the Office of Public Affairs (ASD/PA) and is releasable to the National Technical Information Service (NTIS). At NTIS, it will be available to the general public, including foreign nations.

This technical report has been reviewed and is approved for publication.



ROBERT L. GALLO, Capt, USAF
Project Engineer



DAVEY L. SMITH, Chief
Structural Integrity Branch
Structures & Dynamics Division

FOR THE COMMANDER



RALPH L. KUSTER, JR., Col, USAF
Chief, Structures and Dynamics Division

If your address has changed, if you wish to be removed from our mailing list, or if the addressee is no longer employed by your organization please notify AFWAL/FIBEC, Wright-Patterson AFB, OH 45433 to help us maintain a current mailing list. Copies of this report should not be returned unless return is required by security considerations, contractual obligations, or notice on a specific document.

(16) 2404 (17) 01

SECURITY CLASSIFICATION OF THIS PAGE (When Data Entered)

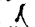
1. REPORT DOCUMENTATION PAGE		READ INSTRUCTIONS BEFORE COMPLETING FORM
2. REPORT NUMBER	3. GOVT ACCESSION NO.	4. RECIPIENT'S CATALOG NUMBER
AFWAL-TR-81-3641-Vol-1	AF-A103657	9
5. TITLE (and Subtitle) EFFECT OF VARIANCES AND MANUFACTURING TOLERANCES ON THE DESIGN STRENGTH AND LIFE OF MECHANICALLY FASTENED COMPOSITE JOINTS. VOLUME 1. Methodology and Data Evaluation		6. PERFORMING ORG. REPORT NUMBER
7. AUTHOR P. Garbo J. M. Ogonowski		8. CONTRACT OR GRANT NUMBER(s) F33615-77-C-3140
9. PERFORMING ORGANIZATION NAME AND ADDRESS McDonnell Aircraft Company P.O. Box 516 St. Louis, Missouri 63166		10. PROGRAM ELEMENT, PROJECT, TASK AREA & WORK UNIT NUMBERS P.E. 62201F W.U. 24010110
11. CONTROLLING OFFICE NAME AND ADDRESS Flight Dynamics Laboratory (AFWAL/FIBEC) Air Force Wright Aeronautical Lab. (AFSC) Wright-Patterson AFB, Ohio 45433		12. REPORT DATE Apr 1981
13. MONITORING AGENCY NAME & ADDRESS (if different from Controlling Office)		14. NUMBER OF PAGES 144
(12) 159		15. SECURITY CLASS. (of this report) Unclassified
16. DISTRIBUTION STATEMENT (of this Report) Approved for public release; distribution unlimited		
17. DISTRIBUTION STATEMENT (of abstract entered in Block 20, if different from Report)		
18. SUPPLEMENTARY NOTES		
19. KEY WORDS (Continue on reverse side if necessary and identify by block number) Bolted Joints Orthotropic Load Distributions Composite Stress Concentrations Stress Analysis Graphite-epoxy Methodology Failure Criteria Fatigue Life		
20. ABSTRACT (Continue on reverse side if necessary and identify by block number) The subject of this program was structural evaluation of mechanically fastened composite joints. Program objectives were threefold: (1) development and verification by test of improved static strength methodology, (2) experimental evaluation of the effects of manufacturing anomalies on joint static strength, and (3) experimental evaluation of joint fatigue life.		

DTIC
JUL 21 1981
C

DD FORM 1 JAN 73 1473

SECURITY CLASSIFICATION OF THIS PAGE (When Data Entered)

403111

Program activities to accomplish these objectives were organized under five tasks. Under Task 1 - Literature Survey, a survey was performed to determine the state-of-the-art in design and analysis of bolted composite joints. Experimental evaluations of joint static strength were performed under Tasks 2 and 3. In Task 2 - Evaluation of Joint Design Variables, strength data were obtained through an experimental program to evaluate the effects of twelve joint design variables. In Task 3 - Evaluation of Manufacturing and Service Anomalies, effects of seven anomalies on joint strength were evaluated experimentally and compared with Task 2 strength data. Bolted composite joint durability was evaluated under Task 4 - Evaluation of Critical Joint Design Variables on Fatigue Life. Seven critical design variables or manufacturing anomalies were identified based on Task 2 and 3 strength data. Under Task 5 - Final Analyses and Correlation, required data reduction, methodology development and correlation, and necessary documentation were performed. 

This report documents all program activities performed under Tasks 2, 3, 4 and 5. Activities performed under Task 1 - Literature Survey, were previously reported in AFFDL-TR-78-179. Static strength methodology and evaluations of joint static and fatigue test data are reported. Analytic studies complement methodology development and illustrate: the need for detailed stress analysis, the utility of the developed "Bolted Joint Stress Field Model" (BJSFM) procedure, and define model limitations. For static strength data, correlations with analytic predications are included. Data trends in all cases are discussed relative joint strength and failure mode. For joint fatigue studies, data trends are discussed relative to life, hole elongation, and failure mode behavior.

This final report is organized in the following three volumes:

- Volume 1 - Methodology Development and Data Evaluation
- Volume 2 - Test Data, Equipment and Procedures
- Volume 3 - Bolted Joint Stress Field Model (BJSFM) Computer Program User's Manual

FOREWORD

The work reported herein was performed by the McDonnell Aircraft Company (MCAIR) of the McDonnell Douglas Corporation (MDC), St. Louis, Missouri, under Air Force Contract F33615-77-C-3140, for the Flight Dynamics Laboratory, Wright-Patterson Air Force Base, Ohio. This effort was conducted under Project No. 2401 "Structural Mechanics", Task 240101 "Structural Integrity for Military Aerospace Vehicles", Work Unit 24010110 "Effect of Variances and Manufacturing Tolerances on the Design Strength and Life of Mechanically Fastened Composite Joints". The Air Force Project Engineer at contract go-ahead was Mr. Roger J. Aschenbrenner (AFWAL/FIBEC); in December 1979, Capt. Robert L. Gallo (AFWAL/FIBEC) assumed this assignment. The work described was conducted during the period 15 February 1978 through 15 April 1981.

Program Manager was Mr. Ramon A. Garrett, Branch Chief Technology, MCAIR Structural Research Department. Principal Investigator was Mr. Samuel P. Garbo, MCAIR Structural Research Department.

Accession For	
NTIS GPO&I	<input checked="checked" type="checkbox"/>
DTIC TAB	<input type="checkbox"/>
Unannounced	<input type="checkbox"/>
Justification	
By	
Distribution/	
Availability Codes	
Avail and/or	
Dist	Special
A	

TABLE OF CONTENTS

<u>Section</u>	<u>Page</u>
I INTRODUCTION	1
II SUMMARY AND CONCLUSIONS	2
III METHODOLOGY DEVELOPMENT AND ANALYTIC STUDIES	5
1. BACKGROUND	5
2. METHODOLOGY DEVELOPMENT	5
3. PREDICTIONS USING BJSFM APPROACH	15
a. Effects of Anisotropy on Stress Distributions	15
b. Hole Size Effects	16
c. Finite Width Effects	17
d. Characteristic Dimension Sensitivity Study	19
e. Biaxial Loading Effects	20
f. Pure Bearing Strength Study	24
g. Effects of Environment	25
IV TEST DATA EVALUATION	26
1. METHODOLOGY VERIFICATION: EVALUATION OF JOINT DESIGN VARIABLES - TASK 2	26
a. Task 2 Test Plan	26
b. Correlation of BJSFM Predictions With Experimental Results and Evaluations	35
(1) Strength of Laminates With Unloaded and Unfilled Holes	35
(2) Strength of Laminates With Loaded Fastener Holes	44
(a) Layup Variation	50
(b) Load Orientation	50
(c) Edge Distance	55
(d) Width	57
(e) Hole Size	57
(f) Load Interaction	64
(g) Fastener Pattern	73
(h) Torque-up	76
(i) Fastener Countersink and Laminate Thickness	77
(j) Stacking Sequence	86
(k) Single-Shear Loading	86

TABLE OF CONTENTS (Concluded)

<u>Section</u>	<u>Page</u>
2. EVALUATION OF MANUFACTURING AND SERVICE ANOMALIES - TASK 3	93
a. Task 3 Test Plan	93
b. Experimental Results and Evaluation	94
(1) Out of Round Holes	94
(2) Broken Fibers on Exit Side of Hole	98
(3) Porosity	100
(4) Improper Fastener Seating Depth	102
(5) Tilted Countersinks	104
(6) Interference Fit	106
(7) Fastener Removal and Reinstallation	109
3. EVALUATION OF CRITICAL JOINT DESIGN VARIABLES ON FATIGUE LIFE - TASK 4	110
a. Task 4 Test Plan	110
b. Experimental Results and Evaluation	115
(1) Layup Variation	117
(2) Stacking Sequence	125
(3) Torque-Up	130
(4) Joint Geometry	135
(5) Interference Fit	138
(6) Single-Shear Loading	138
(7) Porosity	142
V RECOMMENDATIONS	143
VI REFERENCES	144

LIST OF ILLUSTRATIONS

<u>Figure</u>		<u>Page</u>
1	Superposition of Linear-Elastic Stress Solutions . .	6
2	Uniaxially Loaded Infinite Plate	9
3	Assumed Cosine Bolt-Load Distribution	10
4	Characteristic Dimension Failure Hypothesis	12
5	Failure Criteria Comparison	13
6	Superposition of Solutions to Account for Finite Width	14
7	Circumferential Stress Solutions at Unloaded Holes	15
8	Circumferential Stress Solutions at Loaded Holes	16
9	Effect of Hole Size on Stress Distributions	17
10	Correlation of Loaded Hole Analyses	18
11	Effects of Width on Stress Concentrations	18
12	Correlation of Loaded Hole Analysis for Small Edge Distance Cases	19
13	Effect of Characteristic Dimension on Predicted Strength - 30/60/10 layup	20
14	Effect of Biaxial Loading on Predicted Strength . .	21
15	Effect of Biaxial Loading on Failure Location . . .	22
16	Effect of Biaxial Loading on Ply Strain Concentrations	23
17	Effect of Bearing Load Direction on Predicted Strength	24
18	Effect of Moisture and Temperature on Laminate Strength	25
19	Task 2 - Joint Design Variables - Test Matrix . . .	27
20	MCAIR Evaluation of Unloaded Hole Specimens - Test Matrix	29

LIST OF ILLUSTRATIONS (Continued)

<u>Figure</u>		<u>Page</u>
21	MCAIR Evaluation of Loaded Hole Specimens Test Matrix	30
22	Unloaded Hole Specimen Geometry	30
23	Loaded Hole Specimen Configuration	31
24	Specimen Loading Configurations	32
25	Effect of Laminate Stiffness on Specimen Bolt-Load Distributions	33
26	Task 2 - Layup Number and Stacking Sequence	34
27	AS/3501-6 Lamina Mechanical Properties	35
28	Effect of Layup Variation on Unloaded Hole Tensile Strength	36
29	Effect of Hole Size on Unloaded Hole Tensile Strength	37
30	Effect of Variation of R_c on Predicted Tensile Strength	38
31	Predicted Failure Orientations Were Verified	39
32	Effect Off-Axis Loading on Failure Stress	40
33	Effect of Variation of R_c on Predicted Compressive Strength	41
34	Effect of Hole Size on Unloaded Hole Compressive Strength	42
35	Effect of Layup Variation on Unloaded Hole Compressive Strength	43
36	Effect of Temperature on Unloaded Hole Compression Strength	44
37	Two-Bolt-In-Tandem Specimen Baseline Configuration	45
38	Variations of Single Fastener Specimen Configurations	46
39	Variations of Two-Bolt-In-Tandem Specimen Configurations	47

LIST OF ILLUSTRATIONS (Continued)

<u>Figure</u>		<u>Page</u>
40	Variations of Load-Interaction Specimen Configurations	48
41	Fastener Pattern Specimen Geometry	49
42	Effect of Layup Variation on Joint Tensile Strength	51
43	Effect of Layup Variation on Joint Compressive Strength	52
44	Effect of Off-Axis Loading on RTD Pure Bearing Strength	53
45	Effect of Temperature and Moisture on Off-Axis Strength	54
46	Effect of Temperature and Moisture on Compressive Strength	55
47	Effect of Edge Distance on Joint Tensile Strength	56
48	Effect of Fastener Spacing on Joint Tensile Strength	58
49	Effect of Edge Distance on Pure Bearing Strength	59
50	Effect of Specimen Width on RTD Joint Strength	60
51	Effect of Temperature and Moisture on Joint Strength	61
52	Joint Failures Changed at ETW Test Conditions.	62
53	Effect of Hole Size on Joint Strength	63
54	Load Interaction Specimen and Test Setup	64
55	Correlation of Bearing-Bypass Strength of a 50/40/10 Layup	65
56	Correlation of Bearing-Bypass Strength of a 30/60/10 Layup	66
57	Effect of Bearing Loads on Specimen Load-Deflection Behavior	67

LIST OF ILLUSTRATIONS (Continued)

<u>Figure</u>		<u>Page</u>
58	Predicted Critical Plies for Net-Section Failures	68
59	Predicted Critical Plies for Bearing-Shearout Failures	69
60	Tests Verify Predicted Failure Initiation Points	70
61	Load Conditions for Off-Axis Load-Interaction Tests	71
62	Effect of Off-Axis Bearing Loads on Bypass Strength	72
63	Fastener-Pattern Specimen Loading Configurations . .	73
64	Effects of Environment on Fastener-Pattern Joint Strength	74
65	Joint Failures for Fastener-Pattern Specimens . . .	75
66	Corrosion Resulting From Salt-Spray Exposure	76
67	Effect of Layup and Torque-Up on RTD Pure Bearing Strength	78
68	Failures of Pure Bearing Specimens	79
69	Comparison of Loaded and Unloaded Hole Specimen Strength	80
70	Effect of Torque-Up on RTD Pure Bearing Strength 50/40/10 Layup	81
71	Effect of Torque-Up on RTD Pure Bearing Strength 70/20/10 Layup	82
72	Effect of Torque-Up on RTD Pure Bearing Strength 30/60/10 Layup	83
73	Comparison of Effects of Torque-Up on Joint Strength	84
74	Effects of Thickness and Countersink on Joint Tensile Strength	85
75	Effect of Stacking Sequence on Joint Tensile Strength	87

LIST OF ILLUSTRATIONS (Continued)

<u>Figure</u>		<u>Page</u>
76	Correlation of Joint RTD Tensile Strength With Grouped 0° Plies	88
77	Correlation of Joint ETW Tensile Strength With Grouped 0° Plies	89
78	Correlation of Joint RTD Compressive Strength With Grouped 0° Plies	90
79	Comparison of Single and Double-Shear Joint Strengths	91
80	Correlation of Joint Strength With Edge Distance-to- Width Ratios	92
81	Task 3 - Evaluation of Manufacturing Anomalies - Test Matrix	93
82	Specimen Moisture Conditioning Histories	95
83	Summary of Task 3 Strength Reduction Percents	96
84	Out-of-Round Holes - Specimen Details	97
85	Effect of Out-of-Round Holes on Joint Strength	97
86	C-Scans of Laminates With Delaminations at Fastener Holes	98
87	Effect of Delaminations on Joint Strength	99
88	Panel Fabrication Procedures Used to Produce Panel Porosity	100
89	Examples of Panel Porosity	101
90	Freeze-Thaw Exposure Profile	102
91	Effect of Porosity Around Hole on Joint Strength	103
92	Effect of Improper Fastener Seating on Joint Strength	104
93	Tilted Countersink - Specimen Configuration	105
94	Effect of Tilted Countersink on Joint Strength	106

LIST OF ILLUSTRATIONS (Continued)

<u>Figure</u>		<u>Page</u>
95	Effect of Fastener Interference Fit on Joint Strength	107
96	Photomicrographic Examination of Laminates With Interference Fit Holes	108
97	Effect of Fastener Removal and Reinstallation on Joint Strength	109
98	Task 4 - Evaluation of Critical Joint Variables on Fatigue Life - Test Matrix	111
99	Task 4 - Fatigue Specimen Configuration	113
100	Distribution of Hours and Exceedances	114
101	Measured Mix-Truncated Spectrum	114
102	Task 4 Layup Numbers and Stacking Sequence	115
103	Summary of Task 4 Specimen Static Strength	116
104	RTD Baseline Joint Fatigue Life 50/40/10 Layup	117
105	RTD Baseline Joint Fatigue Life 30/60/10 Layup	118
106	RTD Baseline Joint Fatigue Life 19/76/5 Layup	118
107	Comparison of $R = +0.1$ Joint Fatigue Life Trends . .	119
108	Comparison of $R = -1.0$ Joint Fatigue Life Trends . .	119
109	Hole Elongation Fatigue Life Trends 50/40/10 Layup	120
110	Hole Elongation Fatigue Life Trends 30/60/10 Layup	121
111	Hole Elongation Fatigue Life Trends 19/76/5 Layup	121
112	Representative Specimen Fatigue Failures	122
113	Summary of Effects of Environment on Joint Spectrum Fatigue Life	123

LIST OF ILLUSTRATIONS (Concluded)

<u>Figure</u>		<u>Page</u>
114	Effect of $R = +0.1$ Loading on Hole Elongation - Baseline 50/40/10 Layup	124
115	Effect of $R = +0.1$ Loading on Joint Spring Rate - Baseline 50/40/10 Layup	125
116	Effect of Stacking Sequence on Joint Life - 50/40/10 Layup	126
117	Effect of Stacking Sequence on Joint Life - 19/76/5 Layup	127
118	Stacking Sequence - Comparison With $R = -1.0$ Baseline Life Trends	128
119	Stacking Sequence - Comparison With $R = +0.1$ Baseline Life Trends	128
120	Effect of Stacking Sequence - Hole Elongation Levels - 50/40/10 Layup	129
121	Effect of Stacking Sequence - Hole Elongation Levels - 19/76/5 Layup	130
122	Summary of Effects of Stacking Sequence on Joint Spectrum Life	131
123	Effect of Torque-Up on Joint Fatigue Life 50/40/10 Layup	132
124	Effect of Torque-Up on Joint Fatigue Life 19/76/5 Layup	133
125	Specimen Failures for Torque-Up Conditions	134
126	Effect of Geometry on Joint Fatigue Life 50/40/10 Layup	135
127	Effect of Geometry on Joint Fatigue Life 19/76/5 Layup	136
128	Changes in Failure Due to Specimen Geometry	137
129	Effect of 0.005 Inch Interference Fit on Joint Fatigue Life - 50/40/10 Layup	139
130	Effect of Single-Shear Loading on Joint Fatigue Life - 50/40/10 Layup	140
131	Failures of Single-Shear Specimens	141
132	Effect of Porosity on Joint Fatigue Life - 50/40/10 Layup	142

SECTION I

INTRODUCTION

The subject of this program was structural evaluation of mechanically fastened composite joints. Program objectives were threefold: (1) development and verification by test of improved static strength methodology, (2) experimental evaluation of the effects of manufacturing anomalies on joint static strength, and (3) experimental evaluation of joint fatigue life.

Program activities to accomplish these objectives were organized under five tasks. Under Task 1 - Literature Survey, a survey was performed to determine the state-of-the-art in design and analysis of bolted composite joints. Experimental evaluations of joint static strength were performed under Tasks 2 and 3. In Task 2 - Evaluation of Joint Design Variables, baseline strength data were obtained through an experimental program to evaluate the effects of twelve joint design variables. In Task 3 - Evaluation of Manufacturing and Service Anomalies, effects of seven anomalies on joint strength were experimentally evaluated and compared with baseline Task 2 strength data. Bolted composite joint durability was evaluated under Task 4 - Evaluation of Critical Joint Design Variables On Fatigue Life. Seven critical design variables or manufacturing anomalies were identified based on Task 2 and 3 strength data. Under Task 5 - Final Analyses and Correlation, required data reduction, methodology development and correlation, and necessary documentation were performed.

This report documents all program activities performed under Tasks 2, 3, 4 and 5. Activities performed under Task 1 - Literature Survey, were previously reported in Reference 1. The main body of this report (Sections III and IV) documents developed static strength methodology and evaluations of joint static and fatigue test data. Associated analytic studies have been included in Section III to complement methodology development discussions and to illustrate: the need for detailed stress analysis, the utility of the developed "Bolted Joint Stress Field Model" (BJSFM) procedure, and to define model limitations. For static strength data reported in Section IV, correlations with analytic predictions, where applicable, are included. Data trends in all cases are discussed relative to joint strength and failure mode and compared to baseline data. For joint fatigue studies, data trends are discussed relative to life, hole elongation, and failure mode behavior.

This final report is organized in three volumes: Volume 1 - Methodology Development and Data Evaluation, Volume 2 - Test Data, Equipment and Procedures, Volume 3 - Bolted Joint Stress Field Model (BJSFM) Computer Program User's Manual.

SECTION II

SUMMARY AND CONCLUSIONS

Analytic methods were developed which permit strength analysis of bolted composite joints with minimal test data requirements. Methodology was based on anisotropic theory of elasticity, classical lamination plate theory, and a characteristic dimension (R_c) failure hypothesis. The principle of elastic superposition was used to obtain laminate stress distributions due to combined loadings of bearing and bypass. Test data requirements for general method use were minimized by extending the characteristic dimension failure hypothesis to a ply-by-ply analysis in conjunction with known material failure criteria. Unidirectional (lamina) stiffness and strength data were used with an empirical value of R_c to predict stress distributions, critical plies, failure location, and failure load of arbitrary laminates under general loadings. The developed analysis procedure is entitled the "Bolted Joint Stress Field Model" (BJSFM).

The BJSFM methodology was originally developed for unloaded hole analysis by McDonnell Aircraft Company (MCAIR) under an in-house research and development program. The methodology was further verified and extended to the analysis of loaded holes under this program.

Under Task 2 - Evaluation of Joint Design variables, effects of twelve joint design variables on static strength were experimentally evaluated. The BJSFM procedure was used to predict the effects of five of the twelve design variables (layups, load interaction, off-axis loading, hole size, and width). Only experimental evaluation of the remaining variables was possible. The range of test conditions in each design variable was identified in the Task 1 - Literature Survey.

Initial verification of analysis was obtained by correlating strength predictions with data obtained from tests of specimens with unfilled fastener holes. Specimens were tested to failure in tension and compression. Values for R_c of .02 inch for tensile strength predictions and .025 inch for compressive strength predictions were empirically determined for one laminate, each of which were fabricated using the Hercules AS/3501-6 graphite-epoxy system. With these values of R_c and unidirectional ply (lamina) mechanical properties, BJSFM predictions were correlated with unloaded hole strength data for an extensive range of layup variations and, in general, were accurate to within $\pm 10\%$. Predicted failure initiation points were visually verified. Correlation of strength predictions with data indicated that only knowledge of temperature-altered lamina properties is required to predict effects of temperature on general laminate strength; R_c remained unchanged.

Joint load-deflection plots for specimens with either shear-out or bearing failures indicated nonlinear mechanical behavior, with ultimate failure occurring at loads considerably above initial nonlinearities. Strength predictions obtained using the BJSFM procedure correlated with initial points of joint nonlinear deflection behavior. Ultimate strength predictions using the linear-elastic BJSFM procedure became increasingly conservative as this joint nonlinear load-deflection behavior occurred. However, predicted linear-elastic failures of critical plies were due to exceeding lamina fiber or shear strength and implied the type of localized joint failures and load redistribution typical of the failure modes observed in tests.

Under Task 3 - Evaluation of Manufacturing and Service Anomalies, effects of seven anomalies on joint static strength were experimentally evaluated and compared with baseline (no anomaly) strength data. The seven anomalies were selected based on MCAIR experience and an available industry-wide survey (Reference 2).

Results fell into two groups: (1) anomalies which resulted in strength reductions of more than 13 percent (porosity around hole, improper fastener seating depth, and tilted countersinks), and (2) anomalies which resulted in strength reductions of less than 13 percent (out-of-round holes, broken fibers on exit side of hole, interference fit tolerances, removal and reinstallation). For anomalies of the first group, current industry inspection and acceptance criteria would have detected all three and resulted in part rejection or required repair.

Under Task 4 - Evaluation of Critical Joint Design Variables on Fatigue Life, the influence of seven design variables and anomalies on joint durability were evaluated. Tests were performed to provide data on joint fatigue life performance, hole elongation, and failure mode behavior. Single-fastener pure bearing specimens were cycled, under tension-tension ($R = +0.1$) and tension-compression ($R = -1.0$) constant amplitude fatigue loading, and under spectrum fatigue loadings.

During fatigue testing, load-deflection data were obtained at specified increments of accumulated hole elongation. Several tests were performed at environmental conditions previously defined in Task 2. Static and residual strength tests were performed on selected specimens at each test condition.

Joint fatigue life was defined to occur at specimen failure or when hole elongations of .02 inch were measured. Based on this definition, little difference was noted in relative fatigue life between 50/40/10, 30/60/10 and 19/76/5 layups (percent 0°, +45°, 90° plies respectively) under tension-tension ($R = +0.1$) cycling. Under fully reversed load cycling, ($R = -1.0$), hole elongations of .02 inch occurred more rapidly in the matrix-dominant 19/76/5 layup, followed by the 30/60/10 and 50/40/10 layups. Under spectrum fatigue tests of all three layups, no

hole elongation occurred after 16,000 spectrum hours at test limit loads (TLL) of 89% of static strength values. This agreed with constant amplitude fatigue test results; 16,000 hours of spectrum loading at these levels did not produce enough cycles of high loads to produce hole elongation.

Effects of fastener torque-up on joint fatigue life were pronounced. Joints with torque-up values exhibited increased strength and life for all layups tested, under both $R = +0.1$ and $R = -1.0$ cycling. While failure modes were the same, areas of damage were more pronounced for specimens with torque-up and failure occurred more abruptly (rates of hole elongation, once initiated, were faster).

Effects of joint eccentricity and geometry also influenced joint fatigue life characteristics. Single-shear specimens exhibited lower fatigue life as compared to the double-shear baseline configuration. Further reductions occurred with flush-head fasteners relative to protruding head fasteners; attributed to increased fastener flexibility and specimen bending. For the 19/76/5 layup, changes in specimen width caused changes in failure modes and marked changes in both strength and life. However, for the 50/40/10 layup, variations in width and edge distance did not alter failure modes, and strength and life were virtually unchanged.

Effects of remaining variables on joint fatigue life were minor, with failure modes and durability essentially the same as for baseline configurations.

SECTION III

METHODOLOGY DEVELOPMENT AND ANALYTIC STUDIES

1. BACKGROUND - As described in the Literature Survey, analysis of bolted composite joints in aircraft structural components throughout the industry proceeds from overall structural and bolt-load distribution analyses, to assessment of stress distributions and strength predictions at individual fastener holes through utilization of joint failure analysis.

Methods currently used to determine detailed stress distributions in the immediate vicinity of the fastener hole include both theoretical and empirical approaches. Theoretical approaches include analytic, finite element, and strength of materials approximation methods. Analytic methods, preferred because of their potential generality, economy, and exactness, are principally formulated from two-dimensional anisotropic elasticity theory. Empirical approaches lack generality at high cost.

Joint failure analyses, in current use, include: (1) empirical approaches, (2) elastic and inelastic failure analyses, (3) phenomenological failure analysis, and (4) fracture mechanics models. Physical variables considered for accurate solutions were generally agreed upon throughout the industry. However, the degree to which variables were accounted for was different in particular methods. No single methodology accounted for all of the important variables (e.g. orthotropy, finite geometry, non-linear or inelastic material behavior).

In each joint failure analysis approach, after detailed stress distributions are determined, strength is assessed by using some material failure criteria; however, no single material failure criterion is uniformly endorsed. Studies of utilization of various material failure criteria for joint failure analysis are very limited.

Detailed stress analysis performed at individual fastener holes and associated application of failure criteria represents the primary area of analytic development in this program. The methodology developed requires only unidirectional material properties and minimal laminate test data to calculate laminate strength with an arbitrary in-plane loading. Because the method uses closed-form solutions, parametric studies are easily and inexpensively performed.

2. METHODOLOGY DEVELOPMENT - The goal of the methodology development was to provide a technique for predicting the strength of an anisotropic plate with a stress concentration. A closed-form analytic approach was developed to predict stress distributions and perform failure analysis of an anisotropic plate with a loaded or unloaded fastener hole. This section describes the

analytical development of the Bolted Joint Stress Field Model (BJSFM). An associated computer program is described in Volume 3.

The method of analysis is based on (1) anisotropic theory of elasticity, (2) lamination plate theory and (3) a failure hypothesis. The principle of elastic superposition is used to obtain laminate stress distributions due to combined loadings of bearing and bypass (Figure 1). The developed analysis can be used with various material failure criteria and the failure hypothesis to predict laminate load carrying capability.

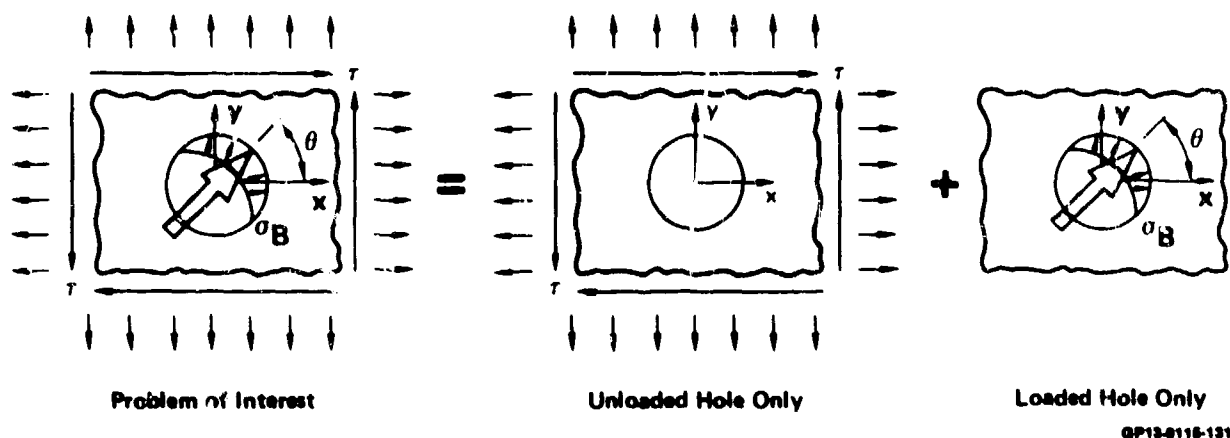


Figure 1. Superposition of Linear-Elastic Stress Solutions

The elastic solution for the stress field in a homogeneous, anisotropic infinite plate with a stress concentration was solved using two-dimensional anisotropic theory of elasticity (Reference 3). Equilibrium and compatibility requirements are satisfied by a stress function, F , which satisfies the generalized biharmonic equation for anisotropic materials,

$$S_{22} \frac{\partial^4 F}{\partial X^4} - 2S_{26} \frac{\partial^4 F}{\partial X^3 \partial Y} + (2S_{12} + S_{66}) \frac{\partial^4 F}{\partial X^2 \partial Y^2} - 2S_{16} \frac{\partial^4 F}{\partial X \partial Y^3} + S_{11} \frac{\partial^4 F}{\partial Y^4} = 0$$

where S_{jk} are laminate compliance coefficients. The general expression for the function F depends upon the roots of the associated characteristic equation. Solving the characteristic equation yields a set of complex conjugate roots ($R_1, \bar{R}_1, R_2, \bar{R}_2$). The stress function can be expressed as

$$F = 2\text{Re} \{F_1(Z_1) + F_2(Z_2)\}$$

where $F_1(Z_1)$, $F_2(Z_2)$ are analytic functions of the complex coordinates $Z_1 = X + R_1Y$ and $Z_2 = X + R_2Y$ respectively. Introducing the functions

$$\phi_1(Z_1) = \frac{\partial F(Z_1)}{\partial Z_1}, \quad \phi_2(Z_2) = \frac{\partial F(Z_2)}{\partial Z_2}$$

general expressions for the stress components are obtained:

$$\sigma_x = 2\text{Re} \{R_1^2 \phi_1' (Z_1) + R_2^2 \phi_2' (Z_2)\}$$

$$\sigma_y = 2\text{Re} \{\phi_1' (Z_1) + \phi_2' (Z_2)\}$$

$$\sigma_{xy} = -2\text{Re} \{R_1 \phi_1' (Z_1) + R_2 \phi_2' (Z_2)\}$$

Superscript primes represent derivatives with respect to the complex arguments. Displacements, ignoring terms for rigid body rotation and translation which in this problem do not affect solutions, can be expressed as:

$$U = 2\text{Re} \{P_1 \phi_1 (Z_1) + P_2 \phi_2 (Z_2)\}$$

$$V = 2\text{Re} \{Q_1 \phi_1 (Z_1) + Q_2 \phi_2 (Z_2)\}$$

where

$$P_1 = S_{11} R_1^2 + S_{12} - S_{16} R_1$$

$$P_2 = S_{11} R_2^2 + S_{12} - S_{16} R_2$$

$$Q_1 = \frac{S_{22}}{R_1} + S_{12} R_1 + S_{26}$$

$$Q_2 = \frac{S_{22}}{R_2} + S_{12} R_2 - S_{26}$$

To obtain exact solutions for an infinite plate with a circular hole (loaded or unloaded) and uniform stresses at infinity, conformal mapping techniques were used. A mapping function was used to map the physical circular boundary of radius, a , in the Z_k plane ($k = 1, 2$) onto a unit circle in the ξ_k plane. The mapping function is given by

$$\xi_k = \frac{Z_k + \sqrt{Z_k^2 - a^2 - R_k^2 a^2}}{a(1 - iR_k)} \quad k = 1, 2$$

The sign of the square root is chosen such that the exterior of a hole is mapped to the exterior of a unit circle.

The above equations contain unknown stress functions $\phi_1(Z_1)$ and $\phi_2(Z_2)$. For infinite plate problems with a stress concentration, these functions will have the general form:

$$\phi_1(Z_1) = B_1 Z_1 + A_1 \ln \xi_1 + \sum_{M=1}^{\infty} A_{1M} \xi_1^{-M}$$

$$\phi_2(Z_2) = B_2 Z_2 + A_2 \ln \xi_2 + \sum_{M=1}^{\infty} A_{2M} \xi_2^{-M}$$

Linear Z_1 and Z_2 terms are required for a uniform stress at infinity. Terms with $\ln \xi_1$ and $\ln \xi_2$ are present whenever the resultant of the applied stresses on the circular boundary are nonzero. Boundary conditions on the circular hole are satisfied by the A_{1M} and A_{2M} series coefficients.

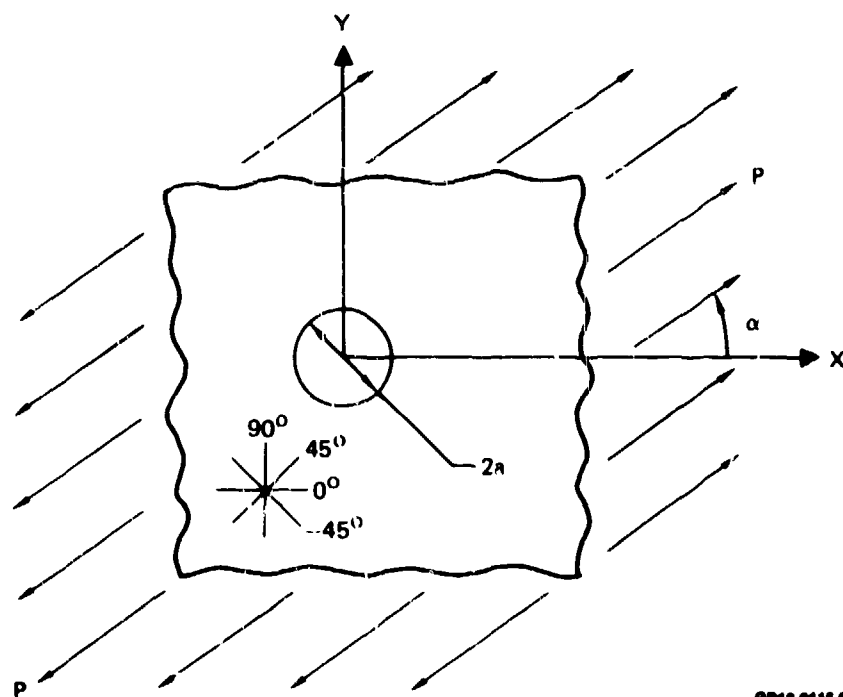
To obtain the solution for a plate with an unloaded hole subjected to a remote uniaxial in-plane stress field, P , at an arbitrary orientation, α , with the X-axis (Figure 2), the imposed boundary conditions at infinity and on the circular boundary result in the stress functions:

$$\phi_1(z_1) = \frac{iPa^2(1-iR_1)}{4(R_1-R_2)} \times$$

$$\left[\frac{R_2 \sin 2\alpha + 2 \cos^2 \alpha + i(2R_2 \sin^2 \alpha + \sin 2\alpha)}{z_1 + \sqrt{z_1^2 - a^2 - R_1^2 a^2}} \right]$$

$$\phi_2(z_2) = \frac{iPa^2(1-iR_2)}{4(R_1-R_2)} \times$$

$$\left[\frac{R_1 \sin 2\alpha + 2 \cos^2 \alpha + i(2R_1 \sin^2 \alpha + \sin 2\alpha)}{z_2 + \sqrt{z_2^2 - a^2 - R_2^2 a^2}} \right]$$



GP13-8115-02

Figure 2. Uniaxially Loaded Infinite Plate

Only the linear terms and first coefficient of the summation are used for the unloaded hole solution.

Loaded hole analysis was performed by specifying a radial stress boundary condition varying as a cosine over half the hole (Figure 3). Boundary conditions at infinity required to satisfy equilibrium result in stress free conditions since the finite force required to balance the bolt load is applied to an infinite boundary. Thus, the linear terms are not required.

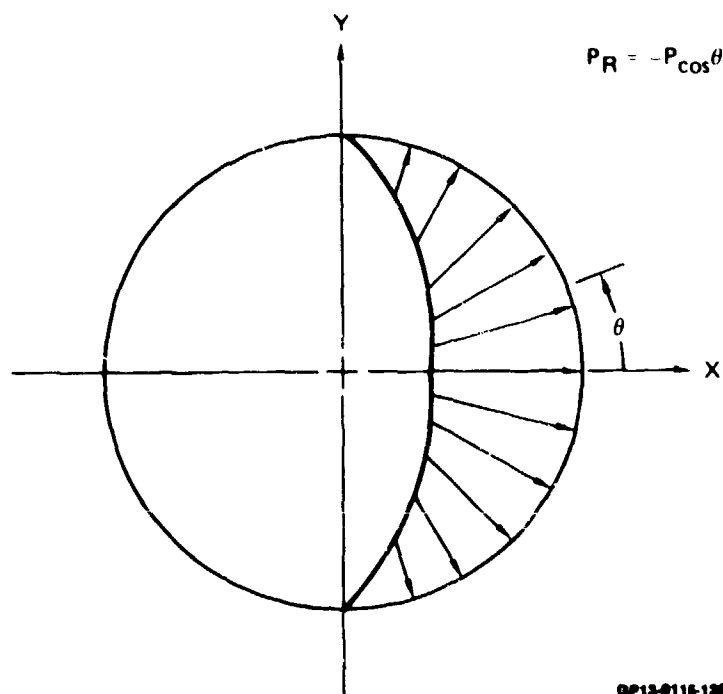


Figure 3. Assumed Cosine Bolt-Load Distribution

Since the specified hole loading is not self-equilibrating on the boundary, single-valued displacement conditions are imposed to determine the log term coefficients. The following set of simultaneous equations are solved for the A_1 and A_2 complex coefficients.

$$A_1 - \bar{A}_1 + A_2 - \bar{A}_2 = P_y/2 \pi i$$

$$R_1 A_1 - \bar{R}_1 \bar{A}_1 + R_2 A_2 - \bar{R}_2 \bar{A}_2 = -P_x/2 \pi i$$

$$R_1^2 A_1 - \bar{R}_1^2 \bar{A}_1 + R_2^2 A_2 - \bar{R}_2^2 \bar{A}_2 = \frac{-S_{12} P_y - S_{16} P_x}{2 \pi i S_{22}}$$

$$A_1/R_1 - \bar{A}_1/\bar{R}_1 + A_2/R_2 - \bar{A}_2/\bar{R}_2 = \frac{S_{12} P_x + S_{26} P_y}{2 \pi i S_{22}}$$

The terms P_x and P_y are net load resultants on the internal boundary in the X and Y directions respectively.

Expressing the radial stress boundary conditions on the hole in terms of a Fourier series and equating the series representation of the solution, the unknown A_{1M} and A_{2M} coefficients are obtained (Reference 4). The resulting expansion can be written as:

$$A_{12} = a\pi i (1 + iR_2)/[16 (R_2 - R_1)]$$

$$A_{22} = -a\pi i (1 + iR_1)/[16 (R_2 - R_1)]$$

for $M = 4, 6, 8, \dots$

$$A_{1M} = A_{2M} = 0$$

for $M = 1, 3, 5, \dots$

$$A_{1M} = -a\pi i (-1)^{(M-1)/2} (2 + iMR_2)/[\pi M^2 (M^2 - 4) (R_2 - R_1)]$$

$$A_{2M} = a\pi i (-1)^{(M-1)/2} (2 + iMR_1)/[\pi M^2 (M^2 - 4) (R_2 - R_1)]$$

These equations give the complete elastic stress distribution in an infinite, two-dimensional, anisotropic material with a circular hole. These solutions are valid only for homogeneous media, but are assumed valid also for mid-plane symmetric laminates. Laminate strains are calculated using material compliance constitutive relations. Laminate compliance coefficients S_{jk} are derived using classical lamination plate theory with unidirectional material elastic constants, ply angular orientations, and ply thicknesses. Assuming that laminate strain remains constant through the thickness, strains for individual plies along lamina principal material axes are calculated using coordinate transformations. Stress distributions resulting from an arbitrary set of in-plane loads (bearing or bypass) are obtained using the principle of superposition (Figure 1).

To account for inelastic or nonlinear material behavior at the hole boundary, the "characteristic dimension" hypothesis of Whitney and Nuismer was adapted (Reference 5). Their hypothesis states that failure of a composite material with a stress concentration can be correlated with analytical predictions of point stresses at a characteristic dimension from the edge of a stress concentration (Figure 4).

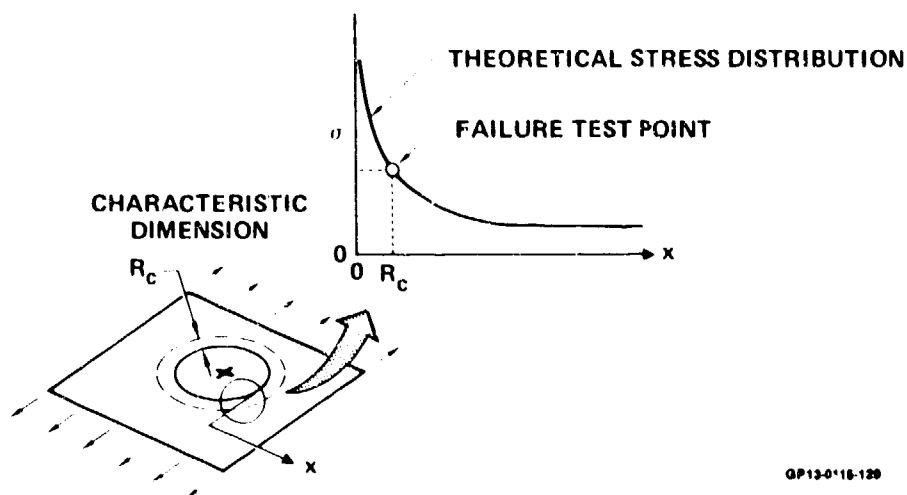


Figure 4. Characteristic Dimension Failure Hypothesis

The application of the characteristic dimension failure hypothesis was extended to permit strength predictions for anisotropic laminates under general in-plane loadings, without requiring extensive laminate test data. To do this, laminate failure is predicted by comparing elastic stress distributions with material failure criteria on a ply-by-ply basis at a characteristic dimension away from the hole boundary.

Various material failure criteria can be used with the characteristic dimension failure hypothesis. Interactive (Tsai-Hill, Hoffman, Tsai-Wu) and noninteractive (maximum stress, maximum strain) criteria were evaluated. Failure envelopes for each criteria for the same set of graphite-epoxy (AS/3501-6) material allowables ignoring matrix failure are illustrated in Figure 5.

Finite width effects have a significant influence on the circumferential stress distribution around a loaded fastener hole. A superposition of stress distributions from loaded and unloaded hole infinite plate solutions can be used to evaluate the effects of finite width (Reference 6). In the loaded hole

analysis, the bolt load, P , is reacted (at infinity) by tensile and compressive loads of $P/2$ (see Figure 6). By superimposing the solution for an unloaded hole under a remote tensile loading of $P/2$ (a stress of $P/2Wt$) the desired loading on the bolt and overall equilibrium is obtained. The resulting stress distribution gives a good approximation of the state of stress in a plate of finite width but differs from an exact solution in that the superimposed normal and shear stresses at the "edge" of the plate are nonzero.

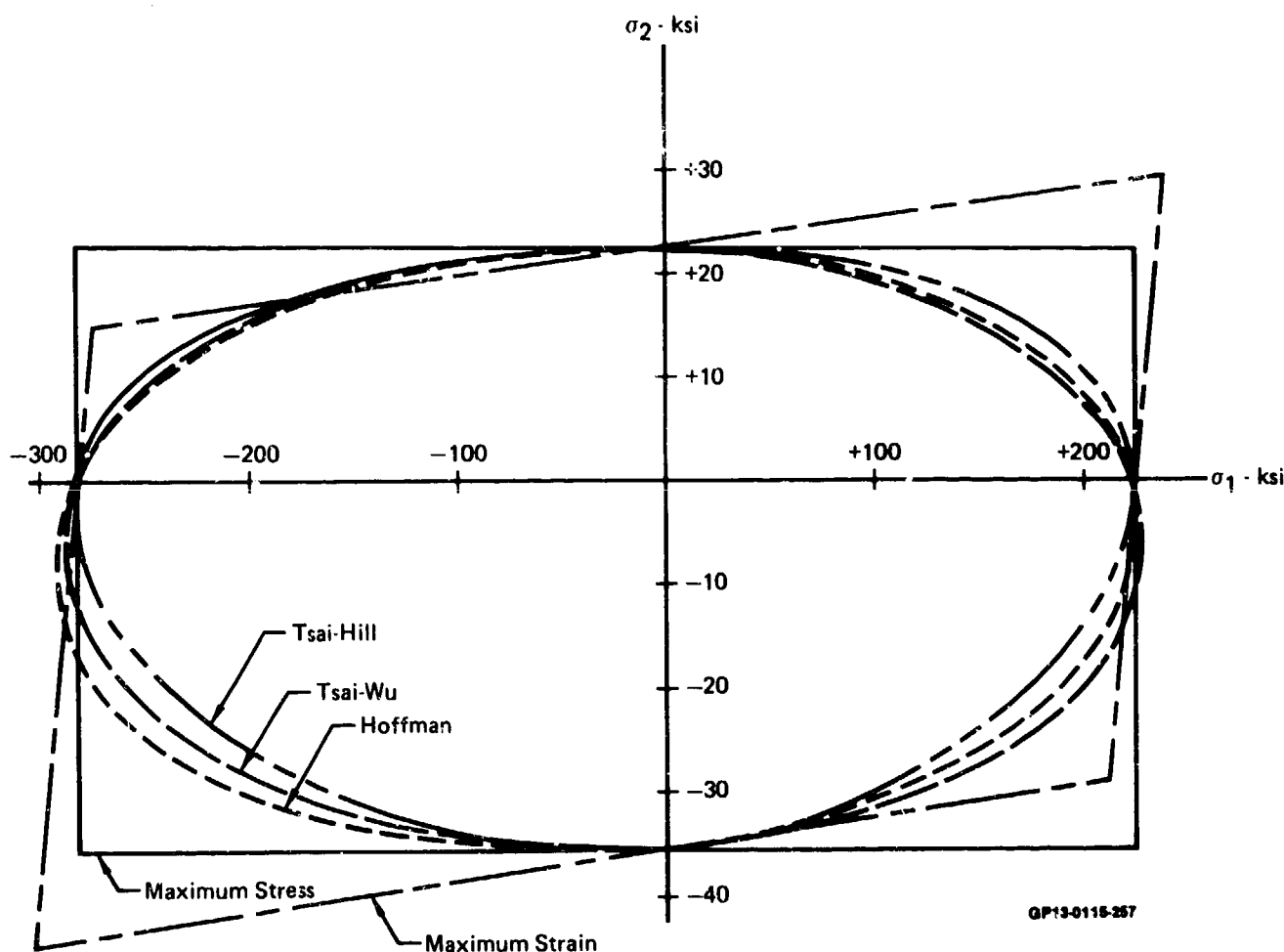
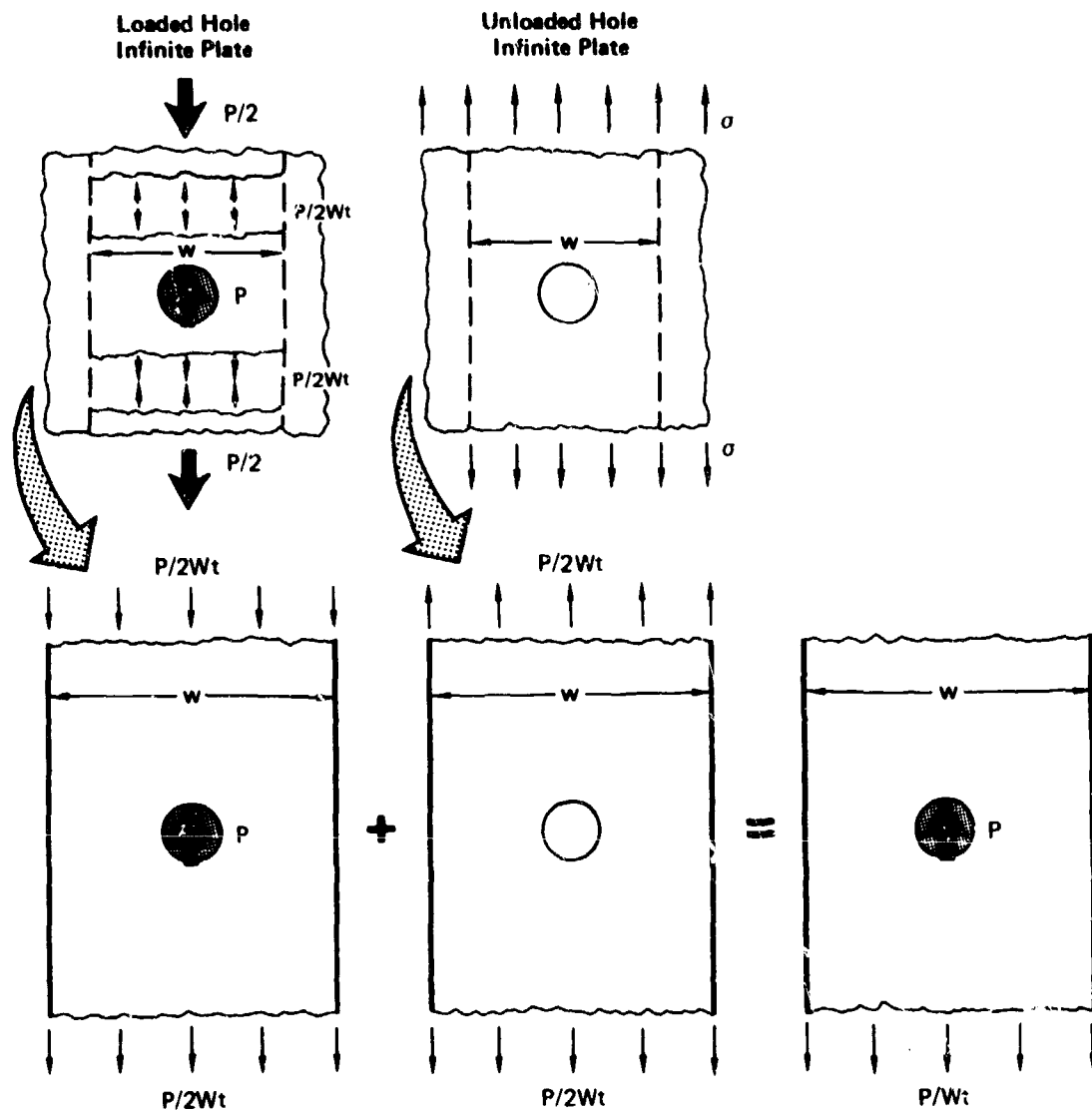


Figure 5. Failure Criteria Comparison



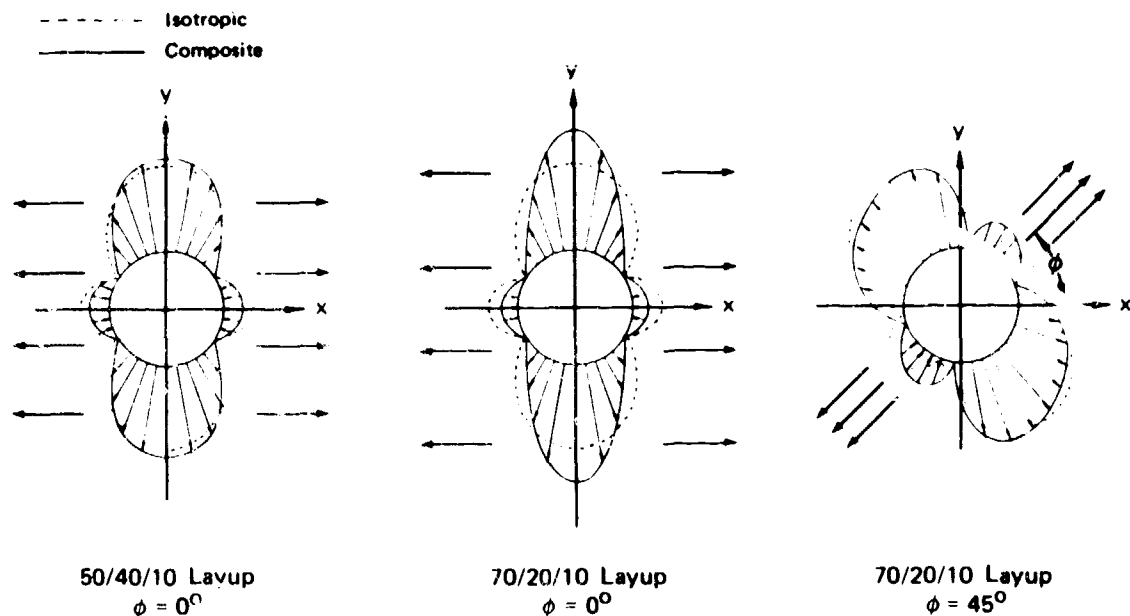
GP13-0115-128

Figure 6. Superposition of Solutions to Account for Finite Width

This methodology has been combined and incorporated into a computer program entitled BJSFM. Capabilities are programmed to handle material anisotropy, general in-plane loadings (tension, compression, biaxiality, shear, bearing), multi-material (hybrid) laminates, and arbitrary hole sizes. Only mechanical properties for the basic lamina (unidirectional ply) are required to obtain strength predictions. A detailed description of the computer program is given in Volume 3.

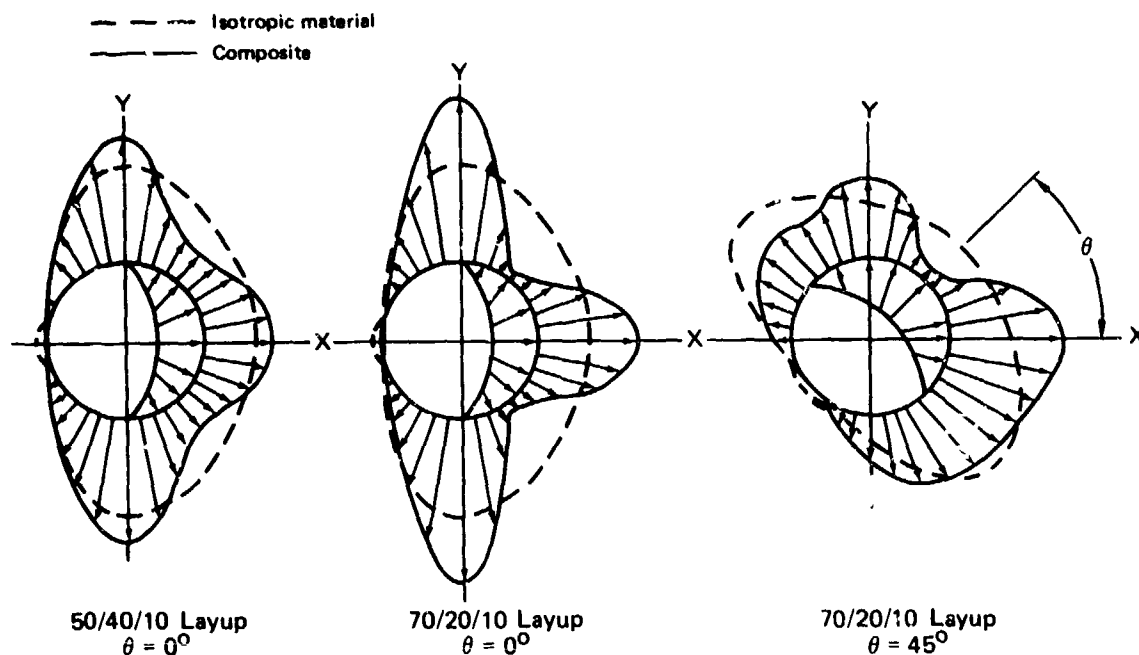
3. PREDICTIONS USING BJSFM APPROACH - Predictions made using the BJSFM are presented in this section to indicate the scope and flexibility of the developed methodology as well as indicate data and information pertinent to analysis of bolted joints in composite structures. The predictions shown are not intended to cover all laminates or loading combinations.

a. Effects of Anisotropy on Stress Distributions - Unlike isotropic materials, stress concentrations in composite materials are affected by layup and load orientation. Predicted circumferential stress plotted at an unloaded fastener hole boundary with uniaxial bypass loads indicates important differences between anisotropic composites and isotropic metals (Figure 7). Layup variations which change laminate stiffness properties affect hole boundary stress distributions and stress concentration factors; however, metal distributions are independent of their stiffness properties. Also, if loading shifts away from principal material axes, shear-extensional coupling creates biaxial states of stress in the laminate. Peak stresses no longer occur 90° to load directions and distributions shift. Loaded holes also show the same dependence on layup and load orientation (Figure 8). These complete stress distributions must be considered to determine failure load, mode and location of failure initiation of composite materials.



GP13-0115-03

Figure 7. Circumferential Stress Solutions at Unloaded Holes



GP13-0115-04

Figure 8. Circumferential Stress Solutions at Loaded Holes

b. Hole Size Effects - Hole size effects are also accounted for analytically. Stress gradients at the edge of the hole vary with hole size and laminate orientation. Smaller diameter holes produce steeper stress gradients which decay rapidly as the distance from the hole is increased (Figure 9). Applying a failure criterion at a constant distance from the hole boundary, hole size is accounted for due to the varying stress gradient with hole size.

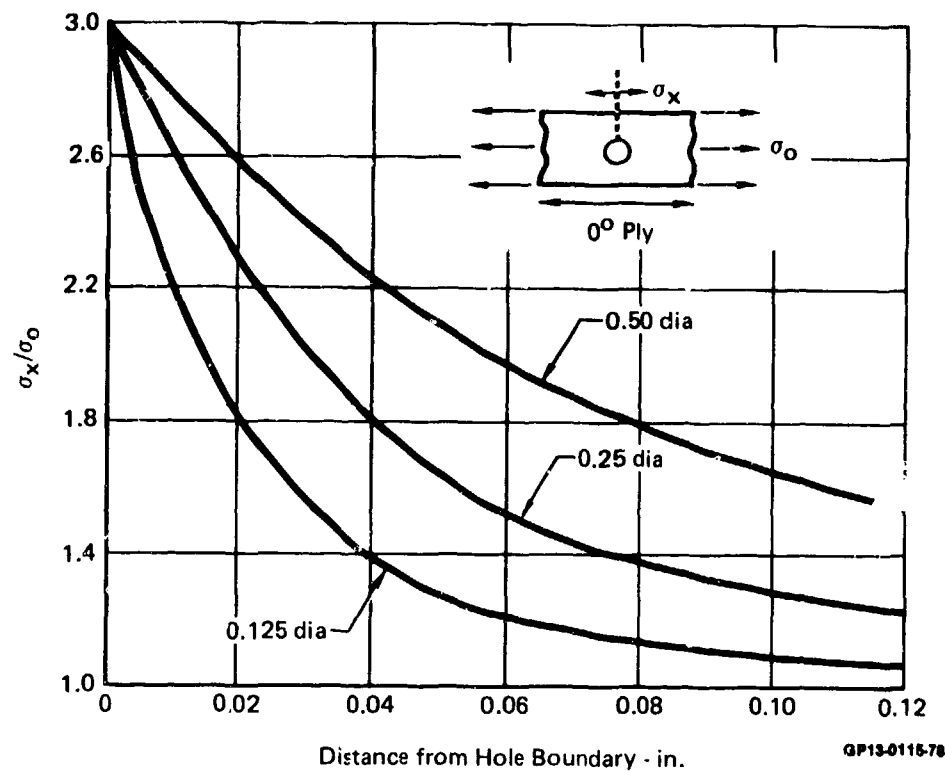


Figure 9. Effect of Hole Size on Stress Distributions

c. Finite Width Effects - To evaluate effects of finite geometry on stress solutions and establish limits on the accuracy of infinite plate solutions, a comparison of BJSFM solutions with finite element solutions was performed. Two example cases are illustrated: (1) a pure bearing specimen with a width-to-diameter ratio (W/D) of 8 and an edge-to-diameter ratio (e/D) of 9, and (2) a pure bearing specimen with a W/D of 6 and an e/D of 3. The results for the first case are presented in Figure 10. Circumferential stresses normalized to the average bolt bearing stress are plotted about the half-circle from directly in front of the neat-fit bolt (0°) to directly behind the bolt (180°). The dashed line indicates the infinite plate BJSFM solution, the solid line represents the BJSFM solution corrected using the DeJong finite-width approximation method, and the triangular symbols represent the finite element solution. Results shown in Figures 10 and 11 indicate that for an e/D of 9, the BJSFM solutions, corrected for finite width, correlate extremely well with finite element solutions where W/D ratios were greater than 4.

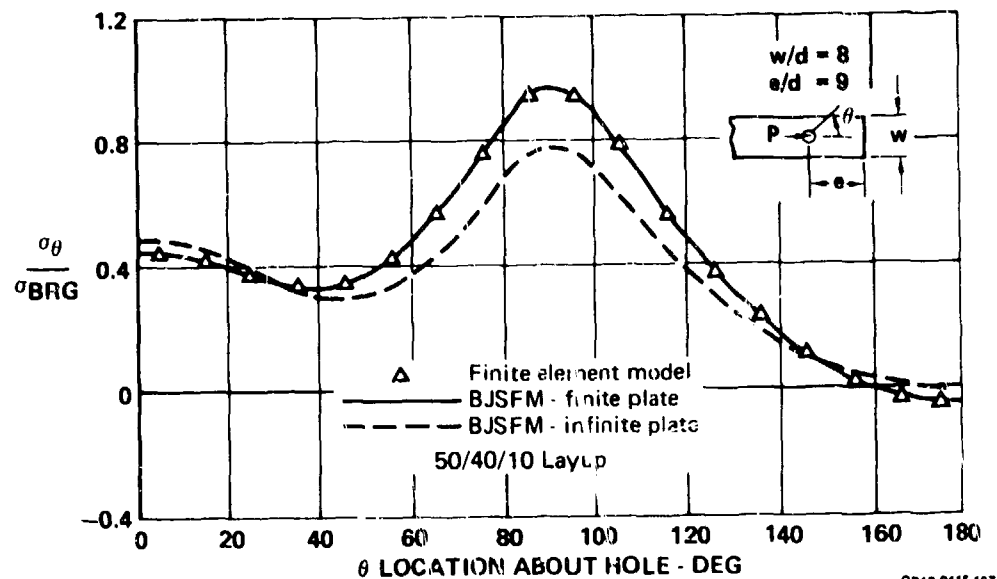


Figure 10. Correlation of Loaded Hole Analysis

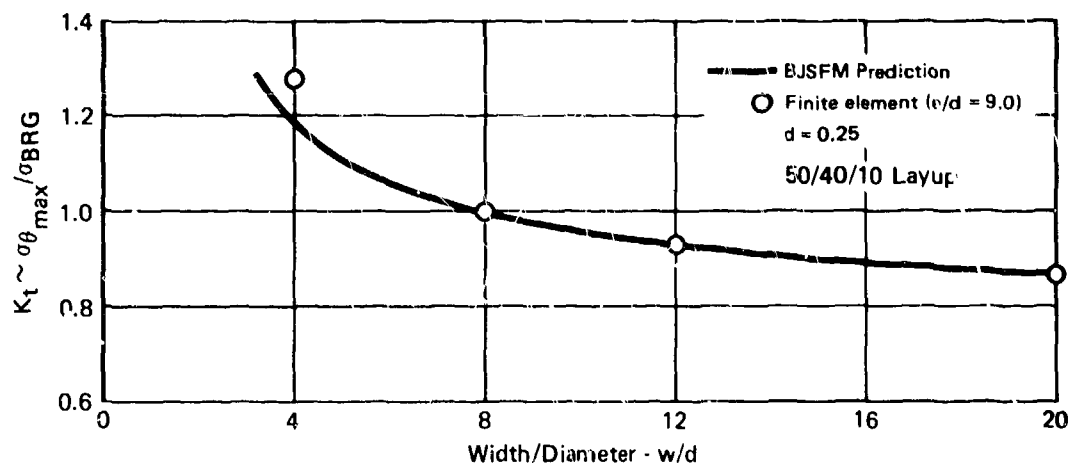


Figure 11. Effects of Width on Stress Concentrations

Sensitivity of solutions to small e/D ratios is illustrated in Figure 12 by results obtained for the second case. At an e/D value of 3, BJSFM infinite-plate solutions, approximately corrected for finite widths (long dash line), are significantly improved over the original BJSFM-infinite plate solution (short dash line), but still differ from the correct finite geometry solution (triangle symbol line).

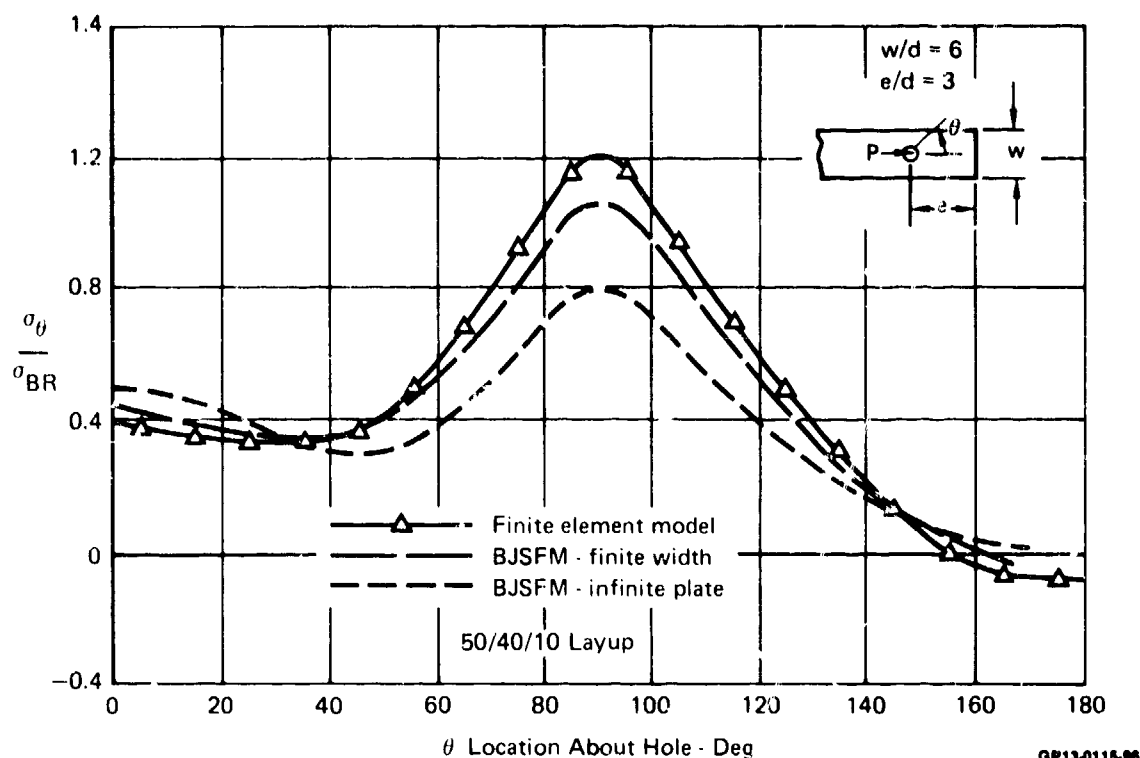
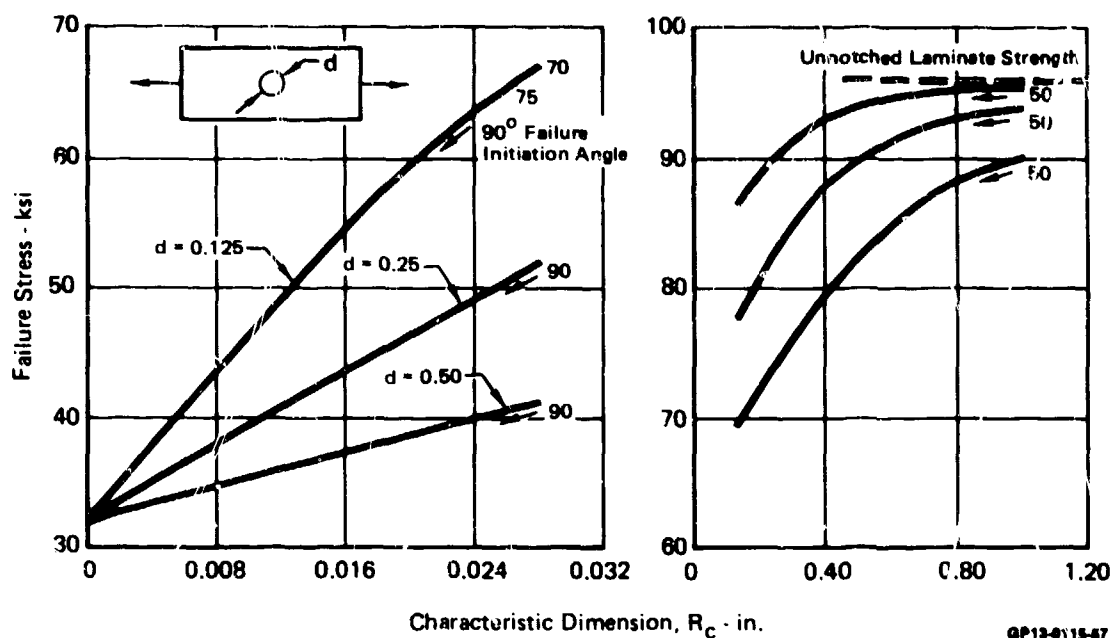


Figure 12. Correlation of Loaded Hole Analysis for Small Edge Distance Cases

d. Characteristic Dimension Sensitivity Study - Various laminate failure criteria can be used with the BJSFM procedure. To fully evaluate the characteristic dimension hypothesis, various correlative and parametric studies were performed. A sensitivity study was performed to determine the effect of various characteristic dimensions on laminate strength predictions. Loading configuration studies included unloaded and loaded fastener holes.

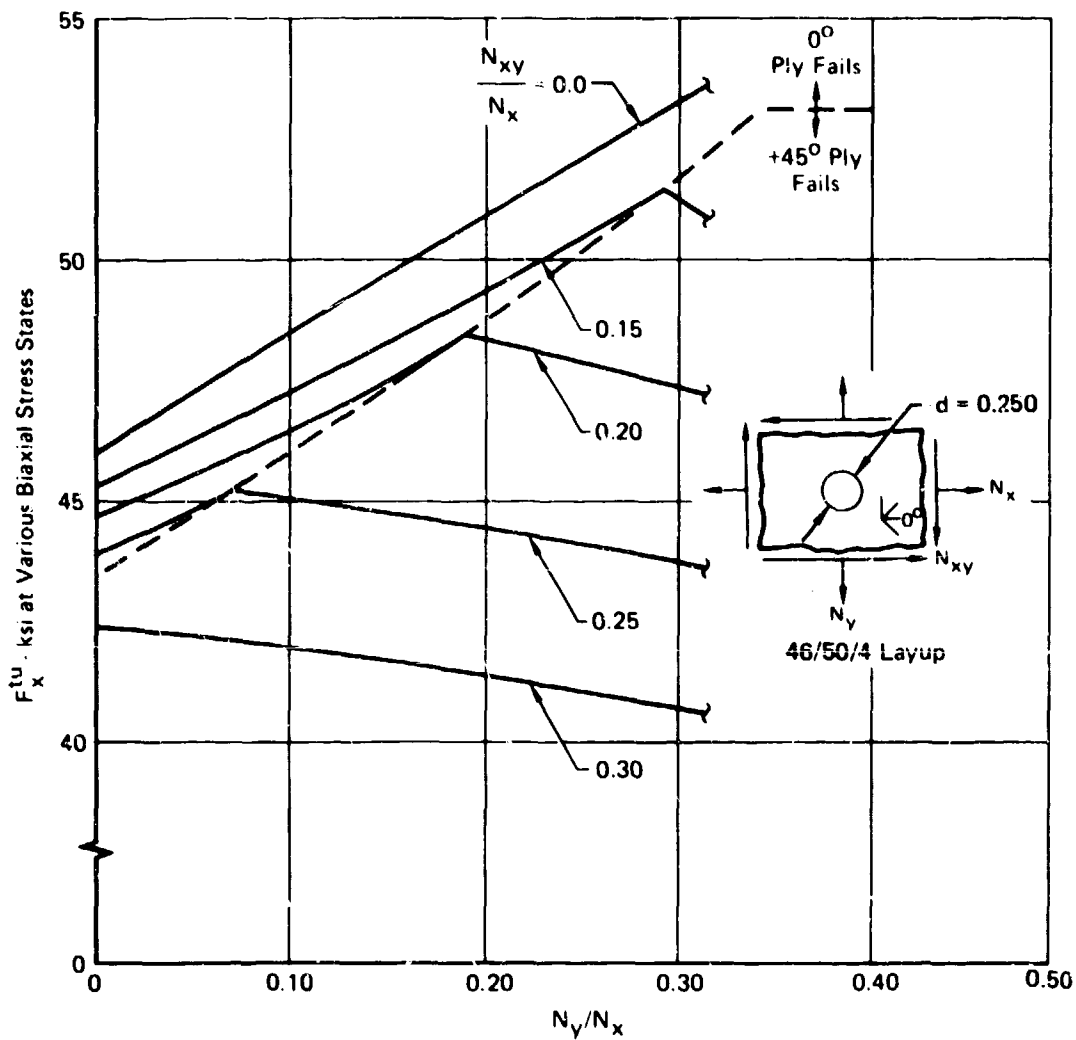
Results for a 30/60/10 layup of graphite/epoxy with unloaded hole sizes of .125, .25 and .50 inch are presented in Figure 13. The Tsai-Hill material failure criterion was used, with strengths predicted when first ply fiber or shear failure occurred. Each curve initiates from a common predicted failure stress level since the theoretical stress concentration at the hole boundary ($R_C = 0.0$) is independent of hole size. Due to stress gradients away from the hole boundary varying with hole size, predicted failure stress levels change with the characteristic dimension. The predicted failure stress curves each asymptotically approach the predicted unnotched laminate strength with an increasing characteristic dimension. These curves indicate that a 10% change in the characteristic dimension yields a maximum 4% change in predicted laminate failure stress for the .125 inch diameter hole and a maximum 2% change for the .50 inch diameter hole. Also, as characteristic dimension changes occur, failure initiation angle predictions change, as indicated in Figure 13.



Figures 13. Effect of Characteristic Dimension on Predicted Strength
30/60/10 Layup

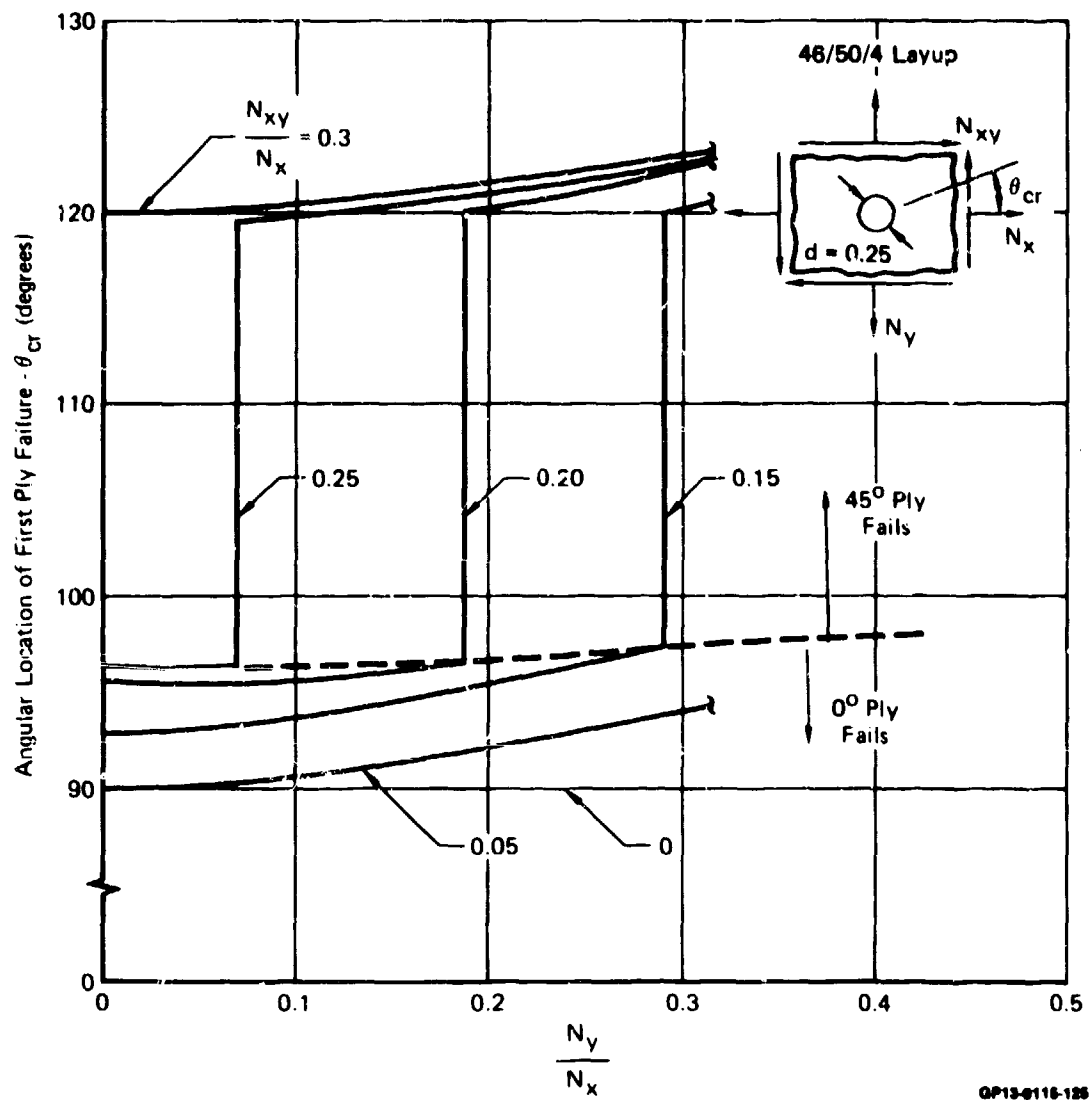
e. Biaxial Loading Effects - To demonstrate the utility of the Bolted Joint Stress Field Model, a parametric analysis was performed to predict interactive effects of biaxial loads on laminates with unloaded fastener holes. Laminate strength, failure location and critical plies were predicted for a representative composite wing skin laminate.

Figure 14 presents predicted failure stress and indicates changes in failure modes as biaxial load ratios increase. Load ratios of increasing (N_y/N_x) for this tension-tension case provide relief at the fastener hole and laminate strength increases. Increasing shear load ratios (N_{xy}/N_x), however, intensify stress concentration effects at the fastener hole; laminate strength decreases and failure modes change from 0° plies to 45° plies. Figure 15 presents the predicted location at the fastener hole boundary of first ply failure. Significant is the indication that at certain biaxial load ratios, a wide arc of the hole boundary may become critical. Figure 16 presents strain concentration factors for critical plies within the laminate with respect to the strain developed under N_x alone.



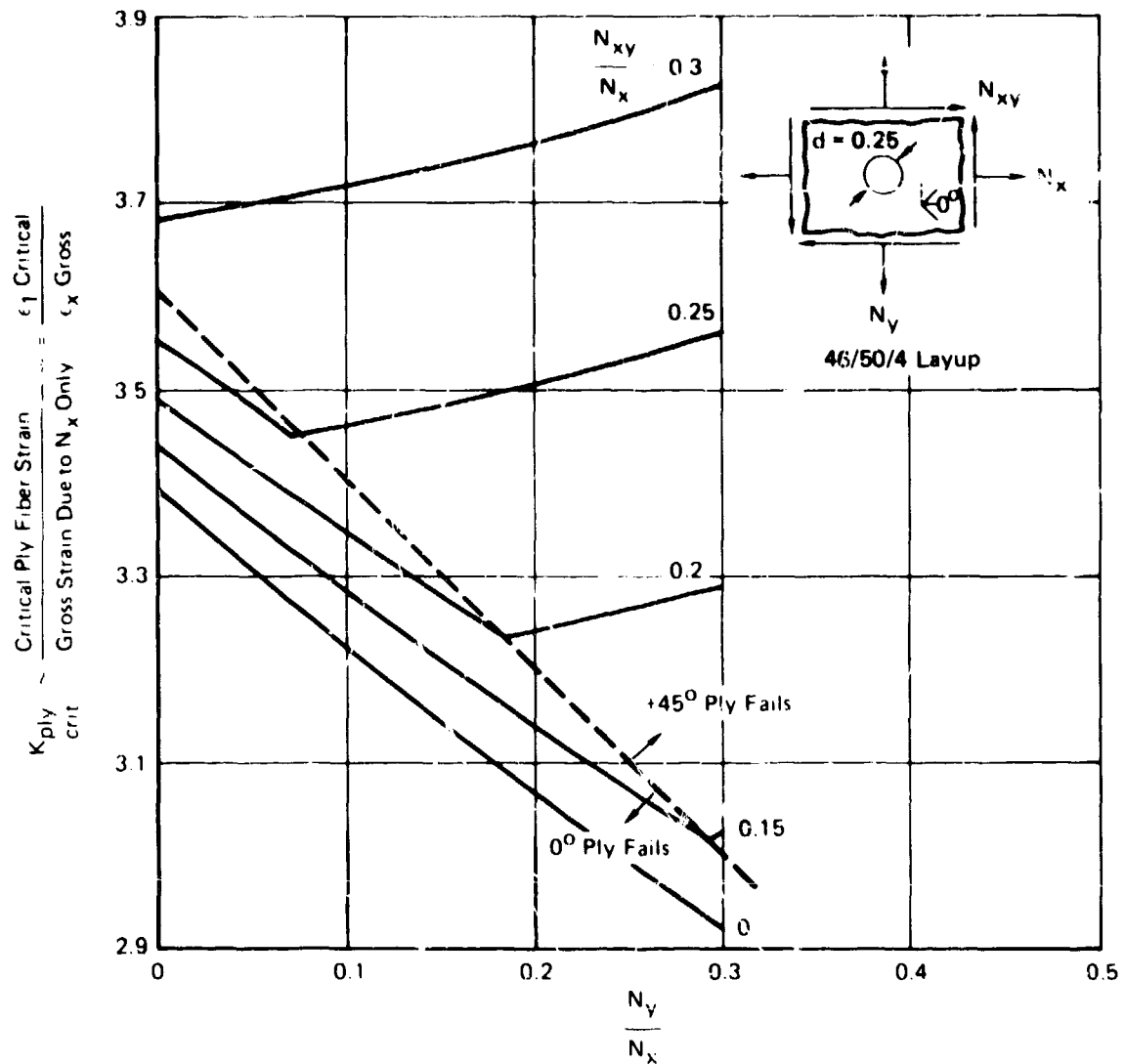
GP13-0118-128

Figure 14. Effect of Biaxial Loading on Predicted Strength



QP13-0116-125

Figure 15. Effect of Biaxial Loading on Failure Location



GP13-0118-27

Figure 16. Effect of Biaxial Loading on Ply Strain Concentrations

Experimental and analytic studies have indicated that failure locations at fastener hole boundaries shift depending on layup and biaxial stress states. The BJSFM methodology accounts for this phenomenon and, further, reveals the critical ply at the failure location. Data shown in Figures 14, 15 and 16 show that failure analysis must account for all locations around the fastener hole, since the critical area is layup and loading dependent. This is best indicated by Figure 15 which shows not only continuous shifts with biaxial loading, but also indicates wide arcs of the hole perimeter may become equally sensitive to failure. This indicates the potential errors which can arise by using methods which predict laminate failure by referencing unnotched laminate strength data at "preselected" or "representative" locations on the hole boundary.

f. Pure Bearing Strength Study - Strength envelopes are predicted based on ply-by-ply analysis to determine critical plies and failure initiation location. The results of a ply-by-ply evaluation of strength based on first ply fiber rupture for the 50/40/10 layup under pure bearing loads is presented in Figure 17. The ply strength envelopes predict initial failure in 90° plies for all load directions with relatively constant laminate strength up to a load angle of 25° and a gradual decrease from 25° to 90°. This predicts that while unloaded holes show a pronounced sensitivity to off-axis, bypass loading, bearing strengths for this laminate are relatively unaffected by off-axis loadings. Analytically, this behavior is a direct result of the differences in local stress distributions resulting from the two loading conditions.

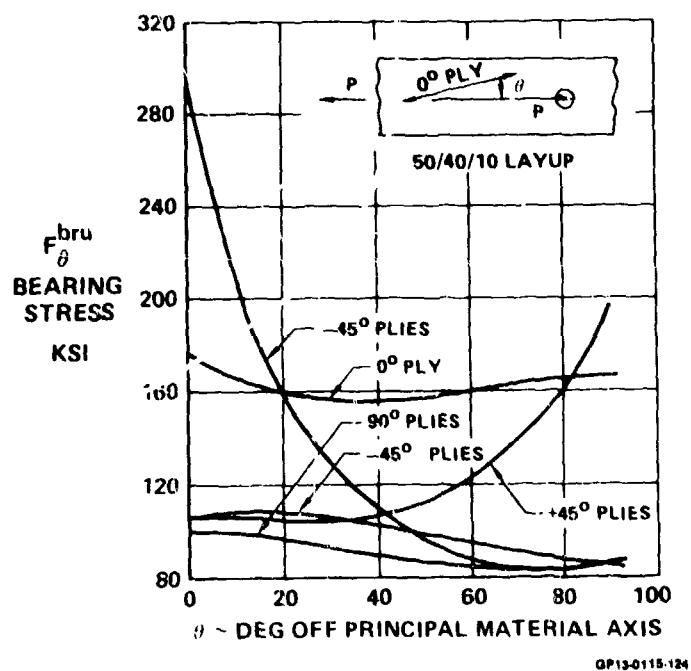


Figure 17. Effect of Bearing Load Direction on Predicted Strength

g. Effects of Environment - Effects of environment on laminate strength can also be accounted for with the BJSFM analysis. Unidirectional material properties (stiffness and strength), as affected by an environment, are used to redefine laminate behavior. Bearing versus bypass failure envelopes were predicted for a 50/40/10 layup at room temperature dry and at elevated temperature with moisture. For this layup, results indicate that little change in predicted strength occurs for high bypass loads associated with fiber dominated modes of failure which are usually not adversely affected by temperature and moisture (Figure 18). However, elevated temperature and moisture do affect matrix properties resulting primarily in lower shear modulus, shear strength and lower compression strength. The lower shear stiffness causes a redistribution of high bearing stresses to the stiffer 45° plies in compression. This, coupled with decreased compression strength, results in fiber compression failures at lower bearing stresses than corresponding RTD properties (Figure 18). Although the failures for this layup initiate in the same vicinity around the hole, different phenomena cause the failures due to changes in material mechanical properties with temperature and moisture.

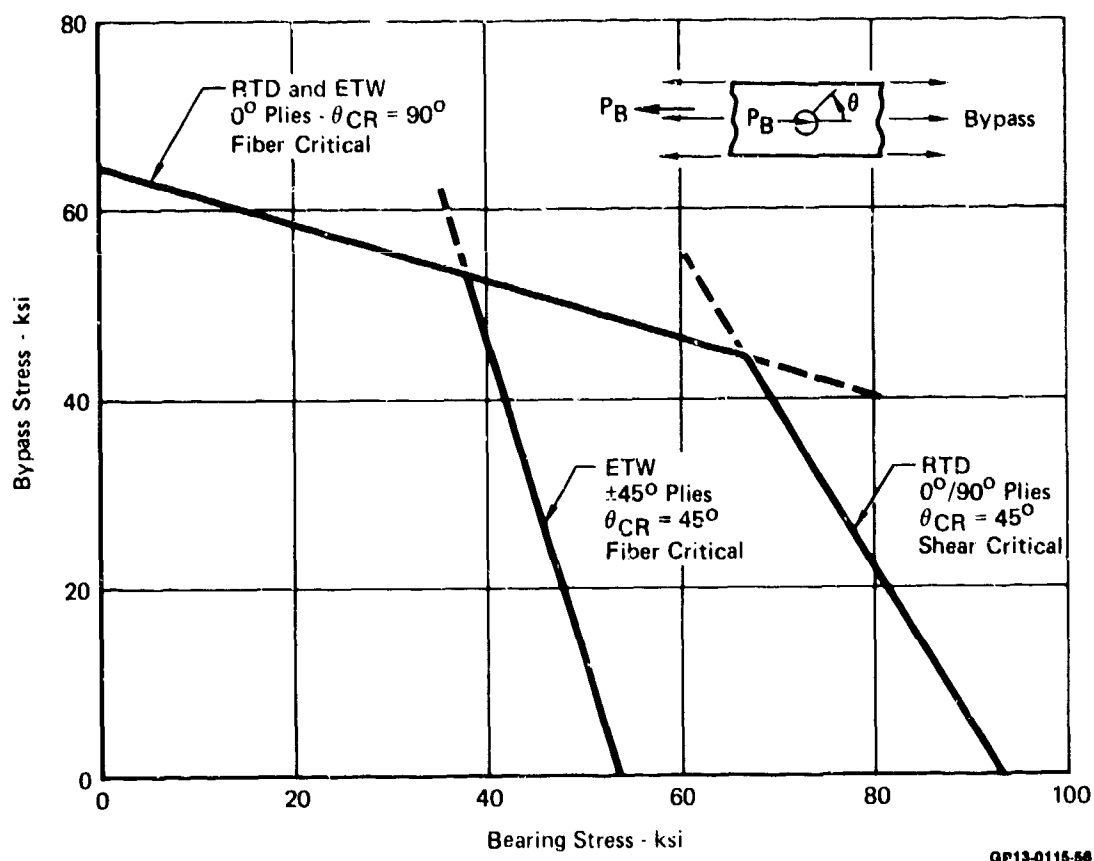


Figure 18. Effect of Moisture and Temperature on Laminate Strength

SECTION IV

TEST DATA EVALUATION




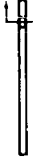
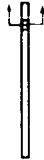


1. METHODOLOGY VERIFICATION: EVALUATION OF JOINT DESIGN VARIABLES - TASK 2 - The primary objective of the Task 2 experimental program was to verify developed methodology through strength tests over a range of bolted composite joint design variables. Test data were also used to provide direction for development of further improvements in the methodology. The Task 2 Test Matrix is presented in Figure 19.

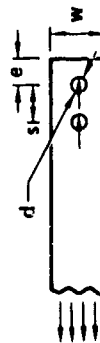
The selection of test variables was guided by information gathered under the Task 1 - Literature Survey. Data obtained from earlier MCAIR in-house test programs were identified under this survey (Reference 1). MCAIR test programs outlined in Figures 20 and 21 were used to supplement the Task 2 experimental data. Ten different layups of the 0°, +45°, and 90° family of ply orientations were tested under tension and compression loadings. Effects of hole size, thickness, countersinking, edge and width distances, and joint eccentricity (single versus double shear) on the strength of laminates with a single loaded or unloaded fastener hole were evaluated. Specimen configurations for unloaded fastener hole and pure bearing evaluations are detailed in Figures 22 and 23.

These MCAIR data provided an initial basis for the effects of layup variations on laminate strength for the two bounds of bolted composite joint load-transfer, i.e., zero bolt bearing (100 percent bypass stress) and total load transfer through a single fastener (pure bearing). The availability of these data permitted early verification of developed methodology, reduced the scope of layup variations to be tested, and permitted Task 2 experimental efforts to include a more comprehensive range of other bolted composite joint design variables.

a. Task 2 Test Plan - The effects of 12 design variables on joint strength were evaluated. Tests were performed at three environmental conditions: room temperature dry (RTD), room temperature wet (RTW), and elevated temperature wet (ETW). Environmental conditions were selected to be realistic with respect to deployment profiles for multi-mission, high-performance supersonic aircraft. Tests were conducted at an elevated temperature of 250°F and, when applicable, specimens were conditioned to an equilibrium moisture content of approximately 0.8 percent by weight. All specimens tested at 250°F were held at temperature 10 minutes before testing. Specimens were loaded in tension or compression to failure. In general, a replication of four tests were performed at each test condition.

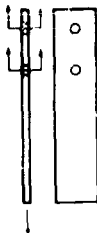
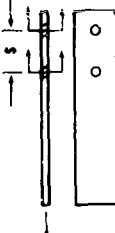
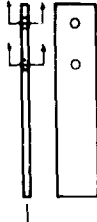
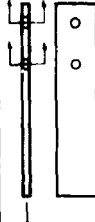

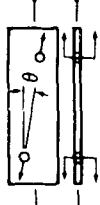
Hercules AS/3501-6 Type II (ten mil thick) graphite-epoxy was used as the principal material for fabrication of test specimens. Limited testing was performed using NARMCO T300/5208 graphite-epoxy.

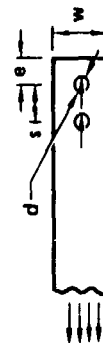
JOINT DESIGN VARIABLE	TEST SPECIMEN	CONFIGURATION		RTD		RTW		ETW		TOTAL TESTS
		LAYUP	VARIATION	TEN.	COM	TEN.	COM	TEN.	CGM	
1 FASTENER TORQUE	TYPE I 	1,2,3	0 IN.-LB	✓,+,+				✓		34
		1,2,3	25	✓,+,+				✓		
		1,2,3	50	✓,+,+				✓		
		1,2,3	75	✓,+,+				✓		
2 STACKING SEQUENCE	TYPE II 	1,2,3	0 IN.-LB	✓,+,+				✓		34
		1,2,3	25	✓,+,+				✓		
		1,2,3	50	✓,+,+				✓		
		1,2,3	75	✓,+,+				✓		
3 SINGLE SHEAR	TYPE I 	1	LAYUP NO. 6	✓	✓			✓		48
		1	LAYUP NO. 7	✓	✓			✓		
		1	LAYUP NO. 8	✓	✓			✓		
		1	LAYUP NO. 9	✓	✓			✓		
4 THICKNESS	TYPE I 	1	Δ	✓				✓		24
		1	$e/d = 2.0$	✓				✓		
		1	$w/d = 4.0$	✓				✓		
		1	$d = 0.375$	✓				✓		
5 COUNTERSUNK FASTENERS	TYPE I 	1	$t_1 = 0.416$	✓	✓			✓		32
		1	$t_2 = 0.524$	✓	✓			✓		
		1	$(h/t)_1 = 0.77$	✓	✓			✓		
		1	$(h/t)_2 = 0.38$	✓	✓			✓		
6 LOAD ORIENTATION (OFF-AXIS LOADS, BEARING AND BYPASS ALIGN)	TYPE I 	1	$(h/t)_3 = 0.26$	✓	✓			✓		20
		1	$(h/t)_1 \& T_i$	✓	✓			✓		
		1	$(h/t)_1 \& A_i$	✓	✓			✓		
		1	$\theta_1 = 10^\circ$	✓	✓			✓		
7 LOAD ORIENTATION (OFF-AXIS LOADS, BEARING AND BYPASS ALIGN)	TYPE I 	1	$\theta_2 = 22.5^\circ$	✓	✓			✓		48
		1	$\theta_3 = 45^\circ$	✓	✓			✓		
		1	$\theta_4 = 90^\circ$	✓	✓			✓		
		1		✓	✓			✓		
SUBTOTAL										264



GP13-0116-122

Figure 19. Task 2 - Joint Design Variables Test Matrix

JOINT DESIGN VARIABLE	TEST SPECIMEN	CONFIGURATION		RTD		RTW		ETW		TOTAL TESTS
		LAYUP	VARIATION	TEN	COM	TEN	COM	TEN	COM	
7 HOLE SIZE	TYPE II 	1	$d_1 = 0.1875$	✓						12
		1	$d_2 = 0.375$	✓						
		1	$d_3 = 0.500$	✓						
8 EDGE DISTANCE	TYPE II 	1	$(e/d)_1 = 1.5$	✓				✓		40
		1	$(e/d)_2 = 2.0$	✓				✓		
		1	$(e/d)_3 = 4.0$	✓				✓		
		1	$s_1 = 2d$	✓				✓		
		1	$s_2 = 3d$	✓				✓		
9 WIDTH	TYPE II 	1	$(w/d)_1 = 4.0$	✓				✓		24
		1	$(w/d)_2 = 5.0$	✓				✓		
		1	$(w/d)_3 = 8.0$	✓				✓		
10 LAYUP	TYPE II 	1	(BASELINE)	✓	✓	✓		✓	✓	56
		2		✓	✓			✓	✓	
		3		✓	✓			✓	✓	
11 FASTENER PATTERNS	TYPE IV 	1		✓	•	•		✓	✓	68
		3		✓	•	•		✓	✓	
		1		✓				✓	✓	
		1		✓				✓	✓	
12 LOAD INTERACTION (BYPASS AND BEARING NONALIGNED)	TYPE III 	1	$\theta = 0^\circ$	✓						22
		3	$\theta = 0^\circ$	✓						
		1	$\theta_1 = 10^\circ$	✓	✓					
		1	$\theta_2 = 22.5^\circ$	✓						
		1	$\theta_3 = 45^\circ$	✓						
TOTAL										478



- 4 tests, T300/5208 Graphite/Epoxy
- ▲ 4 tests after exposure to salt water environment, AS/3501-6

GP-13-9118-123

Figure 19. (Continued) Task 2 - Joint Design Variables-Test Matrix

Laminate Group	% Layers of			No. Pies	Hole Dia.				Loadin.		No. of Tests
	0°	±45°	90°		0.0	0.125	0.250	0.500	Ten.	Com.	
A	70	20	10	40	✓	✓	✓	✓	✓	✓	24
B	50	40	10	40	✓	✓	✓	✓	✓	✓	24
	↓	↓	↓	80		✓	✓	✓	✓	✓	18
				120		✓	✓	✓	✓	✓	18
C	30	60	10	40	✓	✓	✓	✓	✓	✓	24
											108
D	50	10	40	40	✓		✓		✓	✓	12
E	40	20	40	40	✓		✓		✓	✓	12
F	40	50	10	40	✓		✓		✓	✓	12
G	30	30	40	40	✓		✓		✓	✓	12
H	20	40	40	40	✓		✓		✓	✓	12
I	20	70	10	40	✓		✓		✓	✓	12
J	10	80	10	40	✓		✓		✓	✓	12
											84
A	70	20	10	40			X		X	X	6
B	50	40	10	40			X		X	X	6
	↓	↓	↓	80			X		X	X	6
				120			X		X	X	6
C	30	60	10	40			X		X	X	6
											30
Total No. Tests											222

✓ Noncountersunk Specimens

X Countersunk Specimens

GP13-0115-00

Figure 20. MCAIR Evaluation of Unloaded Hole Specimens - Test Matrix

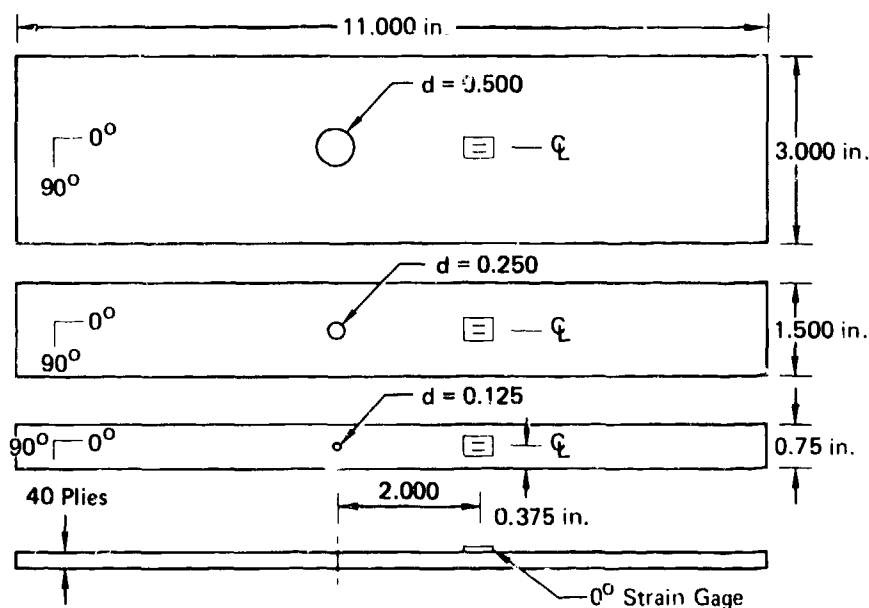
Phase No.	Layup No.	% Layers			No. Plies	Hole Dia					e/d					w/d			Single Shear	Double Shear	Total Specimens
		0°	±45°	90°		0	0.250	0.375	0.500	0.250*	1.5	2.0	2.5	3.0	4.0	4	6	8			
I	1	70	20	10	20	◇	✓	✓	✓	*	✓	✓	✓	✓	✓	✓	✓	✓	✓	-	87
II	2	50	10	40	20	◇	✓	-	-	-	-	✓	-	✓	-	-	✓	-	✓	-	9
I	3	50	40	10	20	◇	✓	✓	✓	*	✓	✓	✓	✓	✓	✓	✓	✓	✓	△	86
II	4	40	20	40	20	-	✓	-	-	-	-	✓	-	✓	-	-	✓	-	✓	-	6
II	5	40	40	20	20	-	✓	-	-	-	-	✓	-	✓	-	-	✓	-	✓	-	6
II	6	30	20	50	20	-	✓	-	-	-	-	✓	-	✓	-	-	✓	-	✓	-	6
I	7	30	60	10	20	◇	✓	✓	✓	*	✓	✓	✓	✓	✓	✓	✓	✓	✓	-	87
II	8	20	40	40	20	-	✓	-	-	-	-	✓	-	✓	-	-	✓	-	✓	-	6
II	9	20	60	20	20	-	✓	-	-	-	-	✓	-	✓	-	-	✓	-	✓	-	6
II	10	10	80	10	20	-	✓	-	-	-	-	✓	-	✓	-	-	✓	-	✓	-	6
II	11	55	40	5	20	◇	✓	-	-	-	-	✓	✓	✓	-	-	✓	-	✓	-	15
-	-	-	-	-	-	15	92	103	72	36	-	-	-	-	-	-	-	-	-	Total	323

Each test replication of 3

GP13-0115-121

- * Countersink
- ◇ Baseline
- △ Two specimens in double shear

Figure 21. MCAIR Evaluation of Loaded Hole Specimens Test Matrix



GP13-0115-120

Figure 22. Unloaded Hole Specimen Geometry

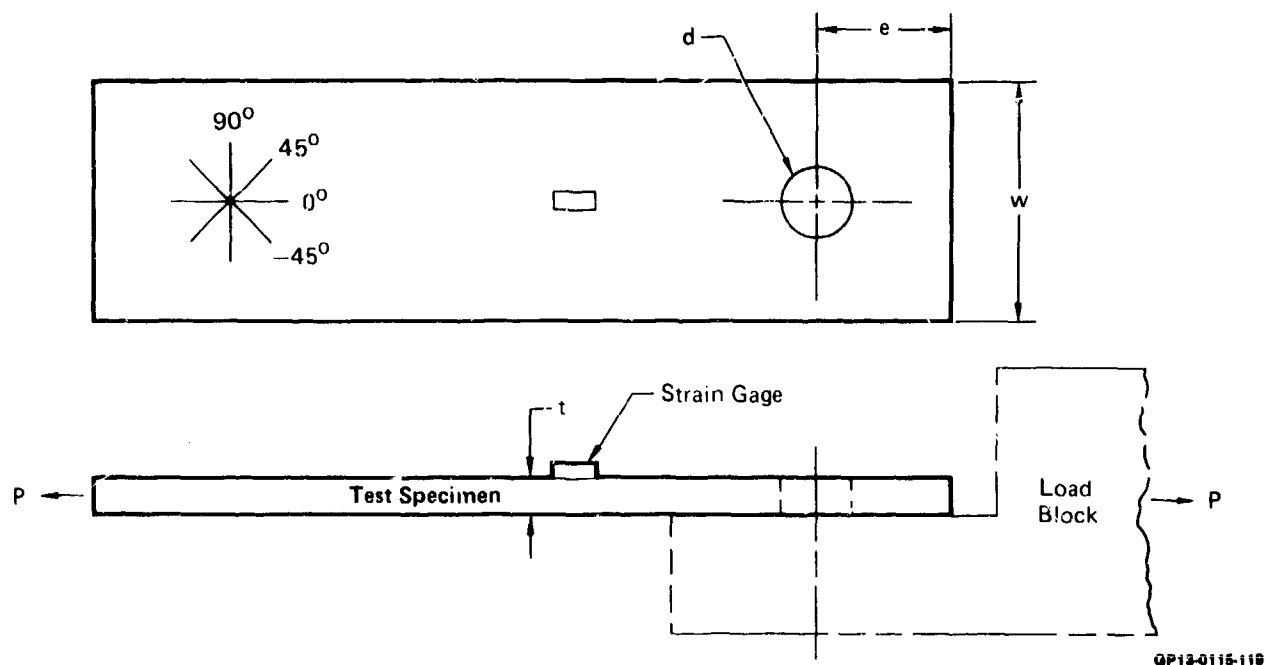


Figure 23. Loaded Hole Specimen Configuration

Four test specimen configurations were used: (1) a single-bolt pure bearing specimen, (2) a baseline two-bolt-in-tandem bearing-bypass specimen, (3) a two-bolt load interaction specimen and (4) a four-bolt fastener pattern specimen. Both single and two-bolt-in-tandem specimens were loaded in either a single-shear or double-shear configuration (Figure 24). All specimens were strain gaged. Recorded data included: failure load and strain, continuous load versus strain plots to failure, selected load versus deflection plots to failure, thickness, width, hole diameter measurements, weight gain of humidity exposure specimens, and selective photographic documentation of failed specimens.

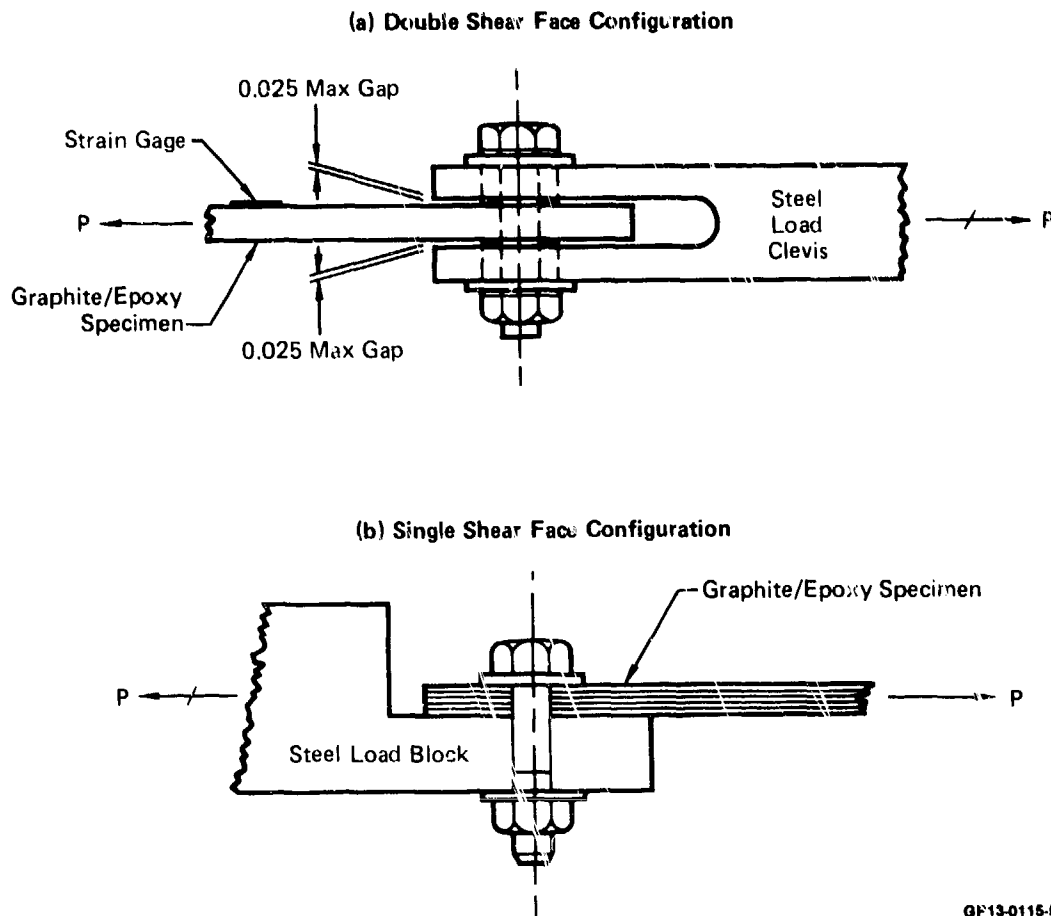


Figure 24. Specimen Loading Configurations

Prior to specification of load-clevis geometry (thickness, width, and material), a parametric study was performed to evaluate the effect of clevis-to-laminate stiffness ratios on load distributions for the baseline two-bolt-in-tandem joint. The objective was to quantify the errors in load distribution which could arise due to material stiffness variability. This would, in turn, provide a theoretical data base to aid in selection of load-clevis geometries and material. The results of this study are presented in Figure 25. Based on these results, a load clevis-to-laminate stiffness ratio of 10 or more was selected. This choice results in unequal bolt loads, but guarantees that no distribution error greater than 0.5 percent should occur due to laminate stiffness variations expected from specimen to specimen.

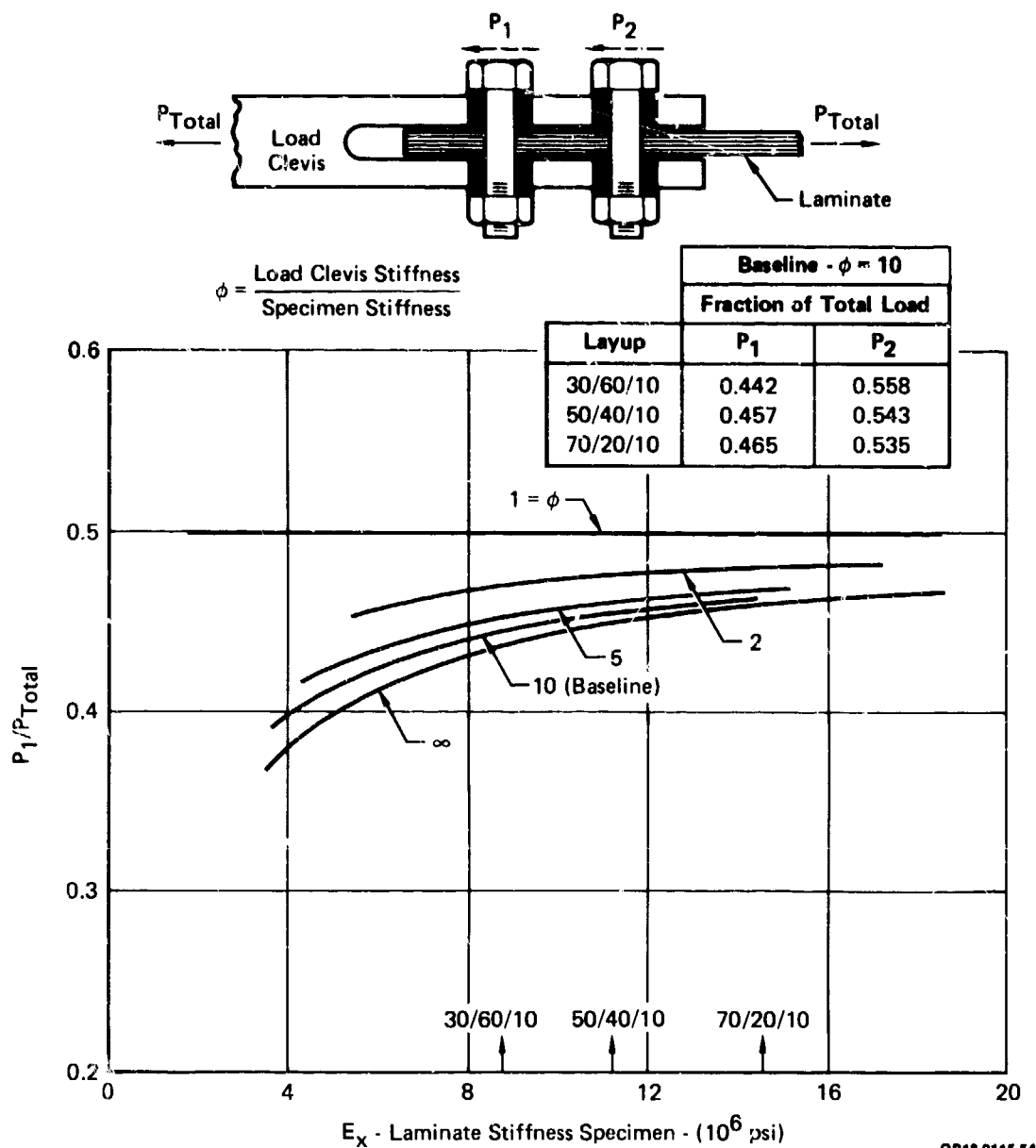


Figure 25. Effect of Laminate Stiffness on Specimen Bolt-Load Distributions

Individual test specimens were fabricated from 19 panels. Stacking sequences are detailed in Figure 26. Panels were cut, collated, and cured per standard MCAIR process specification. All specimens were tested to static failure according to Figure 19 under tensile or compressive loadings. Complete details of all procedures, test results and support requirements are contained in Volume 2 of this report.

PLY NUMBER (TO CENTERLINE)	LAYOUT NUMBER AND PLY ORIENTATION									
	1	2	3	4	5	6	7	8	9	10
1	+	+	+	+	+	+	+	+	+	+
2	0	0	0	0	0	0	0	0	0	0
3	-	-	-	-	-	-	-	-	-	-
4	0	0	0	0	0	0	0	0	0	0
5	90	0	+	90	90	+	90	0	0	0
6	0	0	90	0	0	90	0	0	0	0
7	+	90	-	+	+	-	0	+	0	+
8	0	0	0	0	0	0	0	-	+	90
9	-	0	+	-	-	0	0	0	-	-
10	0	0	-	0	0	0	0	0	90	90
11				+	+					
12				0	0					
13				-	-					
14				0	0					
15				90	90					
16				0	0					
17				+	+					
18				0	0					
19				-	-					
20				0	0					
21					+					
22					0					
23					-					
24					0					
25					90					
26					0					
27					+					
28					0					
29					-					
30					0					
NO. OF PLYS	20	20	20	40	60	20	20	20	20	20
PERCENT OF OP/45°/90°	50/40/10	70/20/10	30/60/10	50/40/10	50/40/10	50/40/10	50/40/10	50/40/10	50/40/10	10/40/50

GP13-6-18-53

- Notes:
1. "+" and "-" refers to 45° ply orientation
 2. Nominal ply thickness is 0.0104 in.
 3. Layouts are all symmetric about centerline

Figure 26. Task 2 - Layout Number and Stacking Sequence

b. Correlation of BJSFM Predictions With Experimental Results and Evaluations - This section compares experimental results obtained under Task 2 and predictions using the BJSFM. Where BJSFM/test correlation was not possible, data trends are discussed. Unless specifically labeled as predictions, lines on graphs are only indicators of data trends.

(1) Strength of Laminates With Unloaded and Unfilled Holes - The test plan of Figure 20 provided data for an initial verification of the BJSFM procedure for the case of an unloaded fastener hole. Using the BJSFM procedure, strength predictions were made for all test layups and test conditions. Laminate elastic properties were calculated using unidirectional ply lamina elastic constants. Laminate failure was assumed to occur when first ply fiber or shear failure was predicted, based on the Tsai-Hill or maximum strain material failure criterion applied at a characteristic dimension away from the hole. Only lamina strength and stiffness data were required for this analysis; these data are shown in Figure 27. RTD data are average values obtained from MCAIR tests performed on unnotched unidirectional laminate sandwich beams, and 0°/90° rail-shear specimens; RTW and ETW data are estimated.

Properties	Room Temperature	RT Wet (Estimated)**	250°F Wet (Estimated)**
Elastic Constants			
• E_1^t (10^6 psi)	18.85	18.85	18.54
• E_1^c (10^6 psi)	18.20	18.20	17.80
• E_2 (10^6 psi)	1.90	1.72	1.27
• G_{12} (10^6 psi)	0.85	0.77	0.60
• ν_{12}	0.30	0.30	0.30
Allowables			
• ϵ_1^{tu} ($\mu\text{in./in.}$)	12,206	12,206	12,735
• ϵ_1^{cu} ($\mu\text{in./in.}$)	17,630	12,694	8,286
• ϵ_2^{tu} ($\mu\text{in./in.}$)	5,380	—	—
• ϵ_2^{cu} ($\mu\text{in./in.}$)	29,080	—	—
• γ_{12} ($\mu\text{in./in.}$) *	20,352	22,470	18,461
• F_1^{tu} (ksi)	230	230	236
• F_1^{cu} (ksi)	321	231	151
• F_2^{tu} (ksi)	9.50	—	—
• F_2^{cu} (ksi)	38.90	35.20	26.00
• F_{12} (ksi)	17.30	17.30	11.00

*Based on linear-elastic behavior

GP13-0116-118

**Approximately 0.86% moisture

Figure 27. AS/3501-6 Lamina Mechanical Properties

Correlation of predicted tensile strength with test data from ten layups is shown in Figure 28. Correlation of predicted effects of hole size on laminate tensile strength with test data is shown in Figure 29. For the AS/3501-6 material system, a characteristic dimension (R_c) of 0.02 inch was used for all tensile failure analysis. This value was obtained by comparing .250 inch hole-size strength data from the 50/40/10 laminate with predictions, as illustrated in Figure 30.

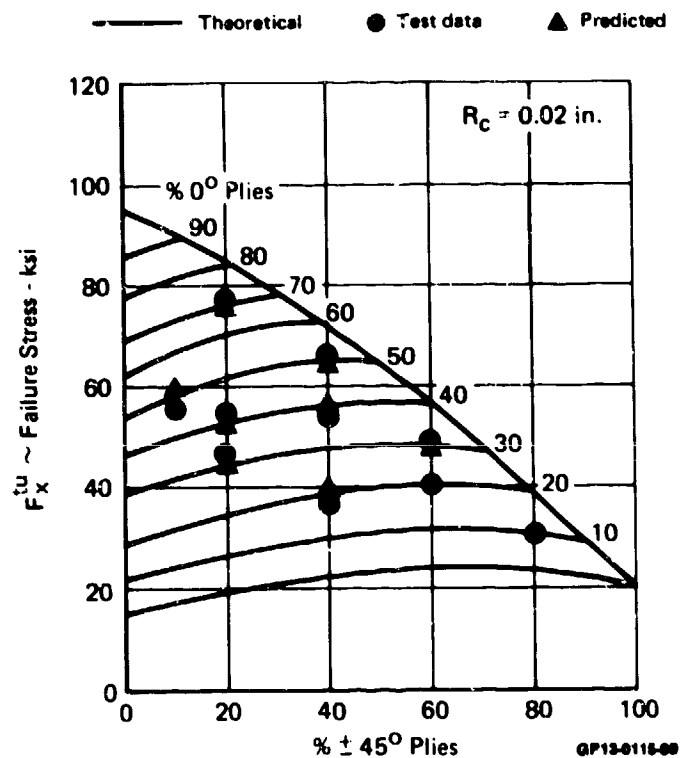
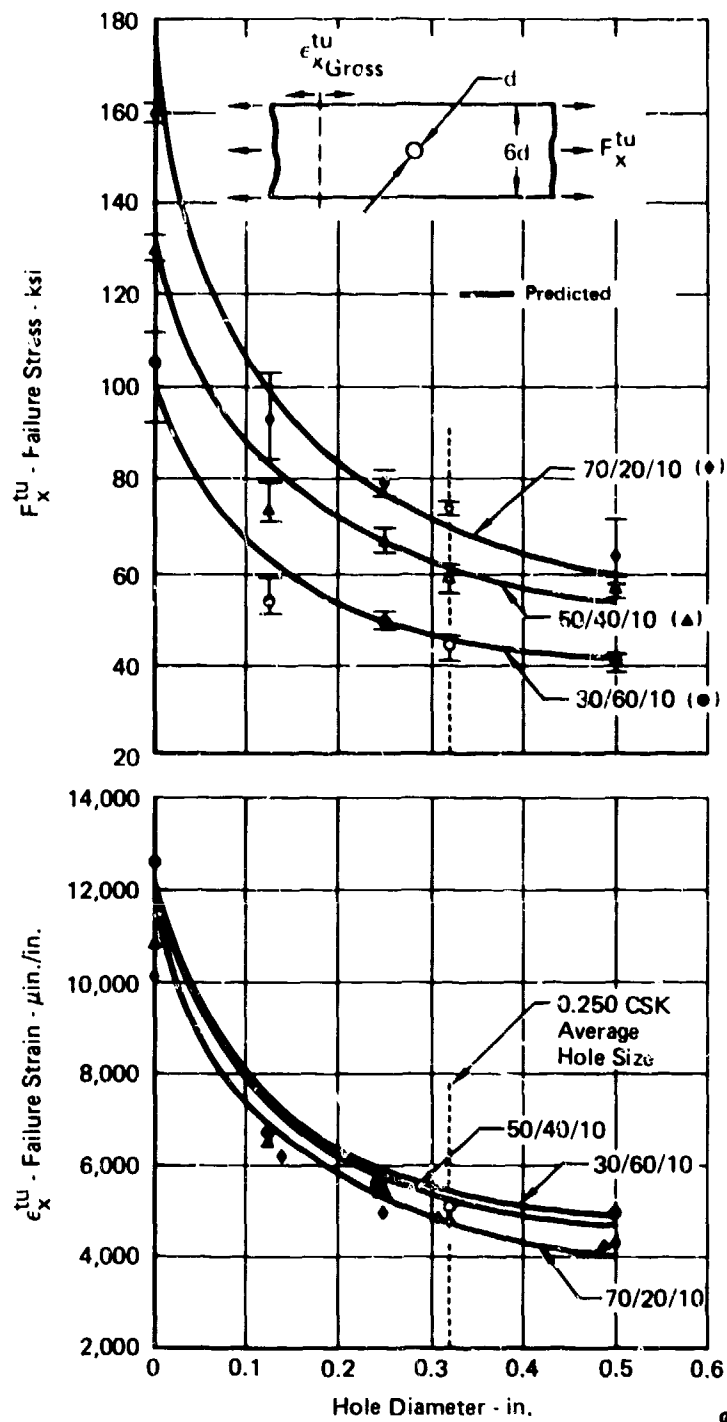


Figure 28. Effect of Layup Variation on Unloaded Hole Tensile Strength



GP13-0116-42

Figure 29. Effect of Hole Size on Unloaded Hole Tensile Strength

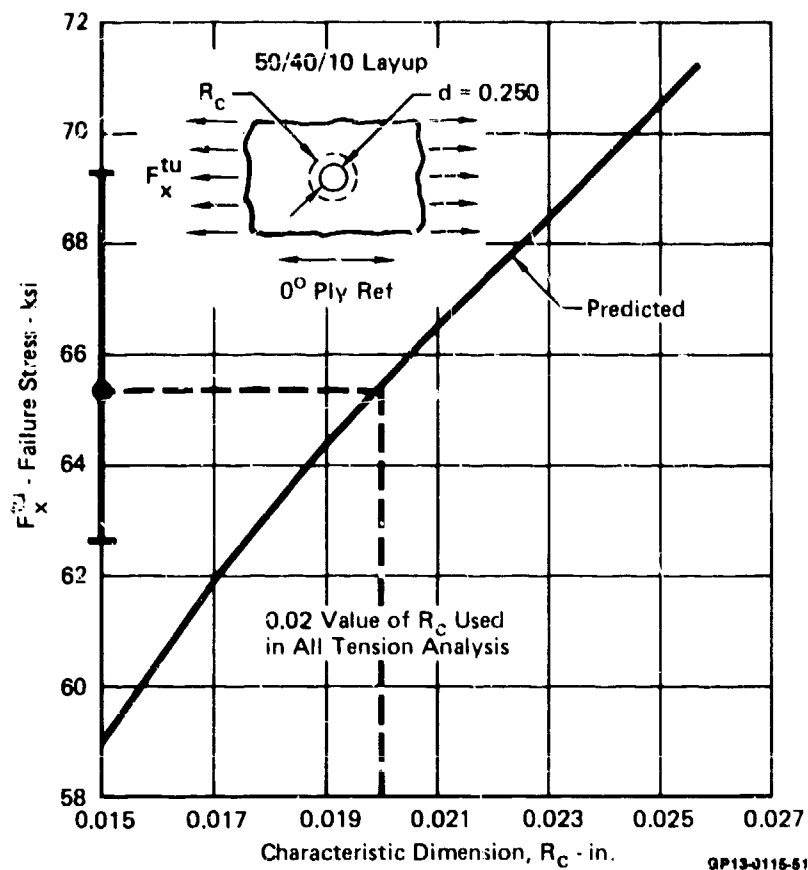


Figure 30. Effect of Variation of R_C on Predicted Tensile Strength

Location of failure initiation depends on layup and hole size. Predicted failure location occurred on the hole boundary and at 90° to the applied load direction for all but two cases. The exceptions are the 70/20/10 layup with 0.250 or 0.500 in. diameter holes. Predicted origins of failure were at 65° for the 0.250 in. diameter hole and 70° for the 0.500 in. diameter hole. In these two cases, failure was predicted in the $\pm 45^\circ$ plies. All predicted locations of failure correlated visually with test data (e.g., Figure 31).

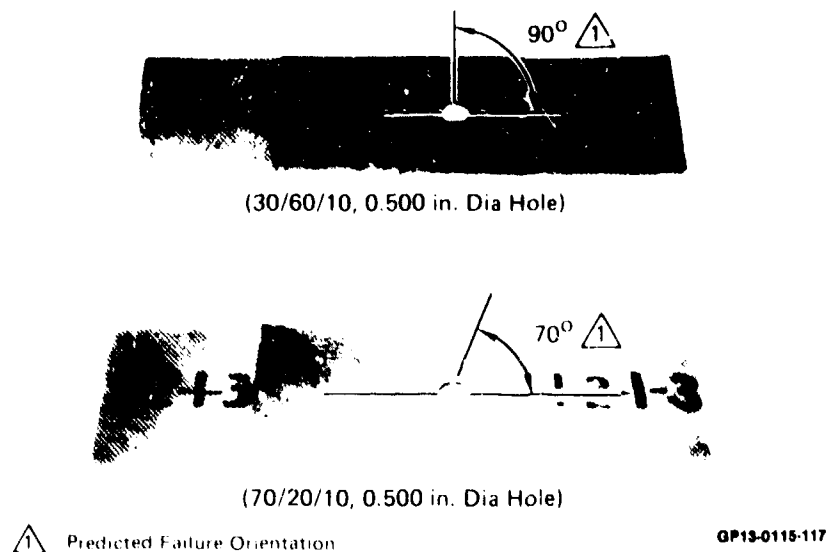


Figure 31. Predicted Failure Orientations Were Verified

Strength predictions for a biaxially loaded laminate with an open fastener hole were also verified by test. This loading condition was achieved with uniaxial loading at various angles relative to the laminate principal material axis. Due to orthotropic material behavior, off-axis uniaxial loading causes shear-extensional coupling which produces a biaxial stress state in the test specimen gage area. Using the 0.02 in. characteristic dimension, correlation of test data with predictions is shown in Figure 32.

A characteristic dimension of $R_C = .025$ inch was used for all compressive failure analysis. As in the tension case, R_C was initially determined using only .250 inch hole size strength data obtained from tests performed on the 30/60/10 laminate (Figure 33); however the final value of .025 inch was based on a best fit of all hole-size strength data for the 30/60/10 layup. Predictions and test data on the effects of hole size on compression strength for this layup as well as the 50/40/10 and 70/20/10 layup are presented in Figure 34. A carpet plot of compressive strength predictions for all ten layups of Figure 20 is correlated with test data in Figure 35. Test data and predictions are for the open hole, .250 inch diameter, specimen configuration.

A preliminary evaluation of the effects of temperature on compressive strength of laminates with .250 inch diameter unfilled fastener holes was also performed. Three different laminates were tested at room temperature and 250°F. Using the BJSFM procedure, strength predictions for both room temperature and 250°F were based on a constant characteristic dimension of 0.025 inch and the Tsai-Hill Failure Criterion. Correlation of

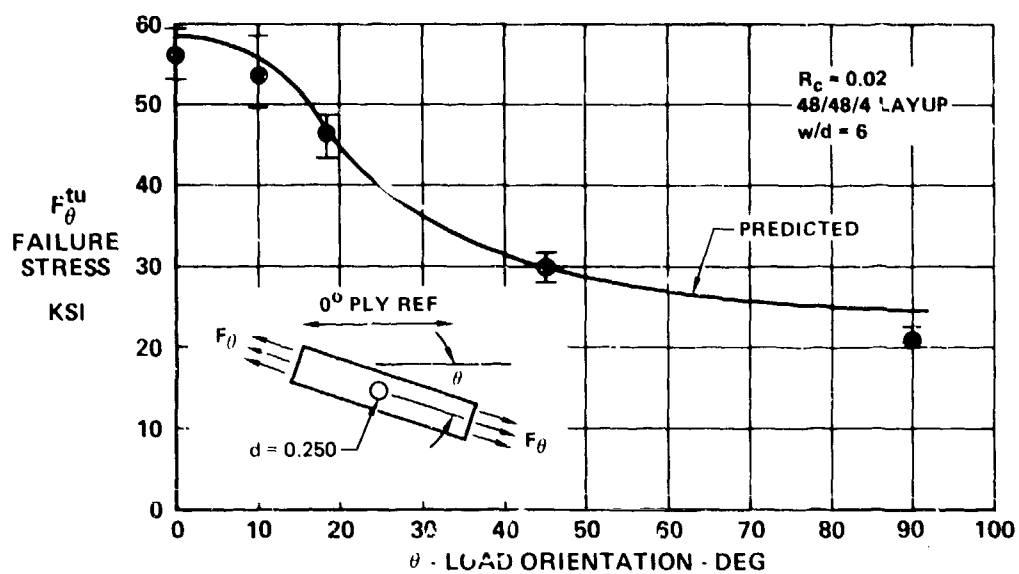


Figure 32. Effect of Off-Axis Loading on Failure Stress

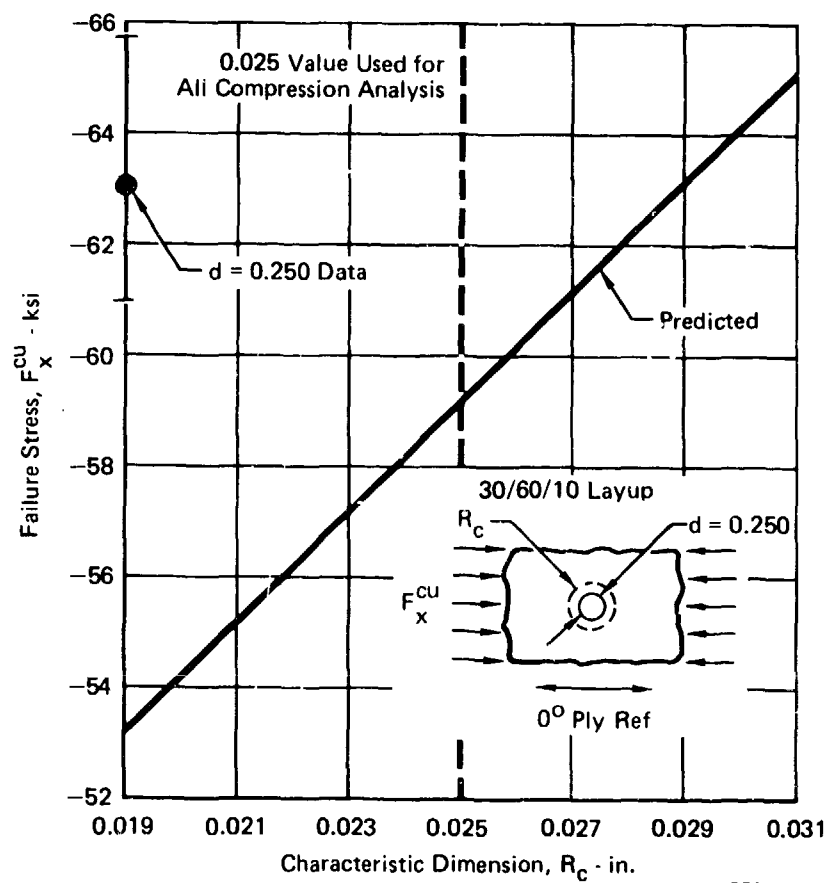


Figure 33. Effect of Variation of R_c on Predicted Compressive Strength

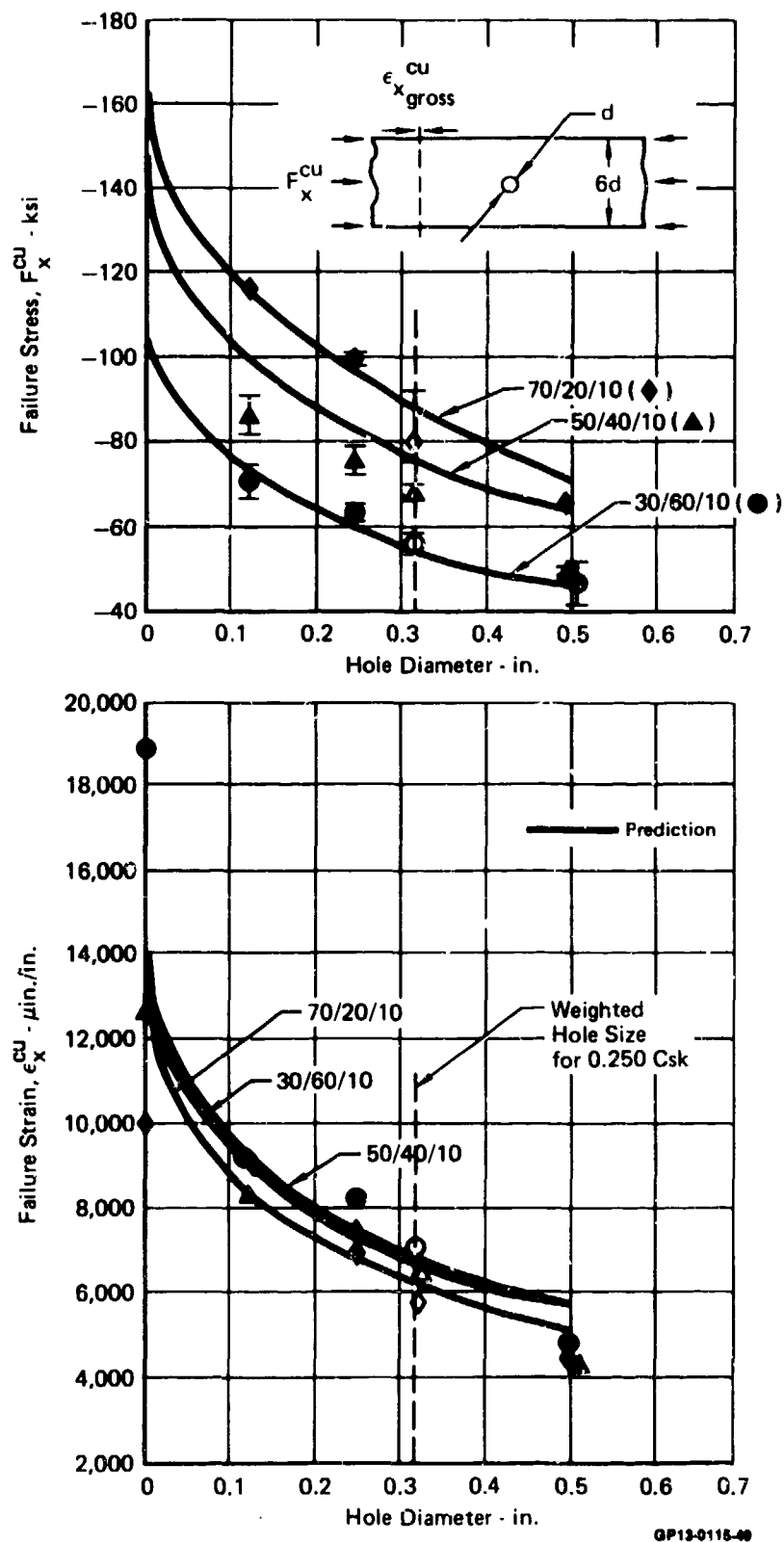


Figure 34. Effect of Hole Size on Unloaded Hole Compressive Strength

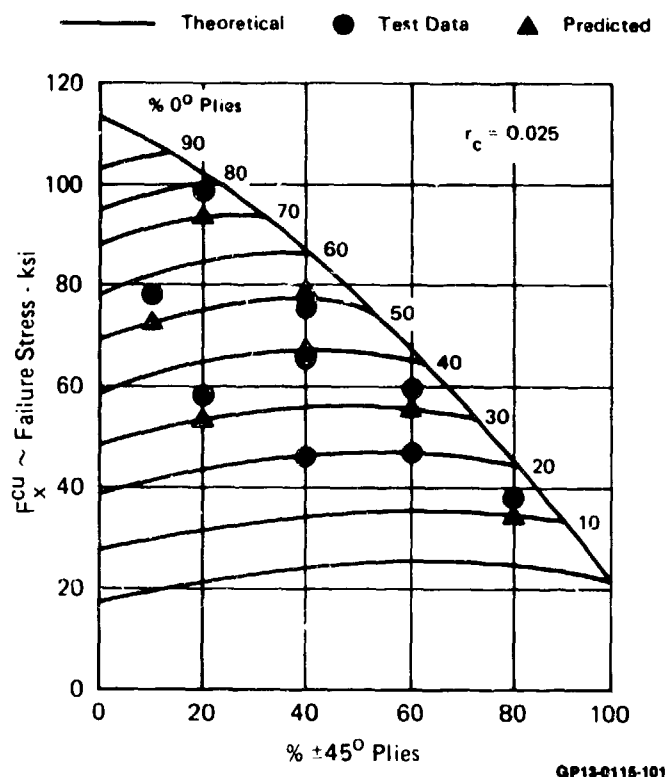


Figure 35. Effect of Layup Variation on Unloaded Hole Compressive Strength

test data and predictions is illustrated in Figure 36. Results indicate that effects of temperature on unloaded hole laminate strength for a wide range of layups can be satisfactorily predicted by using the BJSFM procedure with appropriate temperature-corrected values of lamina elastic constants and lamina strengths.

For all test conditions, compressive failure modes of open hole specimens were similar. Laminate material in the net-section area "broomed-out" symmetrically about the thickness centerline, typical of compressive failures in unnotched laminates.

Failure initiation points were predicted to occur on the hole boundary $85-90^\circ$ from the specimen length axis in all but the highly orthotropic layups. For these latter layups (70/20/10 and 50/10/40), failure initiation points were predicted to occur at 125° . However, due to extensive laminate compressive damage, visual verification of failure initiation points was not possible.

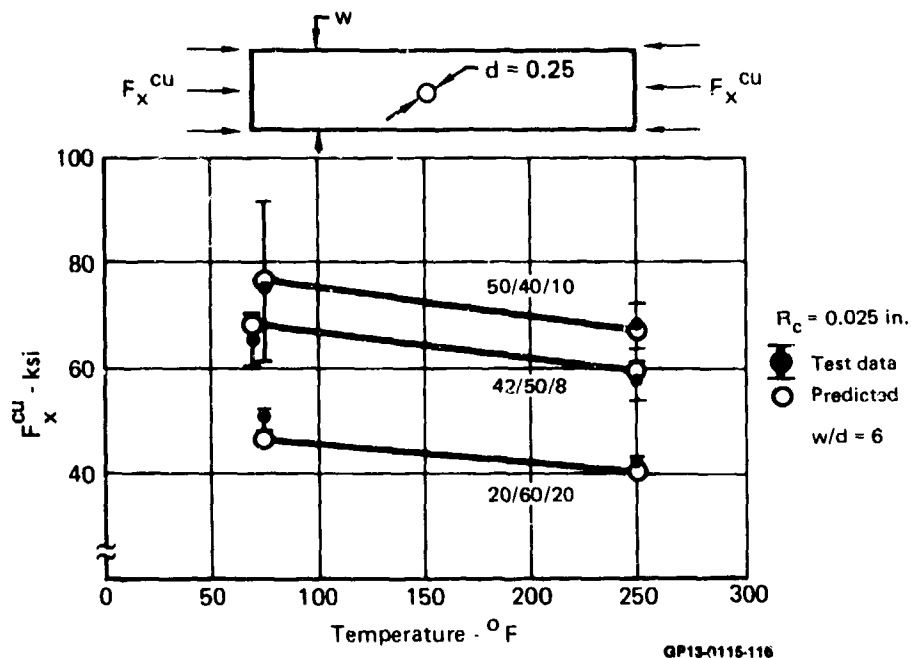
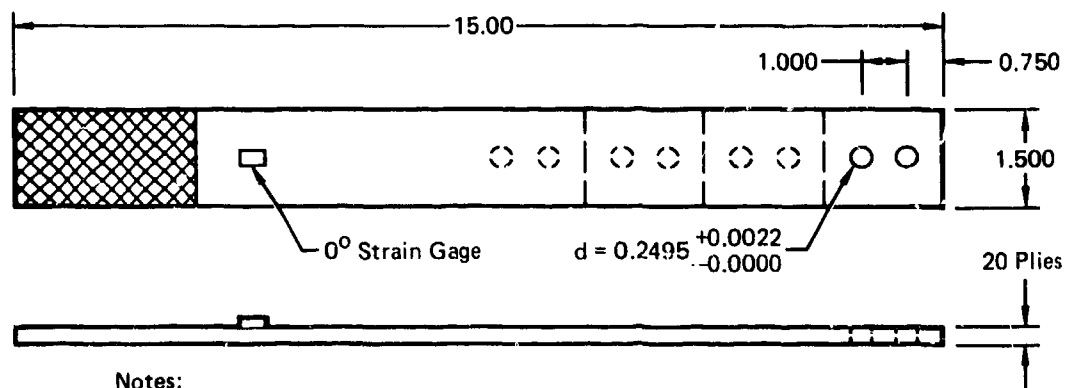


Figure 38. Effect of Temperature on Unloaded Hole Compression Strength

(2) Strength of Laminates With Loaded Fastener Holes

In the Task 2 test matrix (Figure 19), evaluations of bolted composite joint strength can be sub-grouped under four studies: (1) effects of orthotropic mechanical properties, (2) effects of joint geometry, (3) effects of loading and fastener pattern interactions, and (4) effects of through-the-thickness variables. A baseline 50/40/10 layup and joint geometry (single or two fastener-in-tandem configuration) detailed in Figure 37 is used throughout the Task 2 test program as a reference point. Details of specific specimen geometries are shown in Figures 38, 39, 40 and 41.

Evaluation of effects of orthotropic mechanical properties included layup and load orientation variables. Effects of laminate variations (70/20/10 and 30/60/10 layups) on joint strength were compared to the 50/40/10 baseline strength data for the load condition of bearing and bypass loads aligned with a principal material axis. Effects of bearing load, off the principal material axis, on ultimate bearing strength were evaluated for the 50/40/10 layup under pure bearing loadings. As-manufactured and moisture conditioned specimens were tested in tension and compression at room temperature and 250°F.

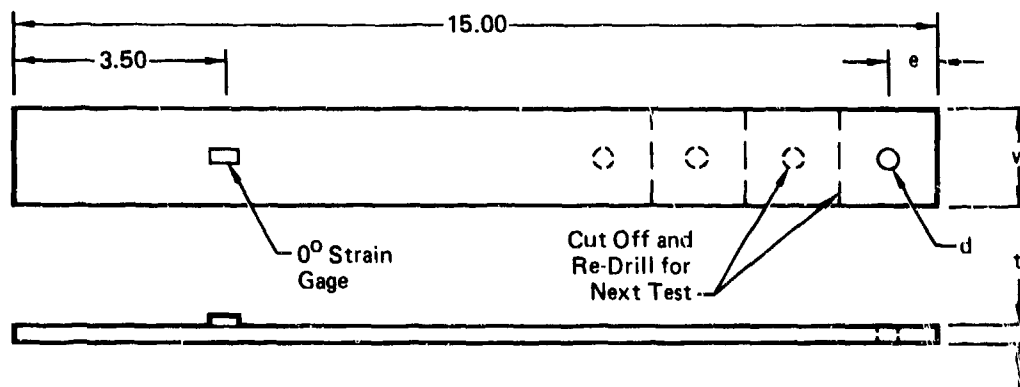


Notes:

Laminate: 50/40/10 Layup
 Stacking Sequence: $[+45^\circ, 0^\circ, -45^\circ, 0^\circ, 90^\circ, 0^\circ, +45^\circ, 0^\circ, -45^\circ, 0^\circ]_s$
 Thickness (t): 0.208 in. Nominal (20 Plies)
 Fastener Type: ST3M 453-4 (0.2495 + 0.0000/-0.0005 in. dia)
 Torque Value: 50 in.-lb (1/4 in. Fastener)
 Load Configuration: Double-Shear

GP13-0115-47

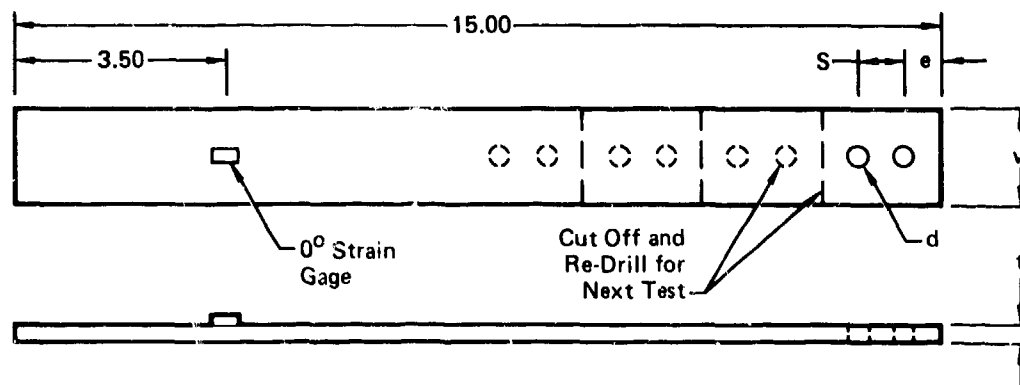
Figure 37. Two-Bolt In-Tandem Specimen Baseline Configuration



Design Variable	Variations	w (in.)	e (in.)	d (in.)	t	
					Plies	in.
Load Orientation	All	1.50	0.750	0.250	20	0.208
Countersink	(h/t) 1	2.25	1.125	0.375	20	0.208
	(h/t) 2	2.25	1.125	0.375	40	0.416
	(h/t) 3	2.25	1.125	0.375	60	0.624
Single Shear (Protruding Hd)	Baseline	1.50	0.750	0.250	20	0.208
	e/d	1.50	0.500	0.250	20	0.208
	w/d	1.00	0.750	0.250	20	0.208
	d	2.25	1.125	0.375	20	0.208
Stacking Sequence	All	1.50	0.750	0.250	20	0.208
Fastener Torque	All	1.50	0.750	0.250	20	0.208
Thickness	t ₁	2.25	1.125	0.375	40	0.416
	t ₂	2.25	1.125	0.375	60	0.624

GP1.3-0115-46

Figure 38. Variations of Single Fastener Specimen Configurations



Design Variable	Variations	w (in.)	e (in.)	d (in.)	S (in.)	t (in.)
Layup	All	1.500	0.7500	0.2500	1.500	0.208
Edge Distance	(e/d) 1	1.500	0.3750	0.2500	1.000	0.208
	(e/d) 2	1.500	0.5000	0.2500	1.000	0.208
	(e/d) 3	1.500	1.0000	0.2500	1.000	0.208
	S1	1.500	0.7500	0.2500	0.500	0.208
	S2	1.500	0.7500	0.2500	0.750	0.208
Width	(w/d) 1	1.000	0.7500	0.2500	1.000	0.208
	(w/d) 2	1.250	0.7500	0.2500	1.000	0.208
	(w/d) 3	2.000	0.7500	0.2500	1.000	0.208
Hole Size	D1	1.137	0.5685	0.1895	0.758	0.208
	D2	2.250	1.1250	0.3750	1.500	0.208
	D3	3.000	1.5000	0.5000	2.000	0.208
Single Shear	All	1.500	0.7500	0.2500	1.000	0.208
Fastener Torque	All	1.500	0.7500	0.2500	1.000	0.208

GP13-0115-45

Figure 39. Variations of Two-Bolt-In-Tandem Specimen Configurations

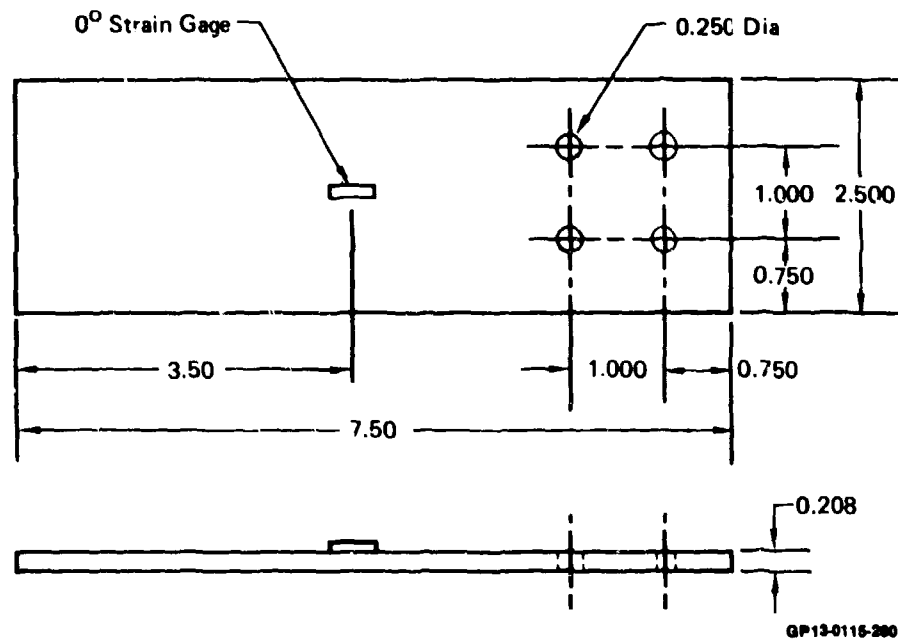


Figure 41. Fastener Pattern Specimen Geometry

In the second group, effects of joint geometry, joint variables evaluated include edge distance (e), width (w), and hole-size (d) for the 50/40/10 laminate. Specimens were tested in tension at room temperature dry and selectively at 250°F after moisture conditioning.

Studies of loading and fastener pattern interaction involved: (1) evaluation of the effect of bearing stress on laminate bypass strength and (2) evaluation of stress concentration interactions in multi-fastener patterns. Bearing-bypass interactions were evaluated for two layups (50/40/10 and 30/60/10) with bearing and bypass loads aligned with the 0° principal material axis and, for the 50/40/10 layup, when bearing loads were oriented at 10°, 22.5°, and 45° relative to bypass loads which were parallel to a principal material axis. Four-bolt specimens were used to evaluate the interaction of fastener stress concentrations for two layups (50/40/10 and 30/60/10) and were tested selectively in tension and compression at room temperature and 250°F after moisture preconditioning.

Five through-the-thickness joint variables - (1) torque-up, (2) single shear (joint load eccentricity), (3) laminate thickness, (4) countersinking fasteners, and (5) stacking sequence - were evaluated to determine the possible three-dimensional interactions at individual fastener holes. Single-fastener pure bearing and two-fastener bearing plus bypass specimens were tested in tension and compression at room temperature dry conditions. Selective tests were performed at room temperature and 250°F with specimens moisture preconditioned. Strength data were compared with the baseline joint configuration.

(a) Layup Variation - Effects of layup variation on laminate bearing strength were evaluated using the two-fastener in-tandem specimen. Three layups (70/20/10, 50/40/10 and 30/60/10) were tested in tension and compression. Tests were performed at RTD, RTW, and ETW. Results of all tension tests are presented in Figure 42. Results of all compression tests are presented in Figure 43. In both sets of data increases in gross failure strain were linear with increases in percent of +45° plies contained in the layup. Parallel trends were observed for moisture conditioned specimens tested at 250°F (ETW), with strains generally lowered by 800-1000 $\mu\text{in/in}$ for all layups both in tension and compression. Specimens of the 50/40/10 layup, which were moisture preconditioned and tested at room temperature (RTW) exhibited little strength changes. Associated ultimate bearing strengths reflected similar trends between RTD and ETW data with approximately a 30-40 KSI loss in bearing strength for all layups tested at ETW.

Associated joint load-deflection data indicated the presence of nonlinear mechanical behavior. Predictions, using the BJSFM procedure, and joint loads at which initial nonlinearity occurred are also presented in Figure 42 and 43. Predictions were based on the previously determined R_c values of 0.02 inch and 0.025 inch for tension and compression respectively.

(b) Load Orientation - Effect of material orthotropy on pure bearing strength was evaluated using a single-fastener specimen fabricated at various angles off the 0° principal material axis. Specimens were tested selectively at room temperature dry and at 250°F after moisture conditioning.

Strengths at room temperature dry conditions are presented in Figure 44. Included are bearing stress values at which initial nonlinearities or abrupt changes were observed in joint load-deflection data. All off-axis test specimens were loaded in double-shear with fastener torque-up of 50 inch-pounds. BJSFM predictions indicate first ply fiber rupture or shear failure, based on a maximum strain failure criterion applied at a characteristic dimension of 0.02 inch away from the hole boundary. Correlation of this linear-elastic analysis with initial points of nonlinear joint deflection behavior, indicates that lamina shear or fiber failures are likely before ultimate bearing failure occurs.

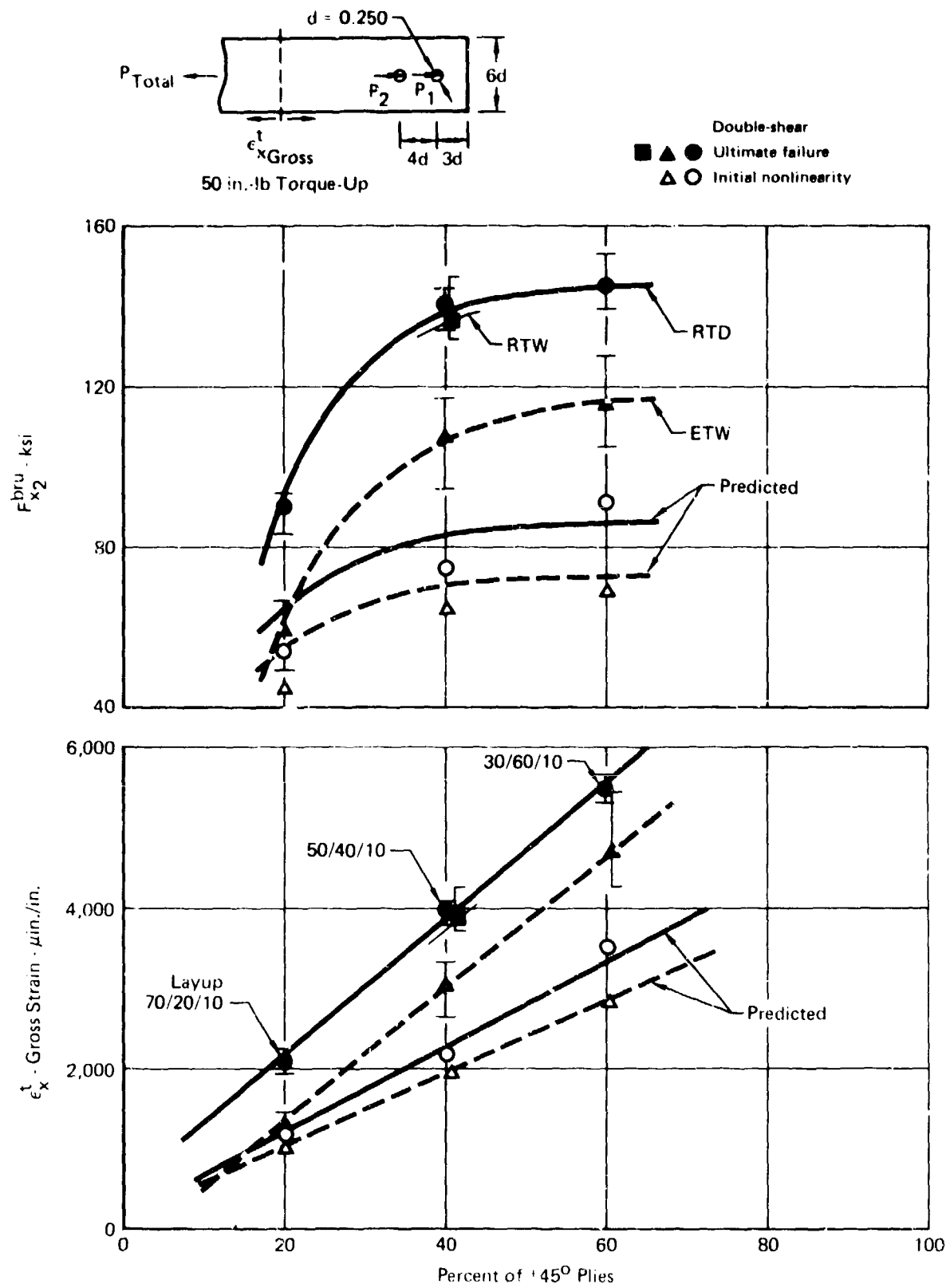


Figure 42. Effect of Layup Variation on Joint Tensile Strength

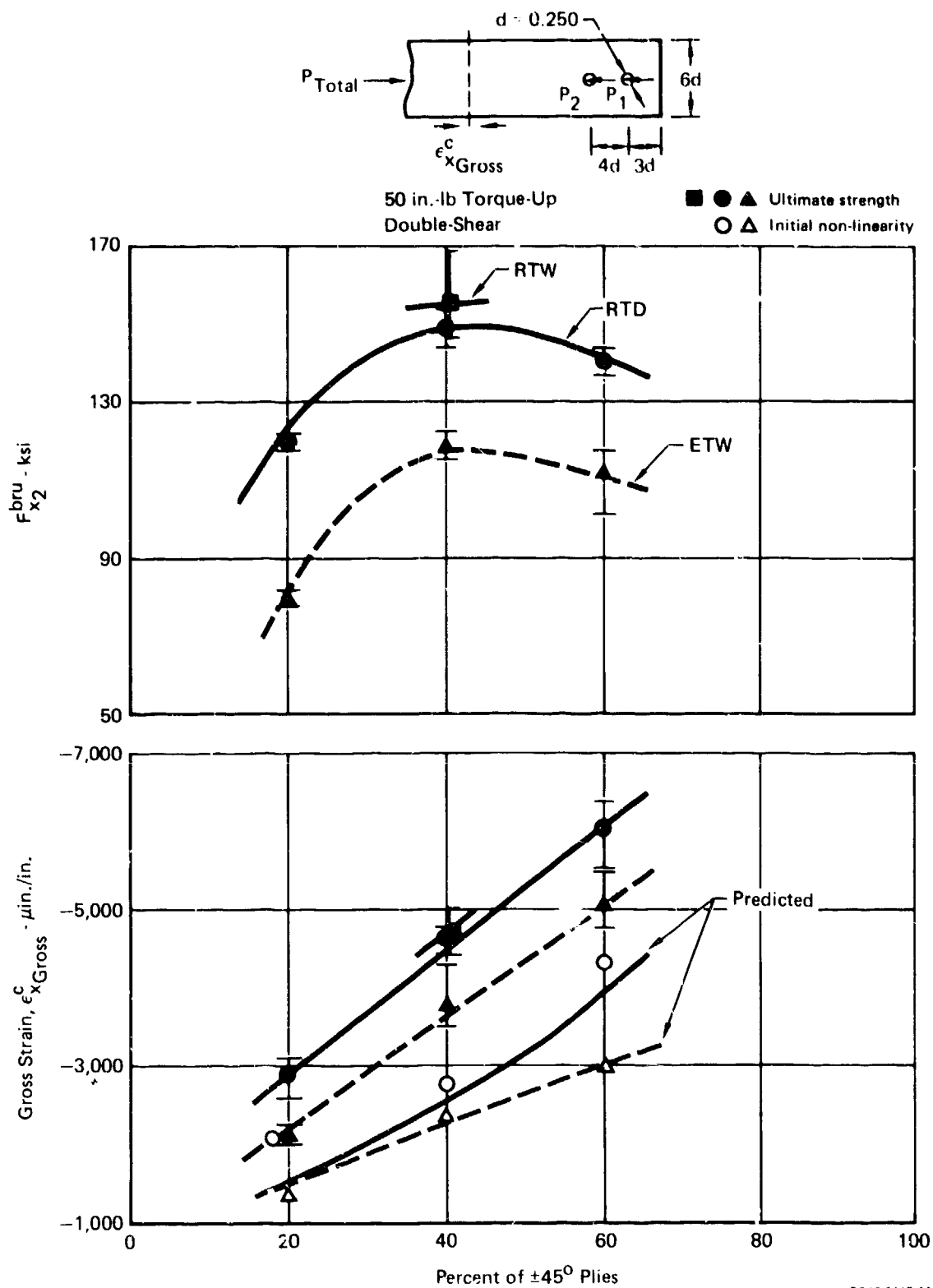


Figure 43. Effect of Layup Variation on Joint Compressive Strength

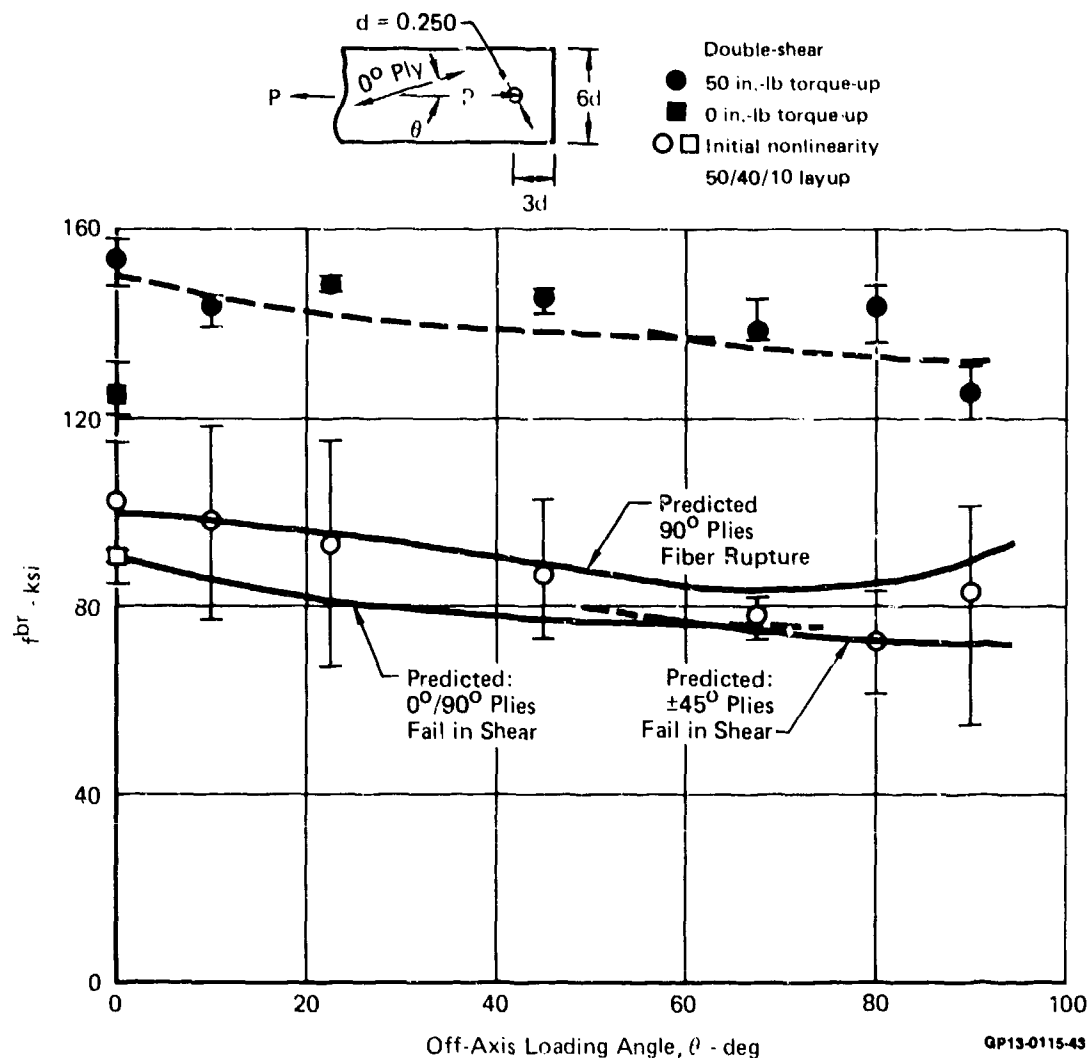


Figure 44. Effect of Off-Axis Loading on RTD Pure Bearing Strength

Strength of moisture conditioned specimens is presented in Figure 45. Trends appear to be similar to RTD results with joint gross failure strains reduced by approximately 700-1000 $\mu\text{in/in}$ and bearing strength by approximately 40 KSI in the moisture conditioned specimens at 250°F. Theoretical predictions at both RTD and ETW are indicated in Figure 45, versus strain data for initial points of nonlinearity. Both ETW and RTD predictions were based on the .02 inch value of R_c . Results from off-axis loading at 10° under compression loading are presented in Figure 46.

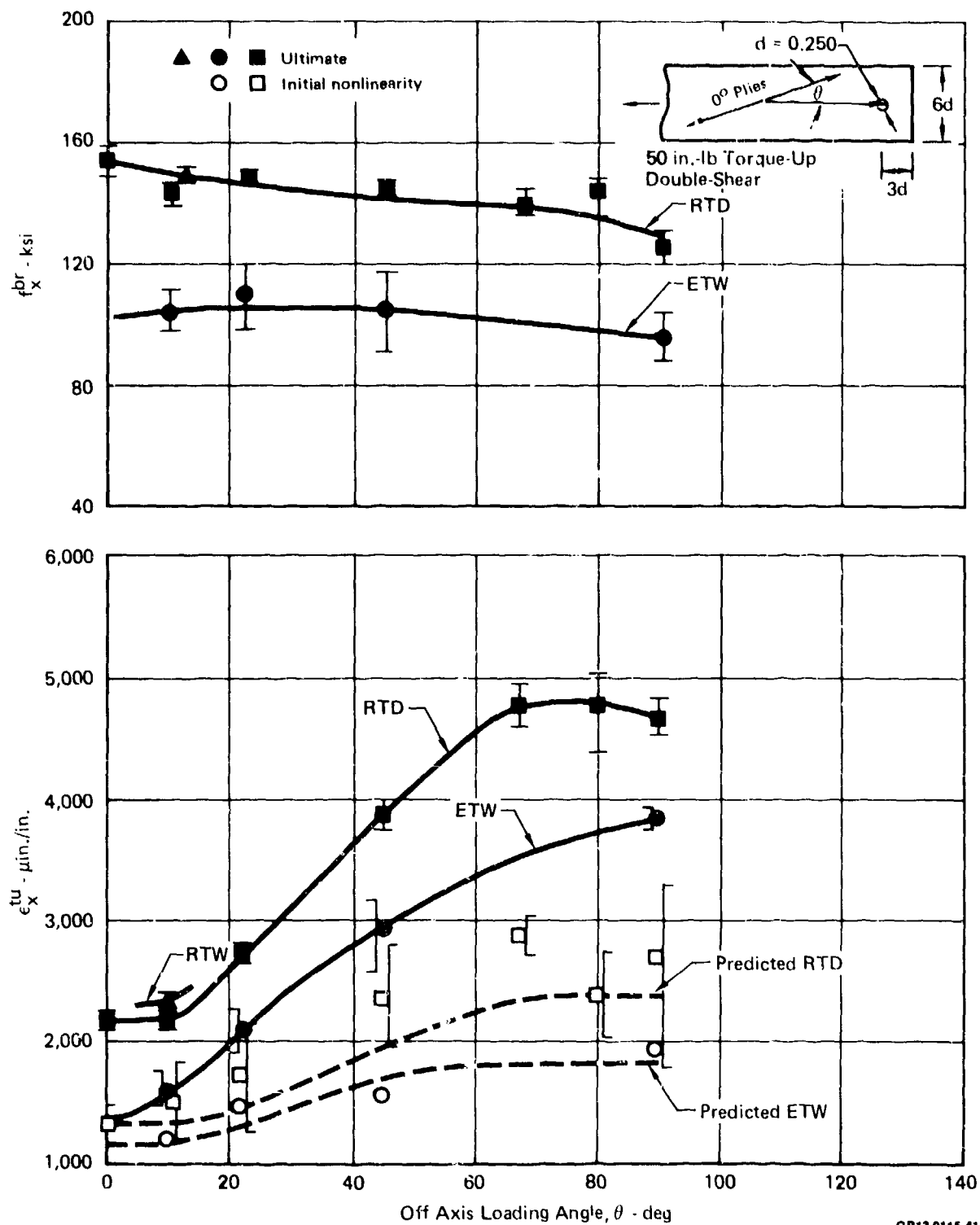
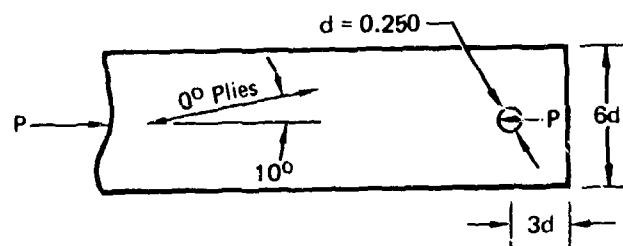


Figure 45. Effect of Temperature and Moisture on Off-Axis Strength



Test Condition 50/40/10 Layup	F_{br} x		Initial Nonlinearity		ϵ_{cu} x	
	ksi	Percent Δ of RTD	ksi	Percent Δ of RTD	$\mu\text{in./in.}$	Percent Δ of RTD
RTD	153	—	113	—	-2,640	—
RTW	157	+2.7	122	+10.4	-2,830	+7.3
ETW	113	-26.3	76	-33.8	-1,980	-25.1

QP13-0115-42

Figure 46. Effect of Temperature and Moisture on Compressive Strength

(c) Edge Distance - Effects of edge distance on joint strength were evaluated by testing two-fastener-in-tandem double shear specimens. Tests were performed on dry specimens at room temperature and on moisture conditioned specimens at 250°F. Specimens were loaded to failure in tension. Additional RTD data on the effects of edge distance on pure bearing (single-fastener) strength were available from an earlier MCAIR in-house program.

Results of RTD and ETW tests are presented in Figure 47. Specimen failure modes at all e/d ratios exhibited shearout to bearing-shearout failures. Joint bearing strength and gross failure strain data exhibit a marked bilinear behavior. Reduced joint strength with earlier insensitivity to e/d ratios was exhibited in the ETW tests.

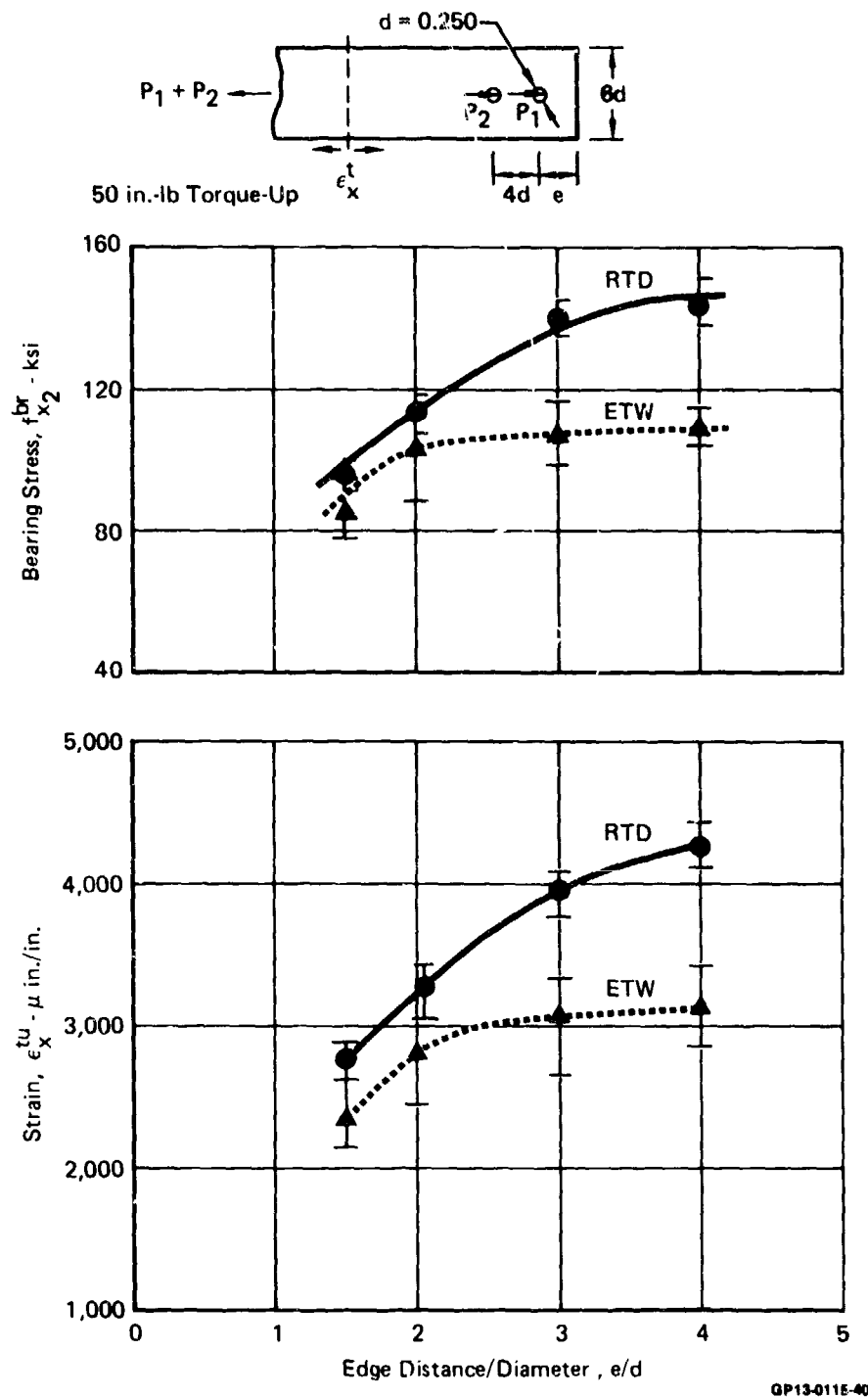


Figure 47. Effect of Edge Distance on Joint Tensile Strength

Effects of fastener spacing (S) on joint strength were evaluated at RTD test conditions. Results (Figure 48) indicate that for high-bearing to bypass joint loadings, strength reductions occur as S/d ratios decrease from 4.0 to 2.0. While fastener spacing creates a beneficial "shadowing effect" at the net-section on stress concentrations, this is not the case in high bearing-to-bypass multi-fastener joints where bearing or shearout failures prevail. The proximity of adjacent fastener holes acts like an edge-of-part to internal fastener holes, reducing bearing strength capability and overall laminate strain capability.

Single fastener (pure bearing) joints were tested in single-shear at RTD for edge distance/diameter values ranging from 1.5 to 3. Effects of torque-up (30.0 increased to 50.0 inch-pounds) are reflected in a 25 KSI increase in bearing strength (Figure 49) for the e/d ratio of 3. The stacking sequence used in these tests was identical to the number 6 stacking sequences of Task 2 (Figure 26). The increased strength of the more homogeneous stacking sequence (number 1) is also indicated in Figure 49.

(d) Width - Effects of width on joint strength were evaluated using the 50/40/10 laminate in a two-fastener-in-tandem double-shear configuration. Specimens were tested to failure in tension at RTD and ETW. Results are presented in Figures 50 and 51. For RTD tests, specimens failed in the net section at the lower w/d ratios of 3 and 4, and failed in bearing-shearout at the w/d ratios of 6 and 8. Effects of temperature (250°F) and moisture content reduced strengths markedly at the higher w/d ratios but not at the lower w/d ratio of 4. This decreased sensitivity reflects a transition to fiber dominant net-section failures which are insensitive to effects of moisture. Failures for RTD specimens occurred in bearing-shearout at w/d ratios of 6 and 8 and transitioned to net-section at w/d ratios of 4 and 5. Decreased shear and compression properties at ETW conditions caused bearing-shearout failures at all but the lowest w/d ratios. Typical failed specimens are illustrated in Figure 52.

(e) Hole Size - Effects of hole size on joint strength were evaluated using the two-fastener-in-tandem double-shear specimen. Specimens were loaded in tension to failure at room temperature. Strengths are illustrated in Figure 53. Bearing strength and gross joint failure strain trends varied linearly over the range of hole sizes tested; however, all torque-up values for these tests were maintained at 50 inch-pounds. The triangular symbol in Figure 53 indicates the increased strength of joints with 160 inch-pounds of torque-up. This indicates a reduced sensitivity to effects of hole-size on joint strength when fastener torque-up values are increased. Predicted joint strengths for a nontorqued configuration are also presented in Figure 53. All specimens failed in bearing-shearout, regardless of hole size.

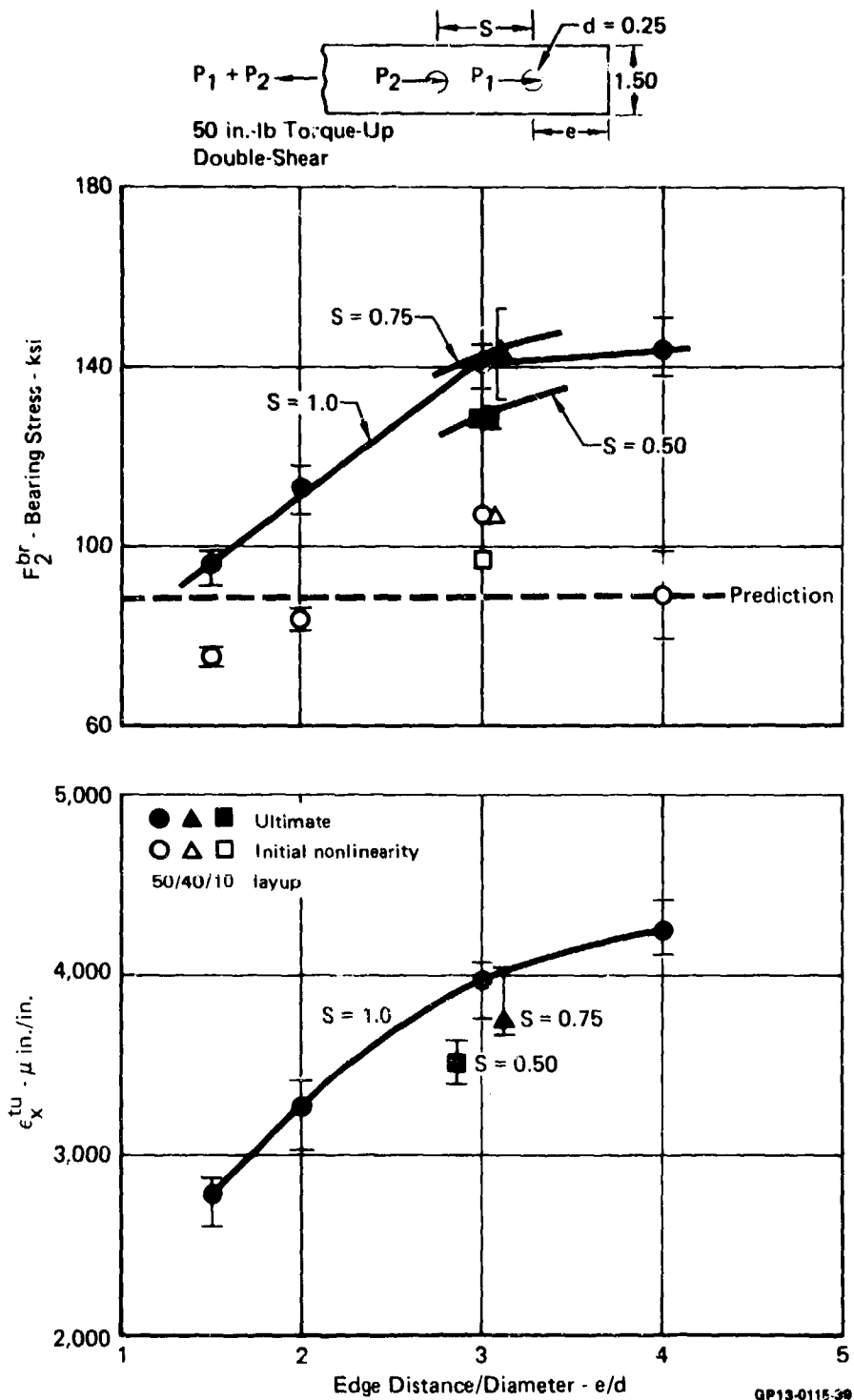


Figure 48. Effect of Fastener Spacing on Joint Tensile Strength

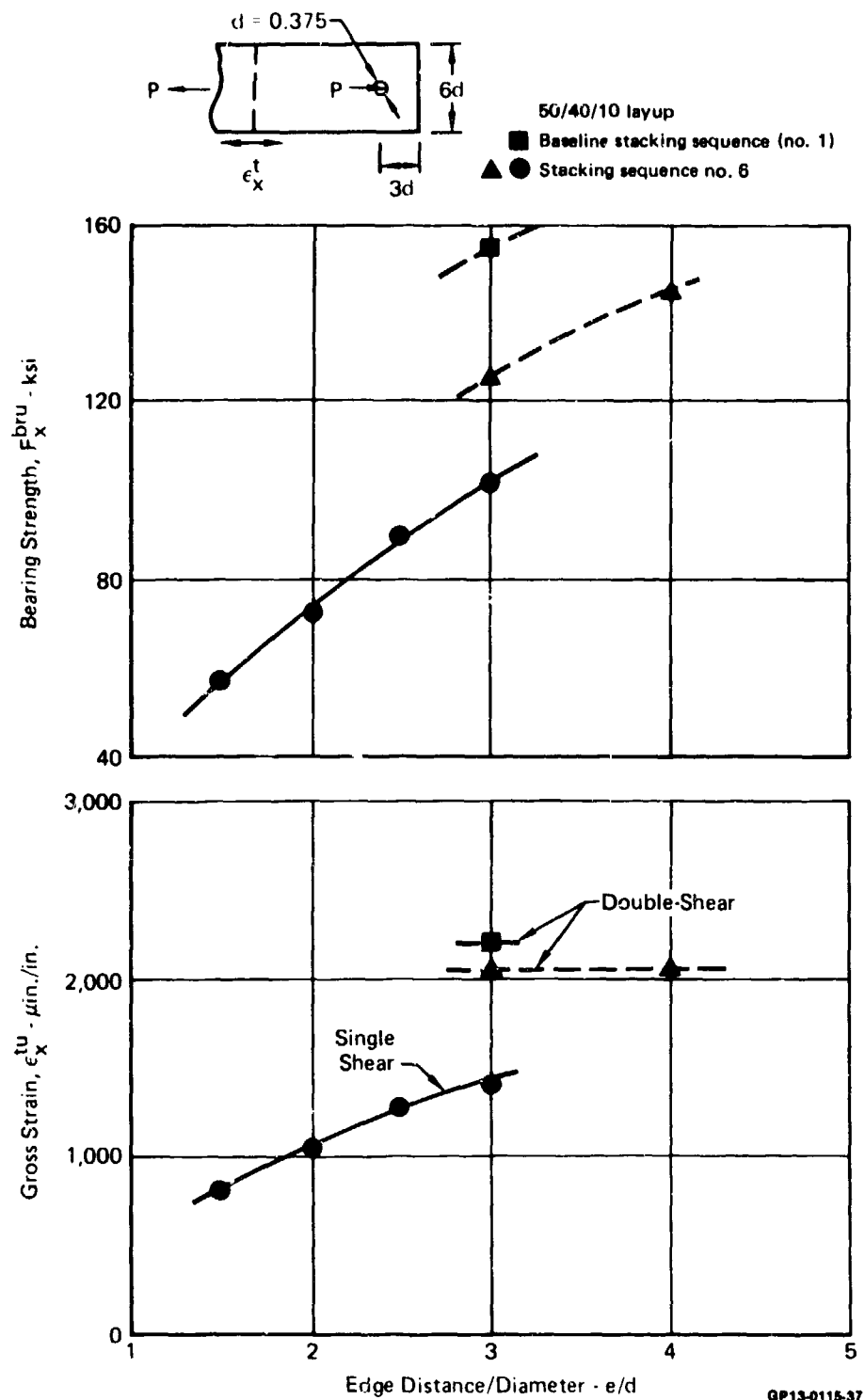


Figure 49. Effect of Edge Distance on Pure Bearing Strength

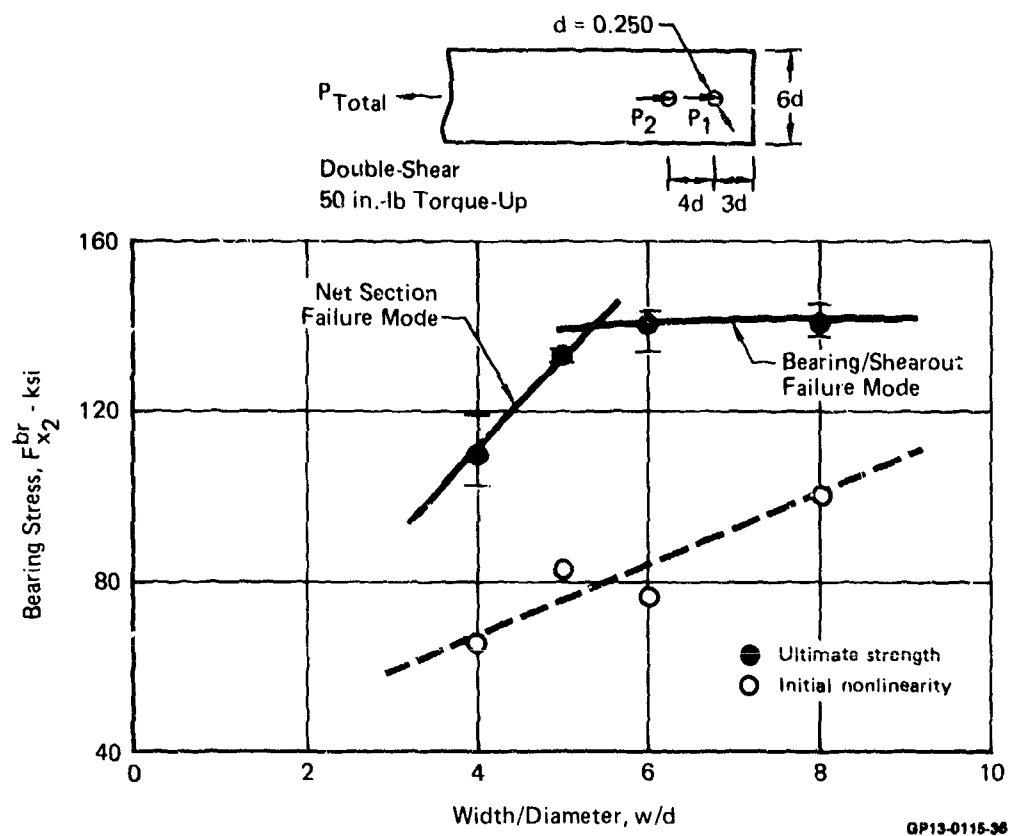


Figure 50. Effect of Specimen Width on RTD Joint Strength

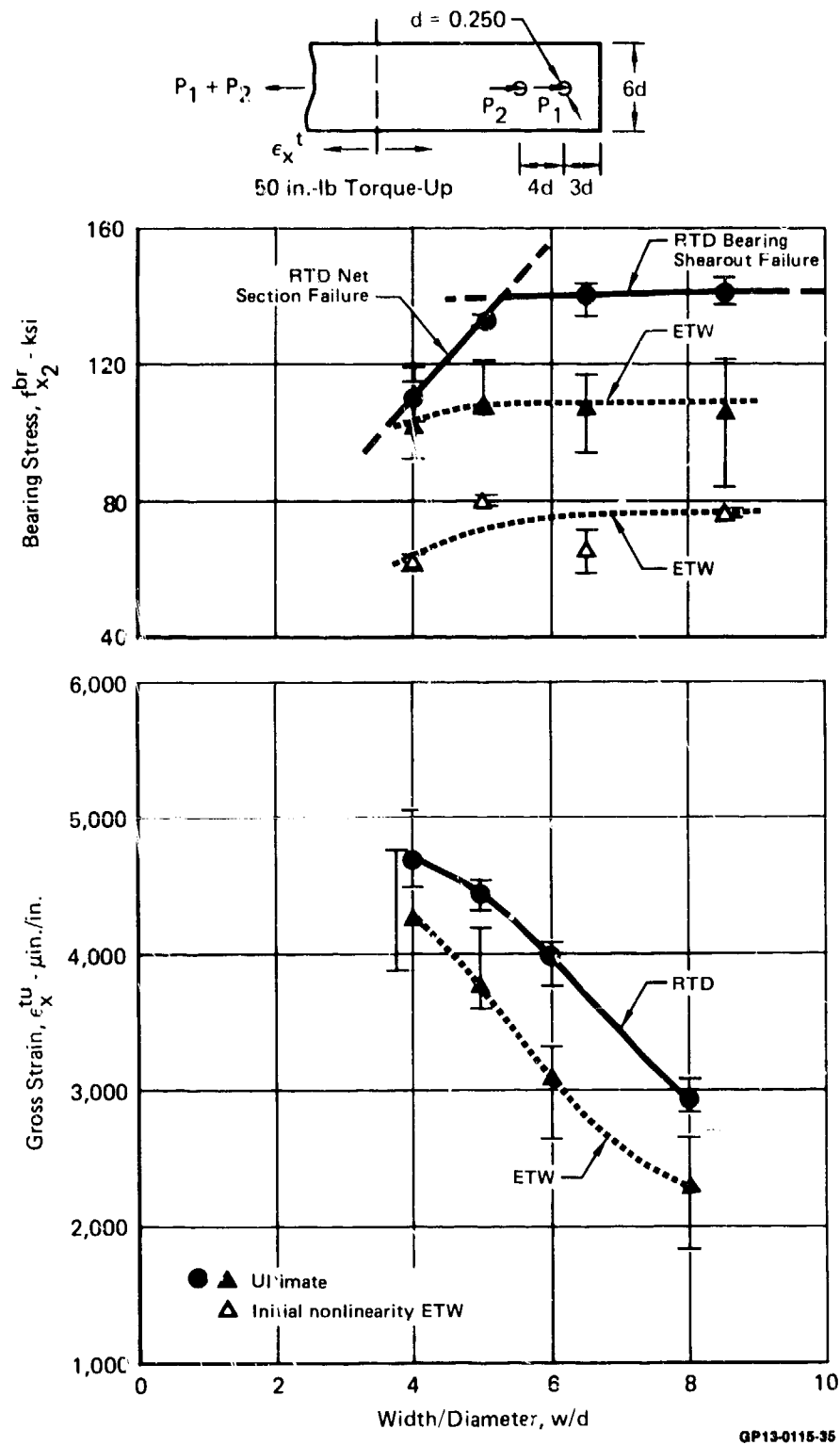
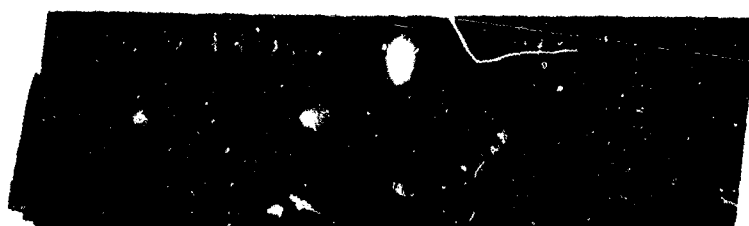


Figure 51. Effect of Temperature and Moisture on Joint Strength



(a) Net-Section at RTD



(b) Bearing-Shearout at ETW

Figure 52. Joint Failures Changed at ETW Test Conditions

GP13-0115-04

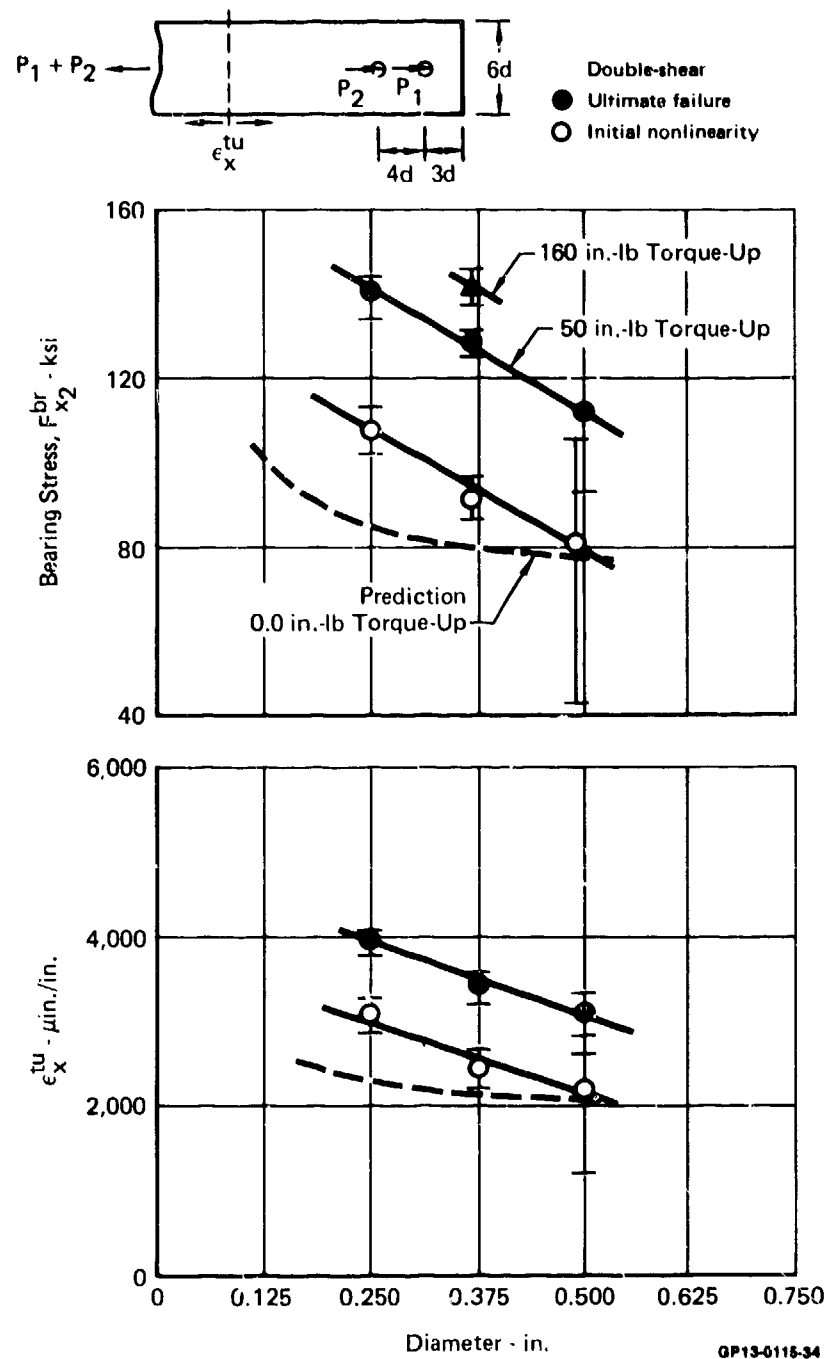


Figure 53. Effect of Hole Size on Joint Strength

(f) Load Interaction - Effects of fastener bearing and bypass stress interaction on laminate strength were evaluated by two load conditions: (1) bearing and bypass loadings aligned parallel to the 0° principal material axis, and (2) bypass loadings with bearing loads at angles of 10° , 22.5° and 45° off the 0° principal material axis. Both studies used a specially designed, hydraulic-actuated, scissor mechanism (Figure 54) to permit bearing loads to be applied to fastener holes independent of bypass loads. In all interaction tests, bearing loads were applied and maintained while bypass loading was increased until specimen failure occurred.

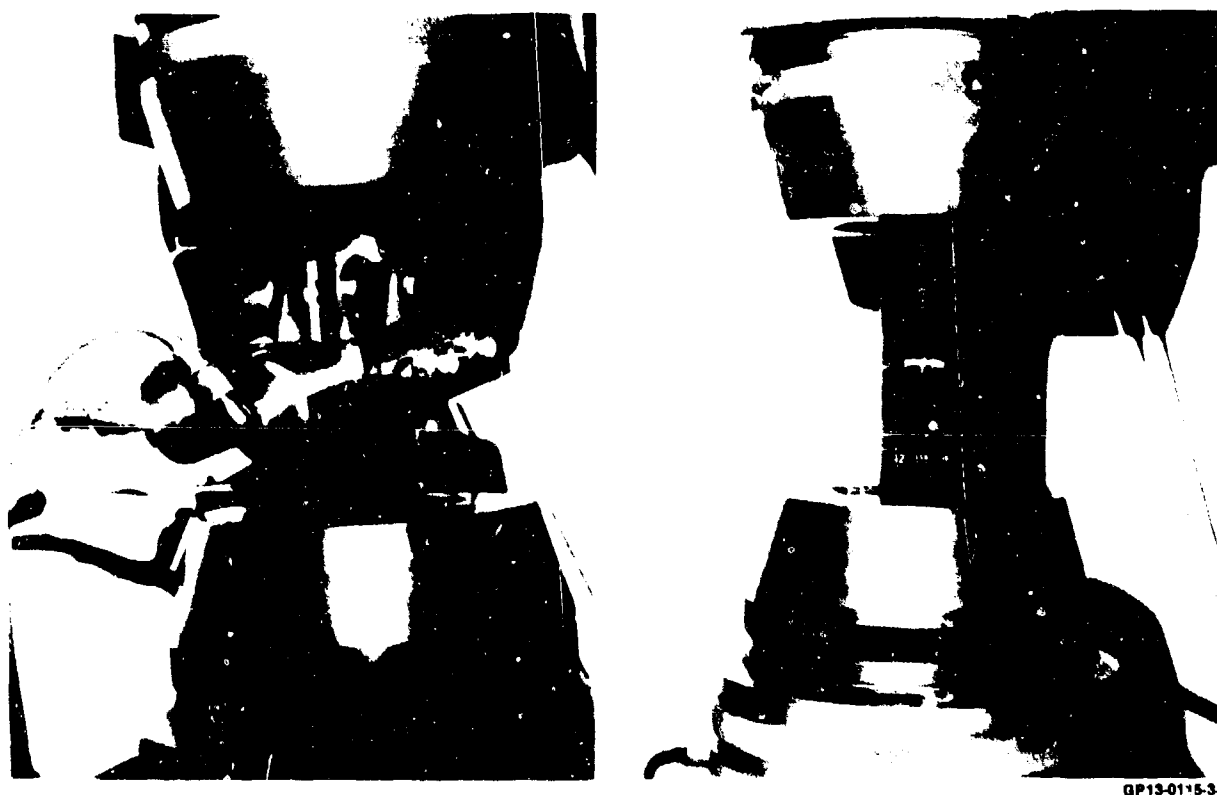


Figure 54. Load Interaction Specimen and Test Setup

The first evaluation provided preliminary data on the effects of aligned bearing and bypass stress on laminate strength for a 50/40/10 and 30/60/10 layup. Unloaded hole (zero bearing stress) and pure bearing (zero bypass stress) data were included

in the study. Predicted strengths are correlated with test data in Figures 55 and 56. Predictions made using the BJSFM are based on the maximum strain failure criterion applied at a characteristic dimension of 0.02 inches away from the hole boundary. Solid symbols indicate occurrence of ultimate static failure, open symbols indicate initial nonlinear or discontinuous load-versus-deflection behavior, if any. For the 50/40/10 layup, the triangular symbol represents strength data obtained from an unfilled single-hole test specimen. This lower strength value indicated the presence of fastener hole interaction ("hole-shadowing") in the bearing-bypass specimen (Figure 40) which tended to reduce stress concentration effects by approximately 10 percent

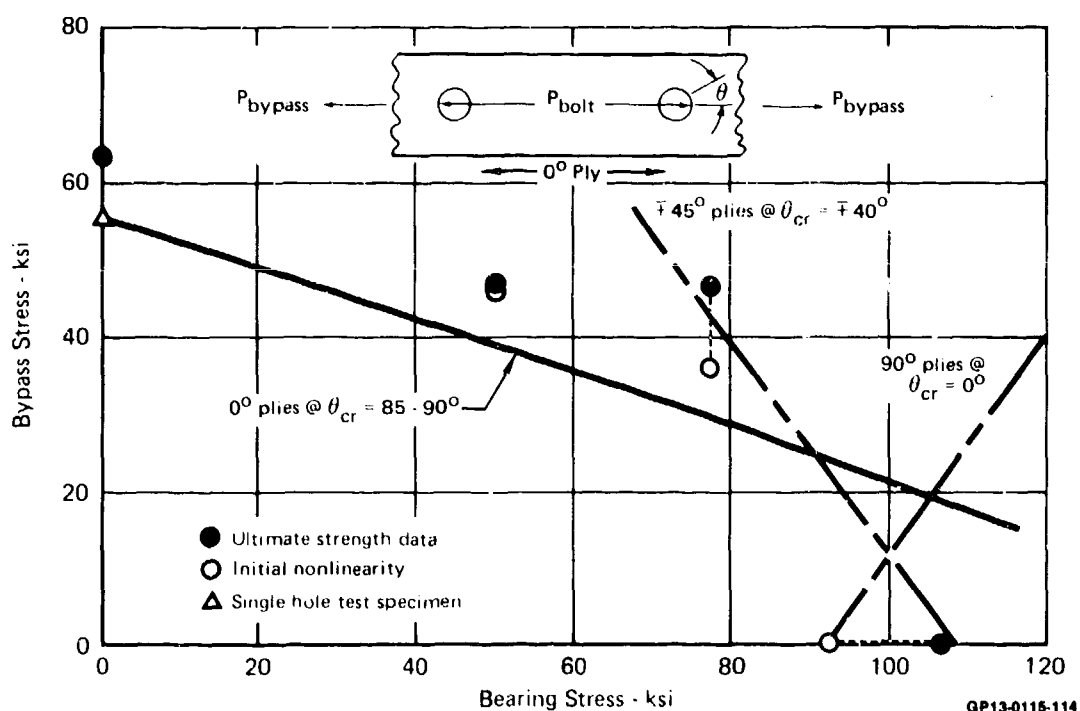


Figure 55. Correlation of Bearing-Bypass Strength of a 50/40/10 Layup

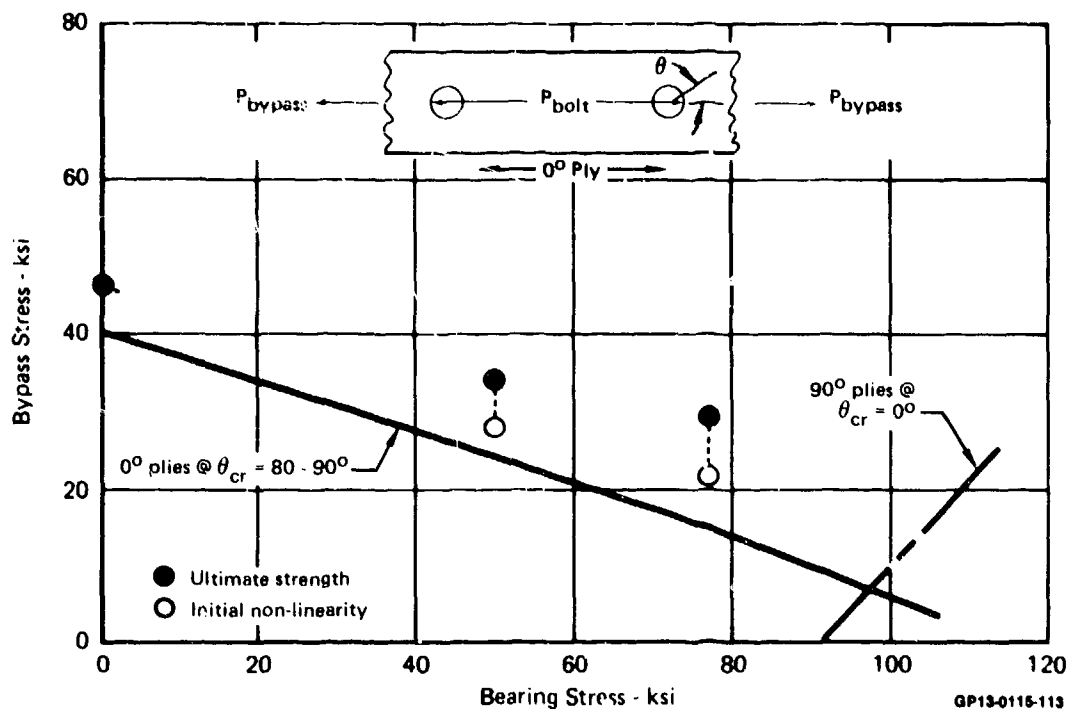


Figure 56. Correlation of Bearing-Bypass Strength of a 30/60/10 Layup

Typical load-versus-deflection trends are illustrated in Figure 57. General trends for both layups were: (1) bypass strength decreased as bearing stresses increased, and (2) initial non-linear or discontinuous load-versus-deflection behavior was present, appeared earlier, and became more marked as bearing stresses increased relative to bypass stress. Predicted failure at low bearing stress was net-section fiber failure of 0° plies; at high bearing stress, failure was predicted to occur in either +45° or 90° plies due to ply shear stress. Figures 58 and 59 indicate graphic representations of predicted critical plies and failure locations. Representative failed specimens in Figure 60 indicate verification of predicted failure modes.

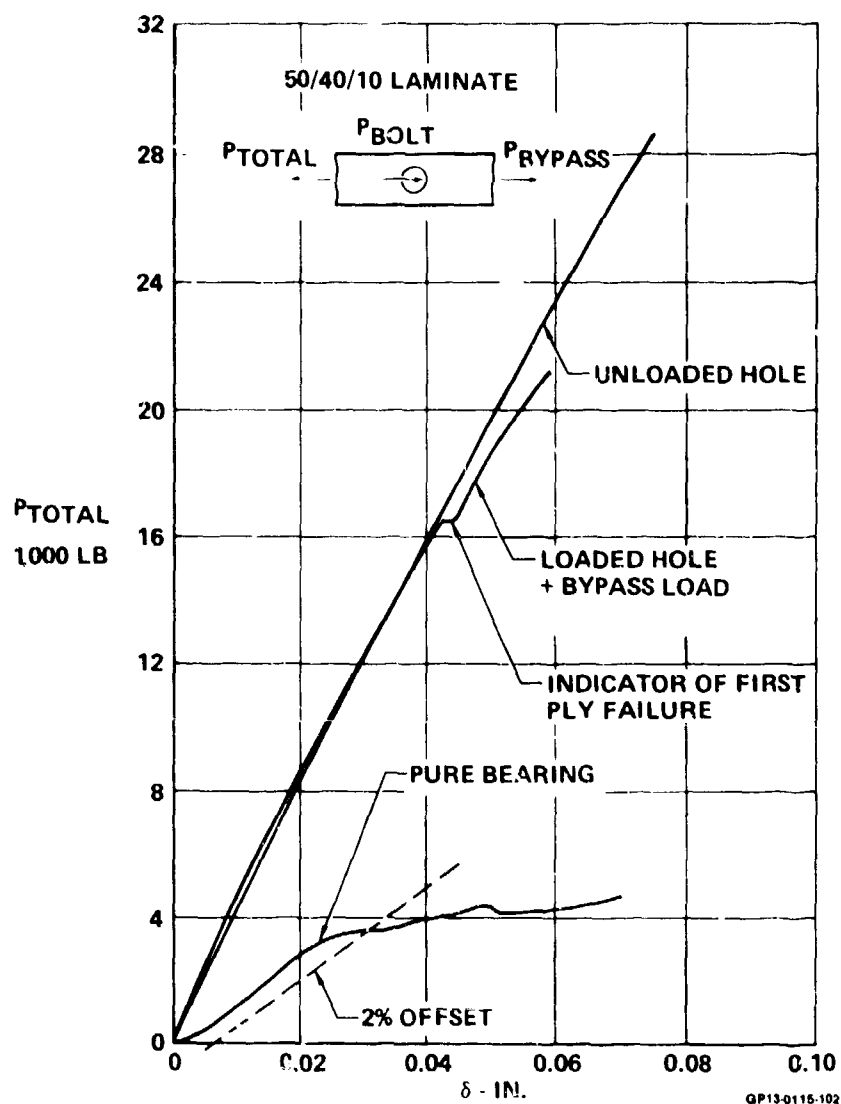


Figure 57. Effect of Bearing Loads on Specimen Load-Deflection Behavior

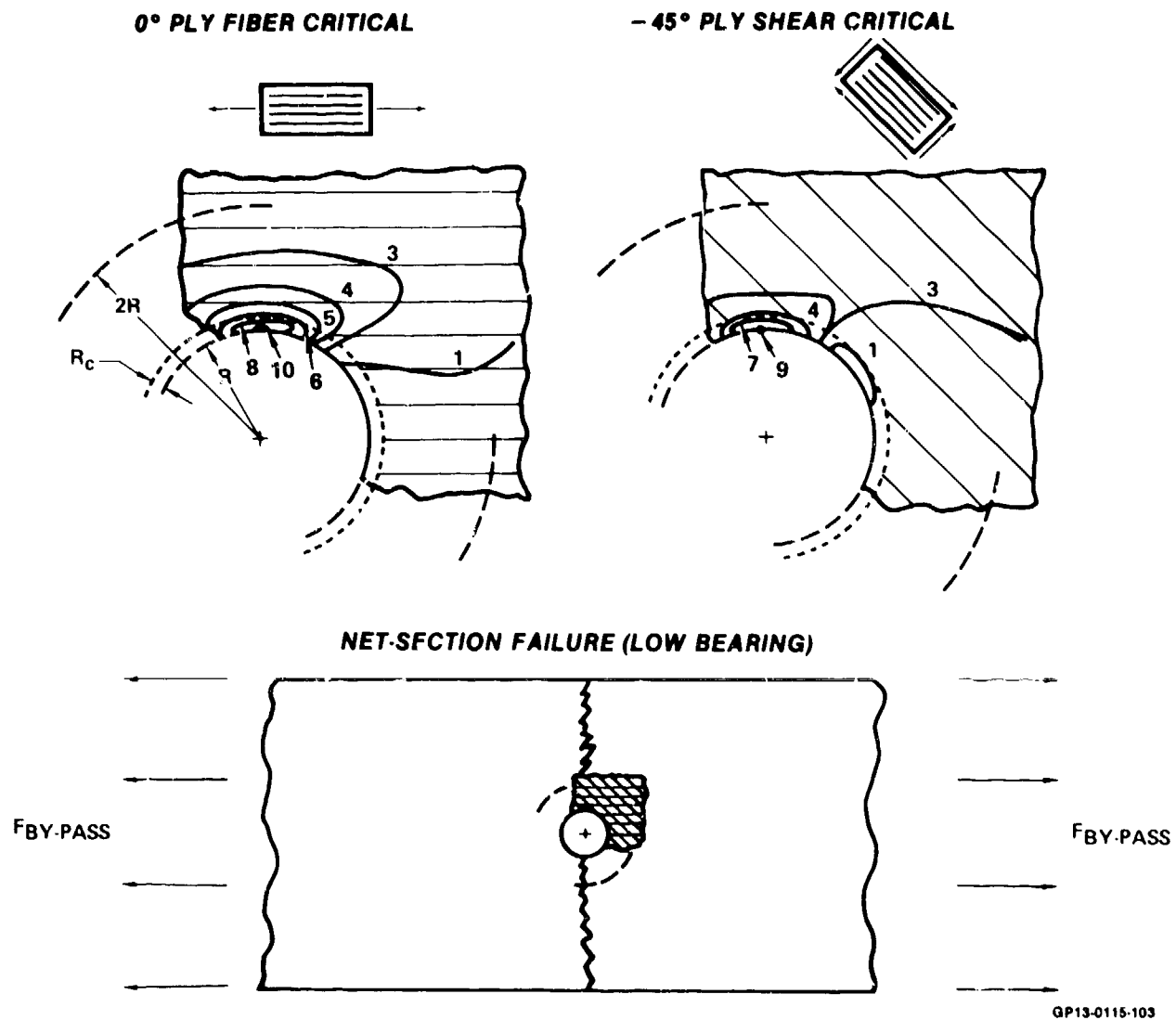


Figure 58. Predicted Critical Piles for Net-Section Failures

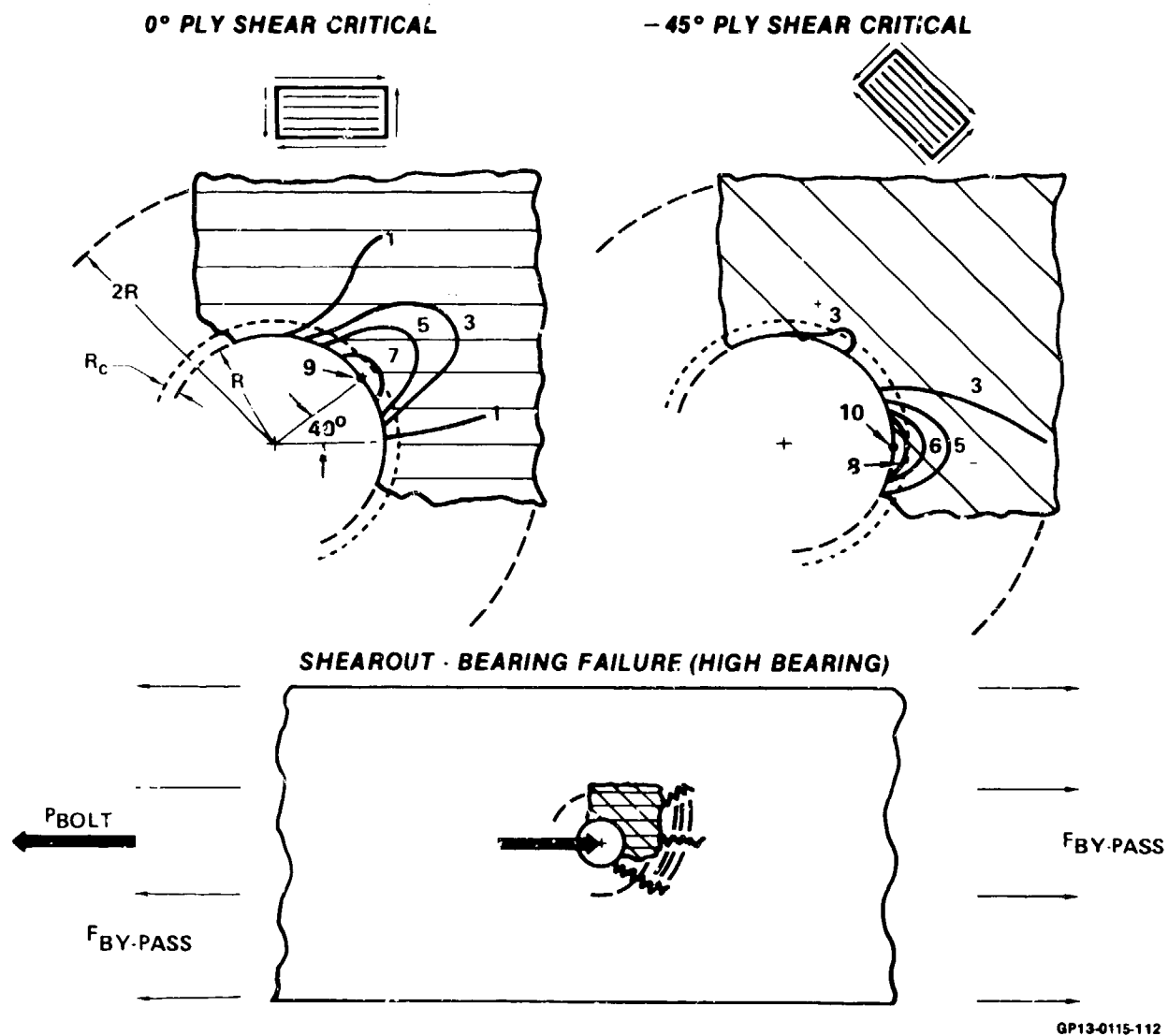
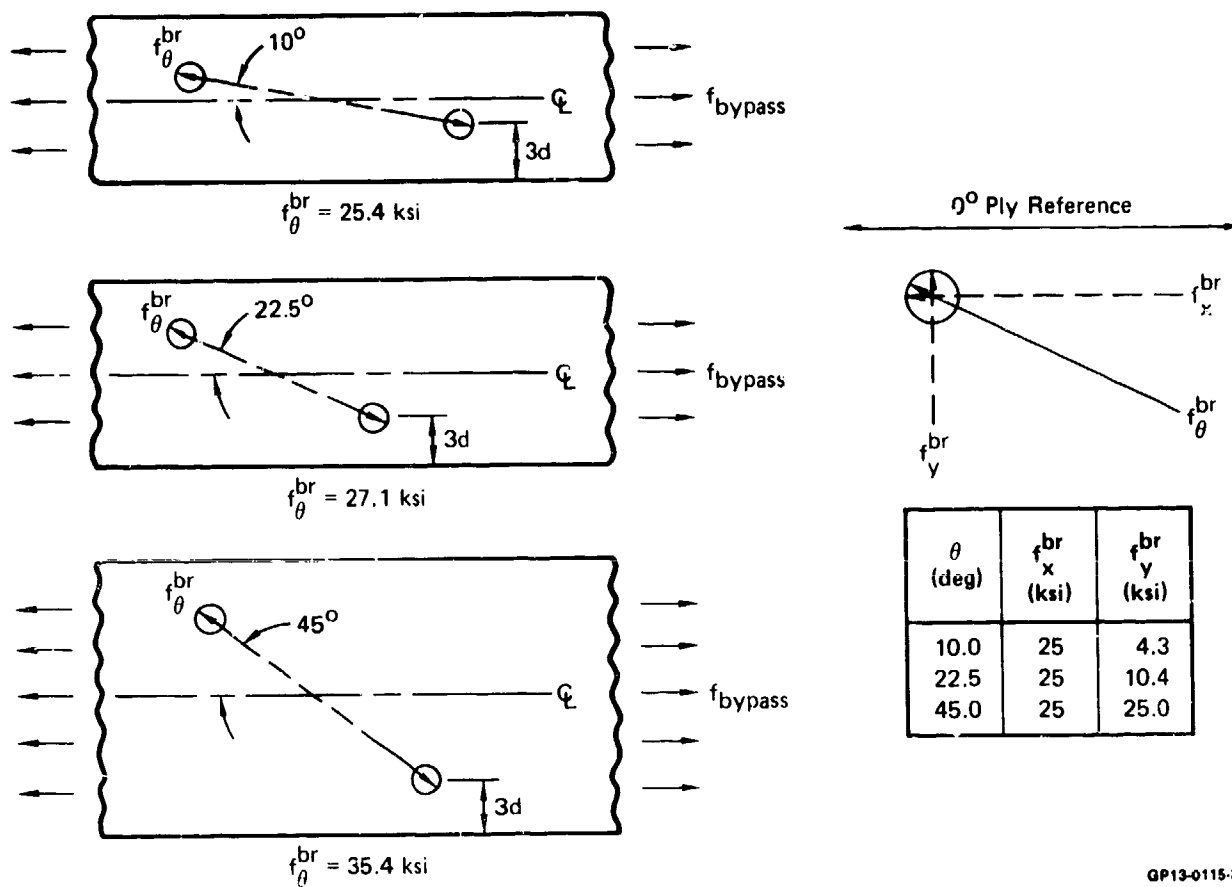


Figure 59. Predicted Critical Piles for Bearing-Shearout Failures



Figure 60. Tests Verify Predicted Failure Initiation Points

The second evaluation examined effects of increasing off-axis bearing stress on laminate bypass strength. For the 50/40/10 laminate, bearing stresses of approximately 25, 27, and 35 KSI were applied to a .250 inch diameter fastener hole at off-axis angles of 10°, 22.5°, and 45° respectively. Bypass loading parallel to the 0° principal material axis was increased from 0.0 pounds until static failure occurred. The resultant bearing loads, and angles of application, were selected to maintain a constant 25 KSI bearing stress component (f_x^{br}) parallel to the bypass loading, while perpendicular bearing stress components (f_y^{br}) increased to values of 4, 10 and 25 KSI (Figure 61). Theory and test data are correlated in Figure 62. For these bearing stresses, all failures were in a net-section mode.



GP13-0115-31

Figure 61. Load Conditions for Off-Axis Load Interaction Tests

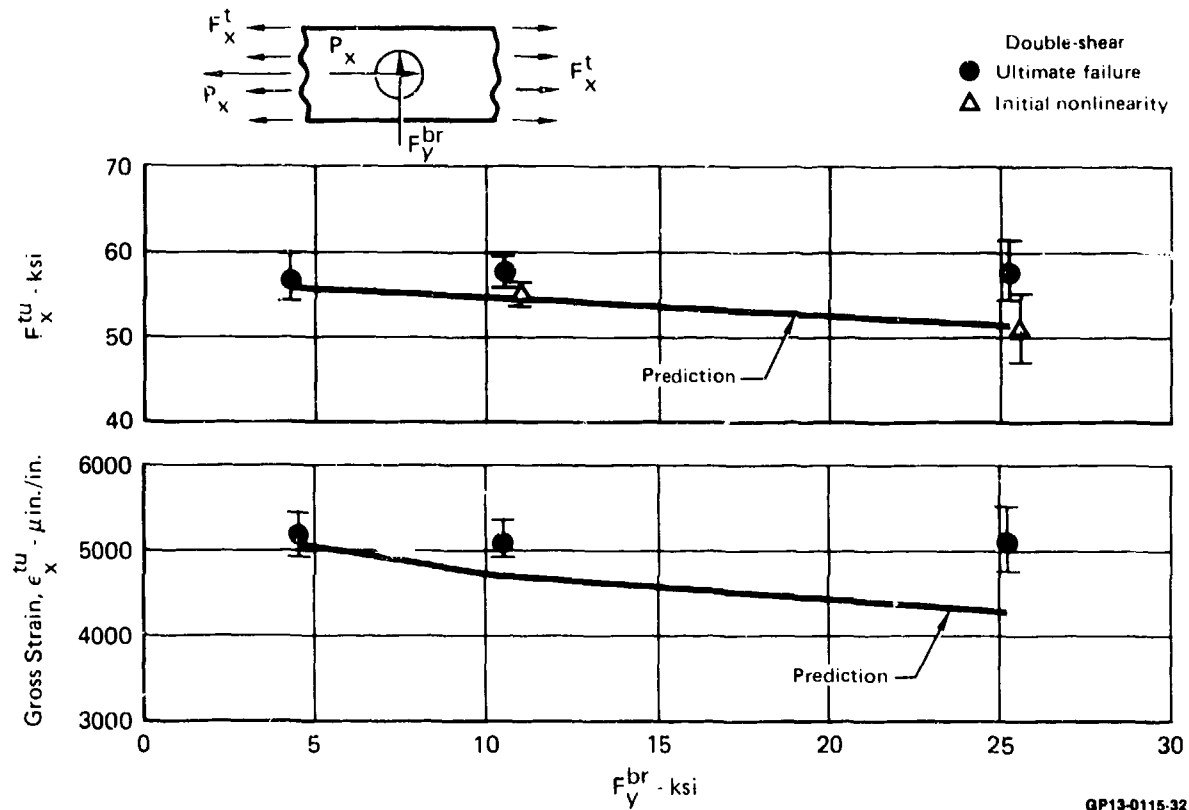


Figure 62. Effect of Off-Axis Bearing Loads on Bypass Strength

For both load-interaction studies, at increased bearing loads, ultimate strengths occurred after initial nonlinearities were observed in joint load-deflection plots. Predicted strengths, based on the linear-elastic EJSFM analysis, correlated with the initial nonlinear indications. High bypass loads with zero to low bearing caused joint net-section failures with plies predicted critical due to excessive fiber strain. Joint load-deflection behavior was linear with catastrophic failure occurring at predicted first ply fiber rupture. At higher bearing stresses, plies were predicted critical due to excessive shear stress, a typically nonlinear ply property. This correlated with observed joint failures which were in bearing or bearing-shearout with nonlinear load-deflection behavior. Failures were localized at the fastener hole with load redistribution occurring prior to failure.

(g) Fastener Pattern - Stress concentration interactions were evaluated using a four-fastener specimen (reference Figure 41). Edge distances and fastener spacings were 3 and 4 diameters respectively. Column spacing was 4 diameters. All fasteners were .250 inch in diameter and specimens were tested to failure at RTD and ETW conditions. Steel, aluminum, and titanium load blocks for the four-fastener specimens were designed to provide joint stiffness ratios between the metal load blocks and the Gr/Ep specimen of approximately 10, 5, and 1 respectively. Test setups are illustrated in Figure 63.

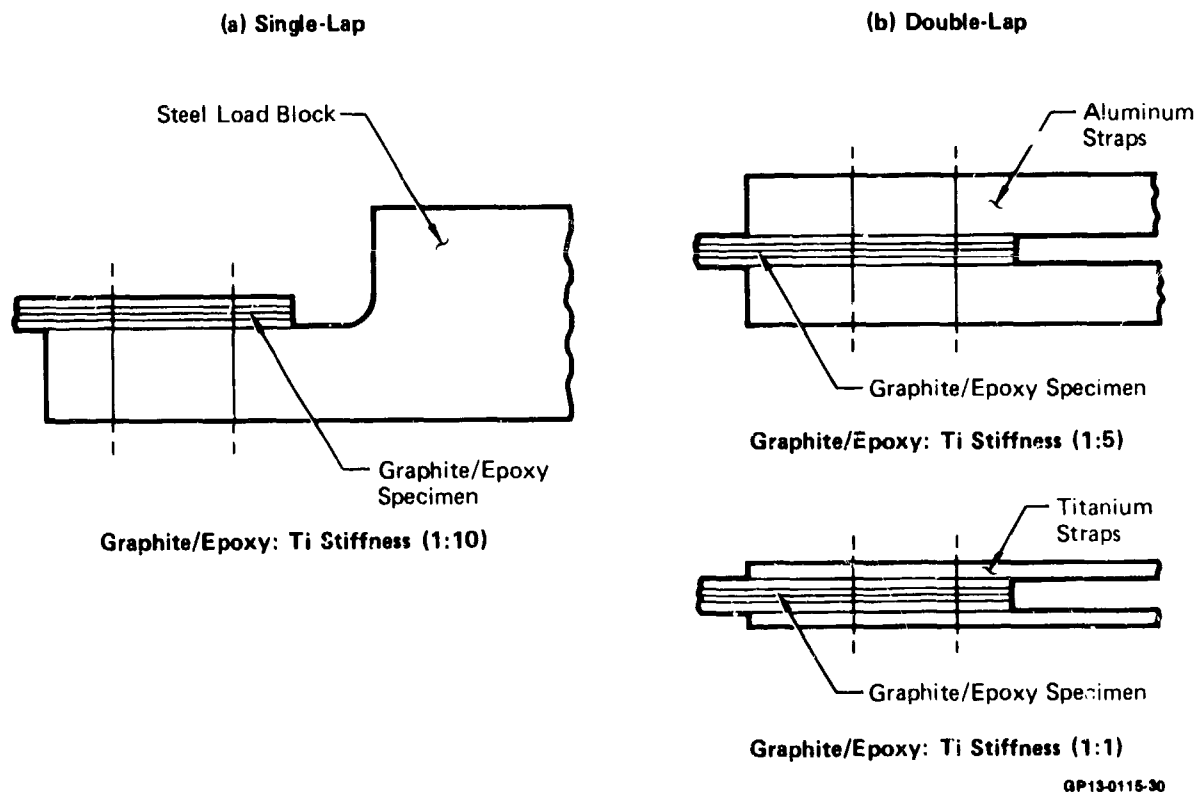
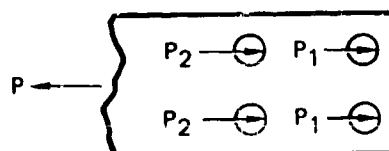





Figure 63. Fastener Pattern Specimen Loading Configurations

Tension strengths are presented in Figure 64. No significant variations in internal load distributions due to variations in joint stiffness were evident. Predicted bolt-loads indicated that the graphite-to-aluminum joint strength should be approximately 4% higher than the graphite-to-titanium joint; however, a slight reduction (6-8%) was noted in test. Based on data from single and two-fastener specimens, small variations in internal bolt-load distribution are probably masked by joint nonlinearities which occur prior to failure. Single-shear joint strengths were similar to the double-shear strengths at RTD, and lower (13-20%) than double-shear strength at ETW. Single-shear joint failures were predominantly shearout. For double-shear joints, failures tended to shift to net-section tension or tension-cleavage as is illustrated in Figure 65. Strengths and failure modes of the single-shear joints reflect joint eccentricity effects. Because bolt-bending was minimal, a physical variable which could account for strength and mode differences is the double lap arrangement of the metal loading members. This arrangement inhibits initiation of localized damage at the fastener hole due to bearing or shearout and creates additional friction load paths.

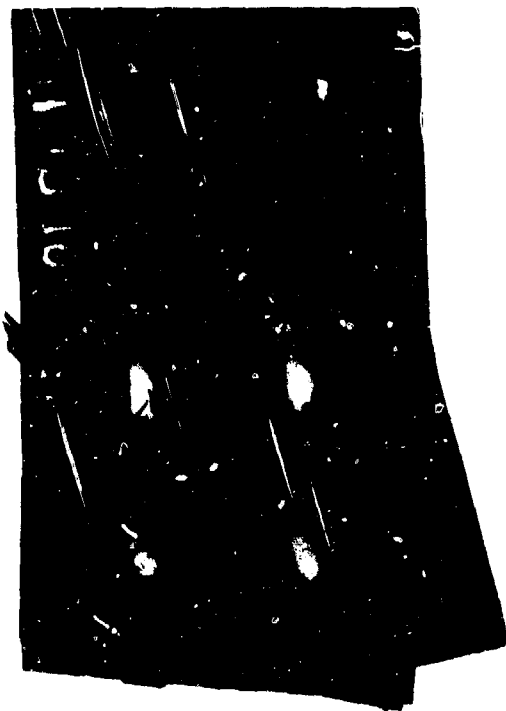


Layup	Configuration	RTD		ETW	
		F_{x2}^{bru} (ksi)	ϵ_{xGross}^{tu} ($\mu in./in.$)	F_{x2}^{bru} (ksi)	ϵ_{xGross}^{tu} ($\mu in./in.$)
30/60/10	Steel Load Block 	123 90	5,470 4,700	110	5,110
50/40/10	Steel Load Block 	130 111	4,350 3,350	101	3,380
50/40/10	Graphite/Epoxy-Ti	133	4,350	112	3,880
50/40/10	Graphite/Epoxy-Al	139	4,610	122	4,220
50/40/10	Graphite/Epoxy-Al (Salt Exposure)	—	—	123	4,580

 T300/5208; all others AS/3501-6

GP13-0115-20

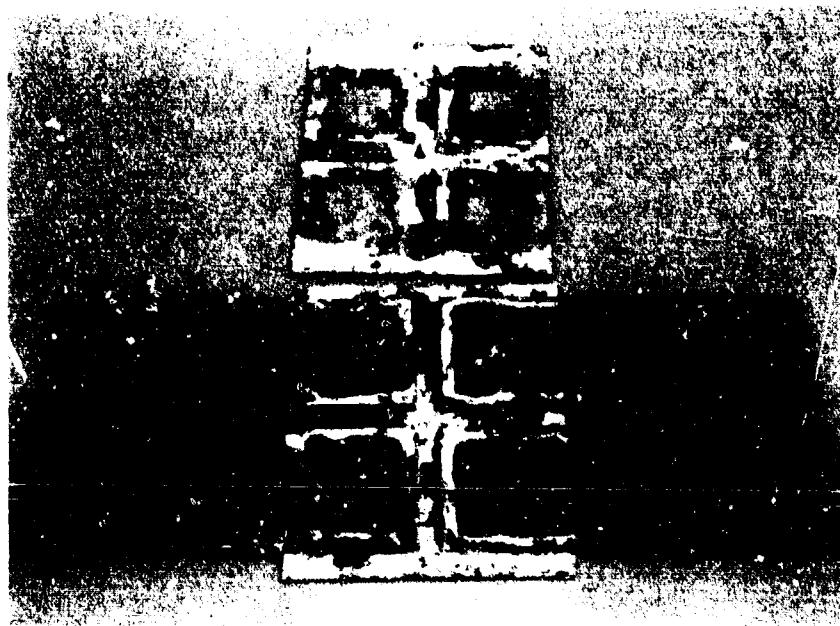
Figure 64. Effects of Environment on Fastener Pattern Joint Strength



GP13-0115-85

Figure 65. Joint Failures for Fastener Pattern Specimens

A limited examination of the galvanic effect of salt-water exposure on graphite-to-aluminum joints was performed with the four-fastener specimen. Specimens were attached to 7075-T76 aluminum plates and exposed to a 5% NaCl salt spray at 95°F. Setup was exposed for 34 consecutive days. Visual appearance after the exposure is indicated in Figure 66. As expected, the exposure resulted in corrosion of the aluminum parts. Because composite member strength was the issue of question, specimens were then attached to pristine aluminum members in a double-lap configuration and tested to static failure at 250°F under tension loadings. As indicated by strength results shown in Figure 64, composite member strength was unaffected by the salt spray exposure.



GP13-0115-86

Figure 66. Corrosion Resulting from Salt-Spray Exposure

Two additional sets of specimens were fabricated from T300/5208 graphite-epoxy in the 50/40/10 and 30/60/10 laminate configurations. These specimens were tested to failure in tension at room temperature. Relative to the AS/3501-6 data, failure modes were similar, but strength values were lower by approximately 14-23 percent (Figure 64).

(h) Torque-Up - Effects of torque-up on bearing strength were evaluated for three layups. In addition, pure bearing (single fastener) and two-fastener-in-tandem (bearing plus bypass) double shear specimens were tested with torque-up values ranging from 0 to 70 inch-pounds.

Pure bearing strengths and associated failure strains are compared in Figure 67. All layups failed in shearout-bearing. Representative failures are illustrated in Figure 68. Layup sensitivity to torque-up appeared to be related to percentage of 0° plies (or lack of $+45^\circ$ plies). For the three layups of 30, 50, and 70 percent 0° plies, respective increases in bearing strength at 50 inch-pounds of torque-up over pin conditions were approximately 15, 21, and 30 percent.

Pure bearing and unloaded hole failure strain data are compared in Figure 69. Higher percentages of 0° plies cause increased strain concentrations which lower laminate gross strain capability. Resulting unloaded hole gross strain concentration factors (K_t 's) range from 2.44 for the 70/20/10 layup, to 2.1 for the 30/60/10 layup, with pure bearing K_t 's respectively of 10.2 and 3.5 for fasteners having 50 inch-pounds torque-up. Removing torque-up entirely increased the effective K_t under pure bearing to 13.6 and 4.1 respectively.

In addition to bearing strength, joint load-deflection plots were examined for nonlinear mechanical response. Points of initial nonlinearities are plotted with ultimate bearing strengths in Figures 70, 71 and 72. Although scatter bands are wider, unlike ultimate strength data, the load values at initial nonlinearities appear to be less affected by torque-up. This correlation of predicted first ply shear failure indicates that joint nonlinearities are associated with localized failure of plies at the hole boundary. For this calculation, the previously determined value of .02 inch was used as the characteristic dimension in conjunction with the maximum strain failure criterion. Strengths of the two-fastener-in-tandem specimens are compared in Figure 73 with pure bearing strengths.

(i) Fastener Countersink and Laminate Thickness - Effects of countersinks on laminate bearing strength were evaluated over a range of countersink depth-to-laminate thickness ratios (.77, .38, and .26). Test specimens were of a single-fastener pure bearing configuration having a .375 inch diameter fastener with the laminate loaded in double-shear. As-manufactured specimens were tested in tension to failure at room temperature. Layup stackings, detailed in Figure 26 were integer multiples of the 50/40/10 baseline 20 ply stacking sequence. These same 40 ply and 60 ply layups were further used to evaluate the effects of thickness without countersinks. The double-shear specimen configuration was used and specimens were loaded to failure in tension and compression. Test conditions included RTW and ETW. RTD strengths are presented in Figure 74. Within data scatter, effects of countersink versus noncountersink on strength appear to be insignificant for the 50/40/10 laminate. However, initial points of nonlinearity indicate a 50% lower onset for countersink 20 ply laminates, becoming less pronounced at the 40 ply thickness and disappearing at the 60 ply thickness. These

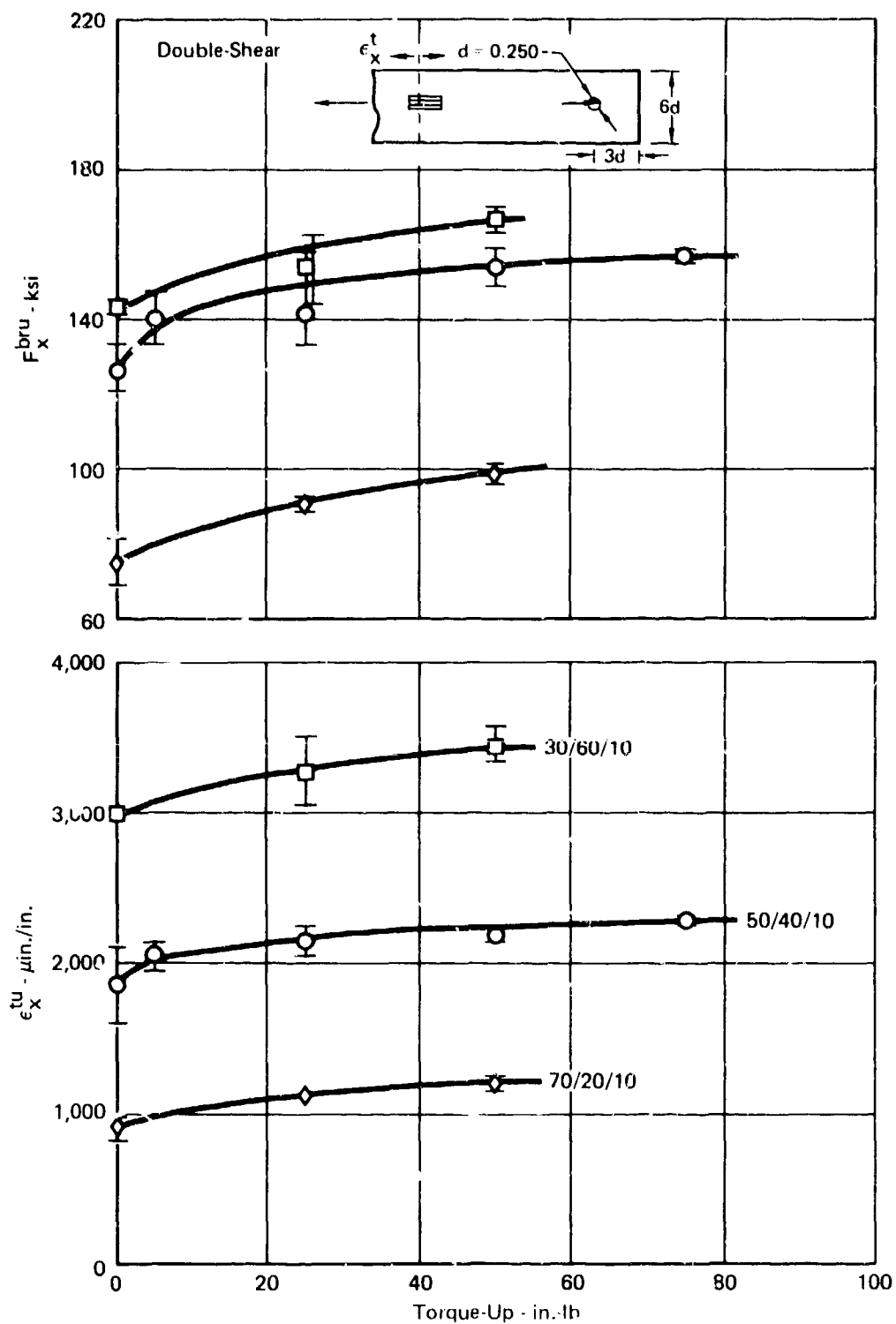
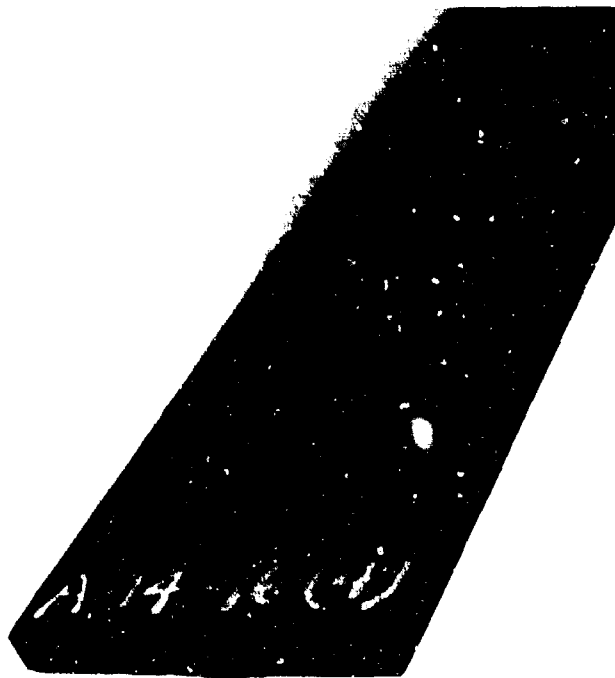


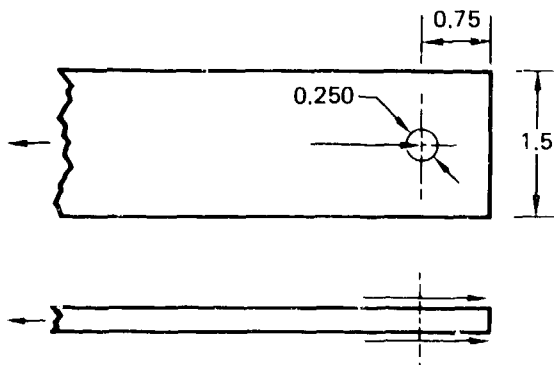
Figure 67. Effects of Layup and Torque-Up on RTD Pure Bearing Strength



70/20/10 Layup



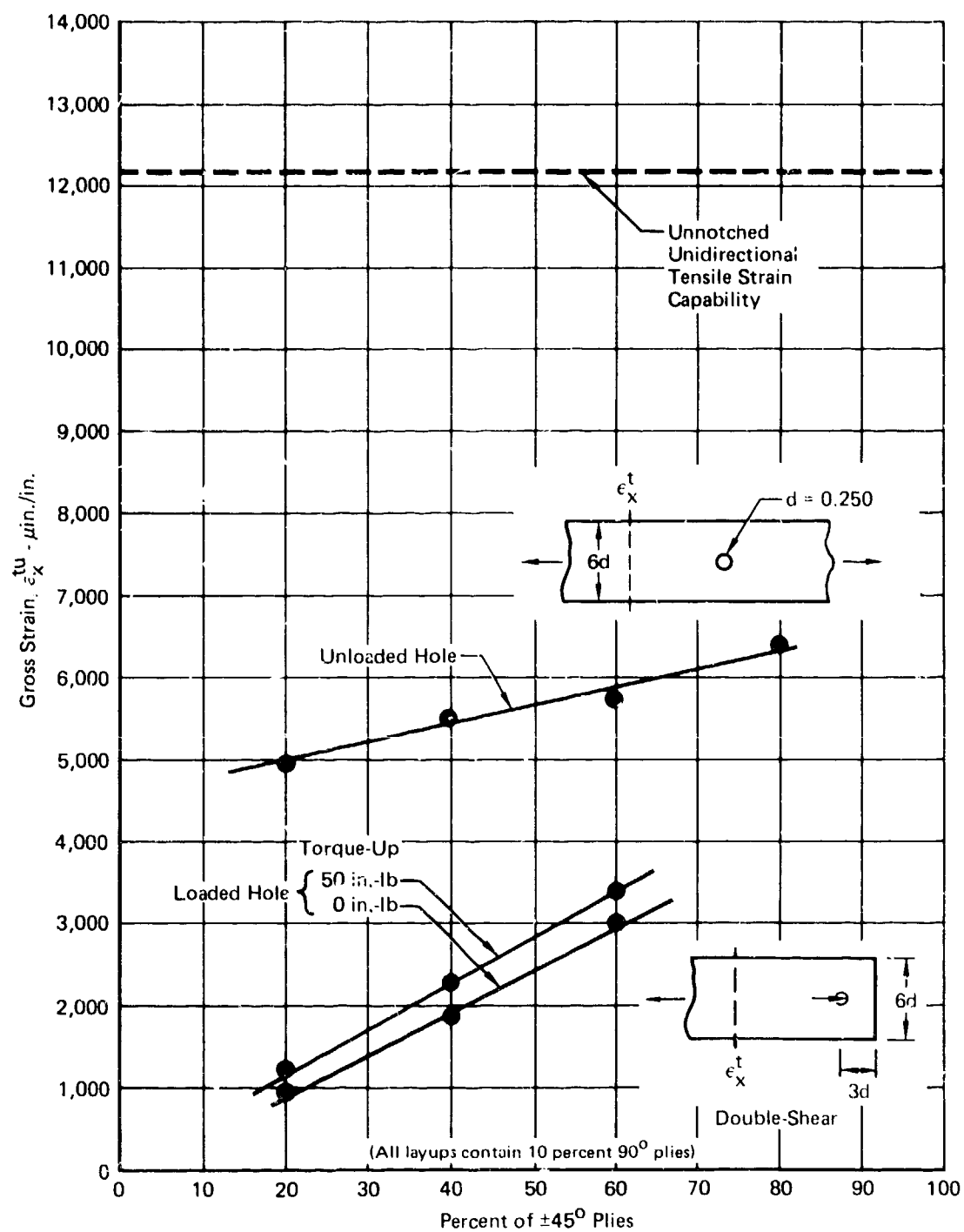
50/40/10 Layup



30/60/10 Layup

GP13-0115-87

Figure 68. Failures of Pure Bearing Specimens



GP13-0115-77

Figure 69. Comparison of Loaded and Unloaded Hole Specimen Strengths

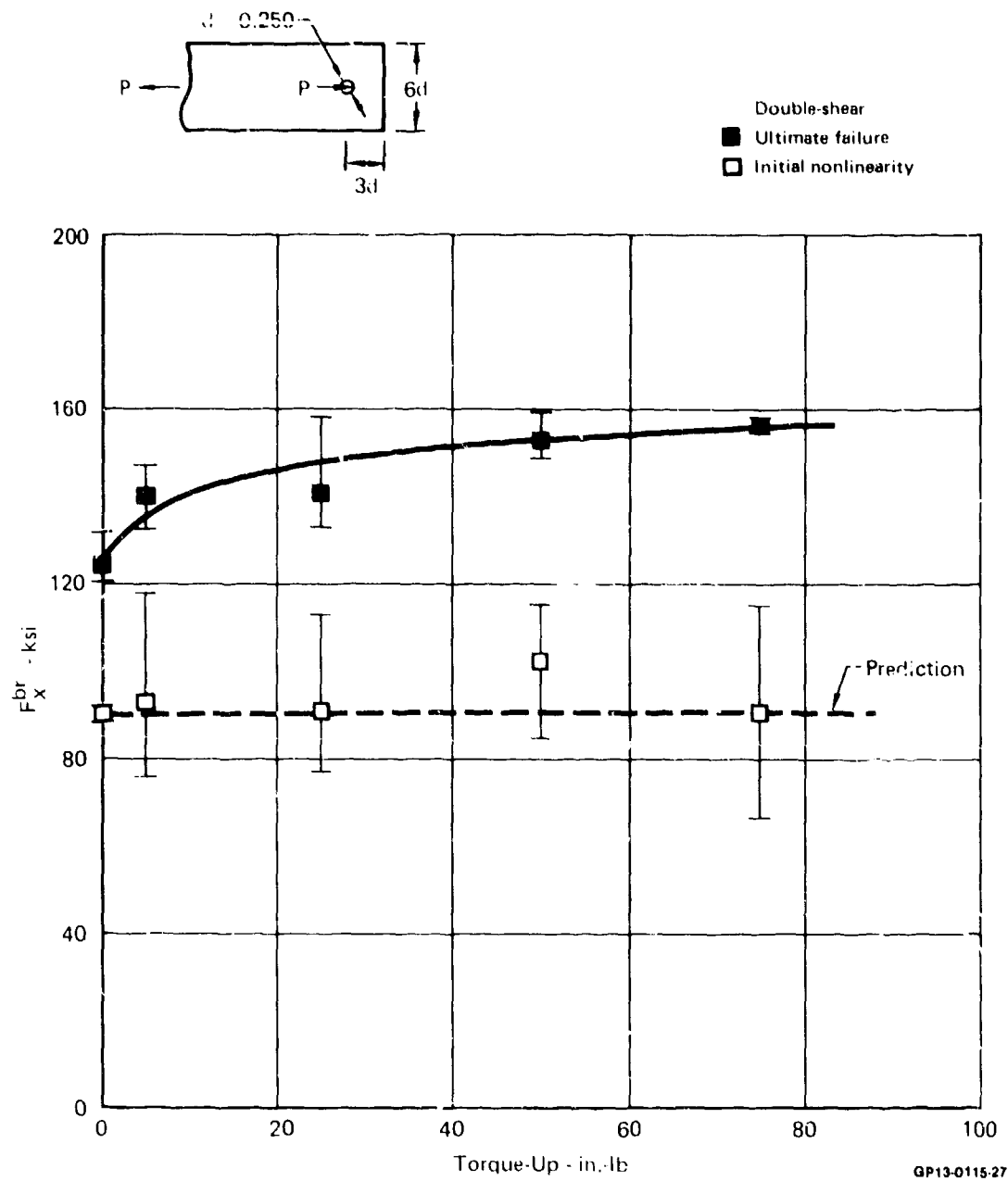


Figure 70. Effect of Torque-Up on RTD Pure Bearing Strength
50/40/10 Layup

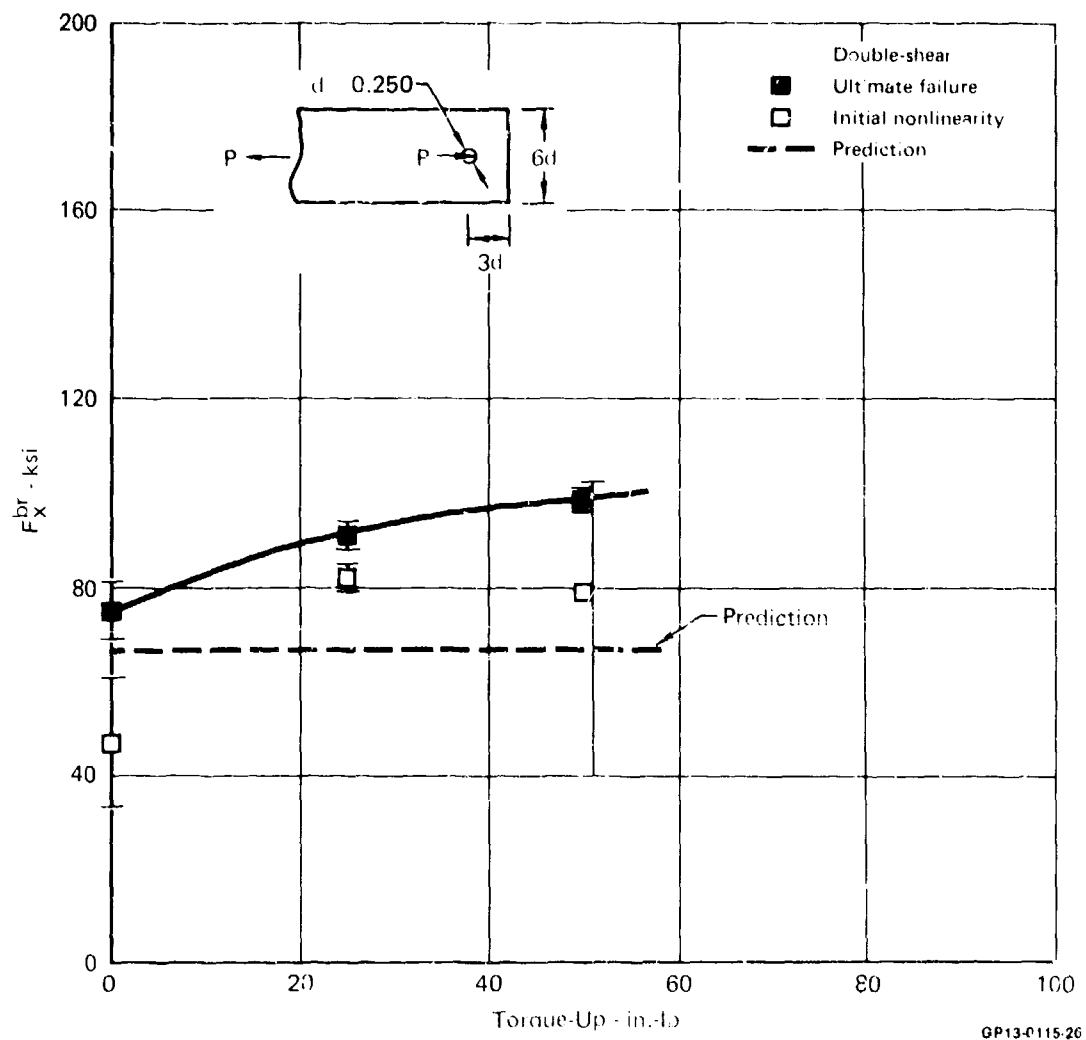
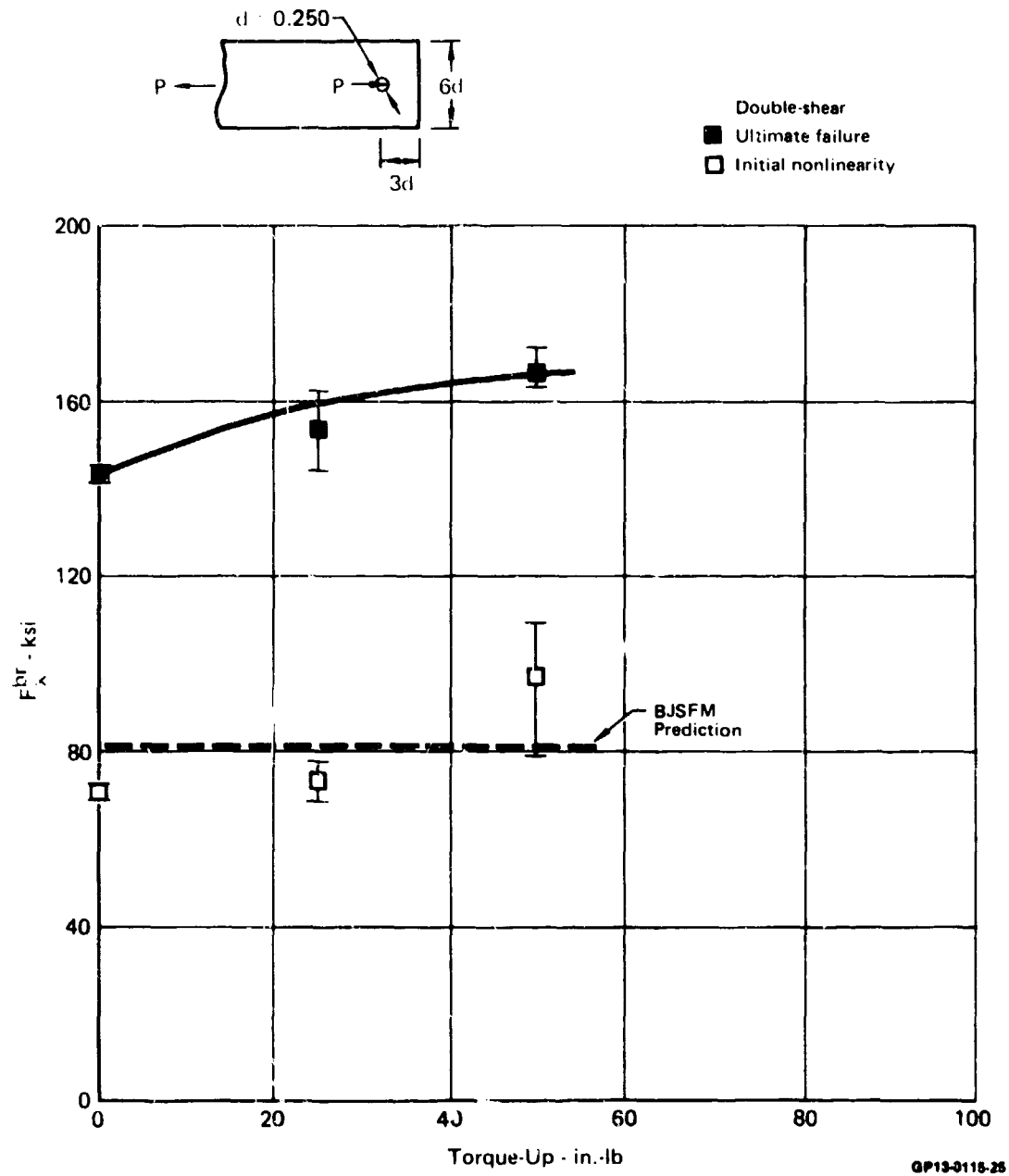
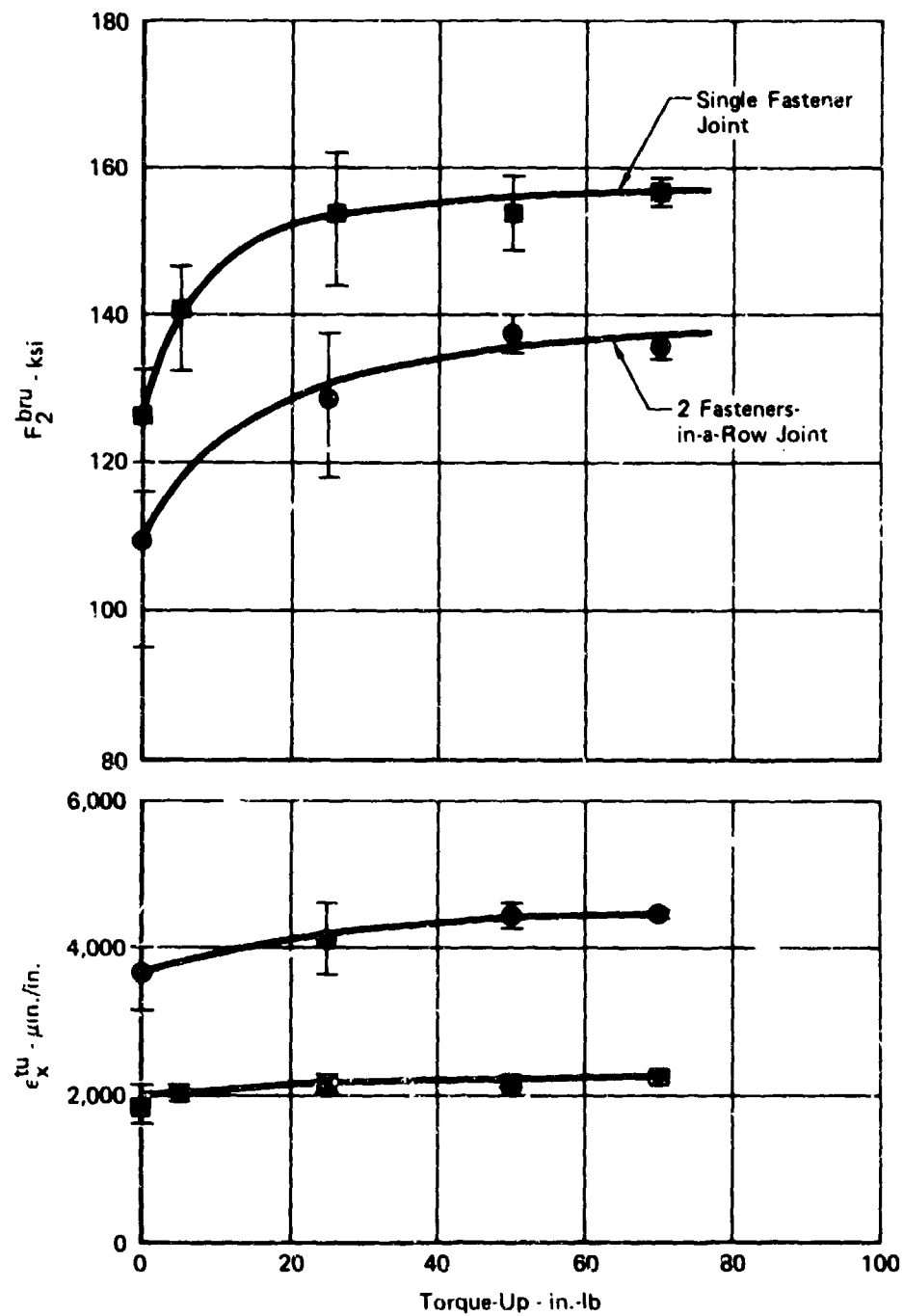
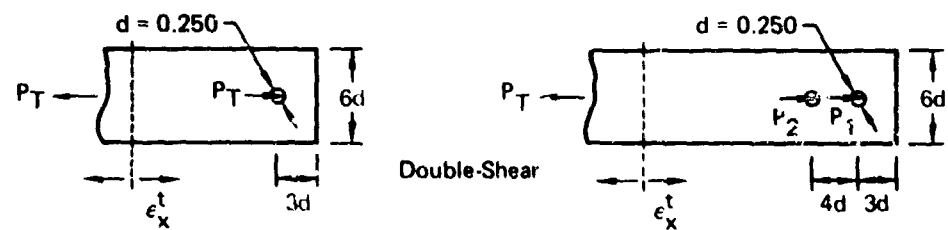


Figure 71. Effect of Torque-Up on RTD Pure Bearing Strength
70/20/10 Layup



**Figure 72. Effect of Torque-Up on RTD Pure Bearing Strength
30/60/10 Layup**



GI 13-0118-24

Figure 73. Comparison of Effects of Torque-Up on RTD Joint Strength

trends indicate the expected effect of local countersink geometry on linear-elastic stress distributions, with differences vanishing due to subsequent joint nonlinear behavior prior to specimen failure.

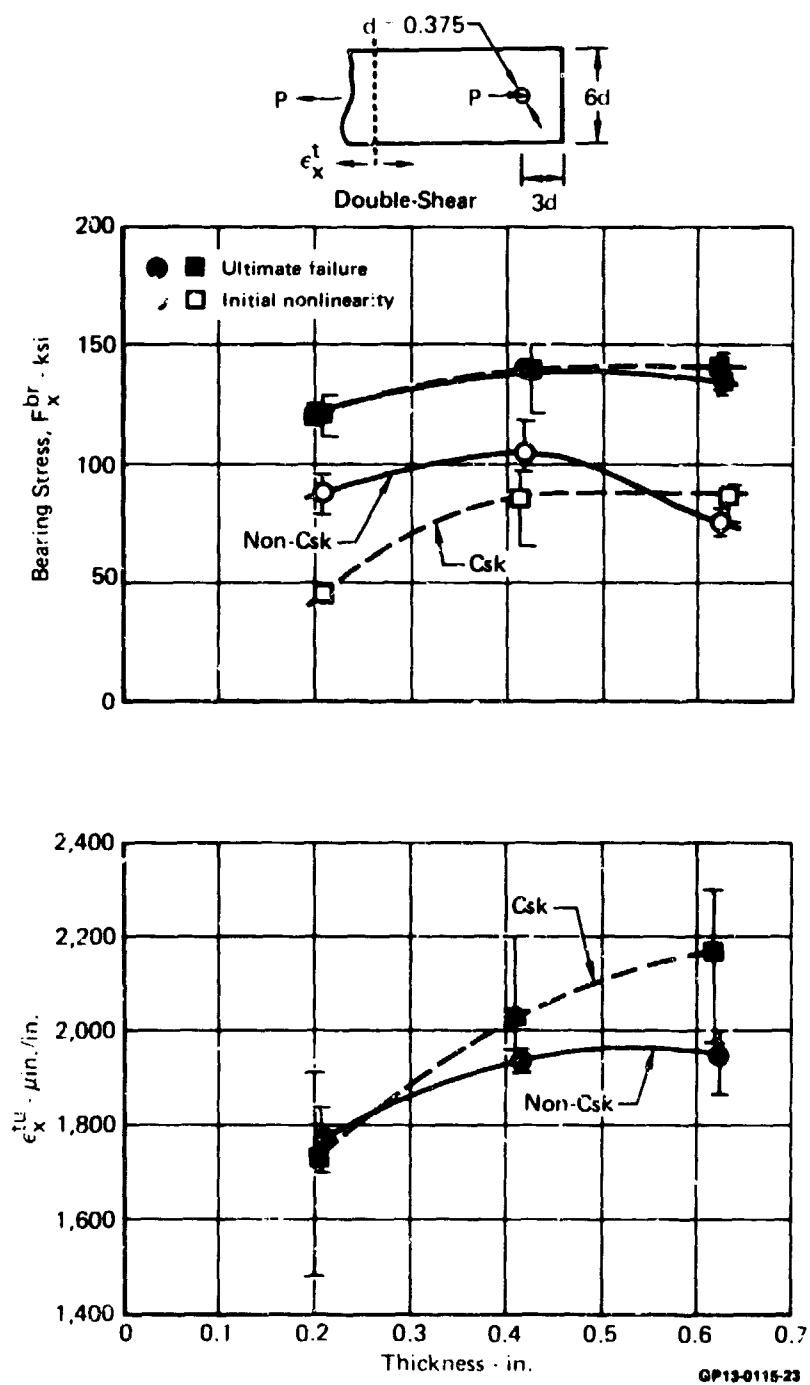


Figure 74. Effect of Thickness and Countersink on Joint Tensile Strength

(j) Stacking Sequence - Five variations of the 50/40/10 layup were tested in pure bearing. Specimens were loaded to failure at room temperature in tension and compression. Effects of moisture content (approximately .8% by weight) and elevated temperature (250°F) on bearing strength were evaluated for tensile loading. The 50/40/10 layup stacking sequences are detailed in Figure 26. The primary variation in stacking sequence was separation of 0° plies.

Tension strengths are presented in Figure 75. Lowest strength values are associated with layups having 60% and 100% of their 0° plies grouped. This type of stacking increases intralaminar shear stresses between each group of 0° plies and the remaining +45° or 90° plies. The dominance of this factor is illustrated in Figures 76 and 77. Both tension RTD and ETW strength trends are presented relative to the maximum percent of grouped 0° plies contained in the 50/40/10 layup. Data trends indicate a linear dependence on 0° ply groupings. Predicted bearing strengths are shown in both plots as a constant value. Effects of through-the-thickness variables on stress distributions are not accounted for in current BJSFM methodology.

For RTD compression data, strengths are plotted versus maximum percent of grouped 0° plies in Figure 78. While compression strength data indicated a linear relation, fastener bearing stresses are quite different than stresses in the previous tensile specimens. While groupings of 0° plies do affect joint compression strength, it would not appear to be through a presence or lack of intralaminar shear planes.

(k) Single-Shear Loading - A comparison of joint single shear versus double-shear strength is presented in Figure 79. Initial points of nonlinearity indicate the expected decrease in joint strength associated with increased joint eccentricity. However, laminate bearing strength at joint failure exceeded bolt shear strength capability in the .250 inch protruding-head single-shear configuration, and composite member failure trends could not be quantified. Single-shear joint strength versus variations in e/w ratios is plotted in Figure 80.

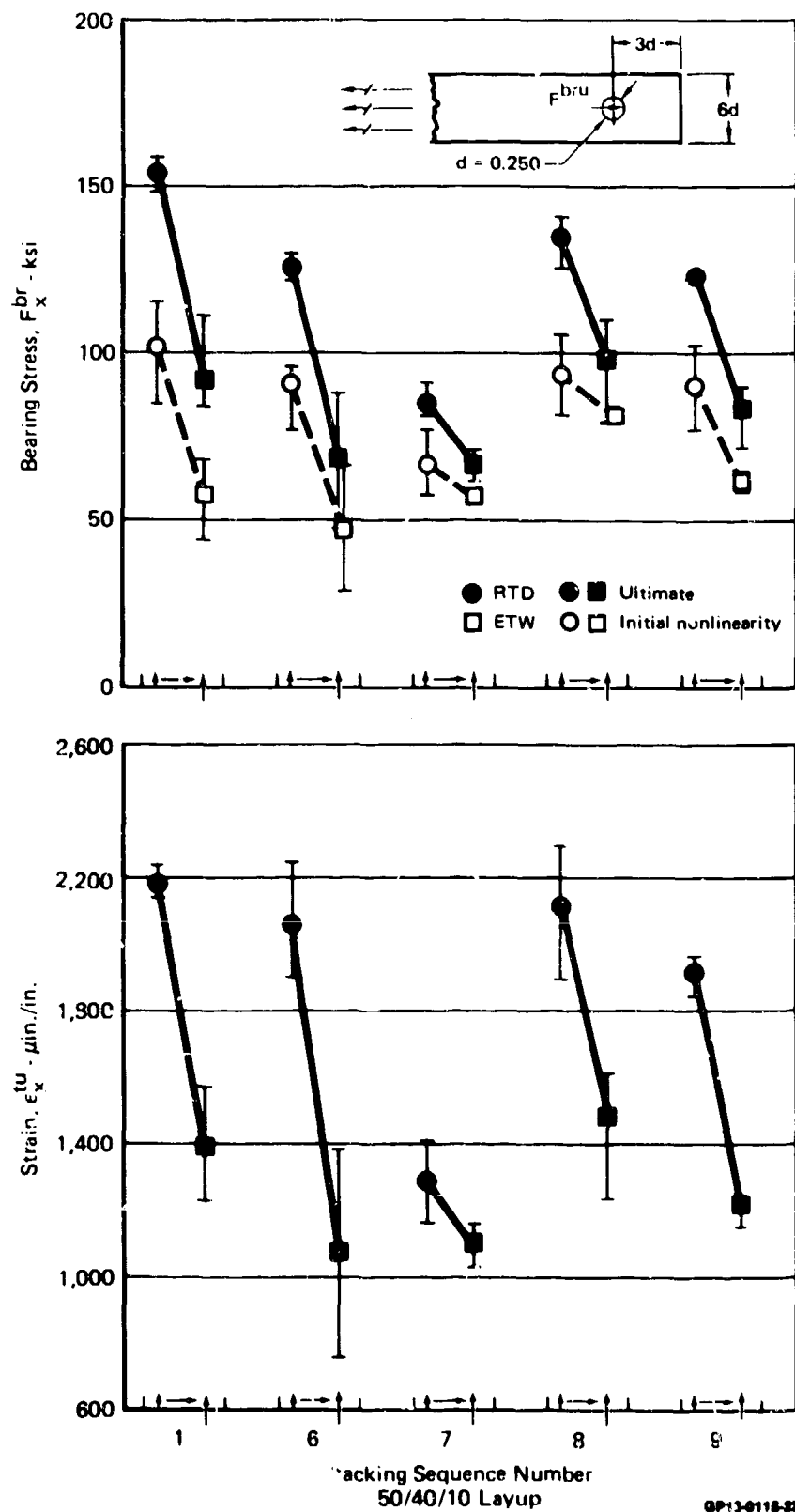


Figure 75. Effect of Stacking Sequence on Joint Tensile Strength

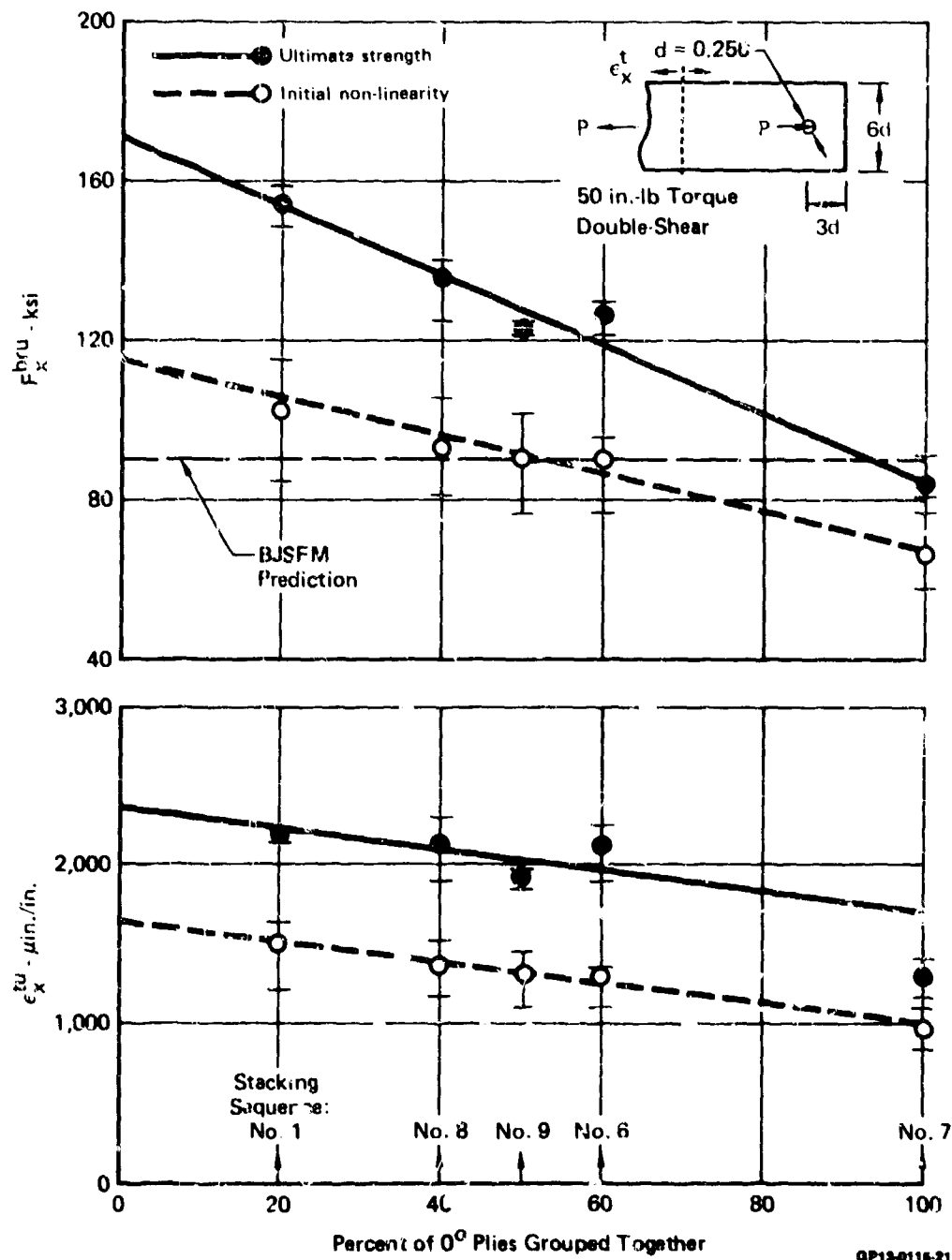


Figure 76. Correlation of Joint RTD Tensile Strength with Grouped 0° Plies

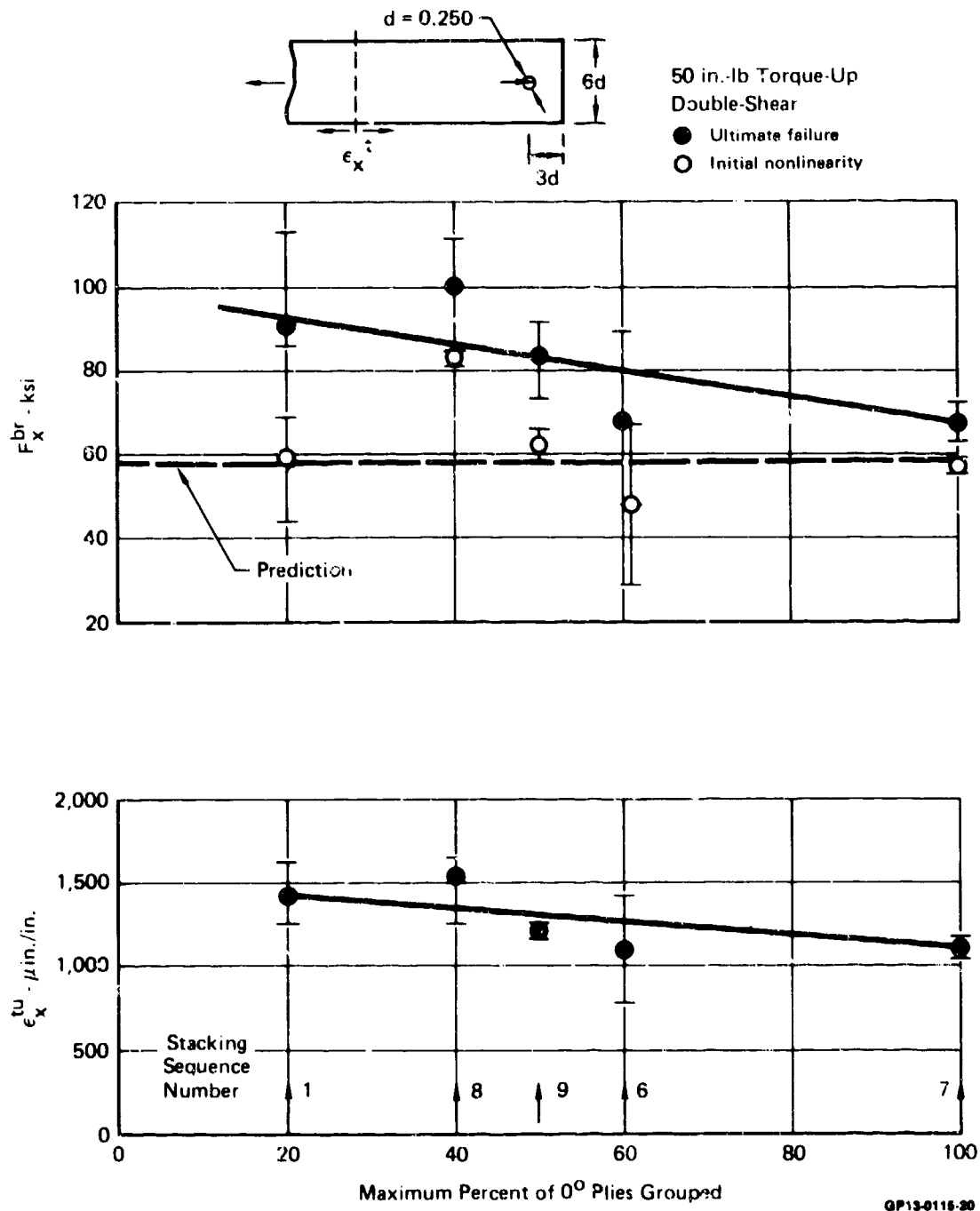


Figure 77. Correlation of Joint ETW Tensile Strength with Grouped 0° Plies

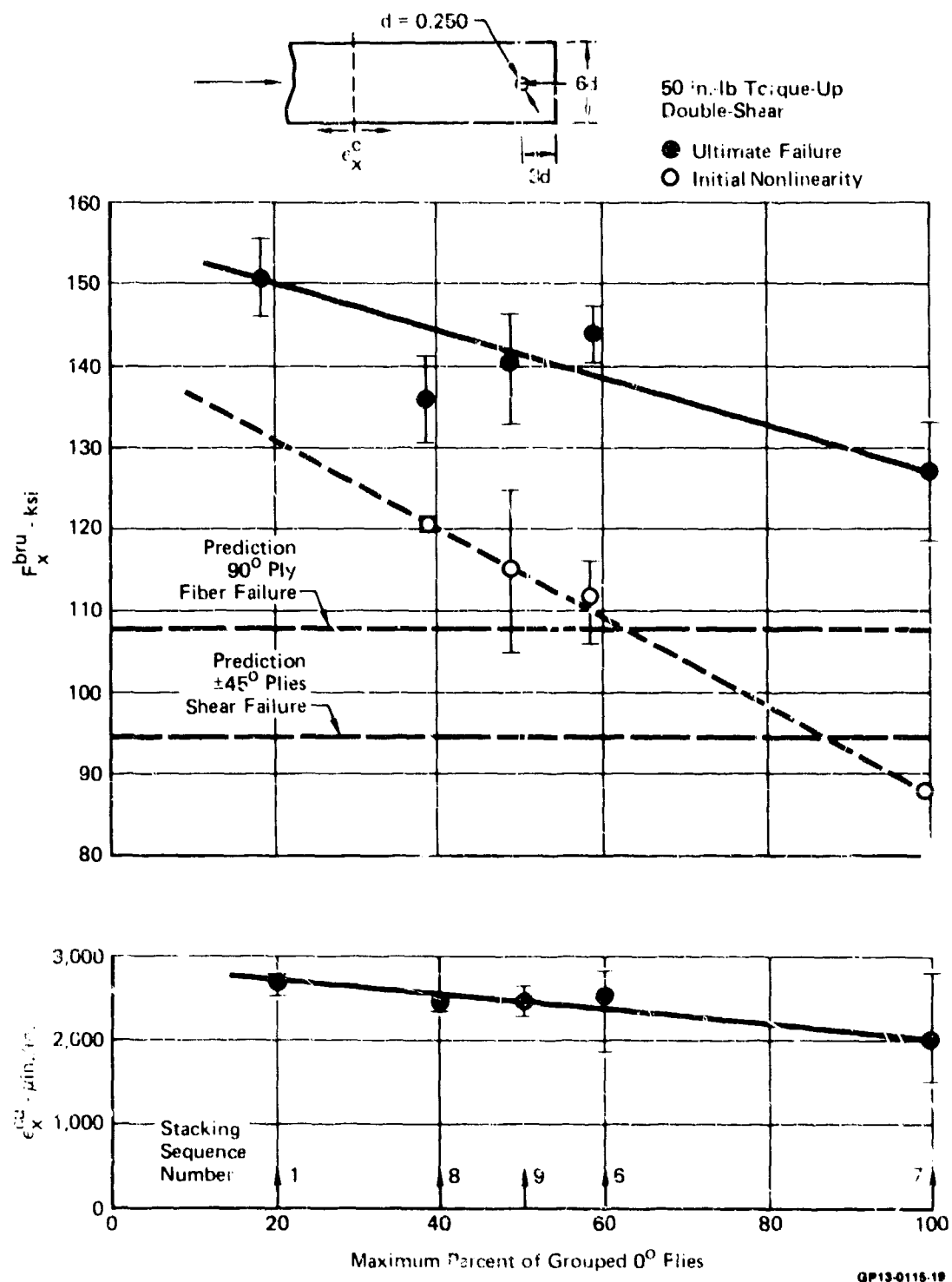


Figure 78. Correlation of Joint RTD Compressive Strength with Grouped 0° Plies

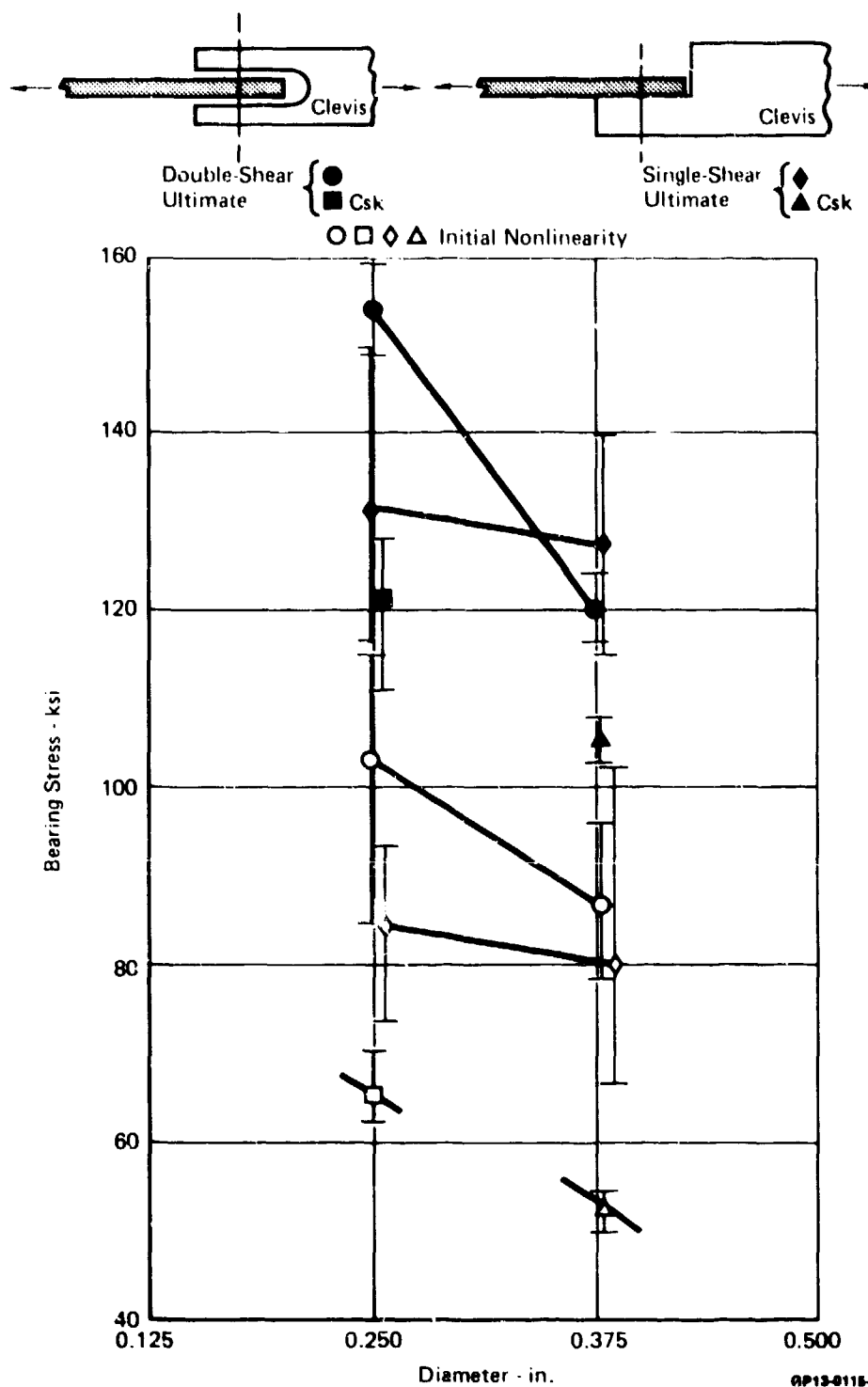


Figure 79. Comparison of Single and Double-Shear Joint Strengths

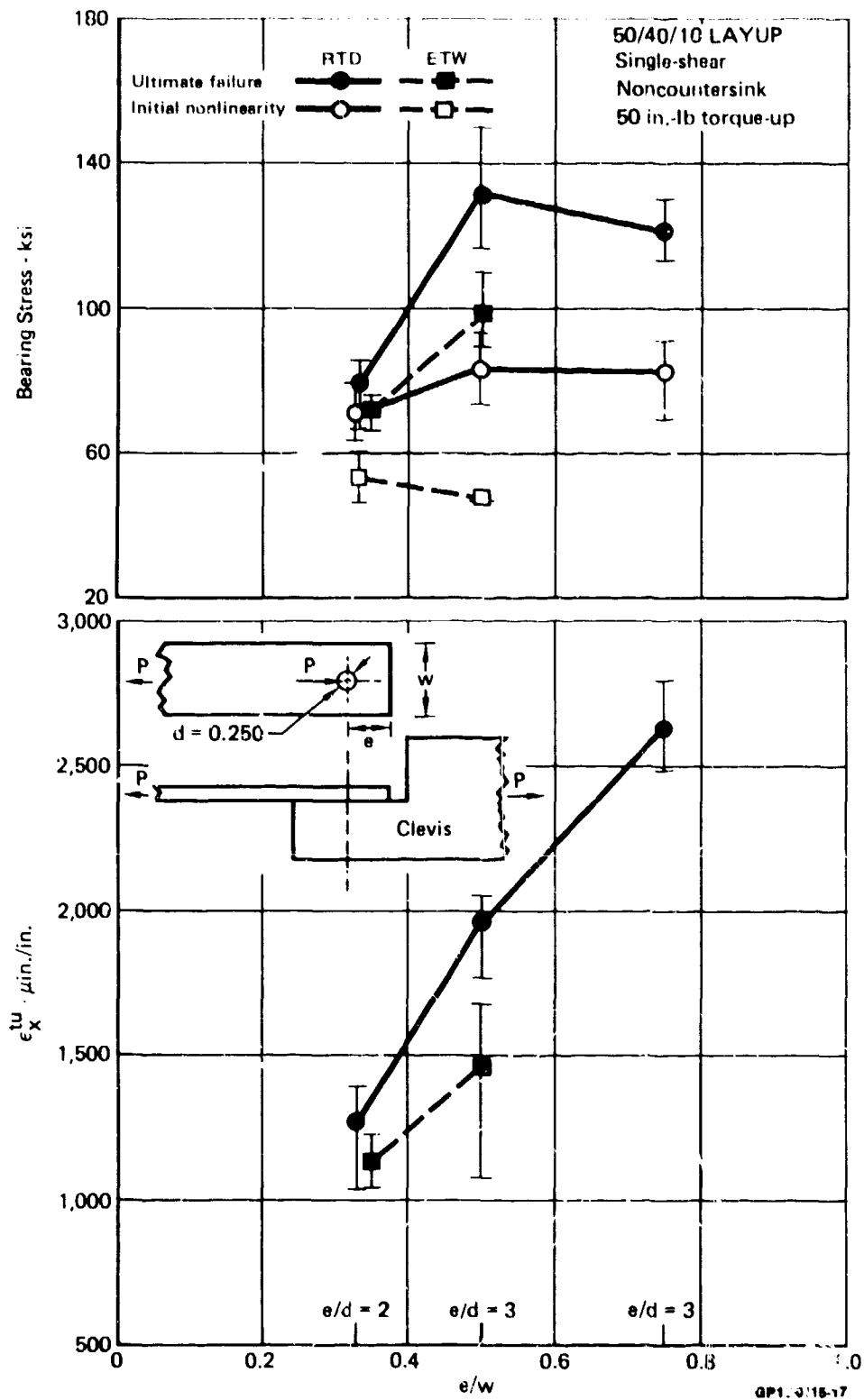
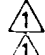





Figure 80. Correlation of Joint Strength with Edge Distance-to-Width Ratios

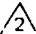
2. EVALUATION OF MANUFACTURING AND SERVICE ANOMALIES - TASK 3

In this task, the effect of common manufacturing and service anomalies on joint static strength were evaluated. The selection of the seven bolted joint anomalies was based on MCAIR experience and results of an industry-wide survey conducted as part of the "Advanced Composite Serviceability Program" (Reference 2). Data from Task 3 were compared with baseline joint strengths (no anomaly) determined from tests performed in Task 2.

a. Task 3 Test Plan - The objective of Task 3 was to evaluate the effects of manufacturing and service anomalies on bolted composite joint static strength. Only laminate quality or hole quality was varied for Task 3 testing. Test Matrix details are provided in Figure 81.

Anomaly		Number of Tests Per Environment			Total Specimen Tests
		RT (Dry) Tension	RT (Wet) Compression	ET (Wet) Compression	
1. Out-of-Round Holes					
"1" Laminate (50/40/10)		4	—	—	4
"2" Laminate (30/60/10)		4	—	—	4
2. Broken Fibers on Exit Side of Hole					
Severe Delamination		4	4	4	12
Moderate Delamination		4	4	4	12
3. Porosity around hole					
Severe Porosity		4	2,2 	4	12
Moderate Porosity		—	2,2 	4	8
4. Improper Fastener Seating Depth					
80% of Thickness		4	—	—	4
100% of Thickness		4	—	—	4
5. Tilted Countersinks					
Away from Bearing Surface		4	—	4	8
Toward Bearing Surface		4	—	4	8
6. Interference	Layup 1	4	—	4 	8
	Fit Tolerances 1	4	—	4	8
	0.003 in. Interference 2	4	—	4	8
	0.008 in. Interference 2	4	—	4	8
7. Fastener Removal and Reinstallation					
100 Cycles		4	—	4	8
Total					116

 After freeze-thaw cycling

 Tension tests

GP13-0115-110

Figure 81. Task 3 - Evaluation of Manufacturing Anomalies-Test Matrix

Test procedures and specimen configurations (Figure 37) used in this task were consistent with those established in Task 2 to insure correlatable results. Specimens were tested to failure in tension and compression at three environmental conditions: room temperature dry (RTD), room temperature wet (RTW), and elevated temperature wet (ETW). ETW tests were conducted at 250°F with specimen moisture contents of approximately .80 percent by weight. Hercules AS/3501-6 graphite-epoxy was used as the material for fabrication of test specimens. All specimens were tested to failure according to Figure 81 under tensile or compressive loadings. Absorption profiles representative of specimens requiring moisture preconditioning are illustrated in Figure 82.

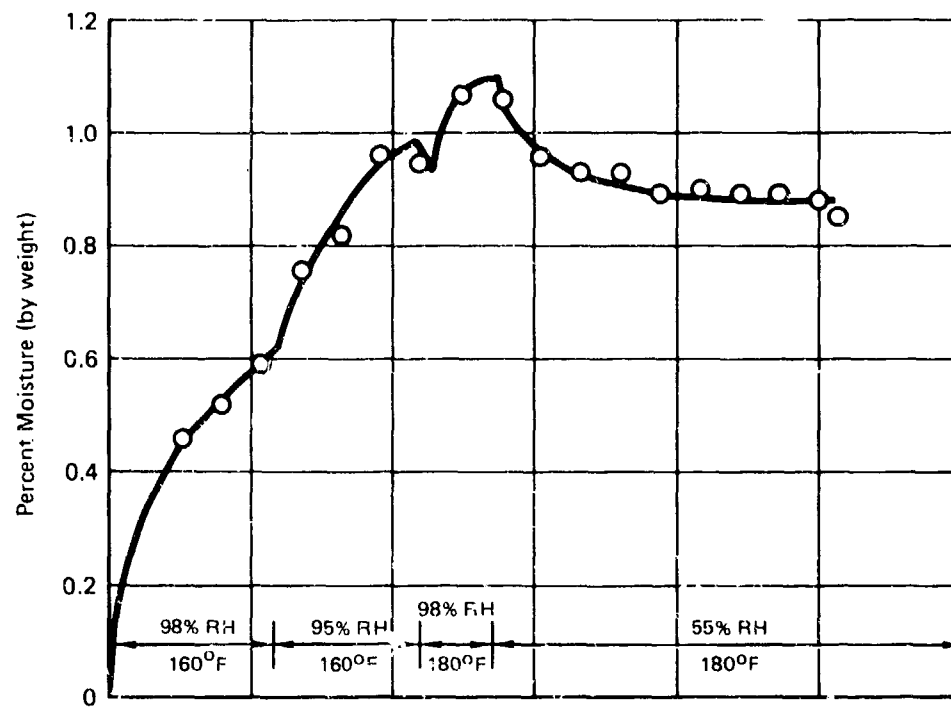
All specimens were instrumented with strain gauges. Documentation included: (1) failure load and failure strain, (2) load-strain plots to failure, (3) thickness, width and hole size measurements of all specimens, (4) resin content of each panel, (5) weight gain of humidity exposure specimens, (5) representative photographs, and (6) selected load-deflection plots to failure. Complete details of Task 3 testing, test procedures, data and support equipment are provided in Volume 2.

b. Experimental Results and Evaluation - Results from all Task 3 tests are summarized in Figure 83. Indicated percentages of increase or decreased strength are based on a comparison of gross failure strains with baseline strength data from Task 2.

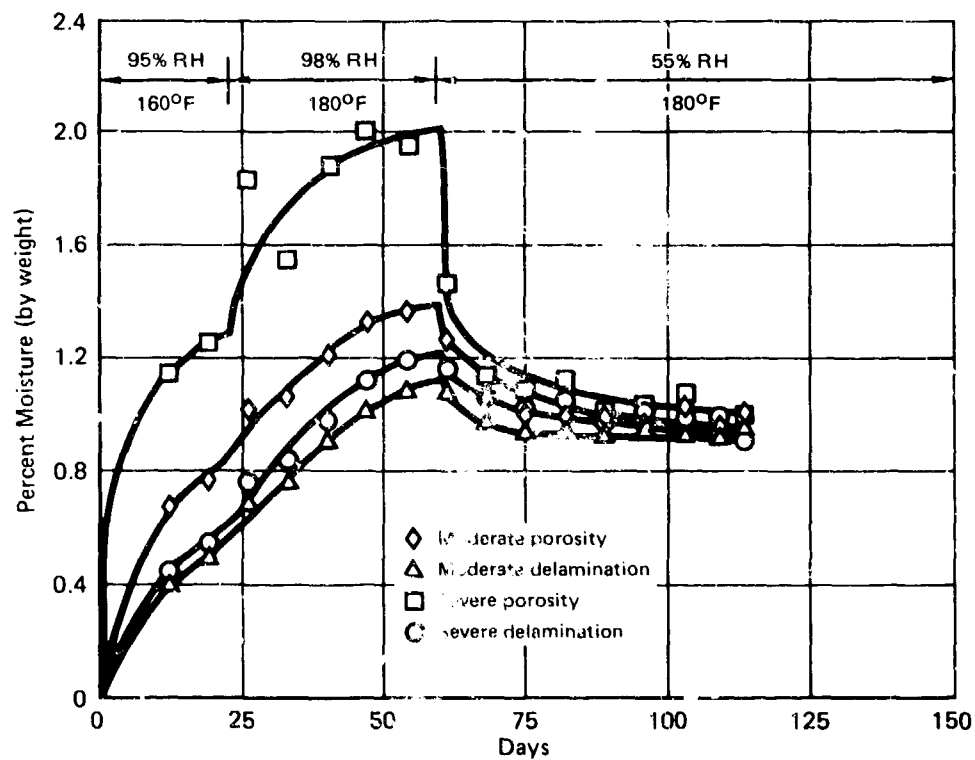
Results can be grouped under two classifications: (1) effects of anomalies which resulted in strength reductions of more than 13 percent and (2) those which resulted in strength reductions less than 13 percent. The first group includes porosity around hole, improper fastener seating depth, and tilted countersinks. Current project inspection and acceptance criteria in the industry would have detected all three of these anomalies and resulted in part rejection or required repair. Detailed results are discussed in the following paragraphs.

(1) Out of Round Holes - Effects of out-of-round holes on joint strength were evaluated by testing specimens produced by drilling offset (.004 inch) holes as shown in Figure 84. The major diameter of the out-of-round hole was fabricated perpendicular to the 0° fibers and the direction of loading.

Joint specimens from two laminates (50/40/10 and 30/60/10) were tested to failure, in tension at room temperature. Test results were compared with baseline data from Task 2. Joint strengths for both layups (Figure 85) indicate little or no sensitivity to out-of-round holes. This is consistent with unloaded hole studies where an out-of-round value of .004 inch (modeled as an elliptic hole) resulted in predicted strength reductions of no more than 1.0 percent.






(a) For Baseline Specimens



(b) For Delaminated or Porous Specimens

GP13-0116-16

Figures 82. Specimen Moisture Conditioning Histories

	RTD TENSION	COMPRESSION	
		RT 	250°F 
OUT-O. ROUND HOLES			
• 50/40/10 LAMINATE	*	-	-
• 30/60/10 LAMINATE	-4.8	-	-
BROKEN FIBERS EXIT SIDE OF HOLE			
• SEVERE	-9.5	-3.5	-12.2
• MODERATE	-4.9	-6.2	*
POROSITY AROUND HOLE			
• SEVERE	*	-12.1	-32.6
• SEVERE WITH FREEZE-THAW	-	-13.3	-
• MODERATE	-	-5.4	-17.9
• MODERATE WITH FREEZE-THAW	-	-7.9	-
IMPROPER FASTENER SEATING DEPTH			
• 80% THICKNESS	-23.2	-	-
• 100% THICKNESS	-56.9	-	-
TILTED COUNTERSINKS			
• AWAY FROM BEARING SURFACE	*	-	-20.0
• TOWARD BEARING SURFACE	-23.9	-	-22.7
INTERFERENCE FIT TOLERANCES (INCH)			
• 50/40/10 @ 0.003	*	-	+14.7
• @ 0.008	*	-	+11.2
• 30/60/10 @ 0.003	*	-	+2.4
• @ 0.008	*	-	*
FASTENER REMOVAL AND REINSTALLATION			
• 100 CYCLES	*	-	-7.4

 0.86% moisture content  Tensile loading *Under 2% change - No test

DP13-0112-105

Figure 63. Summary of Task 3 Strength Reduction Percents

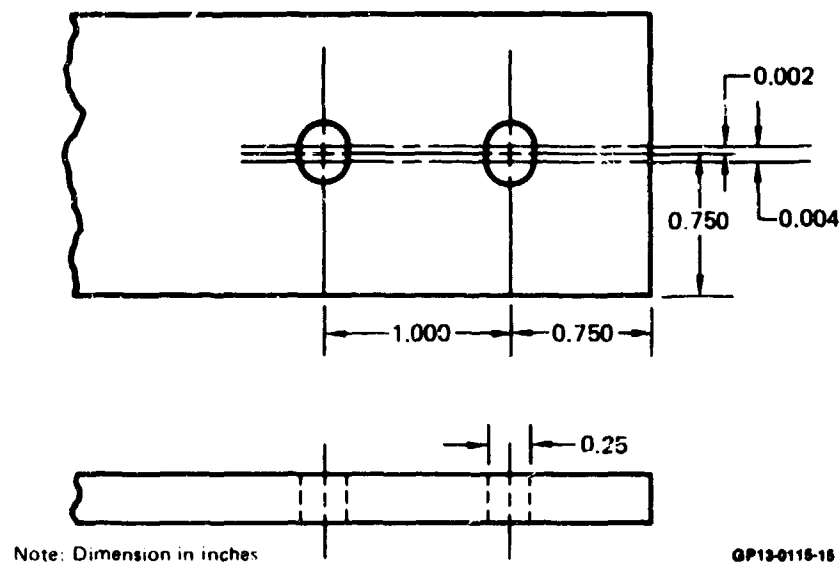
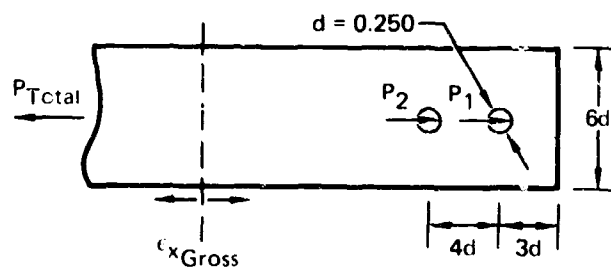


Figure 84. Out-of-Round Holes - Specimen Details



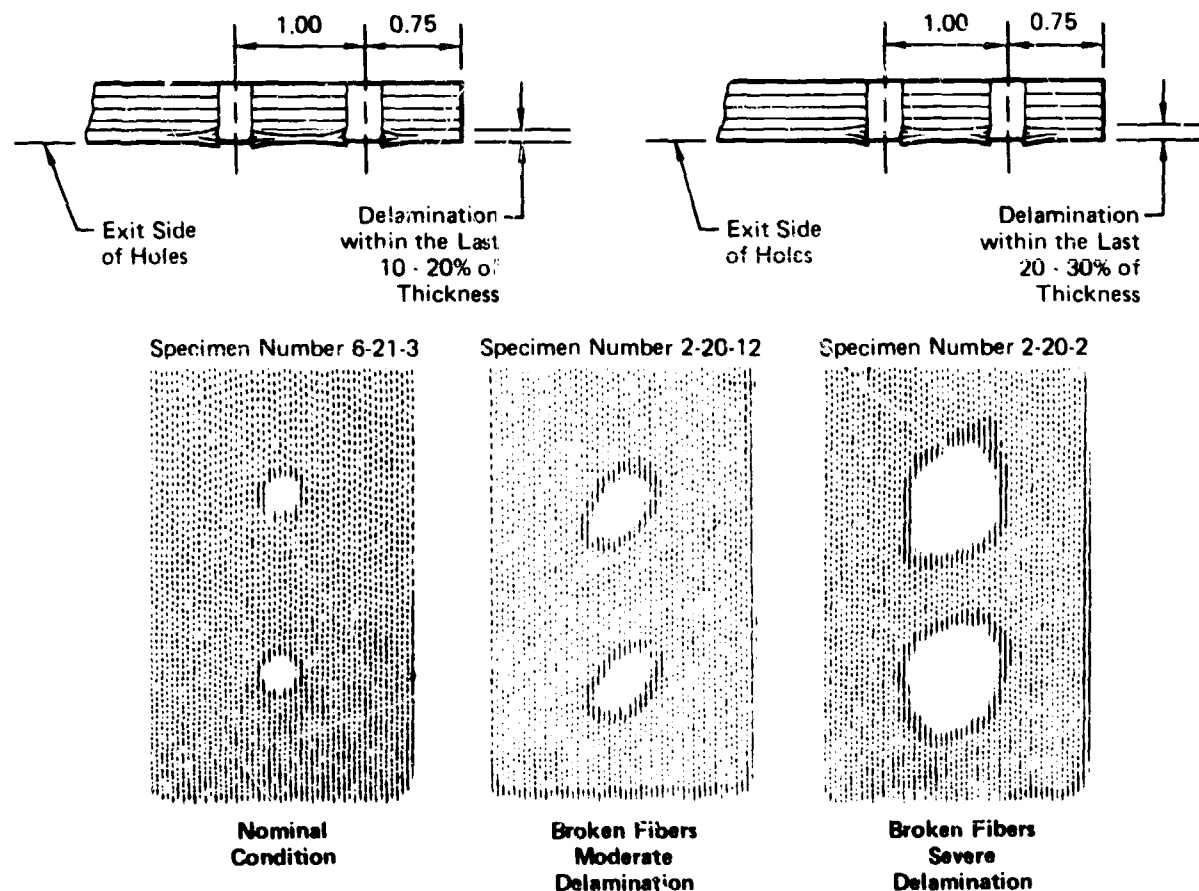
Test Condition Out-of-Round Holes	Task 2 Baseline Data		Task 3 Anomaly Results		% Change		Loading
	F_{x2}^{bru} (ksi)	ϵ_{xGross}^u ($\mu\text{in./in.}$)	F_{x2}^{bru} (ksi)	ϵ_{xGross}^u ($\mu\text{in./in.}$)	F_{bru}	ϵ_{Gross}	
50/40/10 Layup - RTD	140	3,990	146	4,010	+4.3	+0.6	Ten
30/60/10 Layup - RTD	143	5,470	141	5,200	-1.3	-4.8	Ten

QP13-0115-14

Figure 85. Effect of Out-of-Round Holes on Joint Strength

(2) Broken Fibers on Exit Side of Hole - Specimens were tested for two conditions of severity, "moderate" delaminations and "severe" delaminations. In order to obtain the various degrees of delamination, drill procedures included: use of dull bits without backup material, and improper drill and feed speeds. Tests to failure were performed in tension and compression. Compression tests were conducted at room temperature and elevated temperature after specimen moisture conditioning.

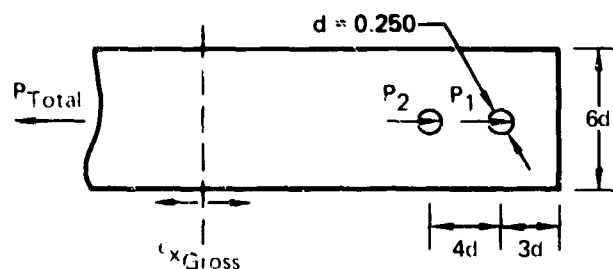
Delaminations were detected visually and with ultrasonic C-scan. Delaminations were defined as "moderate" when they extended over 10-20 percent (2-4 plies deep) of the laminate thickness on the exit side. Delaminations were defined as "severe" when they extended over 20-30 percent (4-6 plies) of the laminate thickness on the exit side. Nondestructive C-scans of holes with moderate and with severe delaminations are illustrated in Figure 86 and compared with a nominal condition.



GP12-0115-13

Figure 86. C-Scans of Laminates with Delaminations at Fastener Holes

Dry laminates at room temperature were tested to evaluate joint strength in tension. Because of its sensitivity to environment, joint compression strengths were evaluated at RTW and ETW test conditions. Strengths are listed in Figure 87 along with the baseline strength data from Task 2. Strength reductions of 2-5 percent and 7-10 percent occurred in RTD tension tests for specimens with moderate and severe delaminations, respectively. Compression strengths at 250°F indicated increased sensitivity with reductions of about 12 percent for specimens with severe delaminations.




Test Condition Hole Delaminations (50/40/10 Layup)	Task 2 Baseline Data		Task 3 Anomaly Results		% Change		Loading
	$F_{bru} \times 2$ (ksi)	ϵ_{xGross}^u ($\mu in./in.$)	$F_{bru} \times 2$ (ksi)	ϵ_{xGross}^u ($\mu in./in.$)	F_{bru}	ϵ_{Gross}	
Moderate:							
RTD	+140	+3,990	+138	+3,790	-2.0	-4.9	Ten
RTW	-155	-4,740	-150	-4,450	-3.2	-6.2	Comp
ETW	-120	-3,790	-115	-3,810	-3.7	+0.6	Comp
Severe:							
RTD	+140	+3,990	+130	+3,610	-7.3	-9.5	Ten
RTW	-155	-4,740	-142	-4,580	-8.4	-3.5	Comp
ETW	-120	-3,790	-109	-3,330	-8.7	-12.2	Comp

GP130115-12

Figure 87. Effect of Delaminations on Joint Strength

Effects of exit side delamination are dependent on depth of damage and on stacking sequence. For uniaxial loadings, greater strength reductions can be expected if delaminations interrupt fibers parallel to loading direction. However, in highly orthotropic layups, delaminations may reduce stress concentrations by reducing the laminate stiffness around the fastener hole. For this particular 50/40/10 stacking sequence (+45, 0, -45, 0, 90, 0, +45, 0, -45, 0)_s, "moderate" exit damage (of 2-4 plies) affected 1-2 of the ten 0° plies, while "severe" exit damage (of 4-6 plies) affected 2-3 of the ten 0° plies. For stacking sequences with more +45° plies towards the surface, considerable differences in strength data would have occurred.

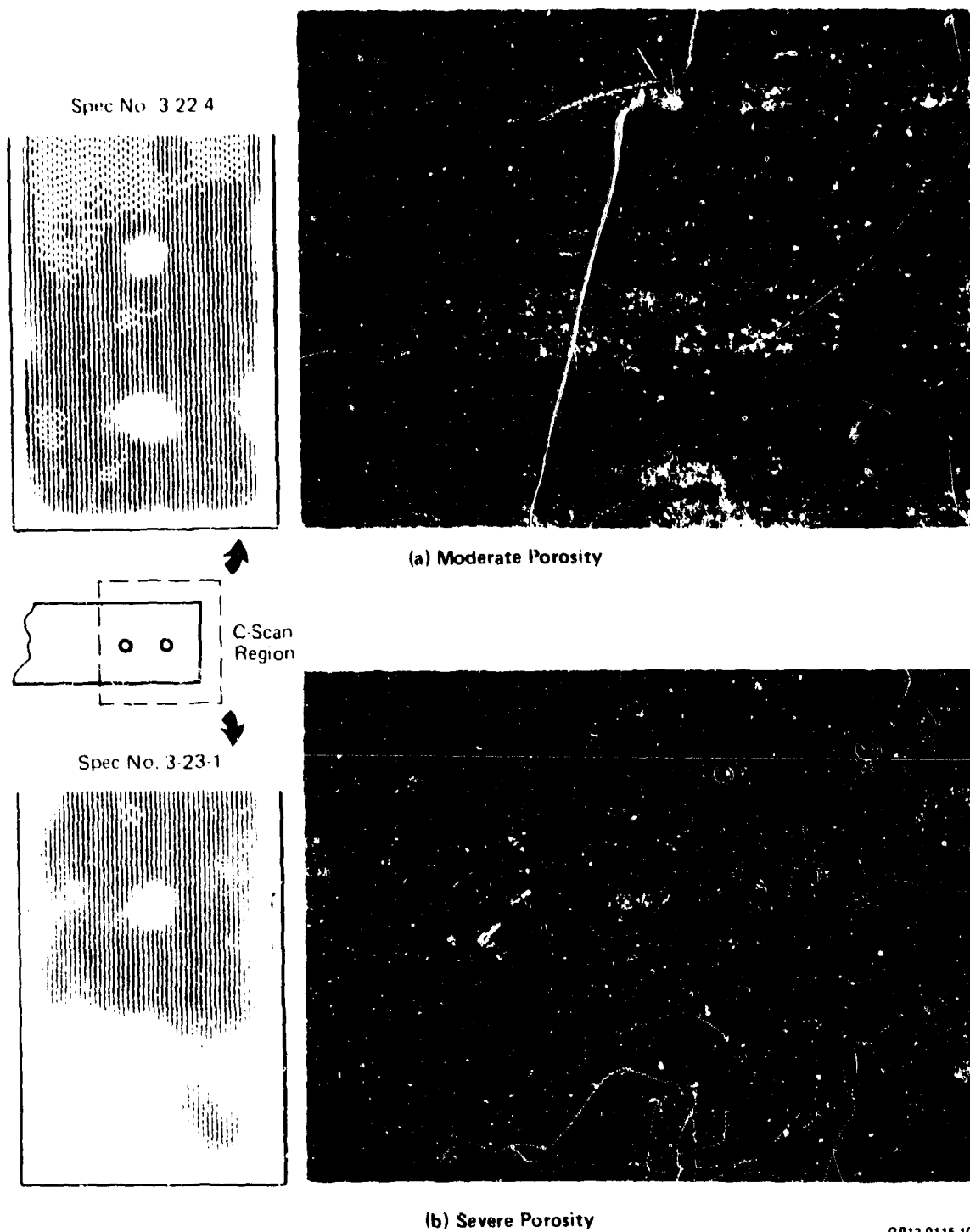
(3) Porosity - Two levels of porosity were evaluated; "moderate" and "severe". Desired levels of porosity in the 50/40/10 laminate were obtained by using the altered collation and curing procedures summarized in Figure 88. Specimens were located within panels such that fastener holes occurred in areas of desired porosity levels as indicated by photomicrograph and nondestructive inspections (Figure 89). Specimens were tested under "worst case" conditions. Under tension loadings, only the effects of severe porosity on joint strength were evaluated at room temperature. Under compressive loadings, effects of moderate and severe porosity on joint strength were evaluated at RTD, RTW, and ETW. Four specimens (two of moderate and two of severe porosity) were loaded to failure in compression at room temperature after moisture conditioning and exposure to freeze-thaw cycling (Figure 90).

Curing Procedure	Process Used for Good Panels	Process Used to Produce	
		Moderate Porosity	Severe Porosity
Vacuum Debulk	Yes	None	None
Intermediate Temperature Hold	1 hr @ 275°F	None	None
Bag Vacuum	0.05 in. Heading	0.8 in. Heading	1.5 in. Heading
Autoclave Pressure	100 psig	50 psig	50 psig
Moisture Induced 	None	Every 7th Ply	Every Ply

 Fine mist sprayed between plies

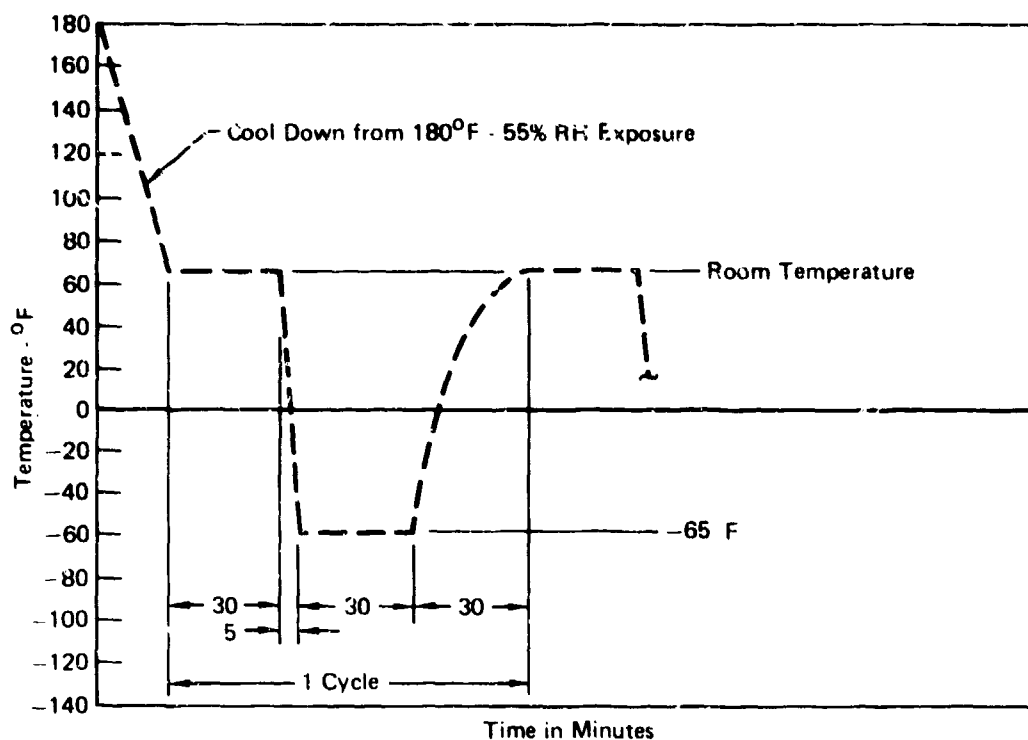
GP13-0115-11

Figure 88. Panel Fabrication Procedures Used to Produce Panel Porosity



GP13-0115-10

Figure 89. Examples of Panel Porosity

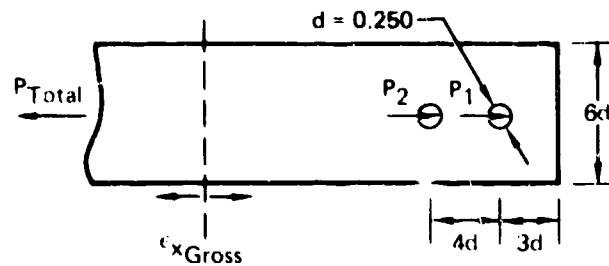


GP13-0115-0

Figure 90. Freeze-Thaw Exposure Profile

Strengths from all tests and baseline (no anomaly) strength data are listed in Figure 91. Little sensitivity to severe porosity was indicated under tensile loading. Under compressive loadings, strength reductions ranged from 4-18 percent for specimens with moderate porosity and 10-33 percent for specimens with severe porosity. The greatest reductions occurred at the 250°F test condition. Specimens with exposures to freeze-thaw cycling indicated a slightly greater loss of strength than specimens not similarly exposed; 3-4 percent added reduction and 1-2 percent added reduction respectively for moderate and severe porosity conditions. Specimens loaded in compression failed in bearing, similar in appearance to specimens with no porosity.

(4) Improper Fastener Seating Depth - Effects of excessive countersink depth on joint strength were evaluated by testing composite joint members having fasteners seated too deeply in the laminate. Two conditions of countersink depth were evaluated at room temperature in tension.



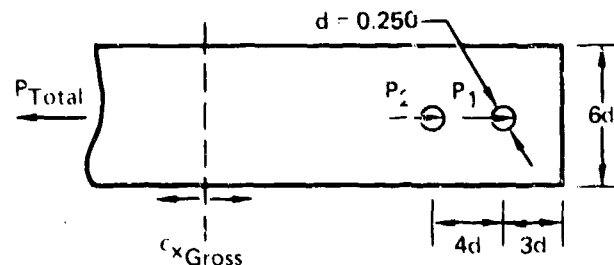
Test Condition Porosity (50/40/10 Layup)	Task 2 Baseline Data		Task 3 Anomaly Results		% Change		Loading
	F_{x2}^{bru} (ksi)	ϵ_{xGross}^u ($\mu\text{in./in.}$)	F_{x2}^{bru} (ksi)	ϵ_{xGross}^u ($\mu\text{in./in.}$)	F^{bru}	ϵ^{Gross}	
Moderate Porosity:							
RTD	+140	+3,990	—	—	—	—	Ten
RTW	-155	-4,740	-184	-4,480	-4.3	-5.4	Comp
RTW (F-T)	-155	-4,740	-142	-4,370	-8.4	-7.9	Comp
ETW	-120	-3,790	-104	-3,110	-12.8	-17.9	Comp
Severe Porosity:							
RTD	+140	+3,990	+140	+3,940	0	-1.2	Ten
RTW	-155	-4,740	-139	-4,170	-10.3	-12.1	Comp
RTW (F-T)	-155	-4,740	-137	-4,110	-11.9	-13.3	Comp
ETW	-120	-3,790	-83	-2,550	-30.3	-32.6	Comp

Note: (F-T) - exposed to freeze-thaw cycles

GP13-0118-8

Figure 91. Effect of Porosity Around Hole on Joint Strength

Strengths are listed with nominal condition strengths in Figure 92. Strengths for joints having improper seating depths are compared with nominal countersunk (52% of laminate thickness) strength data. For the 50/40/10 layup tested, joint strengths for countersink versus noncountersink laminates (Task 2, Reference Figure 74) indicated no significant reductions occurred when fastener seating depth was nominal. The loss of bearing material and the associated knife-edge condition for the 80% and 100% depths may account for the strength reduction. Based on average bearing stresses, countersink depths of 80% and 100% thickness reduce cylindrical bearing area by 28% and 48% respectively, which approximates the percent changes in strength listed in Figure 92. Additionally, the deeper countersink increases the effective diameter of the hole which further reduces laminate strength due to hole size effects.

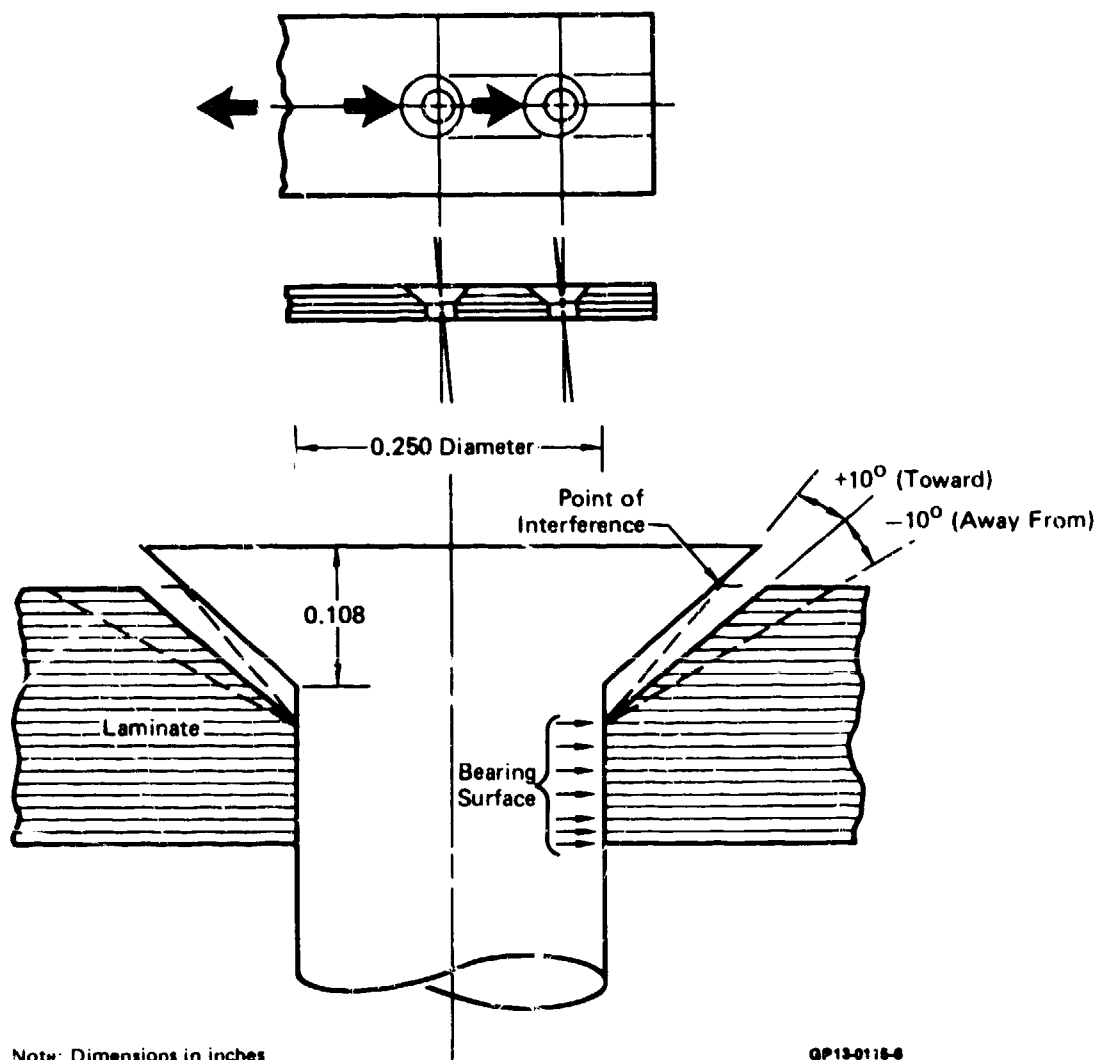


Test Condition Fastener Seating (50/40/10 Layup)	Task 2 Baseline Data		Task 3 Anomaly Results		% Change		Loading
	$F_{bru} \times 2$ (ksi)	ϵ_{xGross}^u ($\mu in./in.$)	$F_{bru} \times 2$ (ksi)	ϵ_{xGross}^u ($\mu in./in.$)	F_{bru}	ϵ_{Gross}	
80% Depth - RTD	140	3,990	117	3,240	- 20	-23	Ten
100% (Knifedge) - RTD	140	3,990	92	2,540	- 53	-57	Ten

GP13-0116-7

Figure 92. Effect of Improper Fastener Seating on Joint Strength

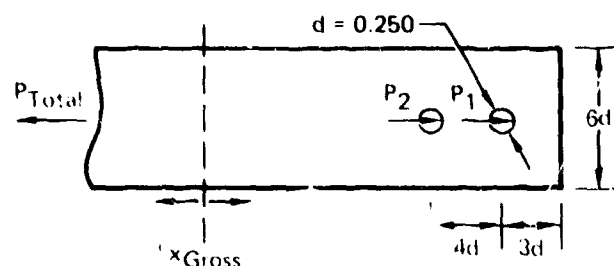
(5) Tilted Countersinks - Countersink perpendicularity was investigated for two conditions of misalignment. The misaligned countersink was tilted 10° away from the bearing surface for one condition and tilted 10° toward it for the other. These tests were conducted in tension at RTD and in compression at $250^\circ F$ after specimen moisture conditioning. As illustrated in Figure 93, tilted countersinks cause interference prior to proper fastener seating and create a gap under the fastener head reducing laminate bearing material. Experimental data indicate approximately equal strength reductions (Figure 94), regardless of direction and magnitude of countersink tilt, for moisture conditioned specimens tested in compression at $250^\circ F$.



Note: Dimensions in inches

GP13-0116-6

Figure 93. Tilted Countersink - Specimen Configuration



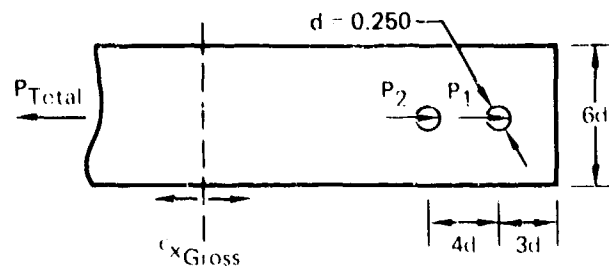
Test Condition Tilted Countersink (50/40/10 Layup)	Task 2 Baseline Data		Task 3 Anomaly Results		% Change		Loading
	$F_{bru} \times 2$ (ksi)	$\epsilon^u \times Gross$ ($\mu in./in.$)	$F_{bru} \times 2$ (ksi)	$\epsilon^u \times Gross$ ($\mu in./in.$)	F_{bru}	$\epsilon^u Gross$	
Away From Bearing RTD ETW	+140	+3,990	+140	+3,910	+1.1	-2.0	Ten
	-120	-3,750	-100	-2,990	-12.6	-20.2	Comp
Toward Bearing RTD ETW	+140	+3,990	+110	+3,030	-18	-24	Ten
	-120	-3,750	-100	-2,898	-14	-23	Comp

GP13-0115-5

Figure 94. Effect of Tilted Countersink on Joint Strength

(6) Interference Fit - The effects of fastener interference fits on joint strength were investigated in two different laminates (50/40/10 and 30/60/10). Two-fastener-in-tandem specimens were tested to failure in tension at RTD and ETW conditions. Strength evaluations were performed on specimens with .003 and .008 inch levels of interference fit.

Results (Figure 95) for both layups indicate an insensitivity to interference at room temperature. Mixed results were obtained at ETW. Joint strength of the more fiber-dominant 50/40/10 layup improved by 8-15% at both levels of interference. Joint strengths of the matrix-dominant 30/60/10 layup showed little or no increase (-1.8 to +4.6 percent) at the ETW test condition.



Test Condition Interference Fit	Task 2 Baseline Data		Task 3 Anomaly Results		% Change		Loading
	F_{bru} x_2 (ksi)	c^u x_{Gross} (μ in./in.)	F_{bru} x_2 (ksi)	c^u x_{Gross} (μ in./in.)	F_{bru}	c_{Gross}	
50/40/10 Layup:							
0.003 Interference							
RTD	140	3,990	140	4,000	+2.1	+0.4	Ten
ETW	110	3,080	120	3,530	+11.8	+14.7	Ten
0.008 Interference							
RTD	140	3,990	140	4,030	+1.0	+0.9	Ten
ETW	110	3,080	120	3,420	+8.1	+11.2	Ten
30/60/10 Layup:							
0.003 Interference							
RTD	140	5,470	140	5,460	+0.2	-0.1	Ten
ETW	120	4,710	120	4,820	+4.6	+2.4	Ten
0.008 Interference							
RTD	140	5,470	140	5,490	-4.6	+0.3	Ten
ETW	120	4,710	120	4,620	+1.5	-1.8	Ten

GP13-0118-4

Figure 95. Effect of Fastener Interference Fit on Joint Strength

Laminate damage due to fastener installation at different levels of interference fit were further evaluated. Fastener interference fits ranging from .002 to .0075 inch were examined. Standard pull-through installation techniques and fastener types were used. Each fastener area was sectioned and photomicrographs taken. Representative results are shown in Figure 96. Photographs indicate little or no damage at a fastener interference of .0035 inch or less; however, damage is indicated at the fastener exit side as well as through-the-thickness for interference fits from .004 through .007 inch.

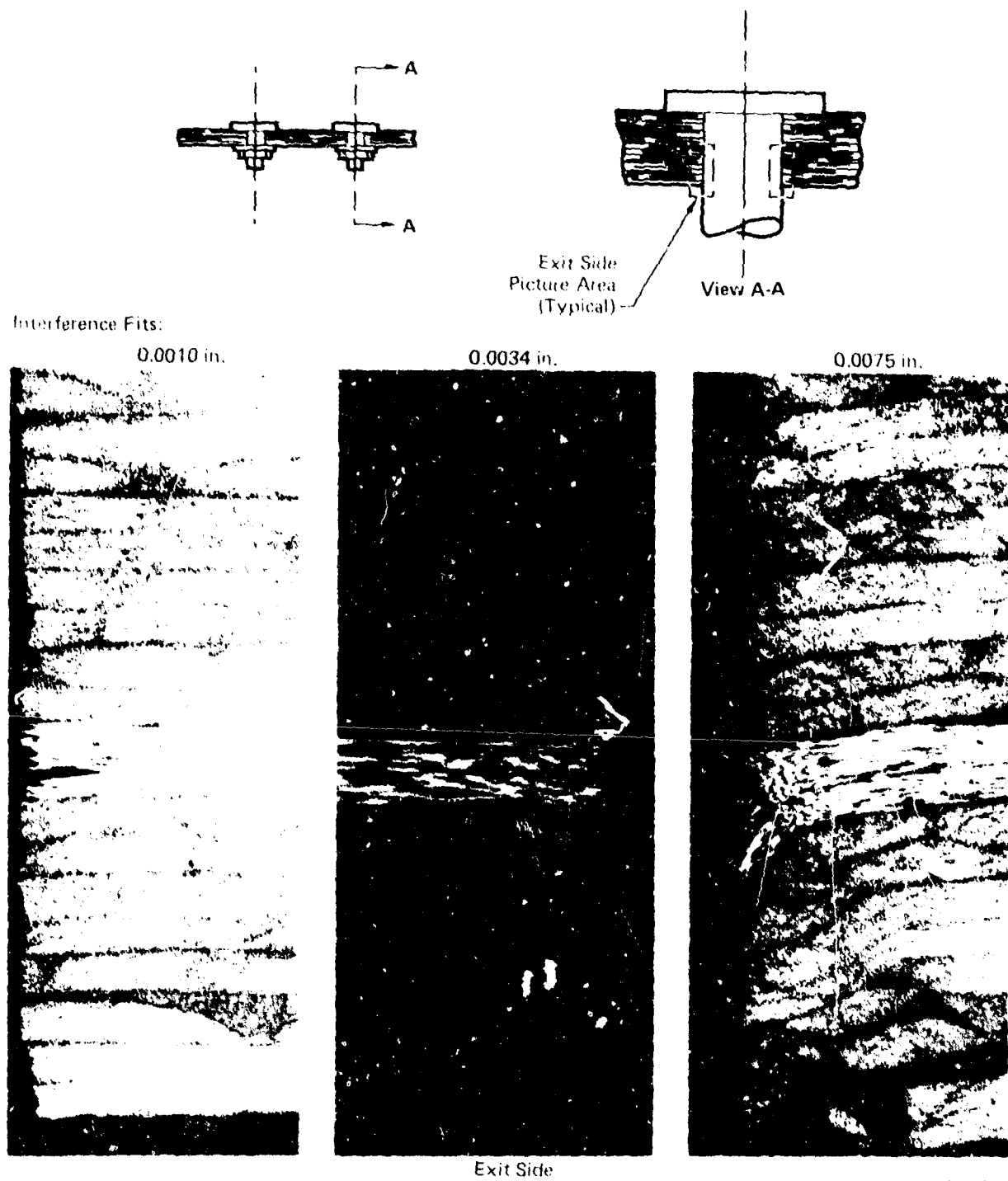


Figure 96. Photomicrographic Examination of Laminates with Interference Fit Holes

(7) Fastener Removal and Reinstallation - Specimens were tested to failure in tension at RTD and in compression at ETW. Fasteners were installed, torqued to 50 inch-pounds, and completely removed. This procedure was repeated 100 times prior to strength testing. These tests were used to evaluate whether repeated fastener torque-up associated with installation and re-installation would locally damage the laminate hole area, and/or affect joint strength. No attempt was made to simulate problems encountered in project or field environments (e.g. part-to-part misfit). While important, these problems require definition of specific structural component and element details for proper evaluation and were beyond the scope of this program.

Visual appearance of all fastener holes after installation and re-installation cycling was unchanged. Strength data listed in Figure 97 indicates little sensitivity to RTD tensile test conditions. Compressive strength values indicated an increased sensitivity (7% reduction); however, test scatter for the compression tests was much larger. No significant effects on joint strength were indicated.

Test Condition Fastener Reinstallation (50/40/10 Layup)	Task 2 Baseline Data		Task 3 Anomaly Results		% Change		Loading
	F_{x2}^{bru} (ksi)	ϵ_{xGross}^u ($\mu in./in.$)	F_{x2}^{bru} (ksi)	ϵ_{xGross}^u ($\mu in./in.$)	F^{bru}	ϵ^{Gross}	
100 Cycles							
RTD	+140	+3,990	+140	+3,900	-1.3	-2.2	Ten
ETW	-120	-3,790	-110	-3,510	-9.3	-7.4	Comp

GP13-0115-2

Figure 97. Effect of Fastener Removal and Reinstallation on Joint Strength

3. EVALUATION OF CRITICAL JOINT DESIGN VARIABLES ON FATIGUE LIFE - TASK 4 - The objective of Task 4 was to evaluate the influence of selected design variables and manufacturing anomalies on joint fatigue life. Seven variables or anomalies shown in Tasks 2 and 3 to have significant effect on static strength were chosen for evaluation. Tests were to provide data on joint fatigue life performance, hole elongation, and failure modes.

A pure bearing test specimen was used to provide basic joint fatigue data while minimizing test difficulties and permitting correlation with Task 2 and Task 3 static test data. All tension-tension ($R = +0.1$) and tension-compression ($R = -1.0$) constant amplitude testing was performed at room temperature with specimens in the as-manufactured condition. Spectrum fatigue testing of the 50/40/10 layup was performed at three environmental conditions: room temperature dry, room temperature wet, and elevated temperature wet. Elevated test temperature (250°F) and the moisture conditioning level (approximately .8 percent by weight) were the same as in Tasks 2 and 3. Hercules AS/3501-6 graphite-epoxy was used for fabrication of all Task 4 test specimens.

a. Task 4 Test Plan - The test plan summarized in Figure 98 was based on literature survey results which indicated that: (1) little generic fatigue life data had been generated for bolted joints, (2) life prediction methods are essentially empirical, and (3) theoretical approaches being pursued, such as the "wear-out" model, require large residual strength data bases for statistical evaluation. This data base would be impractical in size for the seven variables to be evaluated in Task 4. Hence, an empirical approach was adapted to determine the effects of the selected variables on joint fatigue life. Testing of both fiber-dominated laminates and matrix-dominated laminates was included in order to identify differences in failure modes, with sufficient tests under spectrum fatigue loading to indicate major data trends.

The seven test variables selected for evaluation were: (1) stacking sequence, (2) torque-up, (3) single-shear versus double-shear, (4) fastener fit, (5) porosity, (6) layup, and (7) geometry.

Emphasis was placed on generation of hole elongation data and its relevancy to joint fatigue life. All constant-amplitude fatigue specimens were cycled to failure, or 10^6 cycles, whichever occurred first. Constant amplitude fatigue testing was performed at three stress levels for each specimen type. Selection of the stress levels for fatigue testing was based on load-deflection data obtained from static tests. During fatigue testing, load-deflection data were also obtained each time specified hole elongations occurred. All constant amplitude tests were performed at room temperature with as-manufactured specimens. Selected specimens which did not fail in 10^6 cycles were tested to determine residual strength.

Tests were performed to determine effects of spectrum loading on joint life as a function of test limit load. If failure had not occurred after four lifetimes of exposure, selected specimens were static tested to determine residual strength. As in constant amplitude testing, three test limit load levels were selected for each test variable evaluated.

NO.	TEST VARIABLE	MAX FATIGUE STRESS	NO. OF TESTS CONSTANT AMPLITUDE		NO. OF TESTS SPECTRUM FATIGUE			
			R = +0.1	R = -1.0	RTW	RTD	ETW	RTW(TS)
1	BASELINE 50/40/10 $\triangle_2 \triangle_3$	σ_1	3	3	3	3	3	3
		σ_2	3	3	3	3	3	3
		σ_3	3	3	3	3	3	3
		\triangle_1	3	—	3	—	3	3
	30/50/10 $\triangle_2 \triangle_3$	σ_1	3	3	—	3	—	—
		σ_2	3	3	—	3	—	—
		σ_3	3	3	—	3	—	—
		\triangle_1	3	—	—	—	—	—
	19/76/5 $\triangle_2 \triangle_3$	σ_1	3	3	—	3	—	—
		σ_2	3	3	—	3	—	—
		σ_3	3	3	—	3	—	—
		\triangle_1	3	—	—	—	—	—
2	STACKING SEQUENCE 50/40/10 $\triangle_2 \triangle_3$	σ_1	3	3	—	3	—	—
		σ_2	3	3	—	3	—	—
		σ_3	3	3	—	3	—	—
		\triangle_1	3	—	—	—	—	—
	19/76/5 $\triangle_2 \triangle_3$	σ_1	3	3	—	3	—	—
		σ_2	3	3	—	3	—	—
		σ_3	3	3	—	3	—	—
		\triangle_1	3	—	—	—	—	—
3	TORQUE UP T = 160 IN.-LB 50/40/10 \triangle_2	σ_1	3	3	—	3	—	—
		σ_2	3	3	—	3	—	—
		σ_3	3	3	—	3	—	—
		\triangle_1	3	—	—	—	—	—
	T = 160 IN.-LB 19/76/5 \triangle_2	σ_1	3	3	—	3	—	—
		σ_2	3	3	—	3	—	—
		σ_3	3	3	—	3	—	—
		\triangle_1	3	—	—	—	—	—

\triangle_1 Complementing static tests

\triangle_2 d = 0.375 in., w/d = 6, e/d = 3

\triangle_3 Torque up = 0 in.-lb

GP13-0115-108

Figure 98. Task 4 - Evaluation of Critical Joint Design
Parameters on Fatigue Life - Test Matrix

NO.	TEST VARIABLE	MAX FATIGUE STRESS	NO. OF TESTS CONSTANT AMPLITUDE		NO. OF TESTS SPECTRUM FATIGUE			
			R = +0.1	R = -1.0	RTW	RTD	ETW	RTW(TS)
4	GEOMETRY 50/40/10 $\triangle 3$ d = 0.375 w/d = 4 e/d = 3	σ_1	3	-	-	-	-	-
		σ_2	3	-	-	-	-	-
		σ_3	3	-	-	-	-	-
		$\triangle 1$	3	-	-	-	-	-
	19/76/5 $\triangle 3$ d = 0.375 w/d = 4 e/d = 3	σ_1	3	-	-	-	-	-
		σ_2	3	-	-	-	-	-
		σ_3	3	-	-	-	-	-
		$\triangle 1$	3	-	-	-	-	-
	19/76/5 $\triangle 3$ d = 0.375 w/d = 3 e/d = 3	σ_1	3	-	-	-	-	-
		σ_2	3	-	-	-	-	-
		σ_3	3	-	-	-	-	-
		$\triangle 1$	3	-	-	-	-	-
	50/40/10 $\triangle 3$ d = 0.375 w/d = 4 e/d = 4	σ_1	3	-	-	-	-	-
		σ_2	3	-	-	-	-	-
		σ_3	3	-	-	-	-	-
		$\triangle 1$	3	-	-	-	-	-
5	FASTENER FIT (0.003 - 0.008 INTERFERENCE) 50/40/10 $\triangle 2$ $\triangle 3$	σ_1	3	-	-	-	-	-
		σ_2	3	-	-	-	-	-
		σ_3	3	-	-	-	-	-
		$\triangle 1$	3	-	-	-	-	-
6	SINGLE SHEAR (PROTRUDING AND CSK) 50/40/10 $\triangle 2$ T = 160 IN.-LB	σ_1	3	-	-	-	-	-
		σ_2	3	-	-	-	-	-
		σ_2	3	-	-	-	-	-
		$\triangle 1$	3	-	-	-	-	-
	d = 0.375 IN. CSK w/d = 6 e/d = 3 T = 160 IN.-LB	σ_1	3	-	-	-	-	-
		σ_2	3	-	-	-	-	-
		σ_3	3	-	-	-	-	-
		$\triangle 1$	3	-	-	-	-	-
7	POROSITY 50/40/10 $\triangle 2$ $\triangle 3$	σ_1	3	3	-	-	-	-
		σ_2	3	3	-	-	-	-
		σ_3	3	3	-	-	-	-
		$\triangle 1$	3	-	-	-	-	-
					TOTAL TESTS = 351			

$\triangle 1$ Complementing static tests

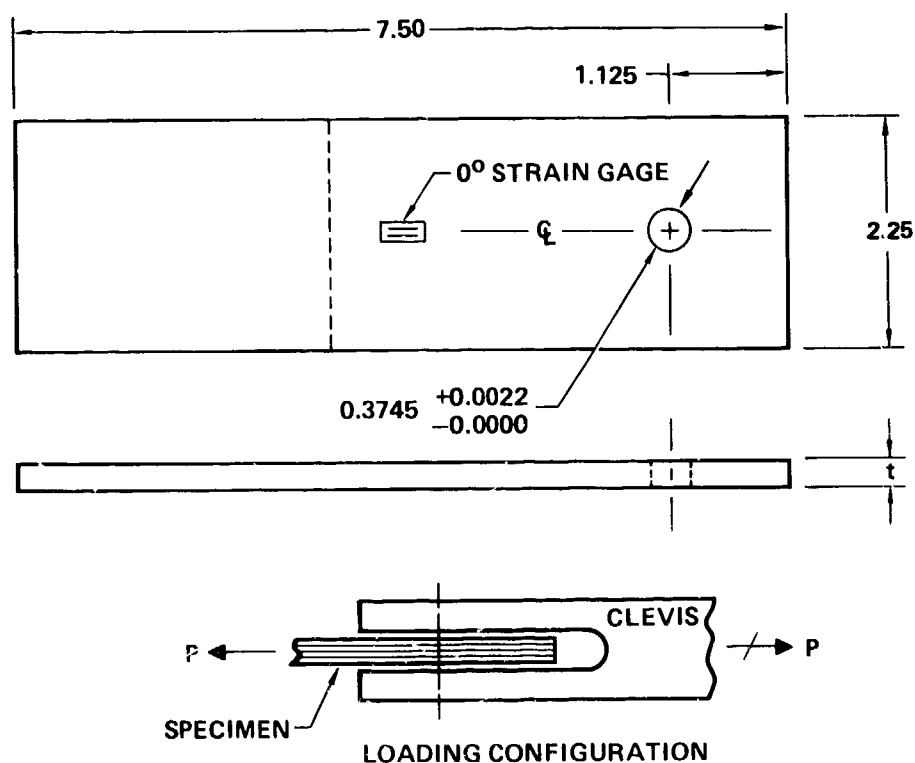
$\triangle 2$ d = 0.375 in., w/d = 6, e/d = 3

$\triangle 3$ Torque up = 0 in.-lb

GP13-0115-202

Figure 98. (Continued) Task 4 - Evaluation of Critical Joint Design Parameters on Fatigue Life-Test Matrix

A baseline joint geometry (Figure 99) was tested to provide a fatigue life reference for all test conditions. Elevated temperature exposure, moisture preconditioning, and thermal spiking were included in this "baseline" series of tests on the 50/40/10 layup. Three sets of the 50/40/10 specimens were tested: (1) one set at room temperature with as-manufactured moisture levels, RTD, (2) one moisture conditioned set at 250°F, ETW, and (3) one moisture conditioned set with thermal spikes (TS) applied intermittently during the humid aging process, RTW(TS). The evaluation of a baseline joint geometry, also included two additional layups (30/60/10 and 19/76/5), which were tested under both constant amplitude and spectrum loading, RTD.



GP13-0115-107

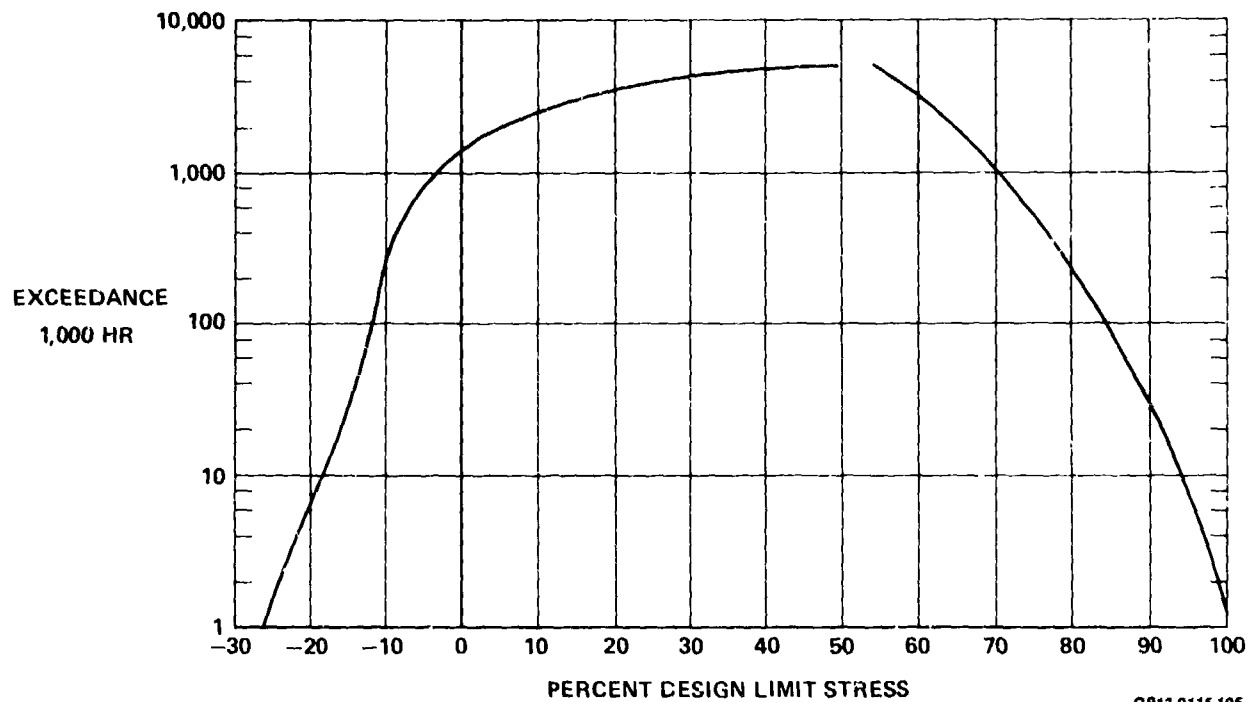
Figure 99. Task 4 - Fatigue Specimen Configuration

The random load spectrum used in Task 4 testing was an "F-15 Measured-Mix Wing Spectrum-Truncated". This spectrum is a combination of three F-15 wing baseline spectra (Air-to-Air, Air-to-Ground, and Instrumentation and Navigation), truncated to eliminate all loads less than 55% design limit load. Truncation was considered appropriate based on the relatively low failure strains associated with static tests of pure bearing (single fastener) joints. The distribution of hours and exceedances for the Air-to-Air, Air-to-Ground, and Instrumentation and Navigation in the Measured Mix spectrum are given in Figure 100. The associated exceedances are illustrated in Figure 101.

	MEASURED MIX	
	HOURS	EXCEEDANCES OF 80% LIMIT STRESS
AIR-TO-AIR	700	3,15
AIR-TO-GROUND	100	140
INSTRUMENTATION AND NAVIGATION	200	10
TOTAL	1,000	3,300

GP13-0115-201

Figure 100. Distribution of Hours and Exceedances



GP13-0115-105

Figure 101. Measured Mix-Truncated Spectrum

Fatigue specimen joint load-deflection response was monitored during the test. Evaluation of joint load-deflection hysteresis data provided hole elongation and overall joint compliance data as a function of cyclic exposure.

Individual test specimens were fabricated from 10 panels. Stacking sequences are detailed in Figure 102.

PLY NUMBERS TO CENTERLINE	LAY UP NUMBER AND PLY ORIENTATION				
	1	2	3	11	12
1	+	+	+	+	+
2	0	0	-	-	0
3	-	-	0	0	-
4	0	0	0	+	0
5	90	+	90	-	+
6	0	90	0	0	-
7	+	-	+	+	+
8	0	0	-	-	-
9	-	+	0	+	+
10	0	-	0	-	-
Q - CENTERLINE				90	90
NO. OF PLIES	20	20	20	21	21
PERCENT OF 0°/±45°/90°	(BASELINE) 50/40/10	(BASELINE) 30/60/10	50/40/10	19/76/5	(BASELINE) 19/76/5

Notes:

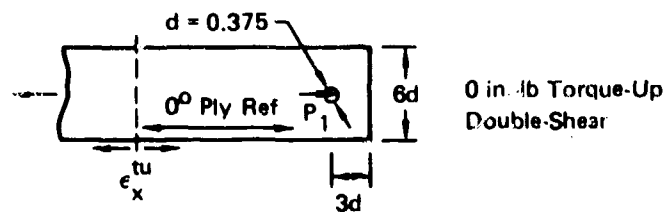
- 1) "+" and "-" refers to ±45° plies.

JP13-0115-248

Figure 102. Task 4 - Layup Numbers and Stacking Sequence

All specimens were tested to static failure or exposed to fatigue loadings according to Figure 98. A double-shear loading configuration (Figure 99) was used for all but the single-shear testing described in a following section. Full details of all Task 4 procedures, test data, and support equipment are provided in Volume 2 of this report.

b. Experimental Results and Evaluation - Static tensile strength data obtained at each test condition for each unique specimen configuration are summarized in Figure 103. Load-versus-deflection curves obtained in these tests were used to select fatigue stress levels.



No.	Test Parameter	Variation	Spring Rate (k - kips/in.)	Bearing Strength (f_{bru} - ksi)	Failure Strain ($\epsilon_{x_{gross}}^{tu}$ - μ in./in.)	Failure Load (lb)
1	Layup:	50/40/10 RTD	400	100	1,400	7,530
		RTW	410	90	1,430	7,250
		RTW (TS)	400	90	1,390	7,020
		ETW	330	50	790	4,210
		30/60/10 RTD	350	100	1,910	7,480
		19/76/5 RTD	330	100	2,650	7,850
2	Stacking Sequence:	50/40/10	390	90	1,330	7,230
		19/76/5	320	100	2,720	8,070
3	Torque-Up: (T = 160 in.-lb)	50/40/10	400	120	1,770	9,350
		19/76/5	300	150	4,160	12,570
4	Geometry:	50/40/10 w/d = 4 e/d = 3	330	100	2,210	7,440
		50/40/10 w/d = 4 e/d = 4	390	100	2,160	7,610
		19/76/5 w/d = 4 e/d = 3	400	100	3,960	7,980
		19/76/5 w/d = 3 e/d = 3	220	80	3,900	6,350
5	0.0045 in. Interference Fit	50/40/10	500	100	1,580	8,100
6	Single Shear: (T = 160 in.-lb)	50/40/10 (PROTR)	350	120	1,830	9,250
		(CSK)	250	110	1,450	8,200
7	Porosity:	Moderate	400	100	1,470	7,810

GP13-0115-1

Figure 103. Summary of Task 4 Specimen Static Strength

Residual strengths were, in general, equal or greater than nonfatigued specimen static strengths; however, in most cases, these specimens had acquired hole elongations of .02 inch or greater during fatigue. For structural applications, hole elongations of .02 inch exceed the usual yield criteria for metallic joints.

(1) Layup Variation - Three laminate variations were tested to determine relative fatigue life; the fiber-dominant 50/40/10 layup and two matrix-dominant layups, 30/60/10 and 19/76/5. These laminates were selected for fatigue evaluation on the basis of Task 2 results where changes were noted in strength, failure mode, and failure initiation point.

Results of tension-tension ($R = +0.1$) and tension-compression ($R = -1.0$) cyclic loading on each laminate at room temperature, dry (RTD) test conditions are summarized in Figures 104, 105, and 106, in terms of fatigue cycles required to produce an 0.02 inch elongation of the fastener hole. The results indicate similar static and fatigue strength for all layups for tension-tension ($R = +0.1$) cycling, as summarized in Figure 107. For tension-compression ($R = -1.0$), the 19/76/5 and 30/60/10 matrix-dominant layups sustained fewer load cycles prior to developing an .02 inch hole elongation, as compared to the 50/40/10 layup (Figure 108).

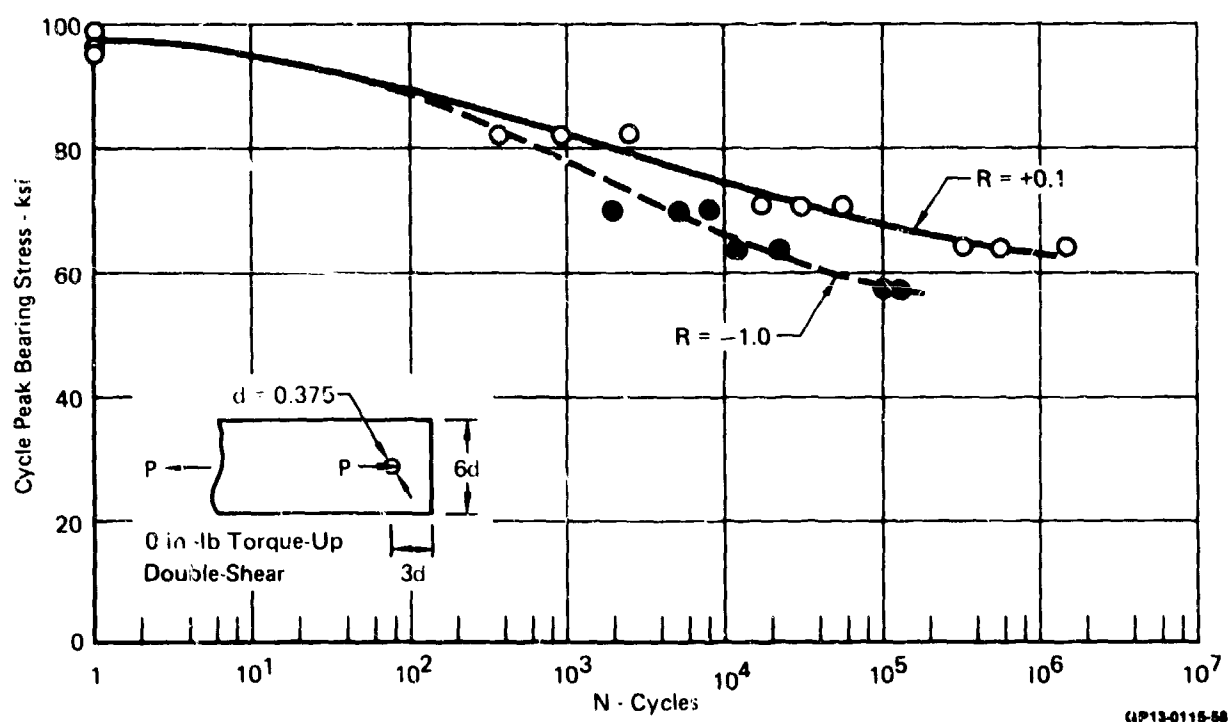


Figure 104. RTD Baseline Joint Fatigue Life
50/40/10 Layup

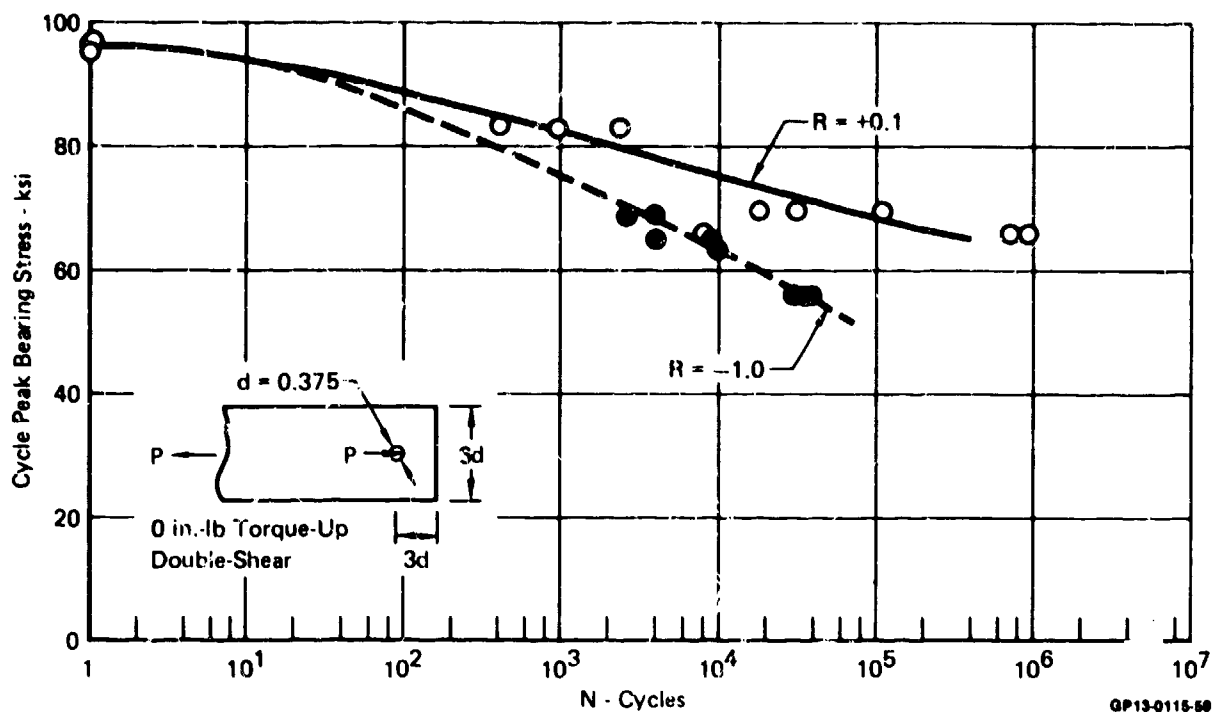


Figure 105. RTD Baseline Joint Fatigue Life
30/60/10 Layup

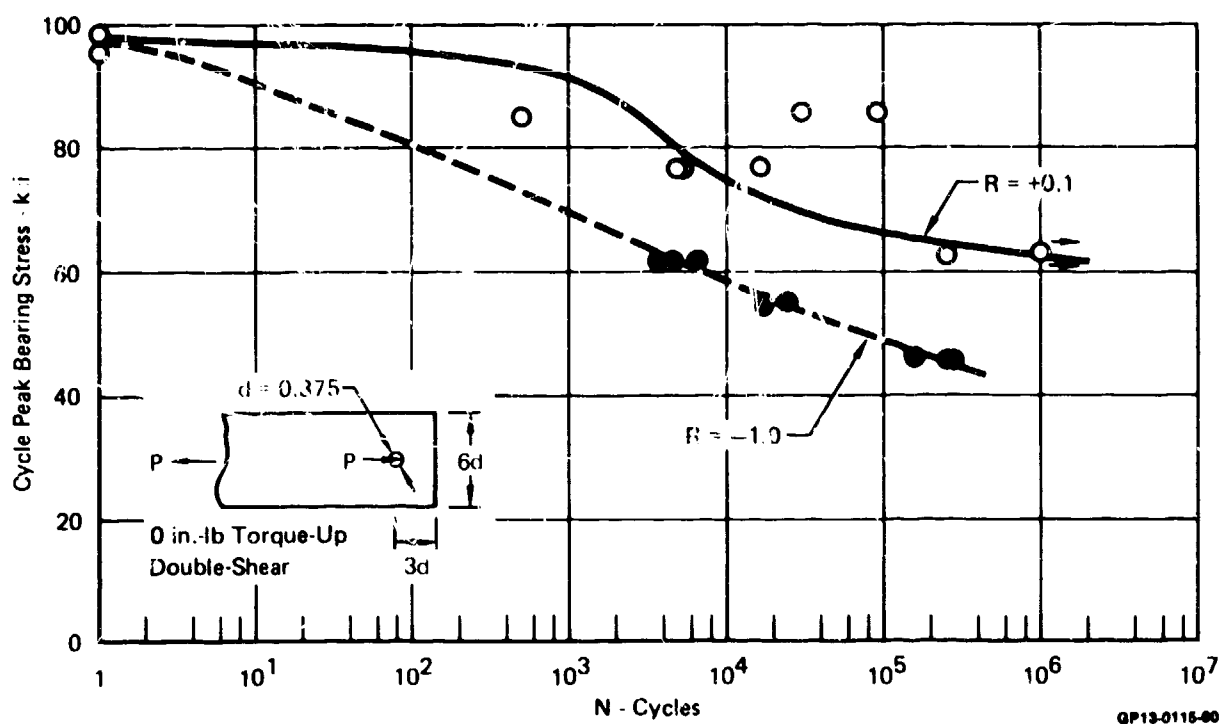


Figure 106. RTD Baseline Joint Fatigue Life
19/76/5 Layup

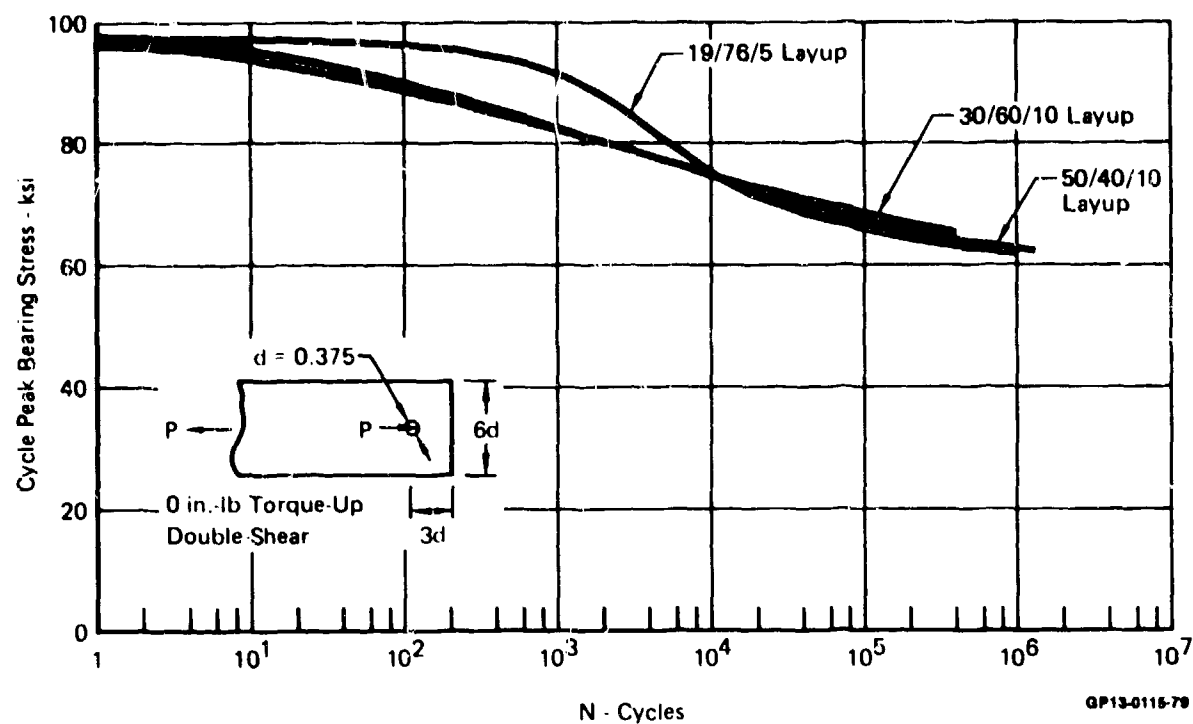


Figure 107. Comparison of $R = +0.1$ Joint Fatigue Life Trends

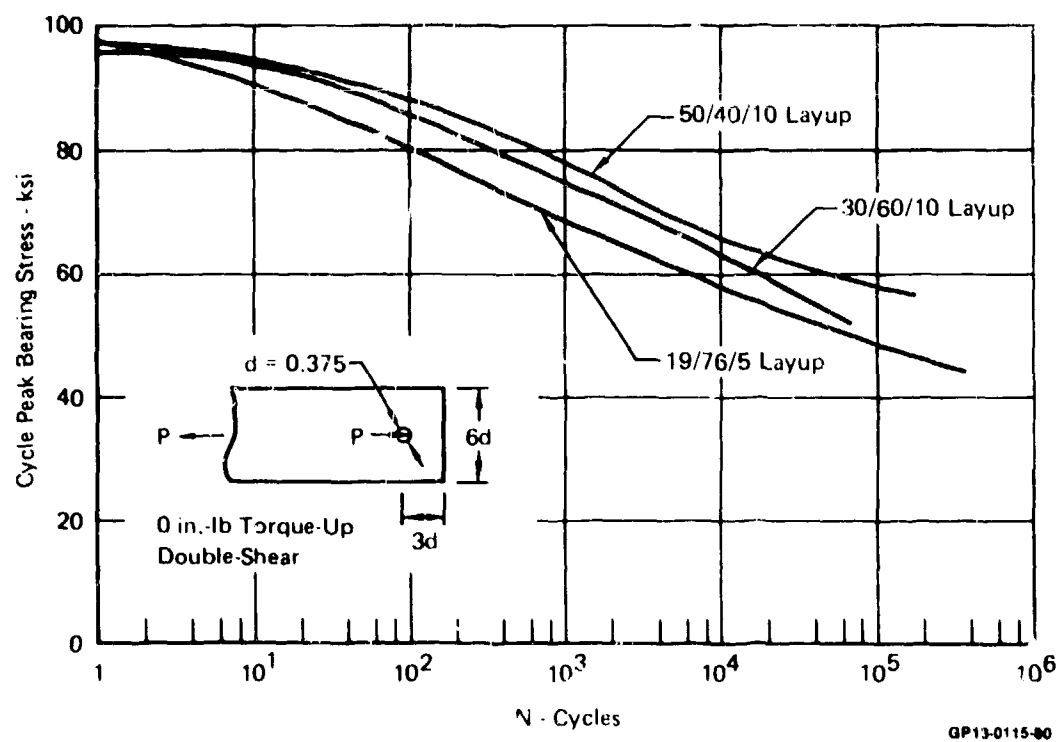


Figure 108. Comparison of $R = -1.0$ Joint Fatigue Life Trends

In order to evaluate the rate of hole elongation in composite joints, the hole elongation data at $R = +0.1$ is summarized in Figures 109, 110, and 111 for three levels of hole elongation (.005, .010, and .020 inch). These data indicate that the matrix-dominant 19/76/5 layup exhibits earliest initiation of hole elongation, but had the most gradual rate of accumulation. Conversely, the fiber-dominant (50/40/10) layup exhibited the most-delayed initiation of hole elongation, but had the most rapid accumulation. The 30/60/10 layup exhibited an intermediate performance. However, hole elongation and associated damage in all three layups resembled bearing failure modes as shown in Figure 112, indicating a possible common matrix failure mechanism with differences in initiation time and accumulation resulting from fiber layup effects.

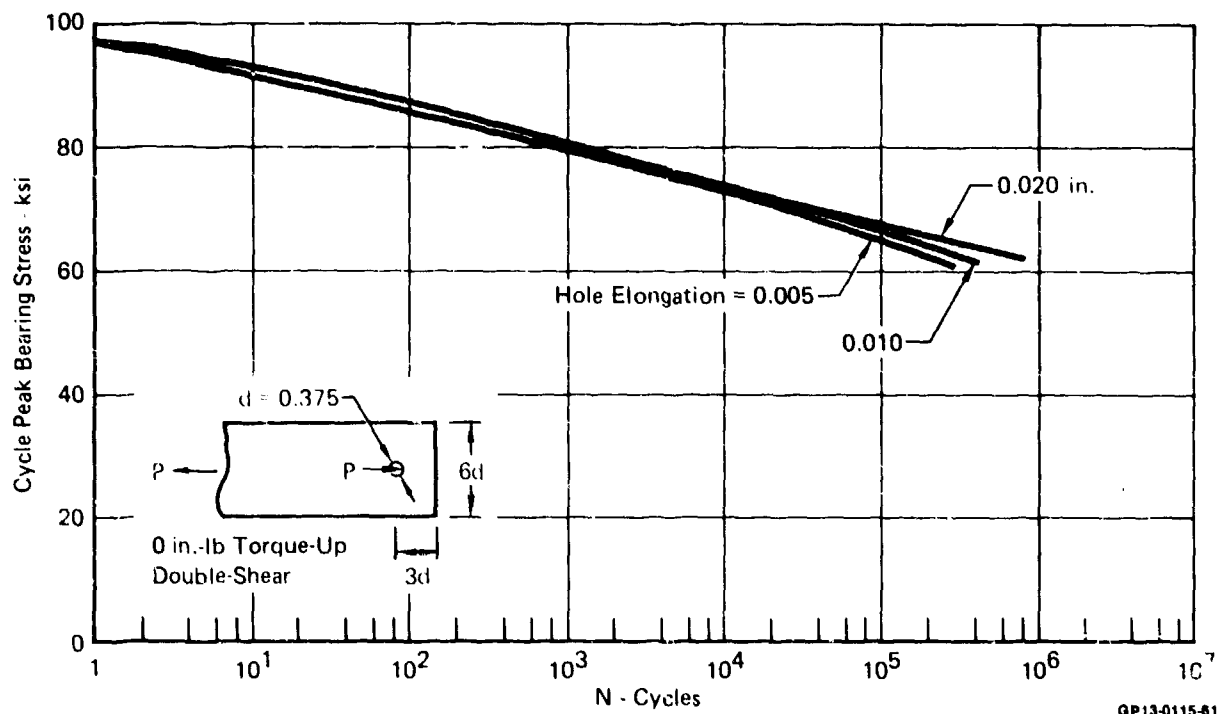


Figure 109. Hole Elongation Fatigue Life Trends
50/40/10 Layup

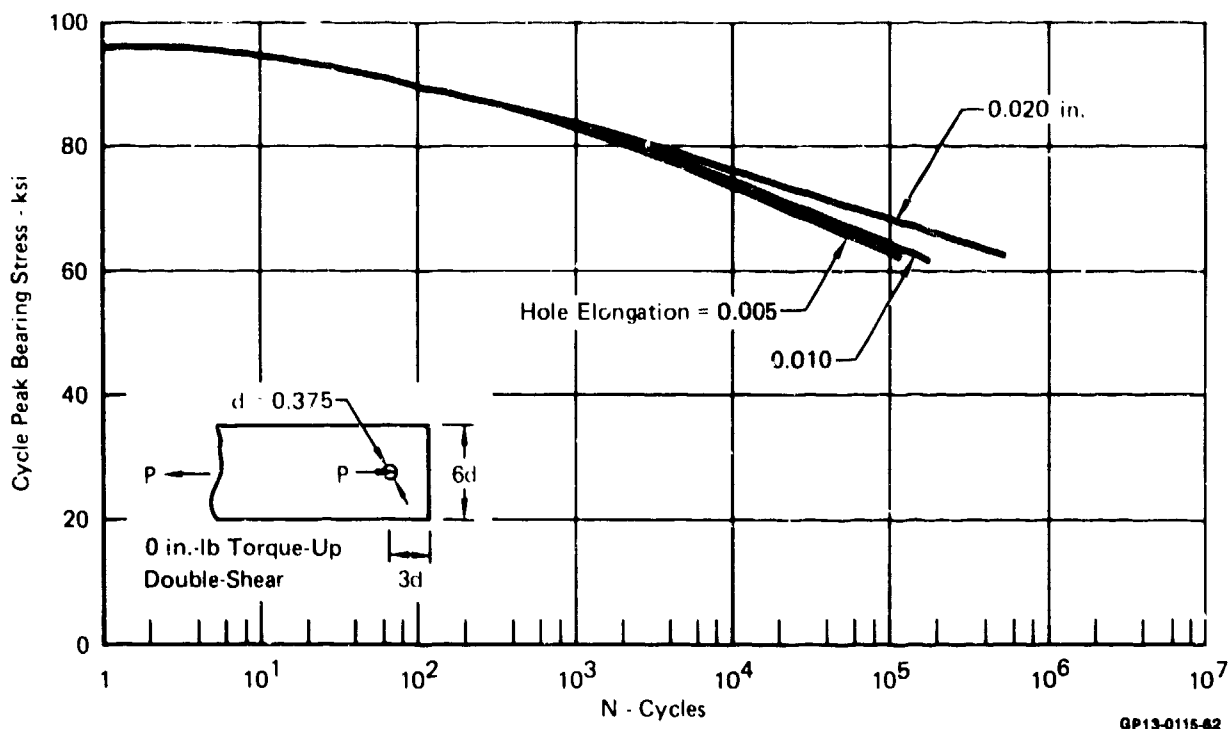


Figure 110. Hole Elongation Fatigue Life Trends
30/60/10 Layup

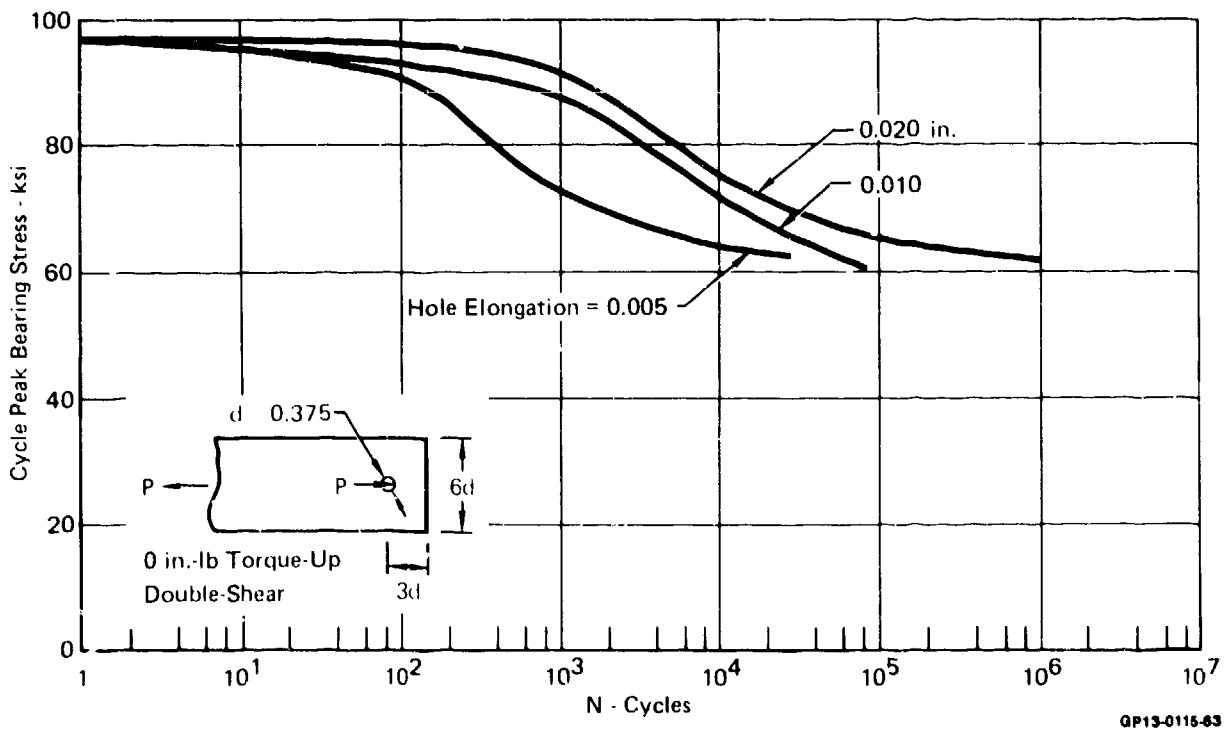
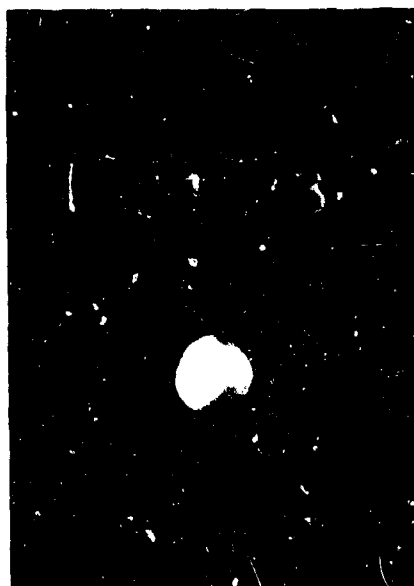
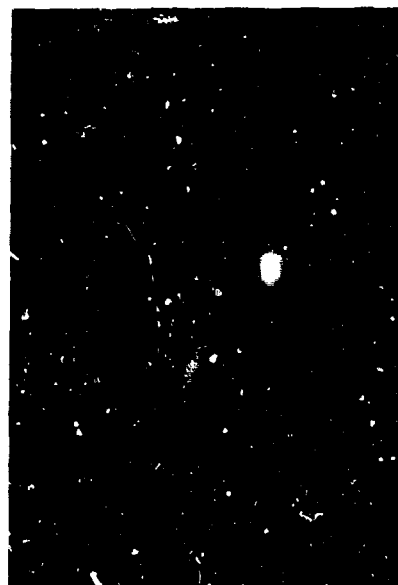


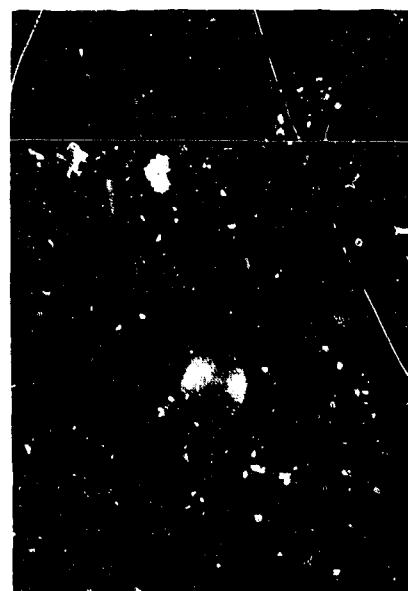
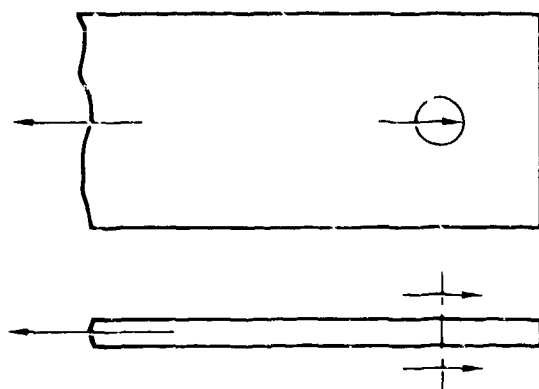
Figure 111. Hole Elongation Fatigue Life Trends
19/76/5 Layup



50/40/10 Layup



30/60/10 Layup



19/76/5 Layup

Figure 112. Representative Specimen Fatigue Failures

GP13-0115-88

Spectrum fatigue tests were conducted for the 50/40/10, 30/60/10, and 19/76/5 layup with test limit load (TLL) defined at 89%, 93%, and 94% of static strength respectively. The results of these tests showed no measurable hole elongation for any of the tested layups after testing equivalent to 16,000 spectrum service hours. Further, for tests with TLL defined at 73%, 87%, and 89% of static strength, no hole elongation was observed after 32,000 spectrum service hours. The differences between constant amplitude results and spectrum results are attributed to the infrequent application of loads high enough to produce hole elongation in any of the three layups tested.

Spectrum fatigue life of the 50/40/10 layup was determined under the RTW, ETW, and RTW(TS) test conditions to identify environmental effects. These results are summarized in Figure 113. Hole elongation was greater for the RTW condition as compared to the RTD condition for test limit load levels above 95% of static strengths with otherwise similar performance below that load level. The RTW(TS) tests produced greater hole elongation than the RTD tests for all TLL above 85% of static strengths; however, the performance of the RTW and RTW(TS) tests is not distinguishable from the test data. All residual strengths were greater than RTD static strength.

Test Conditions	Spectrum Hours Cycled	Hole Elongation (in.) After Fatigue Cycling @ TLL (As a Percent of Static Strength)				Joint Static Strength (lb)
		TLL @ 75%	75 - 85%	85 - 95%	>95%	
50/40/10 RTW	<16,000 16,000	— —	↓ 0.000	(F) ↓ 0.000	(F) ↓ 0.088	7,250
Residual Strength		—	8,560	8,670	8,010	
50/40/10 RTD	<16,000 16,000 16,000 - 32,000 32,000	↓ — — 0.000	— — — —	↓ — (F) ↓ 0.0002 - 0.0006 0.006 - 0.035	(F) ↓ — — 0.03 - 0.048	7,530
Residual Strength		8,980	—	8,080	9,240	
50/40/10 ETW	<16,000 16,000	— —	↓ 0.0006 - 0.0012	↓ 0.000	↓ 0.0008	4,210
Residual Strength*		—	8,660	7,540	8,540	
50/40/10 RTW (TS)	<16,000 16,000	— —	↓ 0.003 - 0.004	(F) ↓ 0.03 - 0.059	(F) ↓ 0.053	7,020
Residual Strength		—	9,140	8,150	8,650	

(F) Specimen failure occurred in some joints tested

* Residual strength tests at RT

-- No test

GP13-0115-04

Figure 113. Summary of Effects of Environment on Joint Spectrum Fatigue Life

The spring rates of the test specimens for the 50/40/10 layup were also determined at various times in the constant amplitude fatigue testing to determine correlation with hole elongation data. Hole elongation data for this layup at RTD, shown in Figure 114, are similar in threshold points and trends to joint spring rate data summarized in Figure 115.

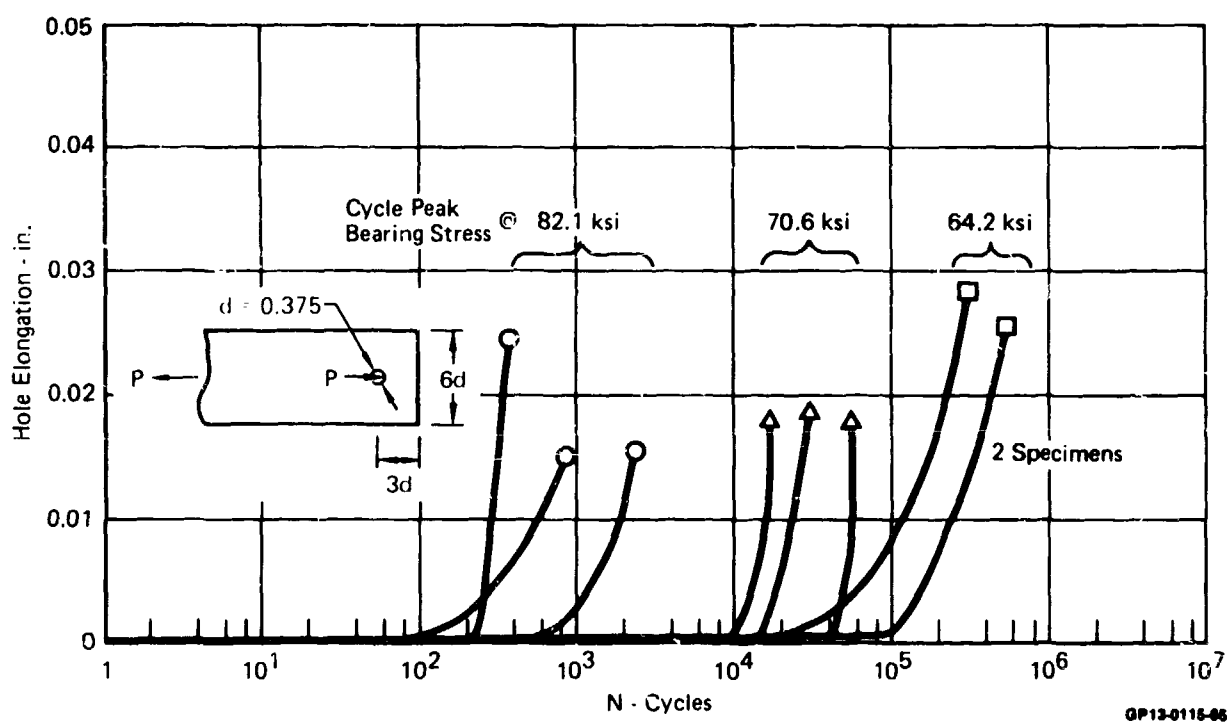
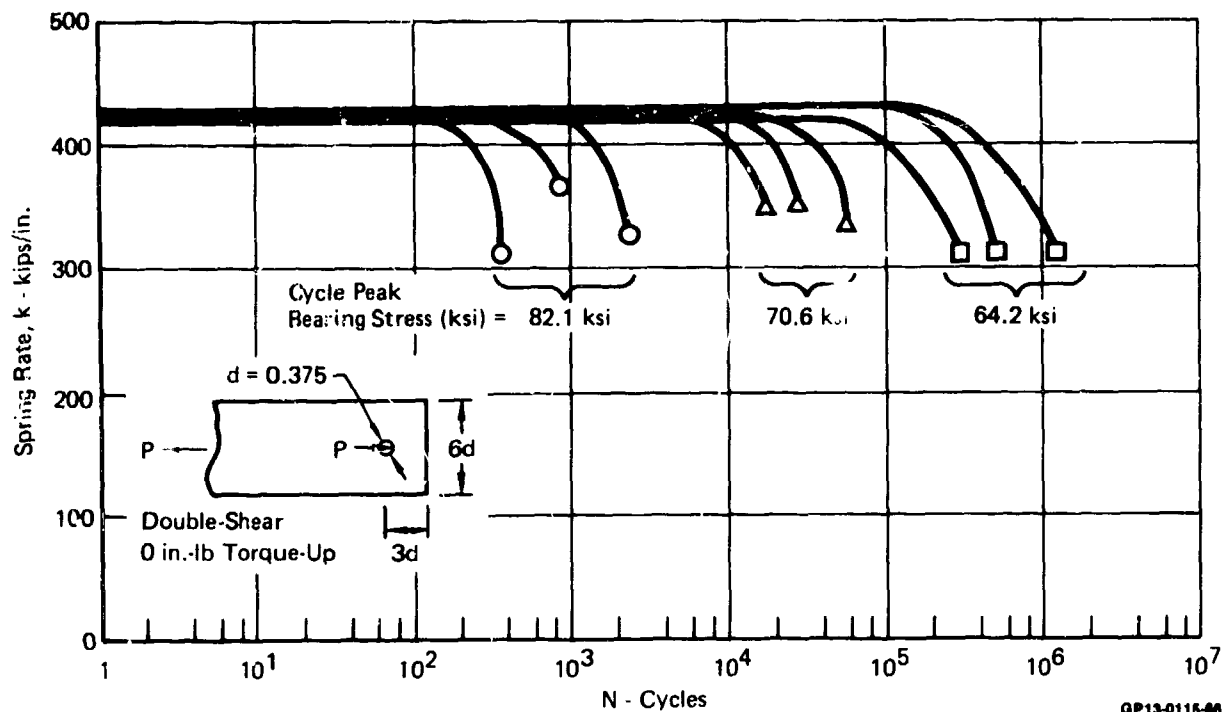


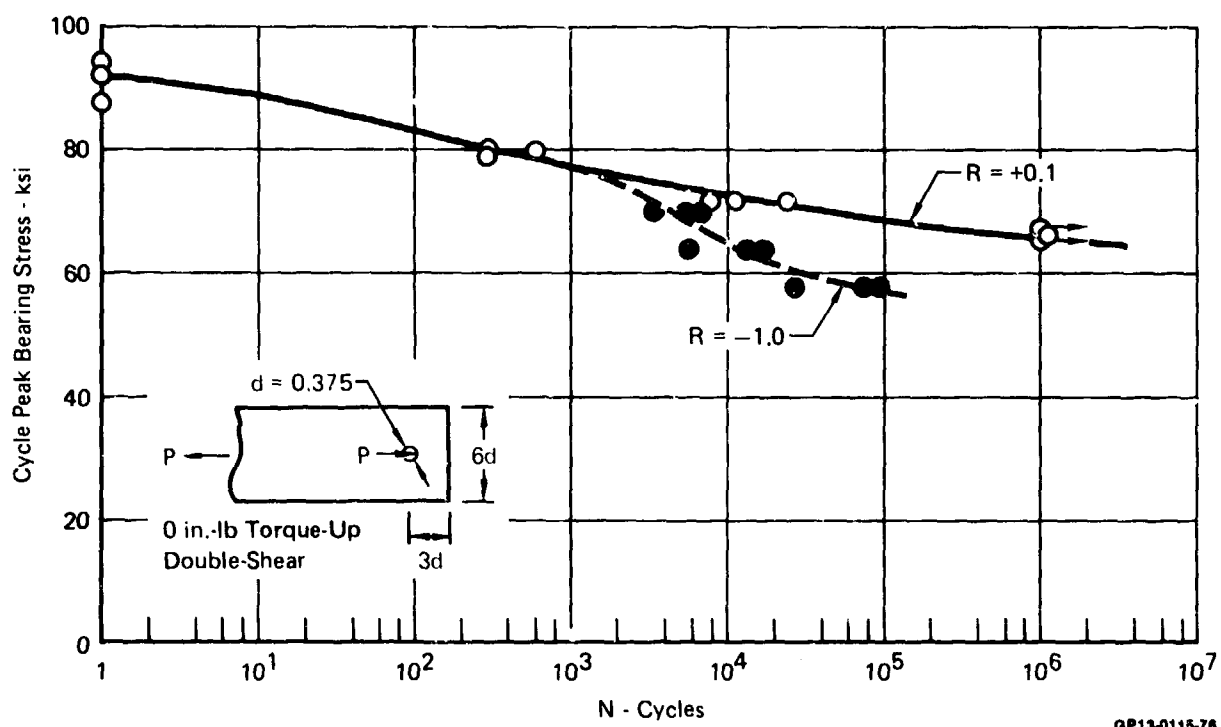
Figure 114. Effect of $R = +0.1$ Loading on Hole Elongation
Baseline 50/40/10 Layup



**Figure 115. Effect of $R = +0.1$ Loading on Joint Spring Rate
50/40/10 Layup**

(2) Stacking Sequence - Tests were conducted to determine the effect of stacking sequence changes on the joint fatigue performance of the 50/40/10 and the 19/76/5 layups. Stacking sequence evaluations compared joint life when laminates had $+45^\circ$ plies grouped in a balanced pair as compared to when $+45^\circ$ plies were uniformly dispersed. In Task 2 testing of the 50/40/10 layup, all alternate stacking sequences which grouped either the 0° plies or the $+45^\circ$ plies exhibited lower static strength. The 0° ply effect was expected; the purpose of these tests was to determine whether the unexpected effect of the $+45^\circ$ ply grouping would extend to fatigue life.

Results obtained under constant amplitude cycling of $R = +0.1$ and $R = -1.0$ are presented in Figures 116 and 117 for the 50/40/10 and 19/76/5 layups respectively. For the 50/40/10 layup, a comparison of static strength data indicated the tested stacking sequence (variation 3, reference Figure 26) failed at approximately 6% lower strengths. No significant difference in static strength was evident between the 19/76/5 baseline and variation stacking sequence data. A comparison of joint fatigue life with baseline data indicates no significant differences in life under constant amplitude cycling (Figures 118 and 119).



GP13-0115-76

Figure 116. Effect of Stacking Sequence on Joint Life
50/40/10 Layup

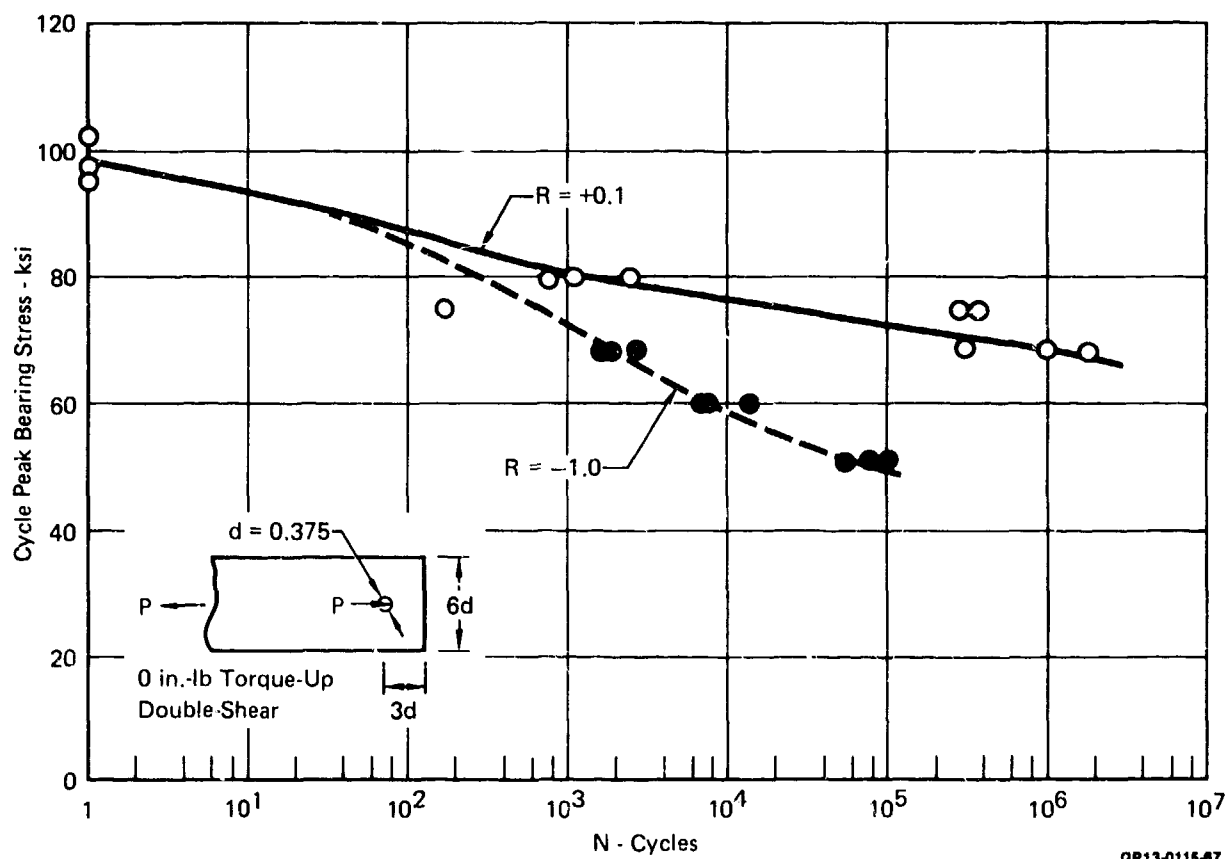
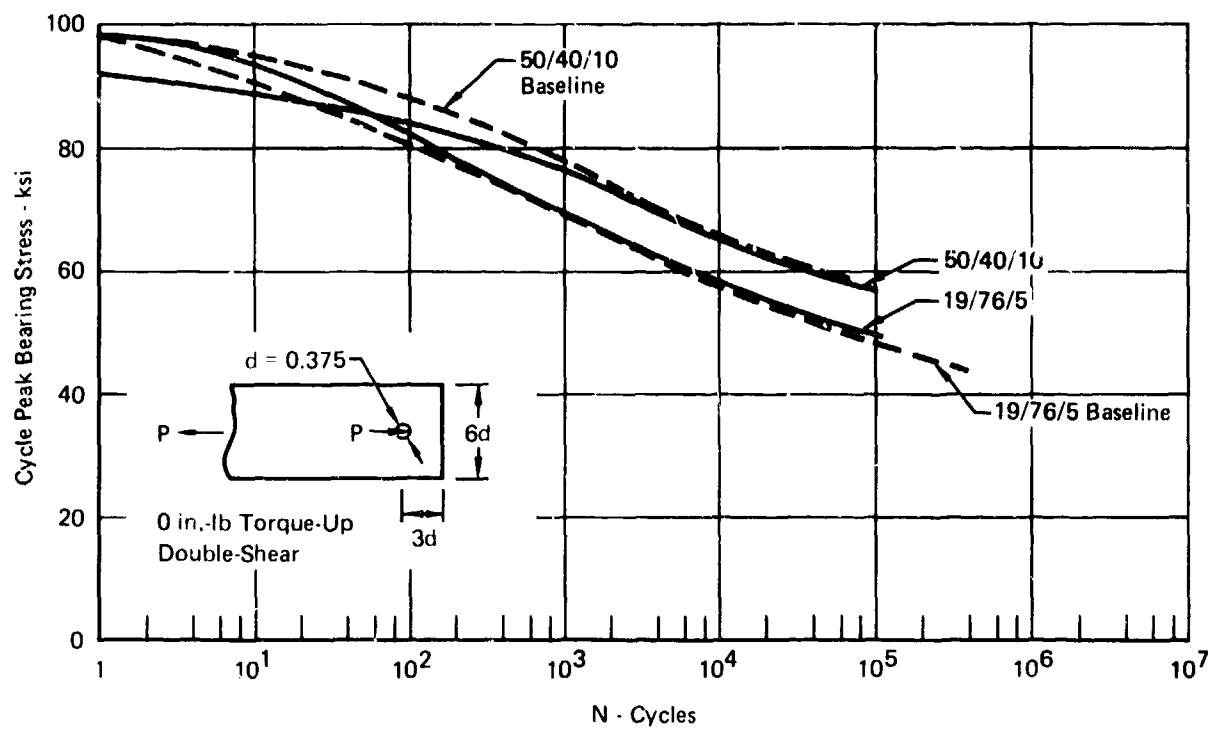
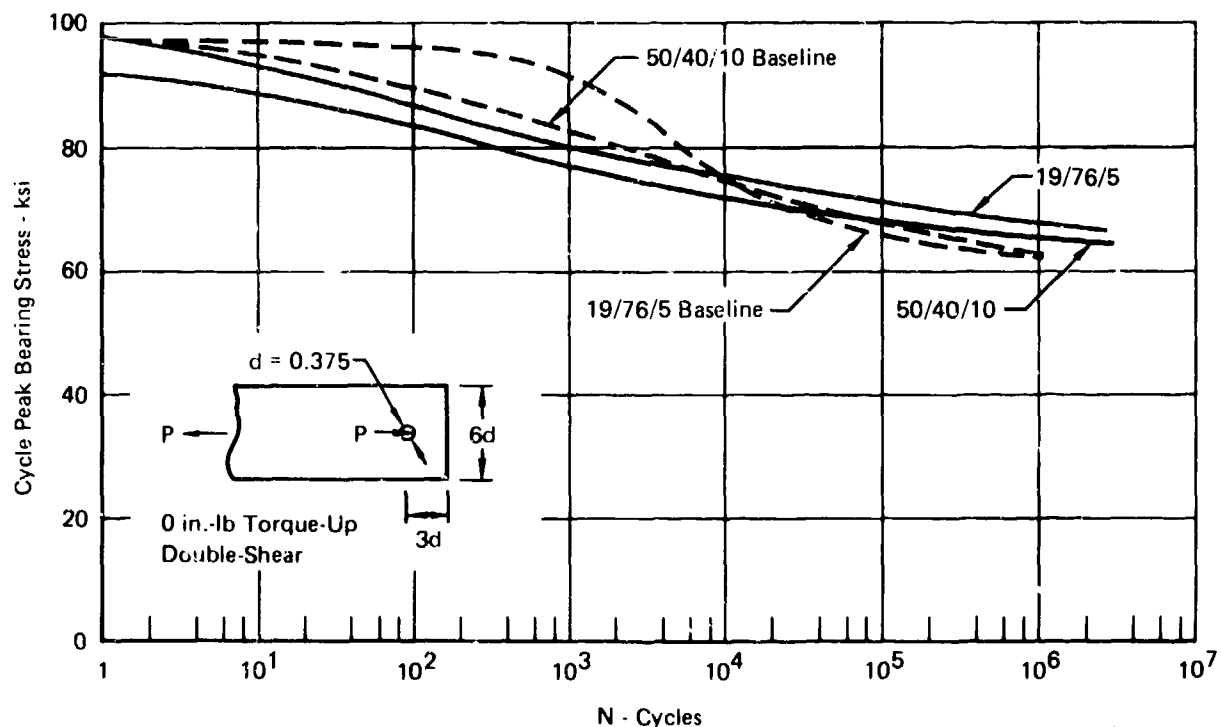


Figure 117. Effect of Stacking Sequence on Joint Life
19/76/5 Layup



GP13-0115-02

Figure 118. Stacking Sequence - Comparison with $R = -1.0$ Baseline Life Trends



GP13-0115-01

Figure 119. Stacking Sequence - Comparison with $R = +0.1$ Baseline Life Trends

Detailed plots of hole elongation intervals of .005 and .010 inch are added to the .020 hole elongation trend line for both stacking sequence variations in Figures 120 and 121 and indicate a closer grouping of elongation levels. This indicates a faster rate of fatigue damage for both of the stacking sequence variations, however in both cases initiation thresholds occurred later.

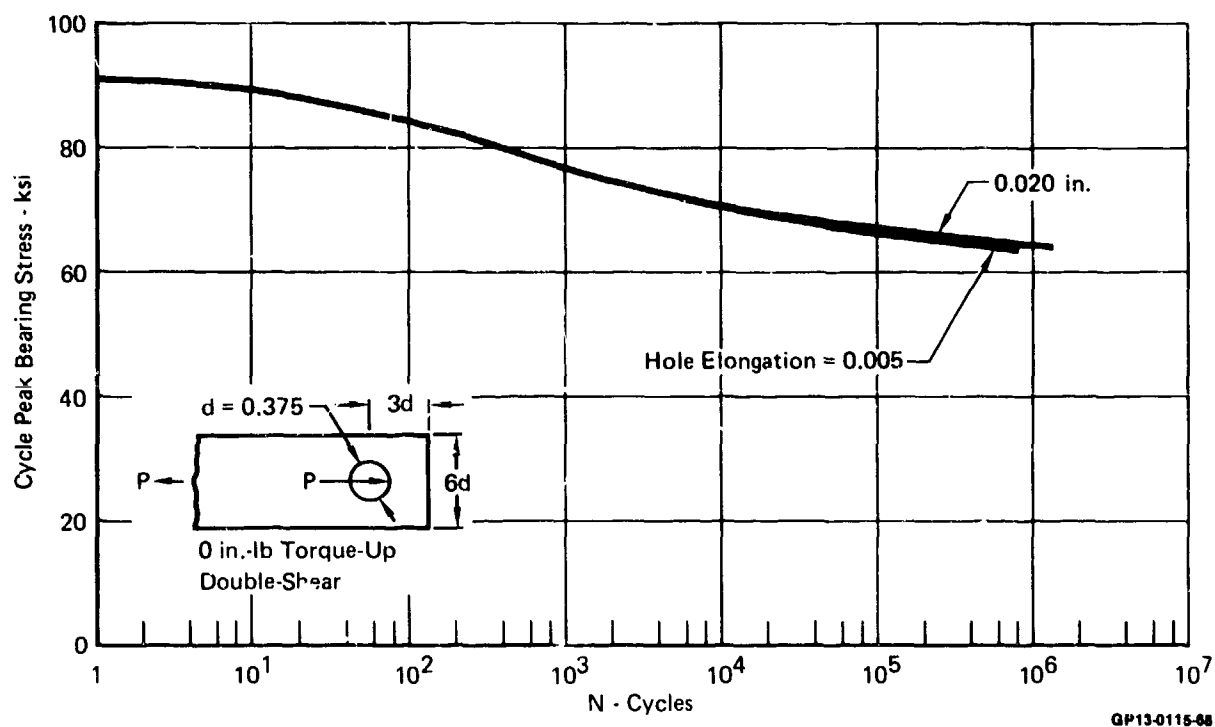


Figure 120. Effect of Stacking Sequence - Hole Elongation Levels
50/40/10 Layup

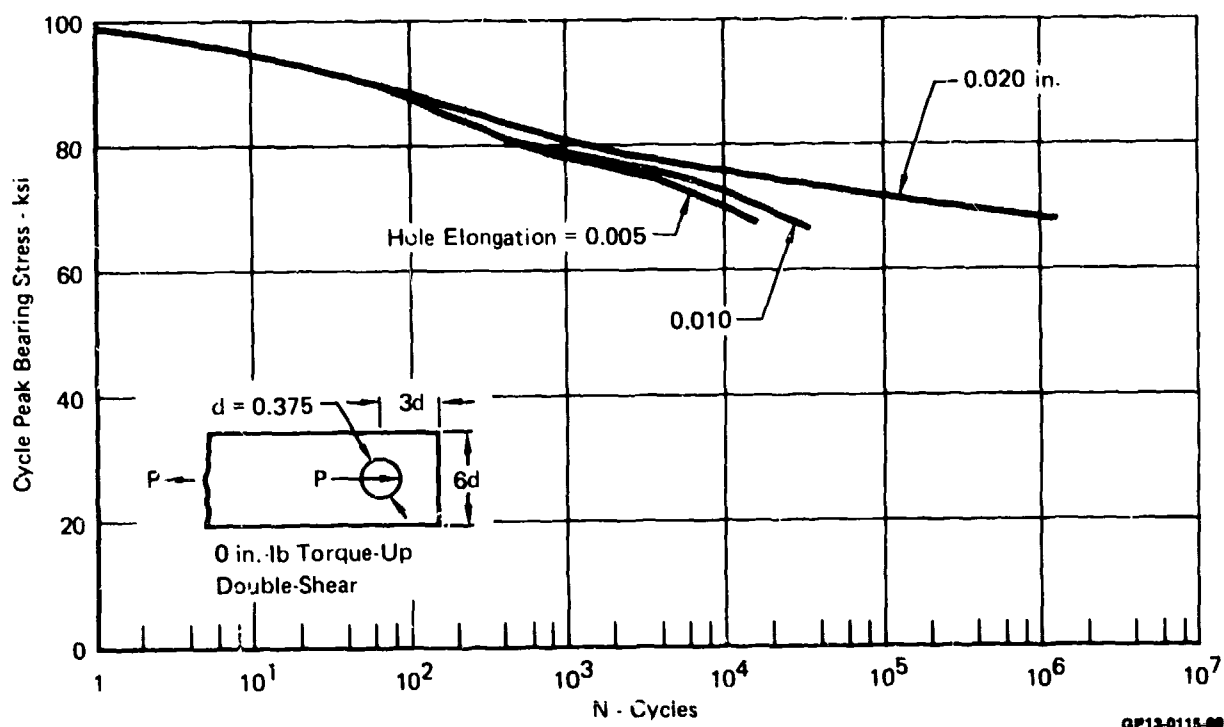


Figure 121. Effect of Stacking Sequence - Hole Elongation Levels
19/76/5 Layup

Effects of spectrum fatigue loading on joint life were similar in all respects to baseline data. Results of hole elongation and residual strength after cyclic exposure are listed in Figure 122. No sensitivity of life or strength was indicated.

(3) Torque-Up - To evaluate the effect of fastener torque-up on joint life, double-shear specimens of the 50/40/10 and 19/76/5 layups were cycled at room temperature, dry, test conditions under constant amplitude tension-tension ($R = +0.1$) and tension-compression ($R = -1.0$) loadings, and under spectrum fatigue loading. Task 2 testing to determine the effects of torque-up on joint strength indicated that both strength and failure mode are altered at 0.0 in-lbs torque-up as compared to typical 160 in-lb torque values for .375 inch diameter fasteners.

Test Conditions	Spectrum Hours	Hole Elongation (in.) After Fatigue Loading at TLL - as a Percent of Static Strength			Joint Ultimate Static Strength (lb)
		TLL @ 75 - 85%	@ 85 - 95%	@ >95%	
50/40/10 RTD	16,000	0	0 - 0.035	0.018 - 0.058	7,230
Residual Strength (lb)		8,680	8,340	8,960	
19/76/5 RTD	16,000	0	0 - 0.001	0.013 - 0.022	8,070
Residual Strength (lb)		10,360	11,280	11,200	

QP13-0115-03

Figure 122. Summary of Effects of Stacking Sequence on Joint Spectrum Life

S-N data for both layups and at both R-ratios are presented in Figures 123 and 124 along with curves obtained from testing of baseline specimens with no fastener torque-up. Significant increases in static and fatigue strength are evident. While failure modes were the same for both torque-up levels, areas of damage surrounding the fastener hole appear more pronounced for specimens torqued to 160 inch pounds (Figure 125) and overall fatigue failures occurred more abruptly (faster rates of hole elongation). This is in contrast to the gradual hole elongation observed in specimens having no fastener torque-up, which permitted specimens to survive additional fatigue cycling while damage progressed slowly.

Fastener torque-up, which constrains material through-the-thickness locally about the fastener hole, inhibited local failures and slowed the initiation of measurable fatigue damage. This effect on strength and life was considerably more pronounced in the 19/76/5 layup (60% increase) as compared to the 50/40/10 layup (20% increase).

Fastener torque-up produced no pronounced changes in joint flexibility or local spring rate. For the 50/40/10 and 19/76/5 layups, no difference in double-shear spring rates for 0.0 in-lbs torque-up and 160 in-lbs of torque-up was indicated. This may be a result of diameter-to-thickness ratio (d/t) greater than one, producing little bolt bending, especially for the double lap configuration. Double-shear specimens exhibited a 13 percent higher spring rate over single-shear specimens for the same 50/40/10 layup.

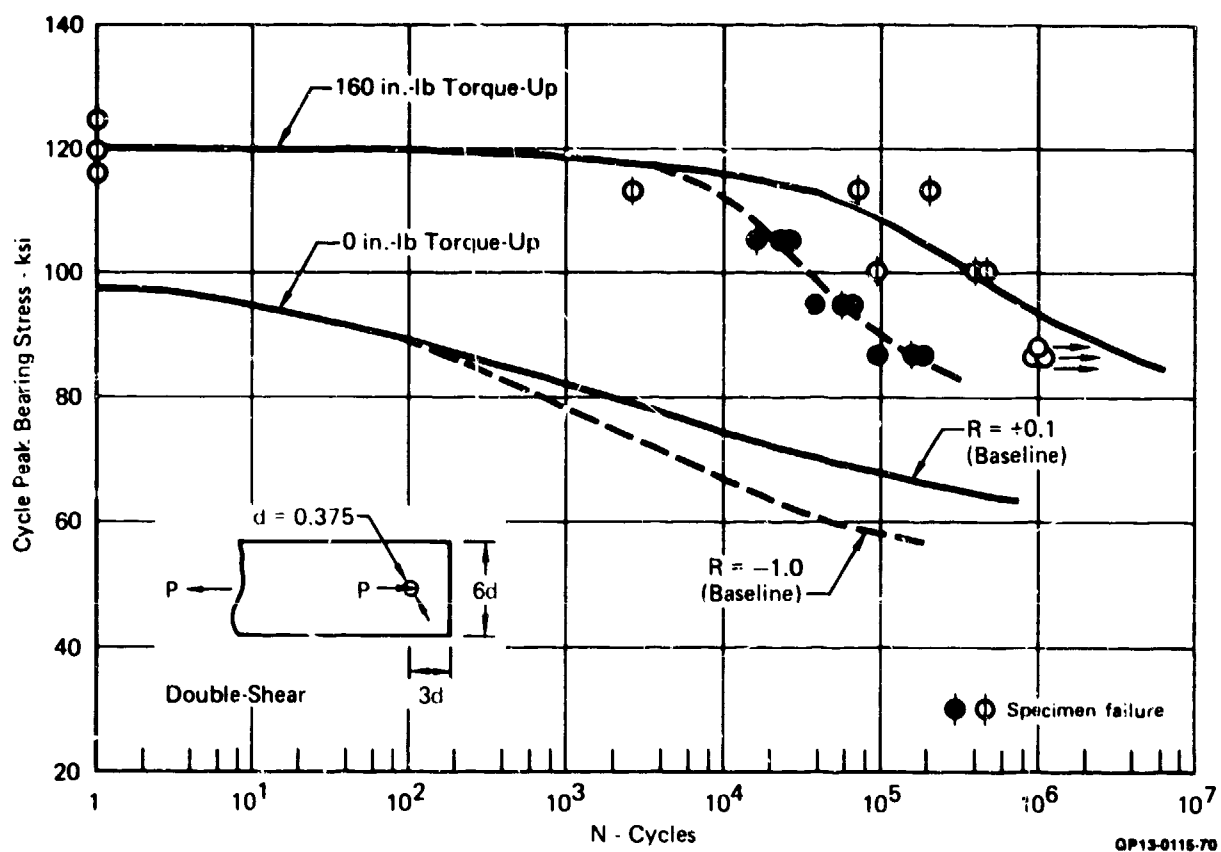


Figure 123. Effect of Torque-Up on Joint Fatigue Life
50/40/10 Layup

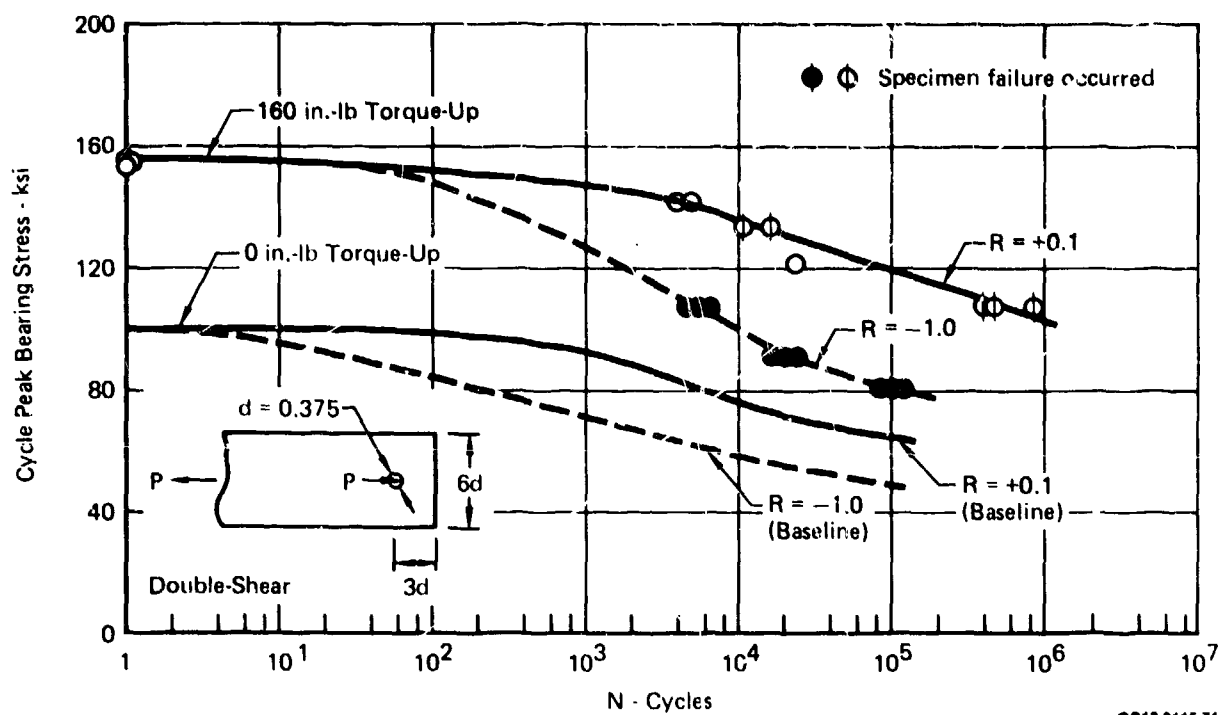
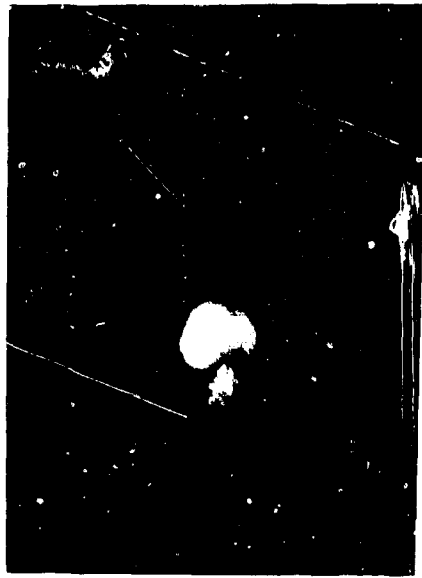


Figure 124. Effect of Torque-Up on Joint Fatigue Life
19/76/5 Layup



(a) 0 in.-lb Torque-Up

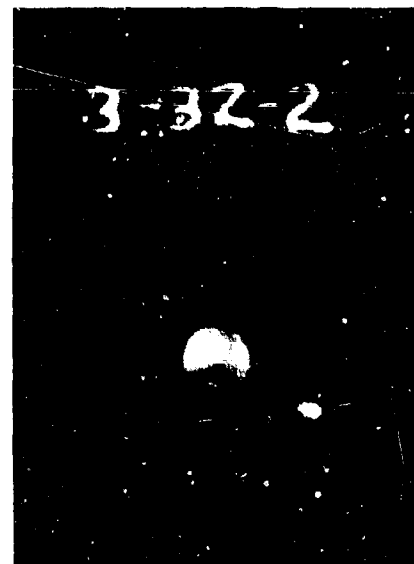


(b) 160 in.-lb Torque-Up

50/40/10 Layup



(c) 0 in.-lb Torque-Up



(d) 160 in.-lb Torque-Up

19/76/5 Layup

GP13-0115-80

Figure 125. Specimen Failures for Torque-Up Conditions

(4) Joint Geometry - The effects of specimen geometry on joint life were evaluated by testing specimens of the 50/40/10 and 19/76/5 layups with different edge distances and widths. In static tests, these variations resulted in changes in joint strength and failure mode. Associated nonlinear joint load-deflection character and static failures in bearing or shearout, as compared to net tension, might alter the fatigue performance as well.

Results for the baseline 50/40/10 layup, in which 4d and 3d edge distances as well as 4d and 6d specimen widths were tested, are summarized in Figure 126. These results indicate virtually identical static and fatigue strength for this layup. Fatigue and static failures were similar for this fiber-dominant layup and did not change with geometry variations.

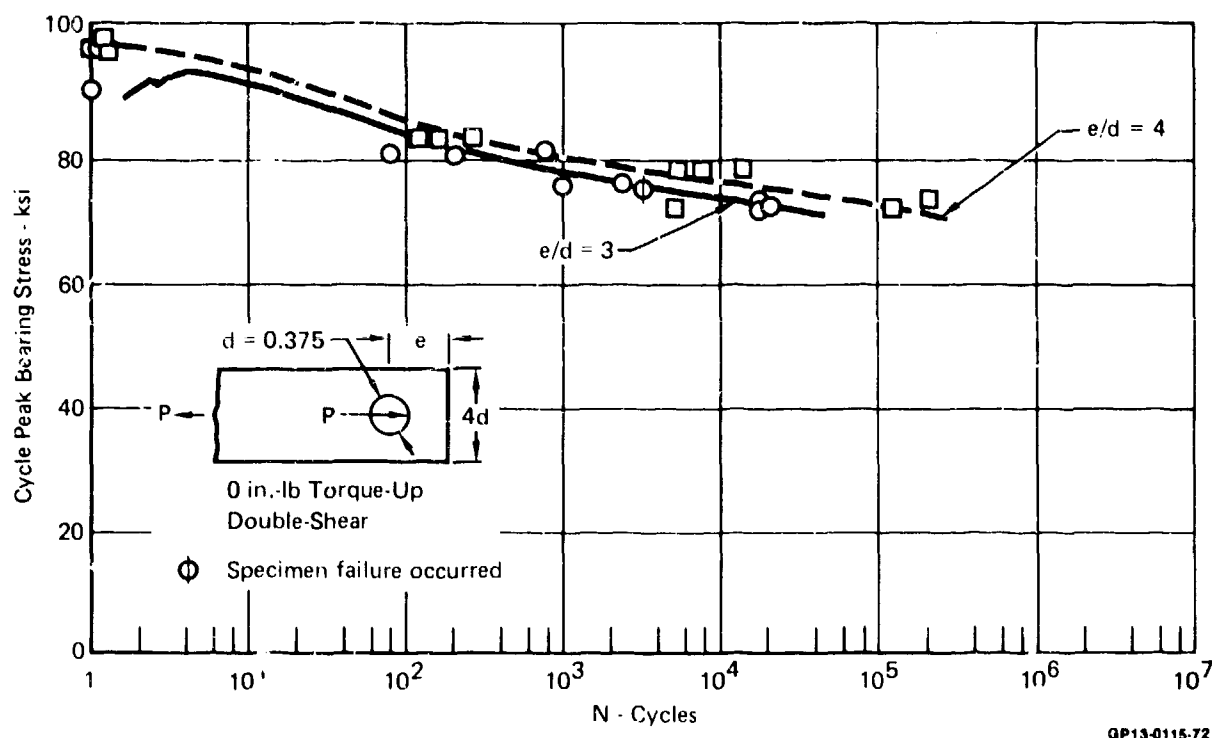


Figure 126. Effect of Geometry on Joint Fatigue Life
50/40/10 Layup

Results for the matrix-dominant 19/76/5 layup, in which variations of specimen widths at 4d and 3d were tested (Figure 127), indicate a pronounced effect on fatigue life. Further, a change of failure from bearing to net section occurred as the w/d ratio was reduced as shown in Figure 128.

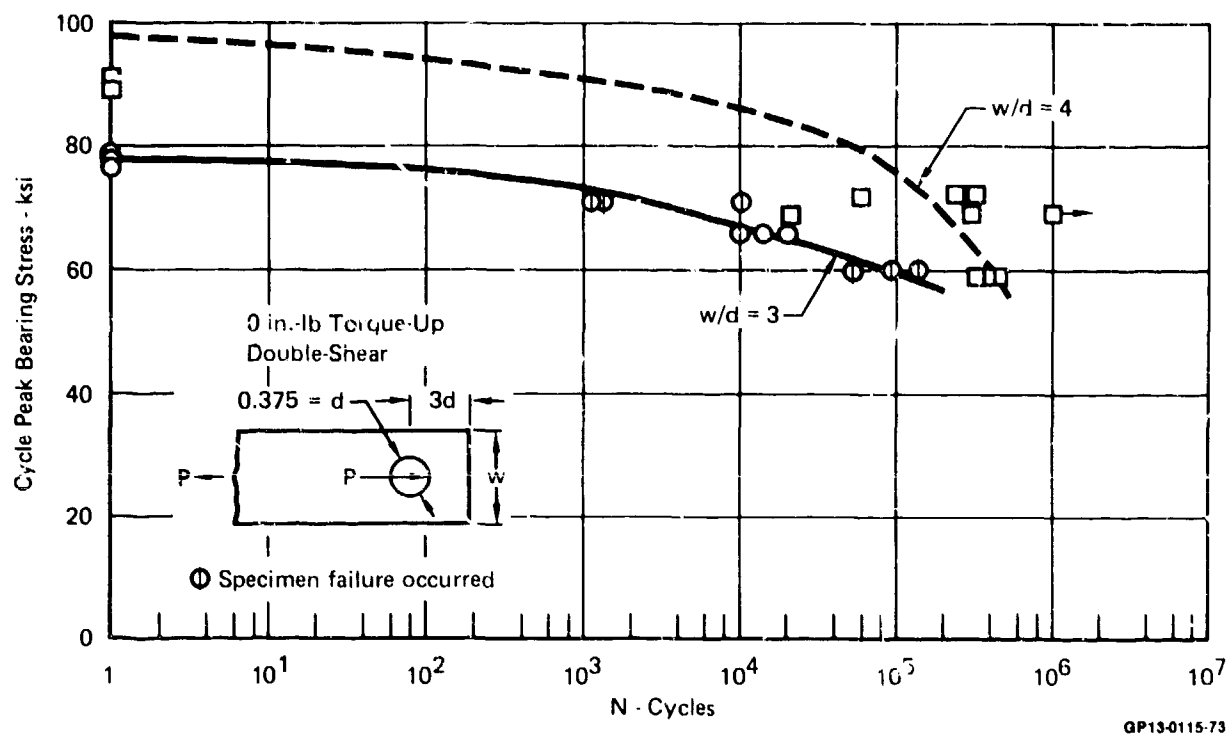
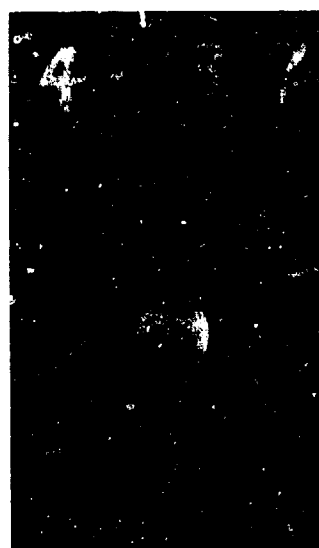


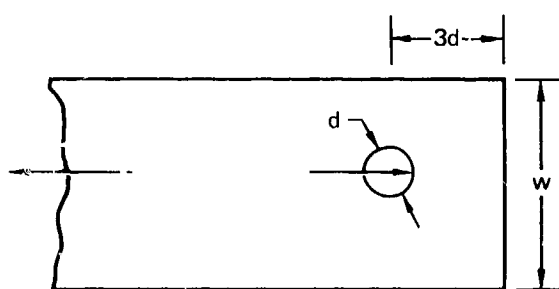
Figure 127. Effect of Geometry on Joint Fatigue Life
19/76/5 Layup



$w/d = 6$



$w/d = 4$



$d = 0.375$ in All Specimens



$w/d = 3$

GP13-0115-90

Figure 128. Changes In Failure Due to Geometry

(5) Interference Fit - This series of fatigue tests were conducted to evaluate the effect of interference fits of .005 inch on the fatigue life of no-torque and torqued joints. In Task 3 testing, interference fits of .003 and .008 inch produced an increase in static strength (up to 14%) over neat-fit specimens; however, evidence of localized cracking and delamination was noted as well. Task 4 tests were to evaluate the effects of these characteristics on fatigue life.

Static strengths of specimens without torque-up were 7.5% higher than baseline (neat-fit) specimens. These data were consistent with earlier Task 3 data.

Fatigue tests, $R = +0.1$, of no torque-up specimens resulted in lower fatigue life relative to neat-fit baseline data. Data are summarized in Figure 129. Associated with lower life was large test data scatter. It was suspected that minor installation damage caused by the interference fit produced the wide scatter in data when no through-the-thickness constraint existed due to zero fastener torque-up. Limited fatigue testing of torqued-up specimens (160 in-lb) produced higher fatigue life relative to neat-fit specimens with the same installation torque. Two specimens were tested at 85% and 94% of the neat-fit static strength, respectively. Both showed fatigue improvements relative to baseline data (Figure 129) with no hole elongation recorded at the 85% load level after 10^6 cycles.

(6) Single-Shear Loading - The effects of joint eccentricities on fatigue life were evaluated using a single-shear specimen configuration (Reference Figure 23). Two types of fastener head configurations were tested; protruding head and countersunk tension-head. As-manufactured specimens were tested under tension-tension, $R = +0.1$, fatigue loading at room temperature. All specimens were torqued to 160 in-lbs for comparison to data from torqued-up double-shear specimens.

Effects on joint life are illustrated in Figure 130. For the protruding head single-lap configuration, static strengths were identical to the double shear configuration. However, the added effect of bending stresses due to the single shear configuration indicates a significant reduction in fatigue life. Further fatigue life reductions were exhibited by the countersunk fastener with its associated loss of direct bearing material and added fastener head flexibility. Joint spring rates for the double-shear, noncountersunk single-shear, and countersunk single-shear specimens were respectively 396,000 lbs/in, 347,000 lbs/in, and 250,000 lbs/in. Representative failures for the three specimen configurations are shown in Figure 131.

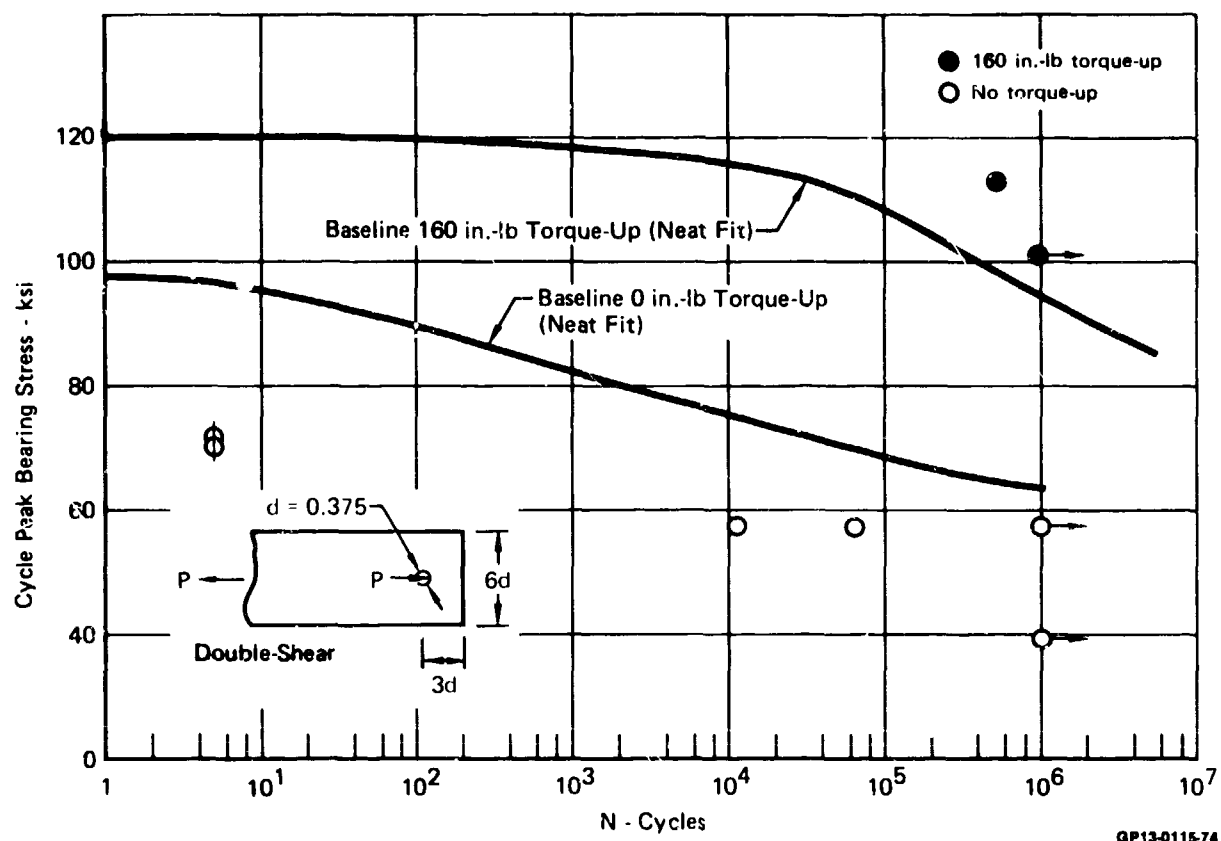
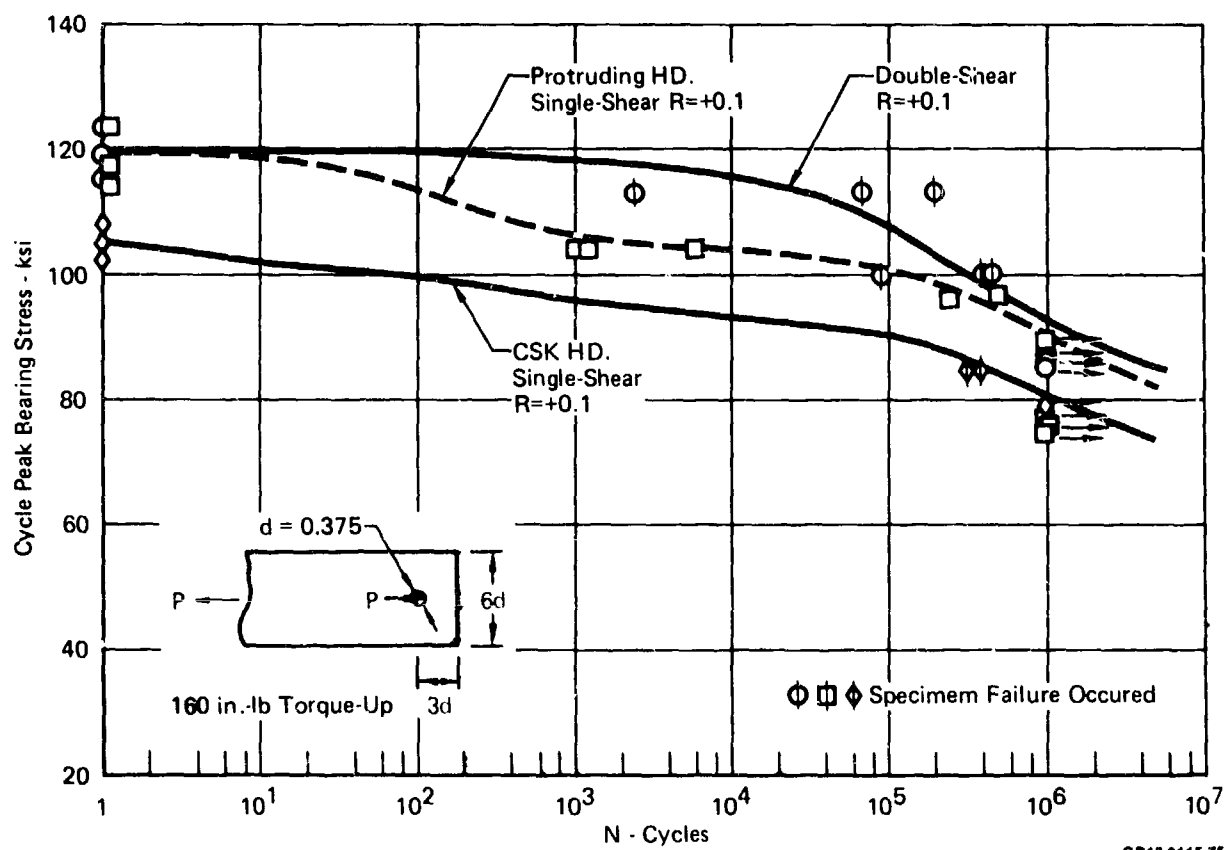


Figure 129. Effect of 0.005 in. Interference Fit on Joint Fatigue Life
50/40/10 Layup

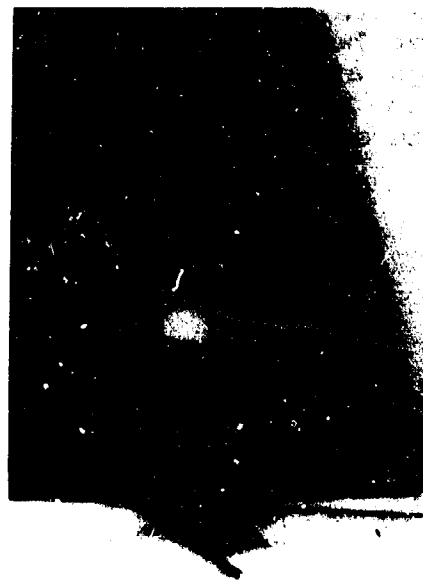


GP13-0115-75

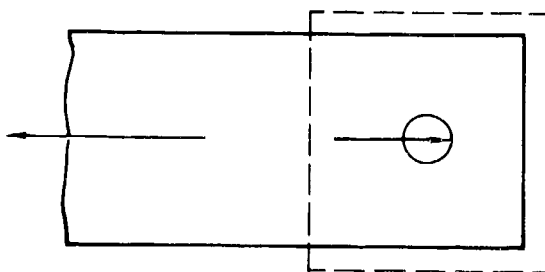
Figure 130. Effect of Single-Shear Loading on Joint Fatigue Life
50/40/10 Layup



(a) Single-Shear
Protruding Head



(b) Single-Shear
Countersunk



160 in.-lb Torque-Up



(c) Double-Shear

QP13-0115-01

Figure 131. Failures of Single-Shear Specimens

(7) Porosity - Tests of specimens with moderate porosity were conducted to evaluate the effects of this anomaly on joint durability. Testing, in Task 3, indicated that moderate levels of porosity had a minor effect on static joint strength at room temperature. Specimens with moderate porosity in regions of fastener holes were tested under $R = +0.1$ and $R = -1.0$ fatigue loadings at room temperature dry conditions. Life data is compared in Figure 132 with baseline data. No reduction of static strength or joint fatigue life was indicated.

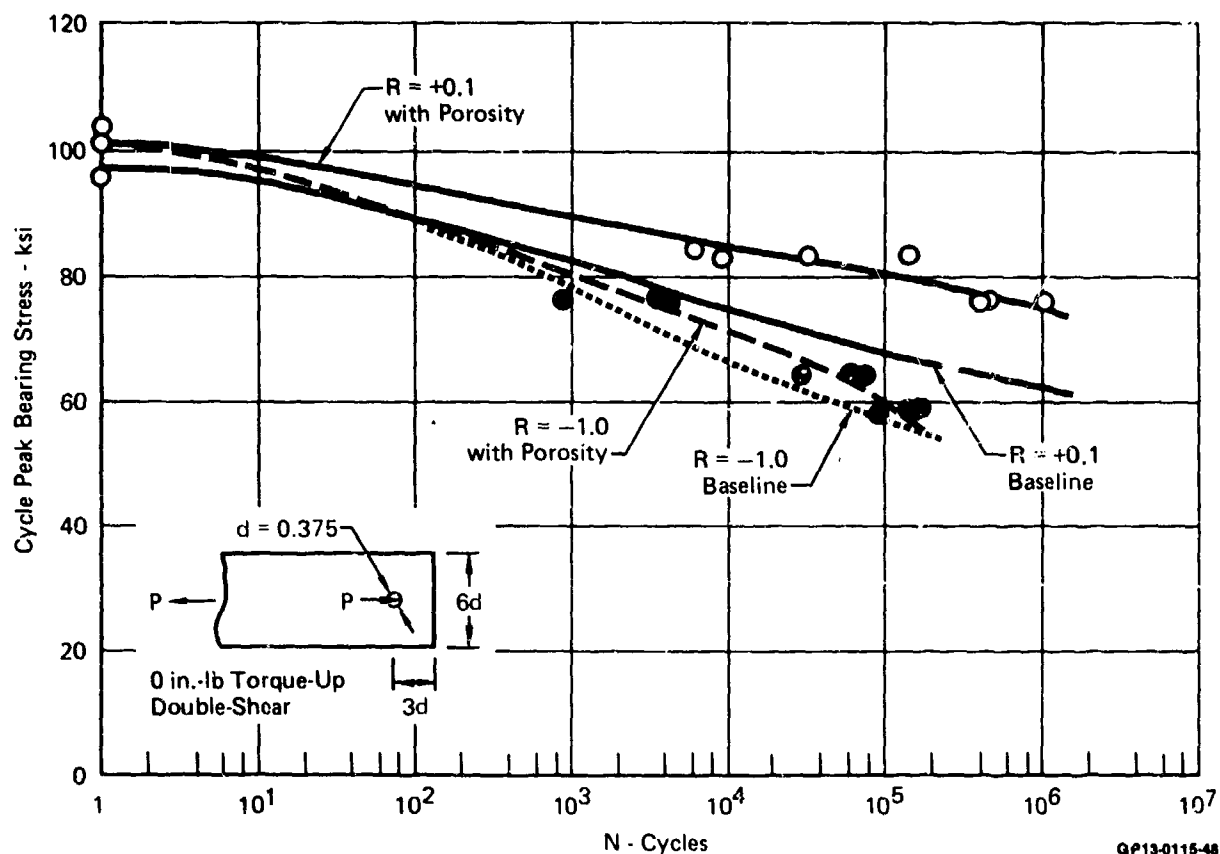


Figure 132. Effect of Porosity on Joint Fatigue Life
50/40/10 Layup

SECTION V

RECOMMENDATIONS

Based on the results of this program, which were summarized in Section II, several areas of future methodology development and experimental verification are recommended.

The analysis procedure developed in this program should be extended to analyze the general class of stress risers in composite structures. Overall geometry and stress concentration interactions (e.g. multiple fastener holes) should be included. Experimental evaluations should be performed to verify developed methodology, with emphasis placed on multifastener joints.

The analysis procedure developed in this program should also be extended to predict the effects of through-the-thickness variables, such as stacking sequence, fastener torque-up, and joint eccentricity. These variables were shown by tests in this program to have a pronounced effect on static and fatigue performance. The improved methodology should be verified by test. The extended analysis technique would permit application of the methodology to a broader range of joint designs.

Hole elongation mechanisms and their relation to joint fatigue life should be further studied. Analytic techniques should be developed to identify critical plies, failure locations, and failure modes for both hole elongation and overall fatigue life. Developed methodology should incorporate the capability to predict effects of finite joint geometry and through-the-thickness variables. An experimental verification program should be conducted to verify the developed methodology for fatigue and hole elongation predictions.

SECTION VI

REFERENCES

1. S. P. Garbo, and J. M. Ogonowski, "Effect of Variances and Manufacturing Tolerances on the Design Strength and Life of Mechanically Fastened Composite Joints," Interim Report AFDL-TR-78-179, 1978.
2. B. Burroughs, et al, "Advanced Composite Serviceability", Rockwell International, F33615-76-C-5344, Quarterlies, 1976 to Present.
3. S. G. Lekhnitskii, "Anisotropic Plates", Gordan and Breach Science Publishers, 1968.
4. J. P. Waszczak and T. A. Cruse, "A Synthesis Procedure for Mechanically Fastened Joints in Advanced Composite Materials", AFML-TR-73-145, Volume II, 1973.
5. J. M. Whitney and R. J. Nuismer, "Stress Fracture Criteria for Laminated Composites Containing Stress Concentrations," J. of Composite Materials, Volume 8, July 1974.
6. T. DeJong, "Stresses Around Pin-Loaded Holes in Elastically Orthotropic or Isotropic Plates", J. of Composite Materials, Volume II, July 1977.